Moving forwards by going outside

Inertial measurement unit-based monitoring of running biomechanics

Marit Zandbergen

MOVING FORWARDS BY GOING OUTSIDE

INERTIAL MEASUREMENT UNIT-BASED MONITORING OF RUNNING BIOMECHANICS

Marit Ariene Zandbergen

The work presented in this thesis was supported in part by the Europees Fonds voor Regionale Ontwikkeling (EFRO) Oost-Nederland through the Runner Assist project.

The publication of this thesis was generously supported by:

ROESSINGH RESEARCH & DEVELOPMENT

Roessingh
Centrum voor Revalidatie

UNIVERSITY OF TWENTE.

Cover design: Jos Spoelstra
Printed by: Gildeprint
Lay-out: Marit Zandbergen
ISBN (print): 978-90-365-5513-5
ISBN (digital): 978-90-365-5512-8
DOI: 10.3990/1.9789036555128
URL: https://doi.org/10.3990/1.9789036555128

MOVING FORWARDS BY GOING OUTSIDE

INERTIAL MEASUREMENT UNIT-BASED MONITORING OF RUNNING BIOMECHANICS

PROEFSCHRIFT

ter verkrijging van
de graad van doctor aan de Universiteit Twente,
op gezag van de rector magnificus,
prof. dr. ir. A. Veldkamp,
volgens besluit van het College voor Promoties
in het openbaar te verdedigen
op donderdag 2 februari 2023 om 16:45 uur

door

Marit Ariene Zandbergen
Geboren op 3 juli 1995
in 's-Hertogenbosch, Nederland

Dit proefschrift is goedgekeurd door

Promotoren
prof. dr. J.H. Buurke
prof. dr. ir. P.H. Veltink

Co-promotor
dr. J. Reenalda

Promotiecommissie

Voorzitter

prof. dr. J.N. Kok	University of Twente

Promotoren

prof. dr. J.H. Buurke	University of Twente
prof. dr. ir. P.H. Veltink	University of Twente

Co-promotor

dr. J. Reenalda	University of Twente

Leden

prof. dr. ir. H.F.J.M. Koopman	University of Twente
prof. dr. ir. J. Harlaar	Delft University of Technology
prof. dr. B. Vanwanseele	KU Leuven, Belgie
dr. A.H. Gruber	Indiana University Bloomington, USA
dr. ir. B.J.F. van Beijnum	University of Twente
prof. dr. K.A.P.M. Lemmink	University of Groningen

Contents

Chapter 1

General introduction

Introduction to running

Running is an accessible leisure time activity. In 2020, running was the second most popular sport in The Netherlands, with 12 percent of Dutch people participating in weekly running sessions [1,2]. Running has many health benefits for the cardiovascular, metabolic, neuropsychiatric, and musculoskeletal systems and runners have a 30-45% lower risk of all-cause mortality [3]. However, runners are at risk for developing running-related injuries such as medial tibial stress syndrome (i.e., shin splints), tibial stress fractures, patellofemoral pain syndrome (i.e., runner's knee), Achilles tendinopathy, plantar fasciitis and iliotibial band syndrome [4]. The incidence of lower extremity running injuries is alarming, with values of up to 79%, depending on the population investigated and the exact definition of an injury [5]. Most running injuries are overuse related and are assumed to be caused by training load errors (i.e., too fast and too far) and running biomechanics [6,7], see Intermezzo "Definitions in motion analysis". A small number of prospective studies have been conducted and found biomechanical differences between runners who acquired an injury and those who remained injury free [6,8,9]. This link between running biomechanics and injuries sparks our interest in measuring running biomechanics and understanding the etiology of running-related injuries.

Intermezzo: Definitions in motion analysis

Biomechanics, kinematics, and kinetics

Biomechanics refers to "the study of biological systems, particularly their structure and function, using methods derived from mechanics, which is concerned with the effect that forces have on the motion of bodies" [10]. Biomechanics is typically subdivided into kinematics and kinetics. Kinematics refer to the study of the description of motion (e.g., position, joint angles, velocity, and acceleration), while kinetics involves the various forces that result in motions (e.g., ground reaction force and torque).

Running gait

Running gait is divided into gait cycles for more straightforward analysis and visualization. A gait cycle starts when a foot first makes contact with the ground (i.e., initial contact) and ends shortly before the same foot makes contact with the ground again, see Figure 1.1. Depending on the strike pattern of a runner, initial contact occurs with the rearfoot, midfoot, or forefoot, of which a rearfoot strike is most common (75-95%) [11].

Gait cycles are further divided into stance and swing phases. The stance phase starts with initial contact (Figure 1.1A) and ends when the foot loses contact with the ground (i.e., toe-off, Figure 1.1D). The swing phase starts with toe-off and ends with initial contact.

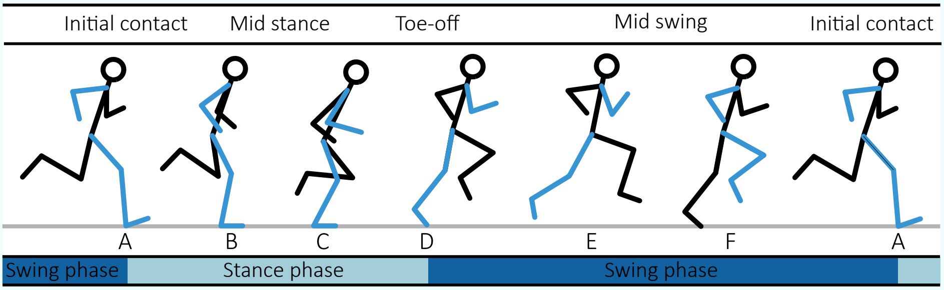

Figure 1.1: *Visualization of a running gait cycle for the right leg. The right leg and arm are shown in blue. The text above the figure shows different moments in the gait cycle. Blocks below the figure show different phases of the gait cycle.*

Running biomechanics

During running, each foot hits the ground around 85 times per minute [12,13]. Every time, ground reaction forces of about 2.5 times body weight are exerted on the body [14], see Figure 1.2. These impact forces cause a rapid deceleration of the foot following initial contact, shortly followed by deceleration of the lower leg, upper leg, pelvis, and upper body. Running kinematics influence these impact forces on the body. A more flexed knee and a smaller angle between the lower leg and vertical axis at initial contact result in smaller peak impact forces [15]. High impact forces and steep increases in impact forces are thought to reflect an increased injury risk [16–18]. Accelerometers can measure acceleration of body segments following initial contact and thereby quantify the decelerating effects of impact forces on body segments.

A commonly reported impact quantity is peak tibial acceleration (PTA) [19], see Figure 1.2. PTA is defined as the peak axial (i.e., in the direction of the long axis of the tibia bone) acceleration typically measured with an accelerometer (or inertial measurement unit (IMU) containing an accelerometer) on the lower leg immediately after initial contact. Typical PTA values during running reach values from (mean (standard deviation)) 5.6 (1.3) to 13.3 (3.4) times the gravitational acceleration (g) [20]. Accelerometers can also quantify peak accelerations of the foot, pelvis, and head [21,22]. The body is expected to minimize proximal accelerations to prevent disturbances of the vestibular and visual systems [23,24]. Shocks, as a consequence of impact forces, are attenuated passively through shoe soles, the Achilles' tendon, plantar fascia, and

bones and actively through muscles and joint kinematics [25,26]. Due to shock attenuation, peak accelerations in the body typically decrease from distal to proximal segments, see Figure 1.2. Shock attenuation is computed from peak accelerations of at least two different body segments as the percentual reduction in peak accelerations. Decreased shock attenuation could indicate that a runner is less able to attenuate impact forces, which is assumed to cause higher forces on biological structures in the body and, therefore, an increased risk of overuse-related running injuries [22,27].

Shock attenuation can change by factors such as fatigue, often encountered when running for prolonged periods of time [28]. With fatigue, the body is hypothesized to move to shock attenuation strategies that rely more heavily on passive structures such as tendons and bones instead of active strategies mainly based on joint angle modulations through coordinated muscle contractions which are energetically costly [15,29,30]. Repetitive loading of tendons and bones is expected to cause overuse-related running injuries [17]. For instance, due to disrupted bone formation and resorption caused by impact forces resulting in accumulation of microfractures in the tibia bone and tibial stress fractures [31] or possibly through muscle traction-related bone resorption in medial tibial stress syndrome [32]. To better understand the link between running-induced fatigue and overuse-related injuries, it is essential to know how running kinematics change due to fatigue.

> Research question **Chapter 2**
> How do running kinematics change due to running-induced fatigue?

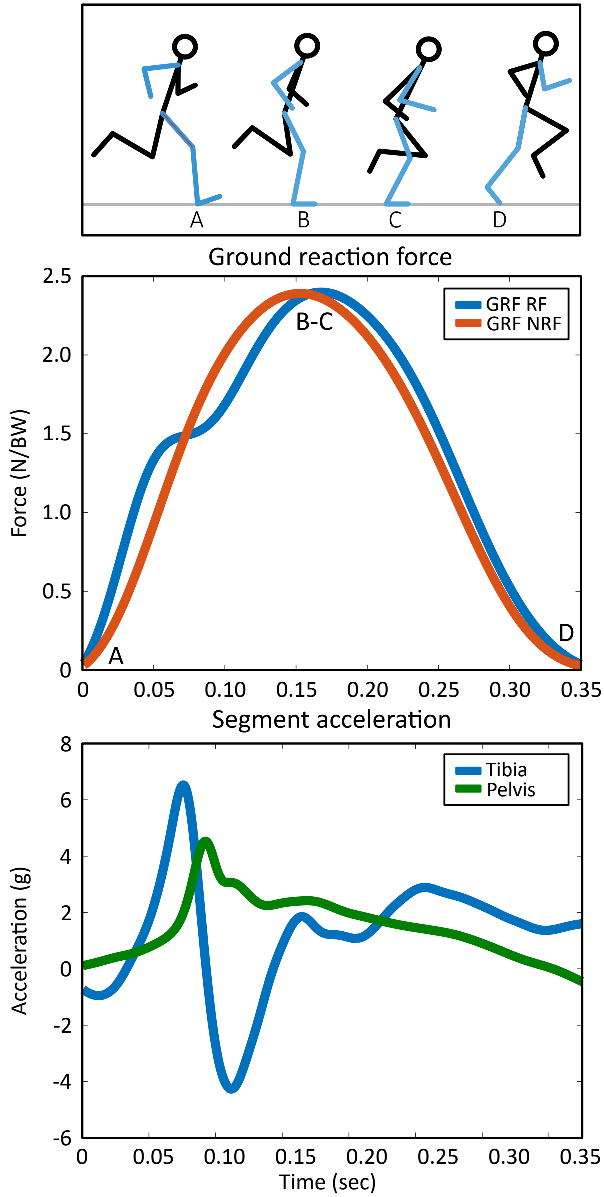

Figure 1.2: *Forces and accelerations during the stance phase of running. Top figure: Visualization of a rearfoot (RF) striking runner at A) initial contact, B-C) midstance, D) toe-off. Central figure: Vertical ground reaction forces (GRF) during the stance phase of running for a RF and non-rearfoot (NRF) striking runner. Letters refer to the gait events presented in the top figure. Bottom figure: Acceleration in the superior direction of the tibia and pelvis segments during the stance phase of running. N = Newton, BW = body weight, GRF = vertical ground reaction force, RF = rearfoot striking runner, NRF = non-rearfoot striking runner, g = gravitational acceleration.*

PTA is one of the most popular quantities to measure when analyzing running gait with IMUs [33]. PTA is often considered a proxy measure for impact forces experienced at the tibia [19]. Higher impact forces are assumed to represent more tibial bone loading and increase the risk of particularly tibial microfractures [34]. Without sufficient rest and recovery, these microfractures result in tibial stress fractures [35]. Prospective preliminary data suggests that runners with a tibial stress fracture tended to have higher PTA values than healthy matched controls before they got injured [36]. Multiple studies found higher PTA values in injured compared to uninjured runners [16,37] and in injured compared to uninjured legs [38]. In some studies, PTA increased with running-induced fatigue, which is thought to reflect an increased injury risk due to higher loads on the body [29,39,40]. PTA is incorporated in multiple commercial products for runners [41–43] and is used as a bio-feedback variable to change the running pattern of runners with high PTA values, with the idea of decreasing their risk of injuries [44–46]. However, tibial bone loading is not only caused by impact forces but is a summation of the (effect of) impact forces and compressive forces from muscle contractions [47,48]. The effect of impact forces compromises no more than 18% of the total tibial compression forces during the stance phase, while muscle contractions of the calf muscles make up 82% [47]. The small contribution of impact-related quantities to tibial compression forces questions the widespread scientific and commercial use of PTA and its assumed relationship with tibial bone loading.

> Research Question **Chapter 3**
> How to quantify and correct for the subject-specific effects of changes in running speed and stride frequency on impact-related running mechanics during a fatiguing outdoor run?

From the laboratory to the outside world

Running kinematics and the effect of running-induced fatigue on running kinematics is typically measured in a laboratory setting with optoelectronic systems while running on a treadmill [49–52]. Such a controlled environment allows researchers to eliminate or minimize the effects of possible confounding factors, such as running speed [53], running surface [54], and inclination [55]. However, these measurements have many downsides, such as an imposed running speed, long processing times, and marker occlusion, which limits the calculation of kinematics. But most importantly, there is no evidence that changes in running kinematics due to fatigue in a controlled environment are similar to those in an uncontrolled environment.

Treadmill running induces more regularity, less variability, and more significant constraints than overground running [56,57]. These differences could result in a poor agreement for multiple kinematic quantities between running in a constrained and unconstrained environment [58]. PTA was shown to differ between treadmill and track running on multiple occasions [54,59]. There is an increasing amount of evidence suggesting that running gait patterns should be measured in a relatively uncontrolled sport-specific setting [33]. However, while controlled settings have their limitations, new limitations arise for uncontrolled settings. Running speed is typically imposed in treadmill running but tends to decrease towards the end of an outdoor fatiguing protocol [11,60,61]. Running speed and stride frequency significantly influences many aspects of the running gait pattern [53,62]. Changes in running kinematics during a fatiguing protocol in a sport-specific setting can be caused by fatigue or a change in speed or stride frequency. Hence, it is necessary to investigate the effect of running speed and stride frequency on changes in running kinematics during a fatiguing protocol in a sport-specific setting such as a marathon.

> Research Question **Chapter 4**
> What is the strength of the relationship between peak tibial acceleration and maximal tibial compression force in running?

Intermezzo: Inertial Measurement Units (IMUs)

Measuring running-related quantities with wearable sensors is very popular in the scientific world [33]. In the last decade, the experience of "going for a run" has also changed for many recreational runners. Runners are using more and more technology to track their progress [63]. In 2014, 86% of competitive half marathon runners reported using a device to monitor how they ran the previous year [64]. Global positioning system (GPS) based devices (e.g., mobile phones and sports watches) are the most popular and can be used to monitor training load. GPS-based devices allow runners to analyze how far, how fast, and how often they run. However, they do not provide information about running biomechanics and injury risks related to running biomechanics. Wearable sensors such as inertial measurement units (IMUs) are affordable and relatively easy to use. IMUs are suitable for monitoring running biomechanics in a sport-specific environment for scientists, competitive and recreational runners.

IMUs consist of three-dimensional (3D) accelerometers and 3D rate gyroscopes and are often combined with 3D magnetometers. These sensors measure the total acceleration (including gravity), angular velocity, and magnetic field in a sensor-fixed coordinate system, respectively. Sensor orientation can be computed through strapdown inertial navigation based on numerical integration of the angular velocity. However, this process is prone to integration drift [65]. Alternatively, data from the rate gyroscope can be combined with accelerometer and magnetometer data for inclination (orientation with respect to vertical) and heading information and be used as input for sensor fusion algorithms to estimate sensor orientation in an Earth-fixed coordinate system (for example [66]). With the orientation of a sensor in an Earth-fixed coordinate system, sensor total acceleration (including gravity) can be rotated from a sensor-fixed to an Earth-fixed coordinate system, in which the gravity component of the total acceleration measured by the accelerometer is always in the same direction. Subtracting gravity from the acceleration signal in the Earth-fixed coordinate system results in the free acceleration, which can be integrated once to obtain change in velocity or twice to obtain change in position. Also these integration operations are prone to drift, which can be reduced by applying supplementary distance measurements or assumptions about the performed movements.

In motion analysis, we are typically interested in data expressed in a coordinate system with functional meaning. Depending on the orientation of a sensor on a body segment, a sensor coordinate system may not have functional meaning while a segment coordinate system is designed to have functional meaning. For example, for the tibia, the first axis of the segment coordinate system can be chosen to be directed in the longitudinal direction of the tibia bone while a second axis can be perpendicular to the flexion-extension rotation axis of the tibia during walking or running. The sensor signals that are measured in the sensor coordinate system can be expressed in the chosen segment coordinate system through a process called sensor-to-segment calibration. When time-synchronized segment orientations of two linked body segments are available, the 3D joint angle between these segments can be computed.

How to measure in the outside world?

Data from IMUs can be used directly (e.g., PTA), or quantities can be computed following multiple processing steps based on the sensor output. For many kinematic quantities of interest, the orientation of body segments is required, such as the orientation of the foot and lower leg at initial contact or for computation of joint angles throughout the gait cycle [29,50,52]. Currently, sensor orientation estimation often relies on the integration of sensor angular velocities. This process is prone to errors and is typically combined with sensor fusion and error modeling, as demonstrated in extended Kalman filtering [67]. Drift reduction and orientation estimation become more challenging during highly dynamic movements or prolonged measurements [67]. Additionally, sensor orientation estimation often relies on extensive calibration procedures and multi-sensor setups. An alternative for Kalman filtering is to use domain-specific assumptions about the movement of interest to correct for drift in orientation estimation. A well-known example is the zero-velocity update method in walking [68]. The foot is assumed to be horizontal and to have zero velocity during the stance phase. This assumption allows for drift corrections in orientation estimation since the foot's orientation during the stance phase is known.

However, these assumptions are not necessarily fulfilled in running. The stance phase in running is short, and runners with a forefoot strike do not always reach a fully horizontal foot position during the stance phase. The difficulties in estimating foot orientations in running through existing domain-specific assumptions make it even harder to estimate orientations of more proximal segments, such as the tibia, as these do not have zero-velocity points. Since running is a quasi-cyclical motion, a new set of domain-specific assumptions based on quasi-cyclical motions can be created to estimate sensor orientation and displacement without many of the previously stated drawbacks.

> Research Question **Chapter 5**
> Can the cyclical nature of running be used to acquire drift-free 3D orientation of a body segment using a single gyroscope?

> Research Question **Chapter 6**
> How to estimate 3D orientation and displacement of a single IMU on the lower leg using the quasi-cyclical nature of running?

General aims and outline of the thesis

This thesis aims to increase our understanding of running biomechanics as measured in and outside the laboratory and explore the challenges regarding wearable motion analysis during running in a sport-specific setting.

Based on this general aim, this thesis aims to answer the following research questions:

Chapter 2 How do running kinematics change due to running-induced fatigue?

Chapter 3 How to quantify and correct for the subject-specific effects of changes in running speed and stride frequency on impact-related running mechanics during a fatiguing outdoor run?

Chapter 4 What is the strength of the relationship between peak tibial acceleration and maximal tibial compression force in running?

Chapter 5 Can the cyclical nature of running be used to acquire drift-free 3D orientation of a body segment using a single gyroscope?

Chapter 6 How to estimate 3D orientation and displacement of a single IMU on the lower leg using the quasi-cyclical nature of running?

Finally, the results of the presented studies and possibilities for future research are discussed in **Chapter 7**.

References

1. Wendel-Vos, W. Sport en Bewegen in cijfers. https://www.sportenbewegenincijfers.nl/kernindicatoren/sportdeelname-wekelijks (2022).
2. Duijvestijn, M., T. Schurink, T., Berg, S. van den, S. Euser, S. & Wendel-Vos, W. RIVM 2021-0117 Sport en beweeggedrag in 2020. (2021).
3. Lee, D. et al. Running as a Key Lifestyle Medicine for Longevity. Prog. Cardiovasc. Dis. 1–11 (2017) doi:10.1016/j.pcad.2017.03.005.
4. Arnold, M. J. & Moody, A. L. Common Running Injuries: Evaluation and Management. Am. Fam. Physician 97, 510–516 (2018).
5. Van Gent, R. N. et al. Incidence and determinants of lower extremity running injuries in long distance runners: A systematic review. Br. J. Sports Med. 41, 469–480 (2007).
6. Willems, T. M., Witvrouw, E., De Cock, A. & De Clercq, D. Gait-related risk factors for exercise-related lower-leg pain during shod running. Med. Sci. Sports Exerc. 39, 330–339 (2007).
7. Nielsen, R. O. et al. Training errors and running related injuries: a systematic review. Int J Sport. Phys Ther 7, 58–75 (2012).
8. Vannatta, C. N., Heinert, B. L. & Kernozek, T. W. Biomechanical risk factors for running-related injury differ by sample population: A systematic review and meta-analysis. Clin. Biomech. 75, 104991 (2020).
9. Messier, S. P. et al. A 2-Year Prospective Cohort Study of Overuse Running Injuries: The Runners and Injury Longitudinal Study (TRAILS). Am. J. Sports Med. 46, 2211–2221 (2018).
10. Aruin, A. S. Biomechanics. Brittanica.
11. Ruder, M., Jamison, S. T., Tenforde, A., Mulloy, F. & Davis, I. S. Relationship of Foot Strike Pattern and Landing Impacts during a Marathon. Med. Sci. Sports Exerc. 51, 2073–2079 (2019).
12. de Ruiter, C. J., van Daal, S. & van Dieën, J. H. Individual optimal step frequency during outdoor running. Eur. J. Sport Sci. 20, 182–190 (2020).
13. Hunter, I. & Smith, G. A. Preferred and optimal stride frequency, stiffness and economy: Changes with fatigue during a 1-h high-intensity run. Eur. J. Appl. Physiol. 100, 653–661 (2007).
14. Cavanagh and Lafortune, M. A. GRF in distance running. J. Biomech. 13, 397–406 (1980).

15. Gerritsen, K. G. M., Bogert, A. J. Van Den & Nigg, B. M. Direct dynamics simulation of the impact phase in heel-toe running. J. Biomech. 28, 661–666 (1995).
16. Milner, C. E., Ferber, R., Pollard, C. D., Hamill, J. & Davis, I. S. Biomechanical Factors Associated with Tibial Stress Fracture in Female Runners. 323–328 (2006) doi:10.1249/01.mss.0000183477.75808.92.
17. Hreljac, A. Etiology, prevention, and early intervention of overuse injuries in runners: A biomechanical perspective. Phys. Med. Rehabil. Clin. N. Am. 16, 651–667 (2005).
18. Schmitz, A., Pohl, M. B., Woods, K. & Noehren, B. Variables during swing associated with decreased impact peak and loading rate in running. J. Biomech. 47, 32–38 (2014).
19. Sheerin, K. R., Reid, D. & Besier, T. F. The measurement of tibial acceleration in runners—A review of the factors that can affect tibial acceleration during running and evidence-based guidelines for its use. Gait Posture 67, 12–24 (2019).
20. Van den Berghe, P., Six, J., Gerlo, J., Leman, M. & De Clercq, D. Validity and reliability of peak tibial accelerations as real-time measure of impact loading during over-ground rearfoot running at different speeds. J. Biomech. 86, 238–242 (2019).
21. Reenalda, J., Maartens, E., Homan, L. & Buurke, J. H. Continuous three dimensional analysis of running mechanics during a marathon by means of inertial magnetic measurement units to objectify changes in running mechanics. J. Biomech. 49, 3362–3367 (2016).
22. Abt, J. P. et al. Running kinematics and shock absorption do not change after brief exhaustive running. J. Strength Cond. Res. 25, 1479–1485 (2011).
23. Pozzo, T., Berthoz, A. & Lefort, L. Head stabilization during various locomotor tasks in humans. Exp. Brain Res. 82, 97–106 (1990).
24. Voloshin, A. S., Mizrahi, J., Verbitsky, O. & Isakov, E. Dynamic loading on the human musculoskeletal system effect of fatigue. Clin. Biomech. 13, 515–520 (1998).
25. Novacheck, T. F. The biomechanics of running. Gait Posture 7, 77–95 (1998).
26. Lafortune, M. A., Lake, M. J. & Hennig, E. M. Differential shock transmission response of the human body to impact severity and lower limb posture. J. Biomech. 29, 1531–1537 (1996).
27. Hreljac, A. Impact and Overuse Injuries in Runners. Med. Sci. Sports Exerc. 36, 845–849 (2004).
28. Derrick, T. R., Dereu, D. & Mclean, S. P. Impacts and kinematic adjustments during an exhaustive run. Med. Sci. Sports Exerc. 34, 998–1002 (2002).

29. Reenalda, J., Maartens, E., Buurke, J. H. & Gruber, A. H. Kinematics and shock attenuation during a prolonged run on the athletic track as measured with Inertial Magnetic Measurement Units Type of Submission. Gait Posture 68, 155–160 (2018).

30. Valiant, G. A. Transmission and attenuation of heelstrike accelerations. (Human Kinetics Publishers, Champaign, IL, 1990).

31. Romani, W. A., Gieck, J. H., Perrin, D. H., Saliba, E. N. & Kahler, D. M. Mechanisms and management of stress fractures in physically active persons. J. Athl. Train. 37, 306–314 (2002).

32. Moen, M. H., Tol, J. L., Weir, A., Steunebrink, M. & Winter, de T. C. Medial tibial stress syndrome- A critical review. Sport. Med. 39, 523–546 (2009).

33. Benson, L. C., Räisänen, A. M., Clermont, C. A. & Ferber, R. Is This the Real Life, or Is This Just Laboratory? A Scoping Review of IMU-Based Running Gait Analysis. Sensors 22, 1–38 (2022).

34. Milgrom, C. et al. Do high impact exercises produce higher tibial strains than running? Br. J. Sports Med. 34, 195–199 (2000).

35. Harrast, M. A. & Colonno, D. Stress fractures in runners. Clin. Sports Med. 29, 399–416 (2010).

36. Davis, I., Milner, C. E. & Hamill, J. Does increased loading during running lead to tibial stress fractures? A prospective study. S58 (2004).

37. Pohl, M. B., Mullineaux, D. R., Milner, C. E., Hamill, J. & Davis, I. S. Biomechanical predictors of retrospective tibial stress fractures in runners. 41, 1160–1165 (2008).

38. Zifchock, R. A., Davis, I., Higginson, J., McCaw, S. & Royer, T. Side-to-side differences in overuse running injury susceptibility: A retrospective study. Hum. Mov. Sci. 27, 888–902 (2008).

39. Lucas-Cuevas, A. G. et al. Effect of 3 Weeks Use of Compression Garments on Stride and Impact Shock during a Fatiguing Run. Int. J. Sports Med. 36, 826–831 (2015).

40. Mizrahi, J., Verbitsky, O. & Isakov, E. Fatigue-related loading imbalance on the shank in running: a possible factor in stress fractures. Ann. Biomed. Eng. 28, 463–469 (2000).

41. Runscribe. https://runscribe.com/metrics/.

42. TgForce 3D. https://tgforce.com/about-tibial-shock/.

43. Moov now. https://welcome.moov.cc/.

44. Clansey, A. C., Hanlon, M., Wallace, E. S., Nevill, A. & Lake, M. J. Influence of Tibial shock feedback training on impact loading and running economy. Med. Sci. Sports Exerc. 46, 973–981 (2014).

45. Crowell, H. P., Milnert, C. E., Hamill, J. & Davis, I. S. Reducing impact loading during running with the use of real-time visual feedback. J. Orthop. Sports Phys. Ther. 40, 206–213 (2010).
46. Crowell, H. P. & Davis, I. S. Gait retraining to reduce lower extremity loading in runners. Clin. Biomech. 26, 78–83 (2011).
47. Scott, S. H. & David, A. W. Internal forces at chronic running injury sites. Med. sci 22, 357–369 (1990).
48. Matijevich, E. S., Branscombe, L. M., Scott, L. R. & Zelik, K. E. Ground reaction force metrics are not strongly correlated with tibial bone load when running across speeds and slopes: Implications for science, sport and wearable tech. PLoS One 14, 1–19 (2019).
49. Siler, W. L. & Martin, P. E. Changes in Running Pattern during a Treadmill Run to Volitional Exhaustion: Fast versus Slower Runners. Int. J. Sport Biomech. 7, 12–28 (1991).
50. Paquette, M. R., Milner, C. E. & Melcher, D. A. Foot contact angle variability during a prolonged run with relation to injury history and habitual foot strike pattern. Scand. J. Med. Sci. Sport. 27, 217–222 (2017).
51. Koblbauer, I. F., van Schooten, K. S., Verhagen, E. A. & van Dieën, J. H. Kinematic changes during running-induced fatigue and relations with core endurance in novice runners. J. Sci. Med. Sport 17, 419–424 (2014).
52. Maas, E., De Bie, J., Vanfleteren, R., Hoogkamer, W. & Vanwanseele, B. Novice runners show greater changes in kinematics with fatigue compared with competitive runners. Sport. Biomech. 17, 350–360 (2018).
53. Orendurff, M. S. et al. A little bit faster: Lower extremity joint kinematics and kinetics as recreational runners achieve faster speeds. J. Biomech. 71, 167–175 (2018).
54. García-Pérez, J. A., Pérez-Soriano, P., Llana Belloch, S., Lucas-Cuevas, Á. G. & Sánchez-Zuriaga, D. Effects of treadmill running and fatigue on impact acceleration in distance running. Sport. Biomech. 13, 259–266 (2014).
55. Mizrahi, J., Verbitsky, O. & Isakov, E. Fatigue-induced changes in decline running. Clin. Biomech. 16, 207–212 (2001).
56. Benson, L. C., Clermont, C. A. & Ferber, R. New Considerations for Collecting Biomechanical Data Using Wearable Sensors: The Effect of Different Running Environments. Front. Bioeng. Biotechnol. 8, 1–8 (2020).

57. Lindsay, T. R., Noakes, T. D. & Mcgregor, S. J. Effect of treadmill versus overground running on the structure of variability of stride timing. Percept. Mot. Skills 118, 331–346 (2014).

58. Lafferty, L. et al. Clinical Indoor Running Gait Analysis May Not Approximate Outdoor Running Gait Based on Novel Drone Technology. Sports Health 1–7 (2021) doi:10.1177/19417381211050931.

59. Milner, C. E., Hawkins, J. L. & Aubol, K. G. Tibial acceleration during running is higher in field testing than indoor testing. Med. Sci. Sports Exerc. 52, 1361–1366 (2020).

60. Chan-Roper, M., Hunter, I., Myrer, J. W., Eggett, D. L. & Seeley, M. K. Kinematic changes during a marathon for fast and slow runners. J. Sport. Sci. Med. 11, 77–82 (2012).

61. Nicol, C., Komi, P. V. & Marconnet, P. Effects of marathon fatigue on running kinematics and economy. Scand. J. Med. Sci. Sports 1, 195–204 (1991).

62. Busa, M. A., Lim, J., Van Emmerik, R. E. A. & Hamill, J. Head and tibial acceleration as a function of stride frequency and visual feedback during running. PLoS One 11, 1–13 (2016).

63. Kuru, A. Exploring Experience of Runners with Sports Tracking Technology. Int. J. Hum. Comput. Interact. 32, 847–860 (2016).

64. Janssen, M., Scheerder, J., Thibaut, E., Brombacher, A. & Vos, S. Who uses running apps and sports watches? Determinants and consumer profiles of event runners' usage of running-related smartphone applications and sports watches. PLoS One 12, 1–17 (2017).

65. Woodman, O. J. An introduction to inertial navigation. Tech. Rep. Univ. Cambridge (2007) doi:10.4271/2000-01-0305.

66. Luinge, H. J. & Veltink, P. H. Measuring orientation of human body segments using miniature gyroscopes and accelerometers. Med. Biol. Eng. Comput. 43, 273 – 282 (2005).

67. Sabatini, A. M. Estimating three-dimensional orientation of human body parts by inertial/magnetic sensing. Sensors 11, 1489–1525 (2011).

68. Park, S. K. & Suh, Y. S. A zero velocity detection algorithm using inertial sensors for pedestrian navigation systems. Sensors 10, 9163–9178 (2010).

Chapter 2

Effects of level running-induced fatigue on running kinematics

A systematic review and meta-analysis

Published as:
Zandbergen, M.A., Marotta, L., Bulthuis, R., Buurke, J.H., Veltink, P.H., Reenalda, J. Effects of level running-induced fatigue on running kinematics: A systematic review and meta-analysis. Gait & Posture, 99, 60-75 (2023).

Abstract

Background: Runners have a high risk of acquiring a running-related injury. Understanding the mechanisms of impact force attenuation into the body when a runner fatigues might give insight into the role of running kinematics on the aetiology of overuse injuries.

Research questions: How do running kinematics change due to running-induced fatigue? And what is the influence of experience level on changes in running kinematics due to fatigue?

Methods: Three electronic databases were searched: PubMed, Web of Science, and Scopus. This resulted in 33 articles and 19 kinematic quantities being included in this review. A quality assessment was performed on all included articles and meta-analyses were performed for 18 kinematic quantities.

Results and significance: Main findings included an increase in peak acceleration at the tibia and a decrease in leg stiffness after a fatiguing protocol. Additionally, level running-induced fatigue increased knee flexion at initial contact and maximum knee flexion during swing. An increase in vertical centre of mass displacement was found in novice but not in experienced runners with fatigue. Overall, runners changed their gait pattern due to fatigue by moving to a smoother gait pattern (i.e., more knee flexion at initial contact and during swing, decreased leg stiffness). However, these changes were not sufficient to prevent an increase in peak accelerations at the tibia after a fatigue protocol. Large inter-individual differences in responses to fatigue were reported. Hence, it is recommended to investigate changes in running kinematics as a result of fatigue on a subject-specific level since group-level analysis might mask individual responses.

Introduction

Running is a popular sport worldwide. With up to 79% of runners acquiring a running-related injury in the lower extremity, runners are likely to get injured [1]. Most injuries are overuse related and assumed to be caused by training load errors (i.e., too fast and too far) and running kinematics [2–4]. During running, the body repetitively endures high-impact forces caused by the feet colliding with the ground. High impact forces on the body and changes in attenuation of these forces with fatigue are expected to result in overuse-related injuries such as tibial stress fractures [5].

Understanding the mechanisms of impact force attenuation into the body when a runner fatigues might give insight into the role of running kinematics on the etiology of overuse injuries. Running kinematics largely influence peak impact forces during running [6–9], possibly by modulating the stiffness of the lower body. Peak accelerations of body segments during running are mostly caused by impact forces and can be used as measures for loading on the body. Peak accelerations can quantify how well the body can attenuate impact forces [10]. A general idea is that higher peak accelerations due to fatigue indicate a higher load on the body and therefore increase the risk of overuse injuries, although this relationship needs further investigation [11,12]. Multiple studies showed an increase in peak accelerations and change in joint angles due to running-induced fatigue, although there is not yet a consensus about the exact effect of fatigue on peak accelerations and joint angles in running [13–15].

The effect of fatigue on running kinematics was previously investigated in three literature reviews. Winter et al. [16] summarized the effects of fatigue on kinematics and kinetics during overground running, while Kim et al. [17] summarized the effects of fatigue on foot plantar pressure and associated kinematic quantities. Apte et al. [18] investigated the effect of fatigue, the severity of fatigue, and the influence of running surfaces on a total of 42 quantities. From these literature reviews, it can be concluded that the maximal vertical ground reaction force ($F_{z,max}$) generally decreases after a fatigue protocol. Spatiotemporal changes with fatigue were dependent on the running surface, and plantar pressure measurements showed that the loading under the metatarsal area was increased after a fatigue protocol. Winter et al. [16], Kim et al. [17] and Apte et al. [18] concluded that it was difficult to compare kinematic results from studies due to small numbers of studies investigating some quantities, differences in subject characteristics (i.e., experience level, familiarity with fatigue protocols, lack of information) and fatigue protocols (i.e., speed, duration, stopping criteria). All three of these literature

reviews do not give us insight into the amount of change in kinematic quantities to expect after a fatiguing protocol. Additionally, Apte et al. [18] mentioned that combining results of runners with different skill levels might lead to confounding effects. Hence, there is a need for a systematic literature review in combination with meta-analyses on the effect of running-induced fatigue on running kinematics, which also takes subject characteristics into account.

The primary aim of this study was therefore to provide an overview of kinematic changes due to running-induced fatigue. The secondary aim was to investigate the influence of experience level on kinematic changes with fatigue.

Many quantities related to running biomechanics have been proposed in the literature. This review focussed on a selection of intertwined quantities related to peak accelerations and shock attenuation because of the assumed link with the development of running-related injuries [11,12]. Quantities included in this review were:

- Peak accelerations
- Shock attenuation
- Vertical and leg stiffness
- Vertical COM displacement (ΔCOM_z)
- Lower body joint angles

It is hypothesized that fatigued runners adopt a stiffer gait pattern to save energy [19], at the cost of higher impact forces on the body. A stiffer gait pattern would result in increased peak accelerations, decreased shock attenuation, decreased ΔCOM_z and decreased joint flexion angles. Experienced runners are hypothesized to show smaller changes in kinematics due to fatigue since they are more familiar with, and accustomed to, running-induced fatigue.

Methods

Search strategy

For this systematic review, three electronic databases were searched: PubMed, Web of Science, and Scopus. The search terms used can be found in Table 2.1, and the search strings can be found in Appendix 2.A. The first literature search was performed in May 2019 (without time constraints), the literature search was repeated in April 2020 (period: 2019-01-01 till 2020-12-31) to ensure no relevant new studies were missing.

Selection criteria

Two researchers independently performed a screening of titles, abstracts, and full-text articles. Disagreements between researchers were solved in a consensus meeting with a third independent researcher when necessary. For a more homogeneous literature review, only studies investigating runners (i.e., people engaging in running-related activities) without injuries and continuously running on a relatively flat surface for a minimum of 3 km were included. A minimum distance of 3 km was chosen to impose a lower threshold for the fatigue protocol and to comply with the definition of long-distance running [21]. To exclude the effect of running speed on running kinematics, only studies in which the running speed during the pre-and post-fatigue measurement was controlled or intended to be similar were included. Exclusion criteria are provided in Table 2.2.

Table 2.1: *Search terms*

Keywords for inclusion
(run OR running OR runner* OR marathon)
AND
(exhaust* OR exert* OR prolong* OR fatigue*)
AND
(kinemat* OR kinet* OR biomechanic* OR mechanic* OR acceler* OR centre of mass OR centre of mass OR center of gravity OR centre of gravity OR ground reaction OR angle OR angular OR force OR moment* OR impact OR shock OR inertia* OR pressure)

Table 2.2: *Exclusion criteria*

Exclusion criteria
• Runners (i.e., people engaging in running-related activities) were not the main subject group
• Runners were injured shortly before or at the time of measurement (healthy control groups were included)
• The fatigue protocol did not satisfy all of the following conditions:
- Minimum distance covered of 3 km
- Continuous running (no interval training)
- Relatively flat surface (no uphill/downhill running, 1% inclination on a treadmill was allowed)
- No imposed step frequency/strike pattern
- Speed during pre- and post-fatigue measurement was controlled/intended to be similar
• No quantities of interest were measured at two time points (pre- & post-fatigue): Exclude if simulations were performed based on a model about fatigue
• The aim of the study was the effect of footwear (including insoles) on the gait pattern
• No full-text article in English was available

Quality assessment

To assess the quality of included studies, 13 out of the 27 questions from the Downs and Black quality assessment checklist [20] were used, resulting in a maximal quality score of 14, see Table 2.3. A description for all included questions and a justification for all excluded questions, and a change in scoring for one question are provided in Appendix 2.B. Quality labels based on the quality score were based on Hooper et al. [22]. A score between 0 and 7 points indicated a study of “Poor” quality, a score of 8 or 9 a study of “Fair” quality, a score of 10 till 12 a study of “Good” quality and a score of 13 or 14 a study of “Excellent” quality.

Table 2.3: *Quality assessment items. Questions for the quality assessment were adapted from the Downs and Black quality assessment checklist [20] and kept the original numbering (first column). A more extensive description of the quality assessment questions and all alterations to the original Downs and Black quality assessment checklist can be found in Appendix 2.B. UTD = unable to determine.*

Quality assessment items		
#	Question	Scoring
Q1	Is the hypothesis/aim/objective of the study clearly described?	0/1
Q2	Are the main outcomes to be measured clearly described in the Introduction or Methods section?	0/1
Q3	Are the characteristics of the subjects included in the study clearly described?	0/1
Q4	Is the fatigue protocol clearly described?	0/1
Q6	Are the main findings of the study clearly described?	0/1
Q7	Does the study provide estimates of the random variability in the data for the main outcomes?	0/1
Q10	Have actual probability values been reported (e.g. 0.035 rather than <0.05) for the main outcomes except where the probability value is less than 0.001?	0/1
Q11	Were the subjects asked to participate in the study representative of the entire population from which they were recruited?	0/1/UTD
Q13	Was the setting of the fatiguing protocol representative for a typical run?	0/1/UTD
Q16	If any of the results of the study were based on “data dredging”, was this made clear?	0/1/UTD
Q18	Were the statistical tests used to assess the main outcomes appropriate?	0/1/UTD
Q20	Were the main outcome measures used accurate (valid and reliable)?	0/1/UTD
Q27	Did the study have sufficient power to detect a clinically important effect where the probability value for a difference being due to chance is less than 5%?	0/1/2/UTD

Quantities of interest

Quantities of interest for this review were related to peak accelerations and shock attenuation in running. To prevent general conclusions based on a small number of findings, only quantities that were investigated in a minimum of two studies were included.

- **Peak accelerations:** Maximum amplitude in the acceleration signal in the axial direction of a body segment (i.e., approximately upward in neutral standing).
  - Peak tibial acceleration
  - Peak sacral acceleration
  - Peak head acceleration

- **Shock attenuation:** Percent reduction in peak acceleration between a distal and proximal location on the body (Equation 2.1).
  - Shock attenuation between the tibia and head
  - Shock attenuation between the tibia and sacrum

$$shock\ attenuation = \left(1 - \frac{Peak\ proximal\ acceleration}{Peak\ distal\ acceleration}\right) * 100 \tag{2.1}$$

- **Vertical and leg stiffness:** Ratio between the peak vertical ground reaction force $(F_{z,max})$ and a measure of compression of the lower body during the stance phase.
  - Vertical stiffness (K_{vert}) (Equation 2.2): Ratio between $F_{z,max}$ and the maximum COM displacement in de stance phase $(\Delta COM_{z,stance})$ [23]
  - Leg stiffness (K_{leg}) (Equation 2.3): Ratio between $F_{z,max}$ and the maximum estimated leg compression in the stance phase (ΔL_{stance}) [24]

$$K_{vert} = \frac{F_{z,max}}{\Delta COM_{z,stance}} \tag{2.2}$$

$$K_{leg} = \frac{F_{z,max}}{\Delta L_{stance}} \tag{2.3}$$

- **Vertical COM displacement** (ΔCOM_z)**:** Maximal vertical COM displacement during either the stance phase or full gait cycle.

- **Lower body joint angles:** Sagittal plane joint angles of the lower body. Joint angles in the transversal and frontal plane were excluded because their range of motion (ROM) in running is small, while they have a relatively large measurement error [25].
  - Ankle dorsi-/plantarflexion angle
  - Knee flexion/extension angle
  - Hip flexion/extension angle

Data extraction

For all quantities of interest, initial (i.e., unfatigued) and final (i.e., fatigued) values were extracted. Obtained data were converted to the same units and recalculated to describe joint angles similarly. When absolute values were not provided, these were estimated from figures using WebPlot Digitizer (Web Plot Digitizer, version 4.5, USA) by two researchers; differences were solved in a consensus meeting. When a study was described in multiple articles, results of the study were included once, although methodological information was extracted from all articles. If two out of three quantities of speed, distance, and time were provided, the third was computed. Additional information about subject characteristics, fatigue protocols, rate of perceived exertion (RPE) [26], measurement systems, and data analyses were extracted from all included articles.

Data analysis

To investigate the effect of fatigue on kinematic quantities, multiple meta-analyses were performed. When absolute initial and final values or the mean difference (MD) for a quantity were provided for two or more studies, a random-effects meta-analysis was performed using the Metafor statistical package in R software (version 4.2.0, R Foundation for Statistical Computing). MDs (fatigued versus unfatigued) were weighted based on their inverse variance. 95% Confidence intervals (CI) of MDs were computed based on p-values when provided. Otherwise, the standard deviation (SD) of the fatigued measurement was used as the SD of the MD [27,28]. P-values provided as "$p < 0.05$" or similar were assumed to be equal to the right-hand operand of the inequality sign. P-values provided as "$p > 0.05$" were treated as if no p-value was provided. In the case of repeated measures analysis of variance, only p-values from post hoc tests between the first and last stage of running, and not from main effects, were used to calculate CI. When a study provided data for multiple independent subgroups, both groups were included for analysis. In the case of dependent subgroups (same runners on different undergrounds [29] or data from both legs [30]), the subgroup most similar to the conditions of all other studies was included for analysis. The percentage variation in estimated pooled effects due to differences between studies rather than chance (i.e., heterogeneity) was estimated using I^2 (I^2<25 was considered small, I^2 = 25-49% as moderate and $I^2 \geq$ 50% as high) [31]. High heterogeneity is an indication that the results of studies are inconsistent, for instance, due to differences in the fatigue protocol or subject characteristics. Statistical significance was defined as $p < 0.05$.

Results

An overview of the literature search process is shown in Figure 2.1. Details about the subject characteristics, fatigue protocols, measurement systems, and data analyses can be found in Table 2.4. The mean quality assessment score was 10 (SD: 1, range: 6-12) out of 14, indicating an overall good quality. Heterogeneity was high for most kinematic quantities, indicating that the variation in results between studies is larger than expected by chance [31]. All quality assessment scores can be found in Table 2.5. Results for all included quantities are presented in Table 2.6 and Table 2.7, where single values between parentheses represent SDs [32–58].

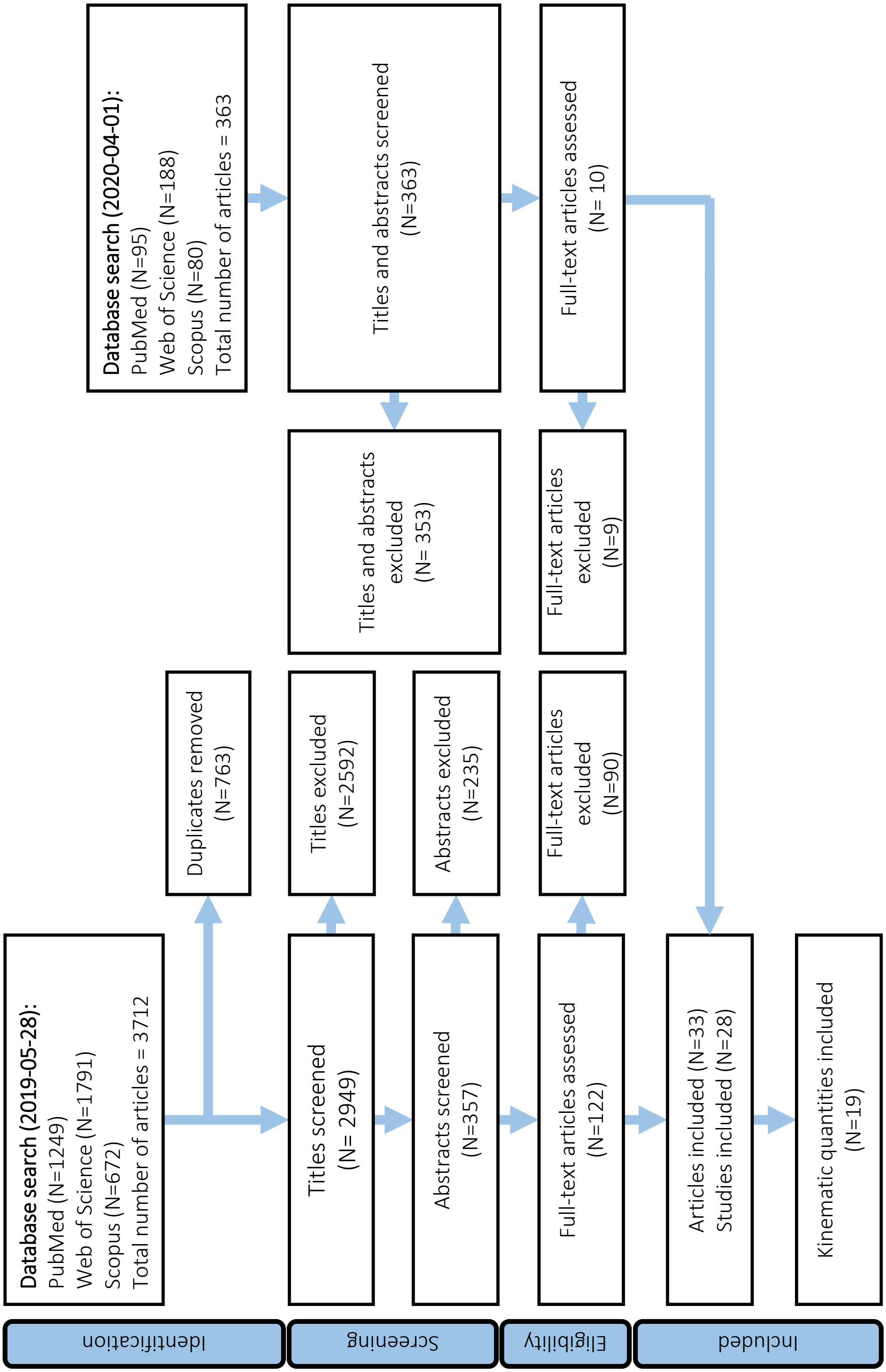

Figure 2.1: *Flow diagram of the literature search process.*

2

Table 2.4: *Study characteristics for all included studies. "Measure" and "Fatigue" refer to a different setting or speed for the measurement and the fatigue protocol. An asterisk (*) indicates that results were not included for meta-analyses. NP = not provided; M = male; F = female; nov = novice runners; com = competitive runners; rec = recreational runners; PTA = peak tibial acceleration; PSA = peak sacral acceleration; PHA = peak head acceleration; COM = centre of mass; FCA = foot contact angle; IMU = inertial measurement unit; uni = unilateral; bil = bilateral; IC = initial contact; MS = midstance; TO = toe-off; cal. = calibration only; IQR = inter quartile range; HR = heart rate; HRmax = maximum HR; VO2max = maximum rate of oxygen consumption; VVO2max = running speed at VO2max; VO2peak = surrogate of VO2max measured during a submaximal exercise; PETCO2 = end tidal carbon dioxide pressure; RPE = rate of perceived exertion.*

1/7	**Abt et al.** [32]	**Avogadro et al.** [33]	**Bazett-Jones et al.** [34]	**Bigelow et al.** [35]
Subject information				
Subject population	Competitive distance runners	Runners or triathletes	Runners or doing running-related activities	Physically active subjects
Subjects (sex), Age (years), Height (cm), Weight (kg)	12 (M+F), 25 (4), 174 (9), 65 (10)	10 (M), 22 (2), 178 (5), 68 (4)	19 (10M+9F), 24 (4), 174 (9), 70 (11)	12, 33 (10), 167 (9), 60 (5)
Training information	Min 3 years, Min 48 km/week, Min 10.7 km/h, No injuries last 3 months	VO2max = 69 (8) ml/kg/min, VVO2max = 18.2 km/h	Min 10 (8) hours/week, No injuries last 6 months	Min 6 weeks, Min 3 hours/week, Never had an injury
Fatigue protocol				
Duration protocol	17.8 (5.7) min	13.8 (2.8) min	36.3 (22.7) min	
Measure of fatigue		Lactate + respiratory data	RPE : 16.6 (1.3)	
Other information			RPE matched to patient group	

1/7	Abt et al. [32]	Avogadro et al. [33]	Bazett-Jones et al. [34]	Bigelow et al. [35]
Measurement system				
Specifications: marker model, sampling frequency, location, axes, operating range, weight	Optical: Plug-in Gait, 120 Hz IMU: forehead, proximal tibia, 3D, 1200 Hz, 25 g, 21 gram	Other: treadmill with 3D forceplate, 1000 Hz	Optical: cluster + anatomical (cal.), 200 Hz	IMU: sacrum, 3D, 1000 Hz, 18 g, 55 gram
Data analysis				
When was data collected	During fatigue protocol: First and last minute	During fatigue protocol: Minute 3 and last minute	Separate trials: Before and after fatiguing run	During fatigue protocol: Continuous
Amount of data analysed	2 x 5 seconds	2 x 20 seconds	2 x 5 strides	16 x 400 meter
Uni-/bilateral data	Uni: dominant leg	Bil: data combined	Uni: matched to patient group	NA
Filtering of data	Markers: low-pass 16 Hz		low-pass 12 Hz	
Quantities				
Peak accelerations	PTA, PHA			PSA
Shock attenuation	PTA/PHA			
Stiffness (vertical/leg)		Leg stiffness*		
Vertical COM displacement				
Ankle angles				
Knee angles	max flexion stance		max flexion stance	
Hip angles			max flexion	
Quality assessment	11- Good	8- Fair	11- Good	10- Good

2/7	Clansey et al. [5]	Derrick et al. [13]	Dierks et al. [36,37]	Dutto and Smith [38]
Subject information				
Subject population	Highly trained distance runners	Recreational runners	Recreational runners	Well-trained runners
Subjects (sex), Age (years), Height (cm), Weight (kg)	21 (M), 36 (13), 180 (8), 75 (12)	10, 26 (7), NP, 71 (10)	20 (5M+15F), 23 (6), 170 (10), 63 (9)	15 (11M+4F), 28 (7), NP, 68 (11)
Training information	72 (37) km/week, Free of injuries now	Free of injuries now	25 (10) km/week, Free of injuries now	Min 40 km/week
Fatigue protocol				
Speed based on	3.5 mM blood lactate concentration	3.2 km time trial	Self-selected (typical traning pace)	80% VO2peak
Speed	Measure: relatively constant at 16.2 (0.8) km/h, Fatigue: constant at 13.8 (2.1) km/h	Constant at 12.2 (1.4) km/h	Constant at 9.5 (1.3) km/h	Constant at 14.5 (1.3) km/h
Setting	Measure: overground Fatigue: treadmill	Treadmill	Treadmill	Treadmill
Stopping criteria	Time	Feeling: unable to continue	Feeling: RPE = 17 or HR: >85% of HRmax	Feeling: unable to continue
Distance covered	9.2 km	3.2 km	7.1 km	13.8 km
Duration protocol	40 min	15.7 min	45 (12) min	57 (19) min
Measure of fatigue	RPE: 17.4 (1.5)		RPE: >15	
Other information	Treadmill with 1% inclination		Stopped due to: RPE = 14, HR = 6	

2/7	Clansey et al. [5]	Derrick et al. [13]	Dierks et al. [36,37]	Dutto and Smith [38]
Measurement system				
Specifications: marker model, sampling frequency, location, axes, operating range, weight	Optical: cluster + anatomical (cal.), 200 Hz IMU: forehead, distal tibia, 2D, 1500 Hz, 16 g	IMU: forehead, distal tibia, 1D, 1000 Hz, 1.8 gram Other: electrogoniometer, 1000 Hz	Optical: cluster + anatomical (cal.), 120 Hz IMU: distal tibia, 1D, 1080 Hz	Other: treadmill with 3D forceplate, 1000 Hz
Data analysis				
When was data collected	Separate trials: Before, middle, after	During fatigue protocol: First, middle and last minute	During fatigue protocol: First and last minute	During fatigue protocol: 0, 25, 50, 75, 100% of duration
Amount of data analysed	3 x 6 strides	3 x 16 seconds	2 x 20 strides	5 x 35-40 steps
Uni-/bilateral data		Uni: right leg	Uni: random	Bil: combined
Filtering of data	PHA/PTA: low-pass 30/60 Hz Markers: low-pass 12 Hz	Markers: low-pass 18 Hz	IMU: low-pass 75 Hz Markers: low-pass 8 Hz	
Quantities				
Peak accelerations	PTA, PHA	PTA, PHA	PTA	
Shock attenuation		PTA/PHA		
Stiffness (vertical/leg)				vertical & leg stiffness
Vertical COM displacement				
Ankle angles	IC			
Knee angles	IC + max flexion stance	IC + max flexion stance	max flexion stance	
Hip angles	IC + MS			
Quality assessment	10- Good	9- Fair	10- Good	8- Fair

3/7	Fuhr et al. [39]	García-Pérez et al. [29]	García-Pinillos et al. [40]	Hanley and Mohan [41]
Subject information				
Subject population	Runners	Recreational runners	Trained endurance runners	Competitive distance runners
Subjects (sex), Age (years), Height (cm), Weight (kg)	9 (F), 32 (4), 167 (7), 58 (7)	20 (11M+9F), 34 (8), 172 (8), 64 (8)	22 (M), 34 (8), 176 (4), 71 (6)	15 (M), 32 (7), 178 (7), 65 (7)
Training information	Min 3 years, 10 km: 35-48 min, Free of injuries now	10 (6) years, 50 (18) km/week, 4 (1) days/week, Stated to be healthy	10 km: 37 (1) min, No injuries last 6 months	10 km: 30-35 min, Free of injuries now
Fatigue protocol				
Speed based on	95% of 10 km time trial	85% of 5 min time trial speed	Self-selected (60 min time trial)	103% of 10 km race
Speed	Constant at 13.2 km/h	Measure: constant at 14.4 km/h, Fatigue: constant at 13.7 (1.4) km/h	Measure: constant at 12.0 km/h, Fatigue: Variable around 15.1 (0.6) km/h	Constant at 17.5 (0.6) km/h
Setting	Treadmill	Treadmill	Treadmill	Treadmill
Stopping criteria	Feeling: unable to continue	Time	Time	Distance
Distance covered	10 km	6.9 km	15.1 km	10 km
Duration protocol	45.3 min	30 min	60 min	34.3 min
Measure of fatigue	RPE: 19 (1)		RPE: 19.3 (0.9)	RPE: start 11 (1), end: 18 (3)
Other information		All rearfoot strikers		11 rearfoot strikers + 4 midfoot strikers

3/7	Fuhr et al. [39]	García-Pérez et al. [29]	García-Pinillos et al. [40]	Hanley and Mohan [41]
Measurement system				
Specifications: marker model, sampling frequency, location, axes, operating range, weight	Optical: cluster + anatomical (cal.), 120 Hz	IMU: forehead, proximal tibia, 1D, 100 Hz, 55 g	Optical: OptoGait (for spatiotemporal parameters), 1000 Hz	Other: high speed camera, 250 Hz
Data analysis				
When was data collected	During fatigue protocol: Every 1500 m	Separate trials: Before and after	Separate trials: Before and after	During fatigue protocol: 1.5 and 9.5 km
Amount of data analysed	8 x 5 strides	2 x 3 strides	2 x 3 minutes	2 x 30 seconds
Uni-/bilateral data		Uni: right leg	Bil: combined	Bil: combined
Filtering of data				low-pass 10 Hz
Quantities				
Peak accelerations		PTA, PHA		
Shock attenuation		PTA/PHA		
Stiffness (vertical/leg)			vertical & leg stiffness	
Vertical COM displacement				
Ankle angles				IC + TO
Knee angles	max flexion + max extension			IC
Hip angles	max flexion			IC + TO
Quality assessment	10- Good	9- Fair	9- Fair	11- Good

2

4/7	Jewell et al. [42]	Koblbauer et al. [30]	Lucas-Cuevas et al. [14]	Maas et al. [43]
Subject information				
Subject population	Recreational active runners	Novice runners	Recreational runners	Competitive (com) and novice (nov) runners
Subjects (sex), Age (years), Height (cm), Weight (kg)	14 (8M+6F), 27 (9), 173 (10), 68 (8)	17 (7M+10F), 26 (3), 172 (10), 67 (11)	40 (20M+20F), 28 (6), 173 (10), 68 (10)	30 (com:10M+5F, nov:9M+6F), com: 22 (4), nov: 21 (1), com: 179 (8), nov: 177 (8), com: 64 (6), nov: 69 (6)
Training information	50 (25) km/week, No injuries last year	Max 10 km/run, Max 2-3 runs/week	27 (4) km/week, No injuries last year, No surgery last 3 years	com: 10 (3) years, com: 77 (17) km/week, nov: max 10 km/week, nov: able to do a 3.2 km run, No injuries last 6 months
Fatigue protocol				
Speed based on	Self-selected (able to run 15 but not 20 min)	RPE 13	80% of 5 min time trial	3.2 km time trial
Speed	Constant at 14.0 (2.2) km/h	Constant at 9.4 (5.8) km/h	Constant at 12.6 (1.1) km/h	Constant, com: measure: 12.0 km/h, fatigue: 17.6 (2.1) km/h, nov: measure: 9.9 (1.8) km/h, fatigue: 9.9 (1.8) km/h
Setting	Treadmill	Treadmill	Treadmill	Treadmill
Stopping criteria	Feeling: unable to continue	Feeling: RPE = 17 or HR: >90% of HRmax	Time	Feeling: unable to continue
Distance covered	3.6 km	3.1 km	6.3 km	com: 4.6 km, nov: 4.7 km
Duration protocol	15.4 (2.2) min	19.7 (7.8) min	30 min	com: 15.8 (4.7) min nov: 28.2 (9.8) min
Measure of fatigue	RPE: 18-19		RPE: 17.1 (0.6)	RPE: min 17
Other information	Forefoot strikers		Placebo group included	

4/7	Jewell et al. [42]	Koblbauer et al. [30]	Lucas-Cuevas et al. [14]	Maas et al. [43]
Measurement system				
Specifications: marker model, sampling frequency, location, axes, operating range, weight	Optical: cluster + anatomical + foot model, 200 Hz	Optical: cluster + anatomical probing, 100 Hz	IMU: forehead, proximal tibia, 3D, 500 Hz, 2.5 gram	Optical: cluster + anatomical, 150 Hz
Data analysis				
When was data collected	During fatigue protocol: First and last minute	During fatigue protocol: First and last minute	During fatigue protocol: Every 5th minute	During fatigue protocol: Second and last minute
Amount of data analysed	2 x 5 strides	20 strides	7 x 15 seconds	2 x 10 seconds
Uni-/bilateral data	Uni: right leg	Bil	Uni:-	Bil: independent legs
Filtering of data	low-pass 12 Hz	low-pass 15 Hz	low-pass 50 Hz	low-pass 15 Hz
Quantities				
Peak accelerations			PTA, PHA	
Shock attenuation			PTA/PHA	
Stiffness (vertical/leg)				
Vertical COM displacement				
Ankle angles	IC + TO + max dorsiflexion	max dorsiflexion		max dorsiflexion
Knee angles	IC + max flexion stance + max extension	max flexion + max extension		max flexion stance
Hip angles		max flexion		
Quality assessment	11- Good	10- Good	10- Good	12- Good

2

5/7	Mizrahi et al. [15,44,45,46]	Murray et al. [47]	Nicol et al. [48]	Paquette et al. [49]
Subject information				
Subject population	Recreational runners	Recreational competitive runners	Experienced endurance runners	Runners
Subjects (sex), Age (years), Height (cm), Weight (kg)	14 (M), 24 (4), 176 (6), 73 (8)	24 (15M+9F), 36.5 (11.2), 172 (9), 73.6 (12.5)	8 (7M+1F), 30, 177 (168-190), 68 (59-93)	21 (14M+7F), 32 (8), 176 (11), 70 (11)
Training information	Min 3 months, 8-10 km/week, Min 2 days/week, Around 12 km/h, Never had an injury	5 years (IQR:1-10), 3 runs/week (IQR: 3-5), Goal: 12 km < 75 min, Free of injuries now		12 (6) years, 56 (21) km/week, No injuries last year
Fatigue protocol				
Speed based on	105% of anaerobic threshold	Race pace 12 km	Training status + last performance	75% of 10 km personal best
Speed	Constant at 12.7 (0.7) km/h	Measure: relatively constant at 15.3 (2.0) km/h, Fatigue: variable around 11.8 km/h	Measure: constant at 14.4 km/h, Fatigue: relatively constant at 13.9 km/h	Constant at 10.8 km/h
Setting	Treadmill	Outdoor race	Measure: treadmill Fatigue: outdoor	Treadmill
Stopping criteria	Time	Distance	Distance	Time
Distance covered	6.4 km	12 km	42.2 km	7.2 km
Duration protocol	30 min	61 (8) min	3.0 hours	40 min
Measure of fatigue	Decrease in PETCO2	RPE: median: 17, IQR: 15-18		
Other information		All rearfoot strikers		Rearfoot and non-rearfoot strikers

5/7	Mizrahi et al. [15,44,45,46]	Murray et al. [47]	Nicol et al. [48]	Paquette et al. [49]
Measurement system				
Specifications: marker model, sampling frequency, location, axes, operating range, weight	IMU: sacrum, proximal tibia, 1D, 1667 Hz, 4.2 gram Other: video camera, 50 Hz	Other: camera, 240 Hz	Other: Video camera, 100 Hz, electric goniometer	Optical: cluster + anatomical, 240 Hz
Data analysis				
When was data collected	During fatigue protocol: Every 5th km	Separate trials: Before and after	Separate trials: Before and after	During fatigue protocol: Every 10 minutes
Amount of data analysed	7 x 20 seconds	2 x 3 strides	2 x 1 stride	4 x 5 steps
Uni-/bilateral data	Uni: right leg	Uni: right leg	Uni: left leg	Uni: right leg
Filtering of data	Markers: low-pass 40 Hz			low-pass 8 Hz
Quantities				
Peak accelerations	PTA, PSA			
Shock attenuation	PTA/PSA			
Stiffness (vertical/leg)				
Vertical COM displacement	X*		X*	
Ankle angles		FCA	IC* + TO*	FCA
Knee angles	IC + max flexion stance* + max extension		IC	
Hip angles			IC*	
Quality assessment	9- Fair	12- Good	9- Fair	11- Good

6/7	Paquette and Melcher [50]	Rabita et al. [51]	Reenalda et al. [52]	Sanno et al. [53]
Subject information				
Subject population	Trained runners	Elite triathletes	Well-trained runners	Recreational (rec) and competitive (com) long distance runners
Subjects (sex), Age (years), Height (cm), Weight (kg)	12 (M), 33 (10), 180 (8), 74 (12)	9 (6M+3F), M: 23 (3), F: 25 (4), M: 182 (2), F: 167 (4), M: 68 (5), F: 58 (3)	10 (M), 31 (5), 183 (3), 76 (9)	25 (rec: 13M + com: 12M), rec: 24 (3), com: 25 (4), rec: 184 (5), com: 182 (6), rec: 81 (7), com: 73 (8)
Training information	9 (5) years, 77 (21) km/week, Long run: 19 (5) km, Free of injuries now	55-75 km/week, VO2max = 72 (7) ml/min/kg, VVO2max = 18 km/h	Min 40 km/week, No injuries last 6 months	10 km: rec: >47.5 min, 10 km: com: <37.5 min
Fatigue protocol				
Speed based on	Self-selected at long run pace	95% VVO2max	96% of 10 km personal best	105% of season's best 10 km
Speed	Measure: relatively constant at 12.2 km/h Fatigue: constant at 12.2 km/h	Relatively constant at 18.3 km/h	Relatively constant at 15.8 (1.4) km/h	rec: constant at 11.5 km/h, com: constant at 15.8 km/h
Setting	Measure: overground Fatigue: treadmill	Indoor synthetic track	Outdoor track	Treadmill
Stopping criteria	Distance	Feeling: unable to continue	Time	Distance
Distance covered	19.2 km	3.3 (0.8) km	5.3 km	10 km
Duration protocol	94.2 min	10.7 (2.6) min	20 min	rec: 52.8 (2.4) min com: 37.5 (1.3) min
Measure of fatigue				RPE: rec: 16.9 (1.3) com: 17.1 (1.2)
Other information	Rearfoot strikers			

6/7	Paquette and Melcher [50]	Rabita et al. [51]	Reenalda et al. [52]	Sanno et al. [53]
Measurement system				
Specifications: marker model, sampling frequency, location, axes, operating range, weight	Optical: cluster + anatomical (cal.), 240 Hz	Other: force platform, 500 Hz	IMU: sacrum, proximal tibia, 3D, 100 Hz, 18 g, 30 gram	Optical: anatomical, 250 Hz
Data analysis				
When was data collected	Separate trials: Before and after	During fatigue protocol: 10, 33, 67, 100 % of total time	During fatigue protocol: Minute 3 and 18	During fatigue protocol: 0.2 km, 0.5 km, and every km
Amount of data analysed	2 x 5 stance phases	4 x 4-6 steps	2 x 20 strides	13 x 20 stance phases
Uni-/bilateral data	Uni: right leg	Bil: combined	Uni: right leg	Uni: right leg
Filtering of data	low-pass 8 Hz			low-pass 20 Hz
Quantities				
Peak accelerations			PTA, PSA	
Shock attenuation			PTA/PSA	
Stiffness (vertical/leg)		vertical & leg stiffness		
Vertical COM displacement		X*		X*
Ankle angles				IC + TO + max dorsiflexion
Knee angles	max flexion stance		IC + max flexion stance	IC + max flexion stance
Hip angles			IC + MS	MS
Quality assessment	11- Good	11- Good	9- Fair	9- Fair

2

7/7	Schütte et al. [54]	Siler and Martin [55]	Strohrmann et al. [56]	Voloshin et al. [57], Verbitsky et al. [58]
Subject information				
Subject population	Novice to experienced runners	Regularly training runners (split into fast and slow runners)	Runners of different skill levels	Non-professional runners
Subjects (sex), Age (years), Height (cm), Weight (kg)	20 (12+8F), 21 (2), 177 (8), 66 (6)	19 (M), fast: 29 (4), slow: 30 (5), fast: 174 (6), slow: 176 (8), fast: 67 (5), slow: 74 (9)	21, NP, NP, NP	22 (M), 31 (5), 174 (7), 70 (9)
Training information	48 (36) km/week, No injuries last 6 months	fast: 5 (2), slow: 4 (3) years, fast: 73 (21), slow: 32 (16) km/week, 10 km: fast<36, slow>40 min, Free of injuries now	0-45 km/wk	Min 2 days/week, Never had an injury
Fatigue protocol				
Speed based on	3.2 km time trial	fast: 87% of VVO2max, slow: 81% of VVO2max	85% of 1 min max speed	Anaerobic threshold
Speed	Measure: constant at max 12.0 km/h, Fatigue: constant at 14.0 (4.5) km/h	fast: constant at 17.0 (0.9) km/h, slow: constant at 13.0 (0.4) km/h	Constant, Beginner: 9-10.5 km/h, Intermediate: 10.5-12 km/h, Advanced: 12-14.5 km/h, Expert: 14.5-17.8 km/h	Fatigued: constant at 9.9 (1.0) km/h, Unfatigued: constant at 9.9 (1.7) km/h
Setting	Treadmill	Treadmill	Treadmill	Treadmill
Stopping criteria	Feeling: unable to continue or RPE = 17	Feeling: unable to continue	Time	Time
Distance covered	4.8 km	fast: 8.4 km, slow: 9.6 km	6.8-13.4 km	5.0 km
Duration protocol	20.5 (6.9) min	fast: 29.5 (5.8) min, slow: 44.2 (7.6) min	45 min	30 min
Measure of fatigue	RPE: >17	RPE: fast: 18.9 (0.3), slow: 19.2 (0.4)		PETCO2
Other information				Split in fatigued and unfatigued group based on PETCO2

7/7	Schütte et al. [54]	Siler and Martin [55]	Strohrmann et al. [56]	Voloshin et al. [57], Verbitsky et al. [58]
Measurement system				
Specifications: marker model, sampling frequency, location, axes, operating range, weight	Optical: anatomical, 150 Hz	Optical: anatomical, 100 Hz	IMU: sacrum, 3D, 100 Hz, 6 g, 22 gram	IMU: sacrum, proximal tibia, 1D, 1667 Hz, 2.3 gram
Data analysis				
When was data collected	Varied: First and last minute	During fatigue protocol: Minute 5 and every 10% of total time	During fatigue protocol	During fatigue protocol: Every 5th minute
Amount of data analysed	2 x 20 steps	10 x 2 strides	2 measurement points	7 x 20 seconds
Uni-/bilateral data	NA	Uni: left leg	NA	Uni: right leg
Filtering of data	low-pass 15Hz	low-pass 5.5-7.5Hz (different for each marker)		
Quantities				
Peak accelerations				PTA*, PSA*
Shock attenuation				
Stiffness (vertical/leg)				
Vertical COM displace-ment	X*		X*	
Ankle angles		max dorsiflexion		
Knee angles		max flexion + max extension		
Hip angles		max flexion		
Quality assessment	11- Good	10- Good	6- Poor	7- Poor

2

Table 2.5: *Quality assessment scores for all included articles. A more extensive description of the questions can be found in Table 2.3 and Appendix 2.B. UTD = Unable to determine.*

	Reporting							Validity					Power		
								External		Internal					
	1. Aim	**2. Main outcomes**	**3. Subject characteristics**	**4. Fatigue protocol**	**6. Main findings**	**7. Estimate of variability**	**10. Probability values**	**11. Subjects representative**	**13. Protocol representative**	**16. Clear about "data dredging"**	**18. Appropriate statistics**	**20. Accurate main outcomes**	**27. Sufficient power**	**Total quality score**	**Quality**
Abt et al. [32]	1	1	1	1	1	1	1	0	0	1	1	1	1	11	Good
Avogadro et al. [33]	1	1	0	1	0	1	1	0	0	1	1	1	UTD	8	Fair
Bazett-Jones et al. [34]	1	1	1	1	1	1	1	1	0	1	1	1	UTD	11	Good
Bigelow et al. [35]	1	1	1	0	1	1	1	1	0	1	1	1	UTD	10	Good
Clansey et al. [5]	1	1	1	1	1	1	1	0	0	1	1	1	UTD	10	Good
Derrick et al. [13]	1	1	0	1	1	1	0	1	0	1	1	1	UTD	9	Fair
Dierks et al. [36,37]	1	1	1	1	1	1	1	0	0	0	1	1	1	10	Good
Dutto and Smith [38]	1	1	1	1	0	1	0	0	0	1	1	1	UTD	8	Fair
Fuhr et al. [39]	1	1	1	1	1	1	0	1	0	1	1	1	UTD	10	Good
García-Pérez et al. [29]	1	1	1	1	1	1	0	0	0	1	1	1	UTD	9	Fair
García-Pinillos et al. [40]	1	1	1	1	0	1	1	0	0	1	1	1	UTD	9	Fair
Hanley and Mohan [41]	1	1	1	1	1	1	1	1	0	1	1	1	UTD	11	Good
Jewell et al. [42]	1	1	1	1	1	1	1	0	0	1	1	1	1	11	Good
Koblbauer et al. [30]	1	1	1	1	1	1	0	1	0	1	1	1	UTD	10	Good
Lucas-Cuevas et al. [14]	1	1	1	1	1	1	1	0	0	1	1	1	UTD	10	Good
Maas et al. [43]	1	1	1	1	1	1	1	0	0	1	1	1	2	12	Good
Mizrahi et al. [15,44,45,46]	1	1	1	1	0	1	0	1	0	1	1	1	UTD	9	Fair
Murray et al. [47]	1	1	1	1	1	1	1	1	1	1	1	1	UTD	12	Good
Nicol et al. [48]	1	1	0	1	1	1	0	0	1	1	1	1	UTD	9	Fair
Paquette et al. [49]	1	1	1	1	1	1	1	0	0	1	1	1	1	11	Good
Paquette and Melcher [50]	1	1	1	1	1	1	1	0	0	1	1	1	1	11	Good
Rabita et al. [51]	1	1	1	1	1	1	1	1	0	1	1	1	UTD	11	Good
Reenalda et al. [52]	1	1	1	1	1	1	0	0	0	1	1	1	UTD	9	Fair
Sanno et al. [53]	1	1	1	1	1	1	0	0	0	1	1	1	UTD	9	Fair
Schütte et al. [54]	1	1	1	1	1	1	1	1	0	1	1	1	UTD	11	Good
Siler and Martin [55]	1	1	1	1	1	1	0	1	0	1	1	1	UTD	10	Good
Strohrmann et al. [56]	1	1	0	1	0	0	1	0	0	UTD	1	1	UTD	6	Poor
Voloshin et al. [57] Verbitsky et al. [58]	1	1	0	1	0	1	0	0	0	1	1	1	UTD	7	Poor
Total of all studies	28	28	23	27	22	27	17	11	2	26	28	28	7		

Peak accelerations

Peak tibial acceleration increased on average 0.39 g (CI: [0.16, 0.62], p = 0.001) after a fatigue protocol, see Table 2.6. There was no significant pooled effect of fatigue on peak sacral acceleration (MD: 0.44 g, CI: [-0.07, 0.95], p = 0.09) and peak head acceleration (MD: 0.08 g, CI: [-0.05, 0.21], p = 0.22). From the study of Bigelow et al. [52], only results for trials on the treadmill fulfilled the inclusion criteria and were included in this literature review. García-Pérez et al. [29] investigated peak tibial accelerations both during treadmill and overground running. Only treadmill running was included in the meta-analysis to prevent dependent inputs. They found no significant effect of fatigue on peak tibial acceleration during overground running (pre-fatigue: 24.6 (10.8) g, post-fatigue: 22.2 (10.3) g)). Findings of the study of Voloshin et al. [50] and Verbitsky et al. [51] were not included in meta-analyses because they lacked absolute values. However, they classified the group of runners into a “fatigued” and “unfatigued” group based on end-tidal carbon dioxide pressure after a fatigue protocol. They found a significant increase of 62 (32)% ($p < 0.05$) in peak tibial acceleration in the group of runners classified as “fatigued” but not in the group of runners classified as “unfatigued” (-1 (14)%, $p > 0.05$). The normalized peak sacral acceleration also significantly increased in the group of “fatigued” runners (37 (30)%, $p < 0.05$) but not in the group of “unfatigued” runners (22 (31)%, $p > 0.05$). Note that there was small to high heterogeneity for peak accelerations, indicating variable results between studies.

Shock attenuation

Fatigue resulted in no pooled significant changes in shock attenuation between the tibia and head (MD: 2.10%, CI: [-0.67, 4.87], p = 0.14) and between the tibia and sacrum (MD: 4.65%, CI: [-3.34, 12.64], p = 0.25), see Table 2.6.

Vertical and leg stiffness

After a fatigue protocol, a significant pooled decrease in K_{leg} was found (MD:-0.73 kN/m, CI: [-1.20,-0.25], p = 0.003), see Table 2.6. The meta-analysis did not show a significant pooled effect of fatigue on K_{vert} (MD:-0.17 kN/m, CI: [-0.59, 0.25], p = 0.43). Results of Avogadro et al. [33] for K_{leg} were not included in the meta-analysis because of a different computation, however, they did not find a significant effect of fatigue on K_{leg} (pre-fatigue:15.12 (3.33) kN/m; post-fatigue: 15.82 (3.52) kN/m, p = 0.24).

Table 2.6: *Random-effects meta-analyses for the effect of running-induced fatigue on peak accelerations, shock attenuation and stiffnesses. An asterisk (*) before the name of the authors indicates that a significant change with fatigue was found in that study. SD = standard deviation; CI = confidence interval; TM = treadmill.*

Peak tibial acceleration	Unfatigued mean (SD) [g]	Fatigued mean (SD) [g]	Subjects	Weight	Mean difference [95% CI]	Mean difference, 95% CI decrease ← → increase
Abt et al. [32]	7.5 (1.1)	7.7 (1.3)	12	39.0%	0.20 [-0.08, 0.48]	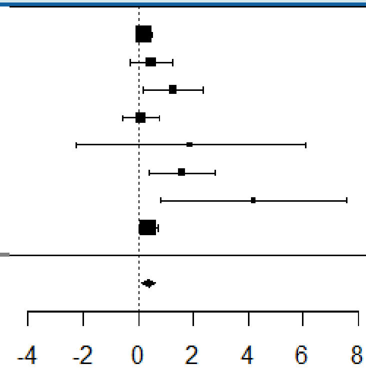
Clansey et al. [5]	11.3 (2.2)	11.8 (1.8)	21	8.3%	0.49 [-0.28, 1.26]	
* Derrick et al. [13]	6.1 (1.0)	7.4 (1.1)	10	4.2%	1.27 [0.17, 2.37]	
Dierks et al. [36]	4.4 (1.4)	4.5 (1.5)	20	11.0%	0.10 [-0.56, 0.76]	
García-Pérez et al. [29] TM	15.3 (6.8)	17.2 (9.5)	20	0.3%	1.90 [-2.26, 6.06]	
* Lucas-Cuevas et al. [14]	6.7 (3.1)	8.3 (4.0)	40	3.6%	1.58 [0.38, 2.78]	
* Mizrahi et al. [15,45,46]	6.9 (2.9)	11.1 (4.2)	14	0.5%	4.20 [0.82, 7.58]	
* Reenalda et al. [52]	5.0 (1.6)	5.3 (2.2)	10	33.2%	0.30 [0.05, 0.69]	
Total (95% CI)			147	100.0%	0.39 [0.16, 0.62]	
Heterogeneity: $I^2 = 14\%$						
Test for overall effect: $Z = 3.28$ ($p = 0.001$)						

Peak sacral acceleration	Unfatigued mean (SD) [g]	Fatigued mean (SD) [g]	Subjects	Weight	Mean difference [95% CI]	Mean difference, 95% CI decrease ← → increase
* Bigelow et al. [35] TM	3.6 (0.6)	4.2 (0.8)	6	40.7%	0.60 [0.49, 0.71]	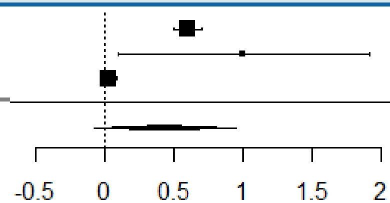
* Mizrahi et al. [46]	2.5 (0.8)	3.5 (1.1)	14	18.0%	1.00 [0.09, 1.91]	
Reenalda et al. [52]	2.5 (0.7)	2.5 (0.6)	10	41.3%	0.03 [-0.03, 0.09]	
Total (95% CI)			30	100.0%	0.44 [-0.07, 0.95]	
Heterogeneity: $I^2 = 98\%$						
Test for overall effect: $Z = 1.68$ ($p = 0.09$)						

Peak head acceleration	Unfatigued mean (SD) [g]	Fatigued mean (SD) [g]	Subjects	Weight	Mean difference [95% CI]
Abt et al. [32]	2.7 (0.4)	2.8 (0.5)	12	23.3%	0.10 [-0.05, 0.25]
* Clansey et al. [5]	1.0 (0.3)	1.3 (0.3)	21	25.1%	0.26 [0.13, 0.39]
Derrick et al. [13]	1.6 (0.3)	1.7 (0.3)	10	22.3%	0.10 [-0.06, 0.26]
García-Pérez et al. [29] TM	2.8 (0.6)	2.7 (0.6)	20	14.2%	-0.10 [-0.36, 0.16]
Lucas-Cuevas et al. [14]	1.8 (0.6)	1.7 (0.8)	40	15.1%	-0.10 [-0.35, 0.15]
Total (95% CI)			103	100.0%	0.08 [-0.05, 0.21]

Heterogeneity: $I^2 = 61\%$

Test for overall effect: $Z = 1.23$ ($p = 0.22$)

Mean difference, 95% CI
decrease ← → increase

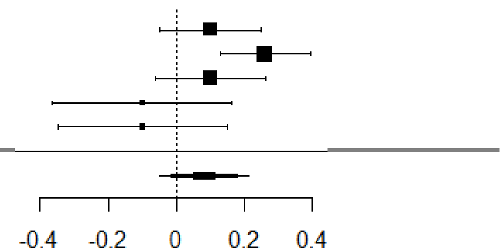

Shock attenuation tibia-head	Unfatigued mean (SD) [%]	Fatigued mean (SD) [%]	Subjects	Weight	Mean difference [95% CI]
Abt et al. [32]	63.2 (7.9)	62.9 (9.6)	12	39.8%	-0.30 [-1.00, 0.40]
* Derrick et al. [13]	74.5 (5.4)	77.5 (4.1)	10	30.1%	3.00 [0.40, 5.60]
García-Pérez et al. [29] TM	75.5 (20.8)	77.9 (13.9)	20	13.7%	2.40 [-3.69, 8.49]
* Lucas-Cuevas et al. [14]	71.0 (18.4)	77.1 (16.9)	40	16.4%	6.05 [0.75, 11.35]
Total (95% CI)			82	100.0%	2.10 [-0.67, 4.87]

Heterogeneity: $I^2 = 71\%$

Test for overall effect: $Z = 1.49$ ($p = 0.14$)

Mean difference, 95% CI
decrease ← → increase

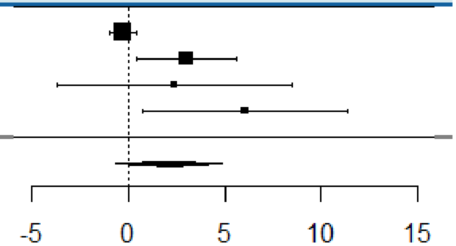

Shock attenuation tibia-sacrum	Unfatigued mean (SD) [%]	Fatigued mean (SD) [%]	Subjects	Weight	Mean difference [95% CI]
* Mizrahi et al. [46]	65.7 (11.2)	75.8 (8.7)	14	35.8%	10.10 [0.94, 19.26]
Reenalda et al. [52]	51.9 (16.2)	53.5 (15.0)	10	64.2%	1.60 [-0.72, 3.92]
Total (95% CI)			24	100.0%	4.65 [-3.34, 12.64]

Heterogeneity: $I^2 = 68\%$

Test for overall effect: $Z = 1.14$ ($p = 0.25$)

Mean difference, 95% CI
decrease ← → increase

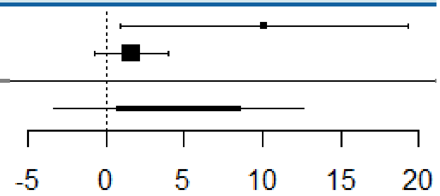

Vertical stiffness	Unfatigued mean (SD) [kN/m]	Fatigued mean (SD) [kN/m]	Subjects	Weight	Mean difference [95% CI]
Dutto and Smith [38]	23.9 (3.2)	23.1 (2.8)	15	8.8%	-0.80 [-2.22, 0.62]
García-Pinillos et al. [40]	23.9 (2.7)	23.8 (2.7)	22	89.7%	-0.12 [-0.56, 0.32]
Rabita et al. [51]	44.4 (7.2)	45.0 (5.3)	9	1.5%	0.60 [-2.86, 4.06]
Total (95% CI)			46	100.0%	-0.17 [-0.59, 0.25]
Heterogeneity: $I^2 = 0\%$					
Test for overall effect: $Z = -0.79$ ($p = 0.43$)					

Mean difference, 95% CI
decrease ← → increase

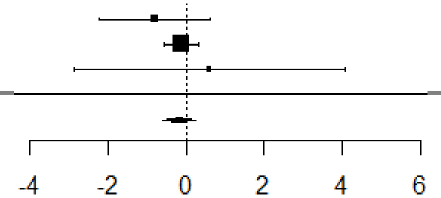

Leg stiffness	Unfatigued mean (SD) [kN/m]	Fatigued mean (SD) [kN/m]	Subjects	Weight	Mean difference 95% CI
Dutto and Smith [38]	9.3 (1.2)	9.0 (1.1)	15	33.4%	-0.30 [-0.86, 0.26]
* García-Pinillos et al. [40]	8.6 (1.5)	7.9 (1.3)	22	43.7%	-0.76 [-1.15, -0.37]
* Rabita et al. [51]	11.7 (1.9)	10.4 (1.0)	9	22.9%	-1.30 [-2.09, -0.51]
Total (95% CI)			46	100.0%	-0.73 [-1.20, -0.25]
Heterogeneity: $I^2 = 54\%$					
Test for overall effect: $Z = -3.01$ ($p = 0.003$)					

Mean difference, 95% CI
decrease ← → increase

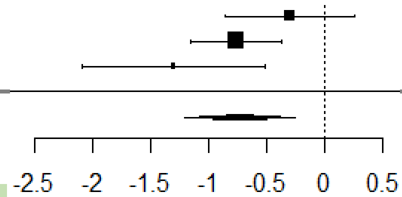

Vertical COM displacement

A total of six studies investigated ΔCOM_z [15,36,40,43,46,47,49], findings were not included in a meta-analysis because the definition of ΔCOM_z differed between studies. Strohrmann et al. [49] found an increase in ΔCOM_z during the complete gait cycle in novice (MD: 8.12%, p = 0.041) but not in more experienced runners (data not provided). Similarly, Sanno et al. [46] found a significant decrease in the COM height at initial contact in recreational runners (pre-fatigue: 1.053 (0.033) m, post-fatigue: 1.047 (0.033) m, $p < 0.05$) but not in competitive runners (pre-fatigue: 1.043 (0.041) m, post-fatigue: 1.039 (0.043) m, $p > 0.05$). They also found a significant decrease in the minimum COM height in recreational runners (pre-fatigue: 0.988 (0.031) m, post-fatigue: 0.980 (0.029) m, $p < 0.01$) but not in competitive runners (pre-fatigue: 0.982 (0.039) m, post-fatigue: 0.977 (0.040) m, $p > 0.05$). Rabita et al. [43] found a decrease in ΔCOM_z during the stance phase (pre-fatigue: 0.045 (0.004) m, post-fatigue: 0.040 (0.006) m, p = 0.025). A surrogate for ΔCOM_z (i.e., hip excursion) was investigated by Mizrahi et al. [15,36]. They found an increase in hip excursion between the moment of maximum hip height and the moment of peak tibial acceleration (shortly after initial contact) (pre-fatigue: 0.051 (0.015) m, post-fatigue: 0.062 (0.012) m, $p < 0.05$). They found no significant effect of fatigue on hip excursion between the moment of peak acceleration and the minimum hip height (pre-fatigue: 0.022 (0.009) m, post-fatigue: 0.019 (0.009) m, $p > 0.05$) or the maximum hip height, minimum hip height or hip height at the moment of peak tibial acceleration (data not provided). No significant effects of fatigue on ΔCOM_z during the full gait cycle were found by Schütte et al. [47] (pre-fatigue: 0.107 (0.013) m, post-fatigue: 0.110 (0.014) m, p = 0.33) and Nicol et al. [40] (no data provided).

The effect of experience level on ΔCOM_z was qualitatively investigated. Two studies measured runners with different experience levels and found significant changes in ΔCOM_z only in novice or recreational runners but not in more experienced runners [46,49]. Additionally, Mizrahi et al. [15,36] included only recreational runners (i.e., low experience level) and found a significant increase in the change in hip height (i.e., surrogate for ΔCOM_z) between the moment of maximal hip height and peak tibial acceleration. Another study included only elite athletes (i.e. high experience level) and found a significant decrease in ΔCOM_z with fatigue [43].

Lower body joint angles

Ankle angles

No significant pooled effect of fatigue on ankle angles at initial contact (MD:-0.06 °, CI: [-1.92, 1.80], p = 0.95), ankle angles at toe-off (MD:-0.05 °, CI: [-1.43, 1.33], p = 0.95) or maximum dorsiflexion angles (MD: -0.31 °, CI: [-0.75, 0.13], p = 0.17) were found, see Table 2.7. No significant pooled effect of fatigue was found for the foot contact angle (i.e., sagittal plane angle between foot and ground at initial contact) (MD: 0.50 °, CI: [-1.12, 2.12], p = 0.54). Results of Nicol et al. [40] were excluded from meta-analyses since they did not provide actual values, however, they reported no significant effect of fatigue on ankle angles at initial contact or toe-off (p > 0.05).

Knee angles

After a fatigue protocol, knee flexion angles at initial contact increased by 1.64 ° (CI: [0.61, 2.66], p = 0.002) and maximum knee flexion during swing increased with 2.92 ° (CI: [0.80, 5.04], p = 0.007]) , see Table 2.7. No significant pooled effect of fatigue was found on maximum knee flexion angles during stance (MD: 0.36 °, CI: [-0.34, 1.06], p = 0.31) or maximum knee extension (MD: 0.37 °, CI: [-0.90, 1.65], p = 0.57). Results of Mizrahi et al. [36] were excluded from meta-analyses since they did not report actual values, however, they stated that the maximum knee flexion angle during stance did not significantly change after a fatigue protocol (p > 0.05).

Hip angles

Meta-analyses showed no significant pooled effects of fatigue on hip angles at initial contact (MD:-0.77 °, CI: [-3.32, 1.78], p = 0.55), midstance (MD:-1.71 °, CI: [-3.93, 0.51], p = 0.13) or maximum hip flexion (MD: 0.57 °, CI: [-0.51, 1.65], p = 0.30), see Table 2.7. Results of Nicol et al. [40] were excluded from meta-analyses since they did not report actual values, however, they found no significant differences in the hip angles at initial contact after a fatiguing protocol (p > 0.05). It should be noted that most quantities related to hip angles were investigated by a small number of studies.

Table 2.7: *Random-effects meta-analysis for the effect of running-induced fatigue on joint angles. An asterisk (*) before the name of the authors indicates that a significant change with fatigue was found in that study. Comp = competitive runners; Recr = recreational runners; Nov = Novice runners; Dom = dominant leg; Fast = group of faster runners; Slow = group of slower runners; SD = standard deviation; CI = confidence interval.*

Ankle angle initial contact	Unfatigued mean (SD) [deg]	Fatigued mean (SD) [deg]	Subjects	Weight	Mean difference [95% CI]
* Clansey et al. [5]	-1.0 (1.9)	-3.5 (2.0)	21	22.6%	-2.50 [-4.40, -0.60]
Hanley and Mohan [41]	2.0 (7.0)	2.0 (7.0)	15	23.4%	0.00 [-1.76, 1.76]
* Jewell et al. [42]	-11.8 (5.3)	-9.3 (6.3)	14	22.9%	2.50 [0.65, 4.35]
Sanno et al. [53] Comp	-8.0 (9.6)	-6.7 (7.6)	12	11.5%	1.30 [-3.00, 5.60]
Sanno et al. [53] Recr	1.2 (6.7)	0.1 (4.5)	13	19.6%	-1.10 [-3.55, 1.35]
Total (95% CI)			75	100.0%	-0.06 [-1.92, 1.80]
Heterogeneity: $I^2 = 71\%$					
Test for overall effect: $Z = -0.06$ ($p = 0.95$)					

Mean difference, 95% CI
decrease ← → increase

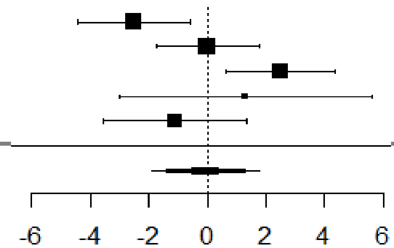

Foot contact angle	Unfatigued mean (SD) [deg]	Fatigued mean (SD) [deg]	Subjects	Weight	Mean difference [95% CI]
Murray et al. [47]	16.7 (6.1)	17.2 (5.0)	24	65.2%	0.50 [-1.50, 2.50]
Paquette et al. [49]	4.6 (6.2)	5.1 (6.4)	21	34.8%	0.50 [-2.24, 3.24]
Total (95% CI)			45	100.0%	0.50 [-1.12, 2.12]
Heterogeneity: $I^2 = 0\%$					
Test for overall effect: $Z = 0.61$ ($p = 0.54$)					

Mean difference, 95% CI
decrease ← → increase

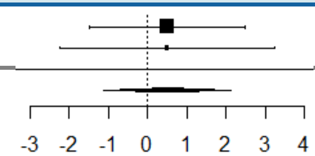

Ankle angle toe-off	Unfatigued mean (SD) [deg]	Fatigued mean (SD) [deg]	Subjects	Weight	Mean difference [95% CI]
Hanley and Mohan [41]	-3.0 (8.0)	-3.0 (6.0)	15	28.0%	0.00 [-1.26, 1.26]
* Jewell et al. [42]	-24.9 (5.4)	-26.2 (5.1)	14	30.3%	-1.21 [-2.25, -0.17]
Sanno et al. [53] Comp	-22.9 (3.7)	-23.6 (3.7)	13	20.6%	-0.70 [-2.71, 1.31]
* Sanno et al. [53] Recr	-21.6 (4.4)	-19.4 (4.2)	12	21.1%	2.20 [0.24, 4.16]
Total (95% CI)			54	100.0%	-0.05 [-1.43, 1.33]
Heterogeneity: $I^2 = 71\%$					
Test for overall effect: $Z = -0.07$ ($p = 0.95$)					

Mean difference, 95% CI
decrease ← → increase

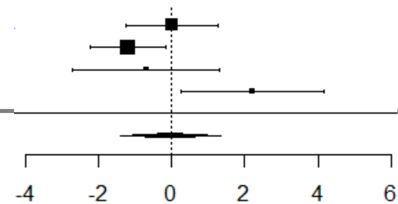

Ankle angle max dorsiflexion	Unfatigued mean (SD) [deg]	Fatigued mean (SD) [deg]	Subjects	Weight	Mean difference [95% CI]
Jewell et al. [42]	14.9 (5.3)	14.3 (4.5)	14	37.2%	-0.59 [-1.31, 0.13]
Koblbauer et al. [30] Dom	18.4 (4.4)	18.1 (4.1)	16	27.3%	-0.30 [-1.15, 0.55]
Maas et al. [43] Comp	-18.2 (4.1)	-19.2 (4.8)	15	3.4%	-1.00 [-3.38, 1.38]
Maas et al. [43] Nov	-17.6 (5.1)	-17.8 (5.3)	15	15.7%	-0.20 [-1.31, 0.91]
Sanno et al. [53] Comp	18.7 (3.0)	18.8 (3.4)	12	5.3%	0.10 [-1.82, 2.02]
Sanno et al. [53] Recr	17.8 (3.6)	17.9 (3.6)	13	5.1%	0.10 [-1.86, 2.06]
Siler and Martin [55] Fast	20.2 (4.1)	21.5 (3.9)	9	3.0%	1.30 [-1.25, 3.85]
Siler and Martin [55] Slow	17.1 (4.9)	17.4 (4.1)	10	3.0%	0.30 [-2.24, 2.84]
Total (95% CI)			104	100.0%	-0.31 [-0.75, 0.13]
Heterogeneity: $I^2 = 0\%$					
Test for overall effect: $Z = -1.37$ ($p = 0.17$)					

Mean difference, 95% CI
decrease ← → increase

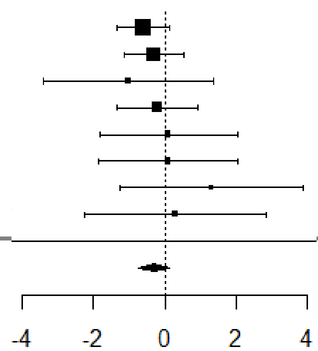

Knee angle initial contact	Unfatigued mean (SD) [deg]	Fatigued mean (SD) [deg]	Subjects	Weight	Mean difference [95% CI]
Clansey et al. [5]	15.0 (2.9)	16.1 (2.8)	21	10.2%	1.15 [-1.08, 3.38]
* Derrick et al. [13]	15.1 (2.3)	19.5 (2.9)	10	5.2%	4.40 [0.59, 8.21]
* Hanley and Mohan [41]	19.0 (6.0)	21.0 (4.0)	15	14.2%	2.00 [0.55, 3.45]
Jewell et al. [42]	9.5 (4.6)	10.4 (4.1)	14	15.4%	0.98 [-0.26, 2.22]
Mizrahi et al. [15,44]	27.3 (6.4)	25.5 (4.3)	14	10.1%	-1.80 [-4.05, 0.45]
* Nicol et al. [48]	29.6 (5.7)	33.4 (5.5)	8	6.9%	3.80 [0.65, 6.95]
* Reenalda et al. [52]	15.8 (7.6)	16.7 (7.6)	10	17.7%	0.90 [0.12, 1.68]
* Sanno et al. [53] Comp	12.7 (3.6)	16.0 (4.0)	12	10.9%	3.30 [1.22, 5.38]
* Sanno et al. [53] Recr	9.5 (4.5)	12.2 (5.7)	13	9.4%	2.70 [0.27, 5.13]
Total (95% CI)			117	100.0%	1.64 [0.61, 2.66]
Heterogeneity: $I^2 = 65\%$					
Test for overall effect: $Z = 3.13$ ($p = 0.002$)					

Mean difference, 95% CI
decrease ← → increase

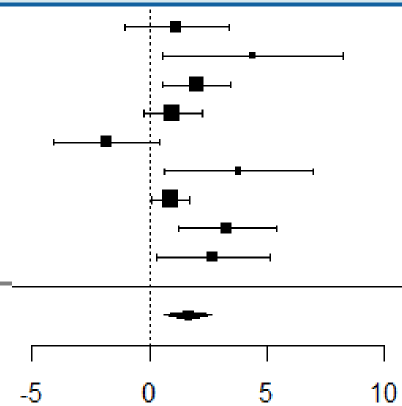

Knee angle max flexion stance	Unfatigued mean (SD) [deg]	Fatigued mean (SD) [deg]	Subjects	Weight	Mean difference [95% CI]
Abt et al. [32]	49.3 (6.6)	49.2 (6.2)	12	12.4%	-0.10 [-0.37, 0.17]
Bazett-Jones et al. [34]	45.1 (4.8)	45.3 (4.8)	19	12.0%	0.20 [-0.25, 0.65]
Clansey et al. [5]	41.2 (4.3)	40.3 (5.3)	21	9.2%	-0.90 [-2.10, 0.30]
* Derrick et al. [13]	52.3 (1.4)	56.2 (1.5)	10	3.2%	3.90 [0.52, 7.28]
Dierks et al. [36,37]	46.3 (5.3)	46.5 (5.4)	20	5.2%	0.20 [-2.17, 2.57]
* Jewell et al. [42]	33.9 (3.7)	36.2 (3.5)	14	10.2%	2.28 [1.33, 3.23]
Maas et al. [43] Comp	43.7 (2.8)	45.1 (3.3)	15	5.4%	1.40 [-0.88, 3.68]
Maas et al. [43] Nov	39.7 (7.0)	39.6 (7.1)	15	11.4%	-0.10 [-0.76, 0.56]
Paquette and Melcher [50]	49.0 (4.3)	47.5 (5.3)	12	7.7%	-1.50 [-3.08, 0.08]
* Reenalda et al. [52]	45.8 (5.2)	45.3 (5.1)	10	12.0%	-0.50 [-0.93, -0.07]
Sanno et al. [53] Comp	43.1 (2.6)	44.3 (2.7)	13	8.1%	1.20 [-0.27, 2.67]
* Sanno et al. [53] Recr	40.5 (6.0)	43.0 (6.1)	12	3.2%	2.50 [-0.87, 5.87]
Total (95% CI)			173	100.0%	0.36 [-0.34, 1.06]

Heterogeneity: $I^2 = 88\%$

Test for overall effect: $Z = 1.02$ ($p = 0.31$)

Mean difference, 95% CI
decrease ← → increase

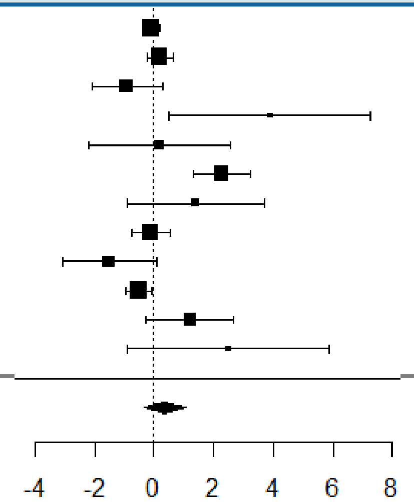

Knee angle max flexion swing	Unfatigued mean (SD) [deg]	Fatigued mean (SD) [deg]	Subjects	Weight	Mean difference [95% CI]
* Fuhr et al. [39]	97.4 (6.6)	101.7 (9.3)	9	34.0%	4.27 [0.64, 7.90]
Koblbauer et al. [30] Dom	89.0 (10.2)	92.2 (12.7)	15	40.0%	3.20 [-0.15, 6.55]
Siler and Martin [55] Fast	120.5 (10.2)	121.9 (9.3)	9	12.5%	1.40 [-4.58, 7.38]
Siler and Martin [55] Slow	103.8 (11.8)	103.9 (9.3)	10	13.5%	0.10 [-5.66, 5.86]
Total (95% CI)			43	100.0%	2.92 [0.80, 5.04]

Heterogeneity: $I^2 = 0\%$

Test for overall effect: $Z = 2.71$ ($p = 0.007$)

Mean difference, 95% CI
decrease ← → increase

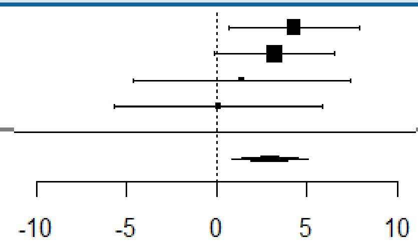

Knee angle max extension	Unfatigued mean (SD) [deg]	Fatigued mean (SD) [deg]	Subjects	Weight	Mean difference [95% CI]
Fuhr et al. [39]	-0.1 (7.0)	0.9 (7.3)	9	6.0%	1.00 [-3.77, 5.77]
Jewell et al. [42]	6.3 (2.5)	6.0 (2.9)	14	34.2%	-0.28 [-0.88, 0.32]
Koblbauer et al. [30] Dom	10.0 (5.4)	9.0 (5.7)	15	25.1%	-1.00 [-2.45, 0.45]
* Mizrahi et al. [15]	13.8 (3.1)	17.2 (4.2)	14	11.7%	3.40 [0.32, 6.48]
Siler and Martin [55] Fast	14.4 (4.4)	16.2 (4.4)	9	12.9%	1.80 [-1.07, 4.67]
Siler and Martin [55] Slow	8.5 (3.8)	8.8 (5.5)	10	10.1%	0.30 [-3.11, 3.71]
Total (95% CI)			71	100.0%	0.37 [-0.90, 1.65]
Heterogeneity: $I^2 = 55\%$					
Test for overall effect: $Z = 0.57$ ($p = 0.57$)					

Mean difference, 95% CI
decrease ← → increase

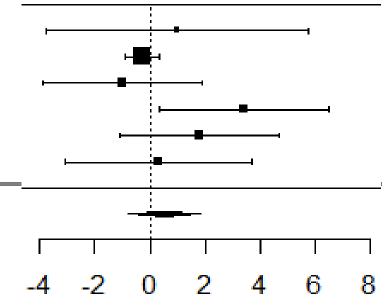

Hip angle initial contact	Unfatigued mean (SD) [deg]	Fatigued mean (SD) [deg]	Subjects	Weight	Mean difference [95% CI]
* Clansey et al. [5]	43.0 (2.6)	39.0 (2.8)	21	26.0%	-4.01 [-7.70, -0.32]
Hanley and Mohan [41]	22.0 (6.0)	23.0 (6.0)	15	31.6%	1.00 [-2.04, 4.04]
Reenalda et al. [52]	33.5 (6.7)	33.4 (7.3)	10	42.4%	-0.10 [-2.10, 1.90]
Total (95% CI)			46	100.0%	-0.77 [-3.32, 1.78]
Heterogeneity: $I^2 = 58\%$					
Test for overall effect: $Z = -0.59$ ($p = 0.55$)					

Mean difference, 95% CI
decrease ← → increase

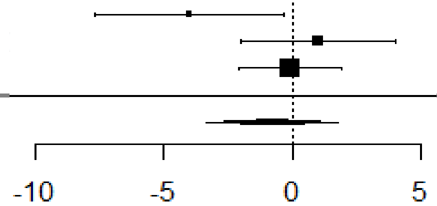

Hip angle midstance	Unfatigued mean (SD) [deg]	Fatigued mean (SD) [deg]	Subjects	Weight	Mean difference [95% CI]
* Clansey et al. [5]	33.1 (9.2)	28.4 (9.0)	21	23.8%	-4.72 [-7.73, -1.71]
* Reenalda et al. [52]	22.5 (5.7)	20.2 (6.5)	10	31.6%	-2.30 [-4.29, -0.31]
Sanno et al. [53] Comp	24.8 (4.7)	24.8 (5.2)	13	25.1%	0.00 [-2.83, 2.83]
Sanno et al. [53] Recr	21.3 (5.4)	22.0 (6.5)	12	19.5%	0.70 [-2.98, 4.38]
Total (95% CI)			56	100.0%	-1.71 [-3.93, 0.51]

Heterogeneity: $I^2 = 60\%$

Test for overall effect: $Z = -1.51$ ($p = 0.13$)

Mean difference, 95% CI
decrease ← → increase

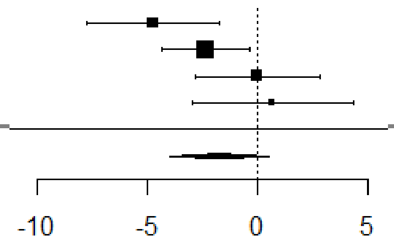

Hip angle max flexion	Unfatigued mean (SD) [deg]	Fatigued mean (SD) [deg]	Subjects	Weight	Mean difference [95% CI]
Bazett-Jones et al. [34]	35.8 (8.4)	35.4 (8.5)	19	38.8%	-0.40 [-1.16, 0.36]
* Fuhr et al. [39]	53.3 (12.3)	57.7 (12.9)	9	7.1%	4.40 [0.66, 8.14]
Koblbauer et al. [30] Dom	43.8 (8.2)	44.3 (9.1)	16	25.8%	0.50 [-0.95, 1.95]
Siler and Martin [55] Fast	40.8 (4.3)	41.8 (3.6)	10	15.7%	1.00 [-1.23, 3.23]
Siler and Martin [55] Slow	33.7 (3.6)	34.7 (4.0)	9	12.6%	1.00 [-1.61, 3.61]
Total (95% CI)			63	100.0%	0.57 [-0.51, 1.65]

Heterogeneity:; $I^2 = 45\%$

Test for overall effect: $Z = 1.03$ ($p = 0.30$)

Mean difference, 95% CI
decrease ← → increase

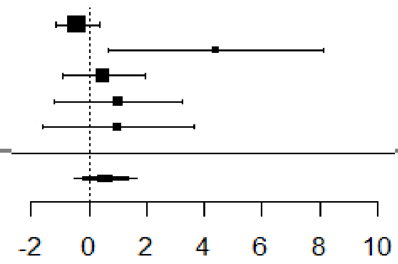

2

Discussion

The primary aim of this study was to provide an overview of kinematic changes due to running-induced fatigue. The main changes in kinematics due to fatigue included an increase in peak accelerations at the tibia, decreased leg stiffness, an increase in knee flexion at initial contact and maximum knee flexion, and an increase in ΔCOM_z in novice, but not in experienced runners. The hypothesis that the lower body would behave stiffer with fatigue was not supported by the results of this literature review. Since most included kinematic quantities are intertwined (i.e., a decrease in stiffness is likely to result in an increase in knee flexion and shock attenuation), the results of this literature review did not support most of the hypotheses. The secondary aim of this study was to investigate the influence of experience level on kinematic changes with fatigue. The hypothesis that experienced runners show smaller changes in kinematics due to fatigue was supported by the finding that ΔCOM_z increased in novice but not in experienced runners with fatigue.

Results from this literature review with meta-analyses were generally in line with results from Apte et al. [18], who investigated seven of the eighteen quantities included in the meta-analyses. They found an increase in PTA, decrease in K_{vert} and K_{leg}, increased knee flexion at initial contact and maximum knee flexion during swing and an increase in ankle dorsiflexion at initial contact [18]. The decrease in K_{vert} and increase in ankle dorsiflexion were not supported by the meta-analyses which can be explained by different exclusion criteria such as including fatigue protocols with a constant versus an uncontrolled running speed. The differences in effects of fatigue between literature reviews emphasize the importance of confounding factors when comparing studies.

Peak accelerations

Peak accelerations at the tibia significantly increased with fatigue. There was no pooled effect of fatigue on peak accelerations at the sacrum and head. An explanation for higher peak tibial accelerations with fatigue could be that in a fatigued state, the body is less capable of coordinating the activation of musculature around the ankle, knee, and hip joints. Decreased coordination might negatively affect the spreading of the impact force impulse over time, resulting in higher peak accelerations [59]. Another explanation for higher peak tibial accelerations is a change in effective mass. The effective mass is the proportion of the body mass that is accelerated during impact and decreases with an increase in knee flexion at initial contact [13]. Since $\sum F = ma$, a decrease in effective mass results in an increase in acceleration when forces remain constant. Since knee flexion angles at initial contact were shown to increase in this literature review, the increase in peak tibial acceleration can partly be explained by a decrease in effective mass.

Shock attenuation

Fatigue resulted in no significant pooled changes in shock attenuation between the tibia and sacrum and the tibia and head. Shock attenuation was expected to increase based on several reasons. Firstly, due to a pooled increase in peak tibial acceleration without a pooled increase in peak sacral and peak head accelerations after a fatigue protocol. Secondly, because of an increase in knee flexion at initial contact [19]. And finally, as a way to keep proximal accelerations low to prevent disturbances of the vestibular and visual systems [60]. It should be noted that the number of included studies for both shock attenuation quantities was limited, and high heterogeneity was present, probably resulting in underpowered meta-analyses.

Vertical and leg stiffness

Vertical and leg stiffness refers to how compliant, respectively, the whole lower body and the lower leg are to the exerted $F_{z,max}$. After a fatigue protocol, K_{leg} decreased while K_{vert} did not significantly change. The number of studies investigating K_{vert} and K_{leg} is limited and heterogeneity was small for K_{vert} and high for K_{leg}. It is unknown if the decrease in K_{leg} was caused by a decrease in $F_{z,max}$ or an increase in ΔL_{stance}. However, a decrease in K_{leg} implies a more compliant lower body with a decreased tolerance for impact forces after a fatigue protocol. Apte et al. [18] found a decreasing trend for K_{vert} which was not shown in this meta-analysis. This difference is likely the result of the methods used to define a trend (median and median absolute deviation versus MD and CI).

Vertical COM displacement

Qualitative subgroup analysis showed that ΔCOM_z increased with fatigue in novice, but not in more experienced runners. Differences in responses to fatigue based on experience level might be caused by a better ability of experienced runners to adopt an energetically efficient gait pattern with smaller ΔCOM_z [61,62]. A larger ΔCOM_z in novice runners might be caused by an increase in knee flexion because of more pronounced knee extensor strength loss with fatigue [40,63].

Lower body joint angles

Fatigue significantly increased knee flexion angles at initial contact and maximum knee flexion angles during the swing phase. An increase in knee flexion at initial contact increases the oxygen cost of running and is energetically costly [19]. This increase in knee flexion could be caused by knee extensor strength loss and decreased tolerance to imposed stretch loads with fatigue [40,63]. Other explanations for more knee flexion at initial contact include a decrease in the effective mass or an increase in active shock absorption [13]. An increase in maximum knee flexion angles during the swing phase could indicate that runners tried to decrease the moment of inertia of the leg about the hip joint, making it easier to swing the leg forward by decreasing required hip flexor torques while possibly increasing activation and metabolic costs of hamstrings and calf muscles [56,64]. None of the other investigated joint angles showed a pooled significant effect of fatigue. This lack of significant findings might be caused by conflicting significant changes in joint angles with fatigue or due to small sample sizes. Heterogeneity was moderate to high for multiple joint angles. Hence, it is likely that there is an additional confounding factor that could explain the conflicting findings for many joint angles. Possible confounding factors include the effect of foot strike pattern, experience level, running surface, shoe wear, sex, and familiarity with running till exhaustion. However, not enough information was available to perform subgroup analyses for the aforementioned factors.

Effect of different fatigue protocols

Fatigue protocols can differ in terms of distance, duration, speed, running surface, stopping criteria, etcetera. The speed of a fatigue protocol influences both kinematics [65] and the presence of kinematic changes after a fatigue protocol. Voloshin et al. [50] and Verbitsky et al. [51] split their subjects into a “fatigued” and “unfatigued” group based on their end-tidal carbon dioxide pressure after a fatigue protocol with a fixed speed. They found a significant increase in both peak tibial and peak sacral accelerations for the “fatigued” group but not for the “unfatigued” group. One subject who fell into the “unfatigued” group repeated the fatigue run on a different day and at a slightly higher fixed speed. During the second fatigue protocol, he was classified for the “fatigued” group and showed an increase in peak tibial acceleration. These findings strengthen the idea that there is a subject-specific threshold above which kinematic changes occur due to fatigue. This subject-specific threshold is expected to apply to running distance and duration as well. Studies typically did not provide enough information to determine if all runners reached their subject-specific threshold and were, therefore, truly fatigued. The distance of each fatigue protocol needed to be at least 3 km to impose a lower threshold on running-induced fatigue and to comply with the definition of long-distance running [21]. The assumption was made that all runners in all studies were fatigued after the fatigue protocol and that kinematic changes caused by running-induced fatigue did not differ between runs of different distances, speeds, or durations.

A measure of fatigue was provided by sixteen studies. Most studies reported RPE scores that were always 15 or higher, indicating that runners experienced the fatigue protocol from "hard" to "very, very hard" [26]. When subjects could decide to terminate the fatigue protocol, subjects were instructed to either run to volitional exhaustion or until a certain RPE score was achieved [26]. When RPE scores were used as a stopping criterion, none of the included quantities showed significant effects of fatigue [35,44,47,53,54]. This implies that terminating a fatigue protocol based on an RPE score below volitional exhaustion might not be sufficient to reach the subject-specific fatigue threshold for kinematic quantities included in this review.

Running kinematics have been shown to be largely comparable between treadmill and overground running [66]. However, one of the included studies investigated the effect of running surfaces on fatigue [29]. Peak tibial and head accelerations were found to be significantly lower on a treadmill versus an athletic track in an unfatigued state but not in a fatigued state. These differences in an unfatigued state might be related to lower reaction forces and alterations in the effective mass [29]. For this literature review, subgroup analysis for running surface was not possible since only six studies performed the pre-and post-fatigue measurements overground [5,29,39,42,43,45]. For two quantities, running surfaces tended to result in different effects of fatigue. The maximum knee angle during stance tended to decrease or show no change in overground measurements [5,42,44,45] while it tended to show no change or increase in treadmill measurements [13,32,34,35,46,53]. Additionally, the hip angle at midstance decreased in overground measurements [5,45] while it remained the same or increased in treadmill measurements [46]. It is unclear if these differences are truly caused by a difference in running surface or by other confounding factors, but it is recommended to more thoroughly investigate the effect of running surface on running kinematics in future research.

Effect of subject characteristics

Investigation of the effect of subject characteristics on kinematic changes due to fatigue heavily depended on the provided information from articles and was therefore limited to ΔCOM_z. As a response to fatigue, novice runners increased ΔCOM_z while more experienced

runners did not show a significant change on a group level. Less experienced runners showed larger kinematic changes due to fatigue than more experienced runners [49]. Multiple studies reported differences between less and more experienced runners. More experienced runners showed less maximal ankle plantarflexion after a fatigue protocol [35] while less experienced runners showed more ΔCOM_z, a smaller maximum ankle dorsiflexion angle, less ankle plantarflexion at toe-off and more maximum knee flexion during stance [46,48,49]. Since there are differences in responses to fatigue for runners with different experience levels, the training history of subjects should be reported, and the results of a fatigue study cannot easily be generalized to the total population of runners.

Most studies analyzed changes in kinematic quantities on a group level. However, inter-individual differences in running kinematics were already present in an unfatigued state [40,49,55] and became even more apparent in a fatigued state [40,43,48,49,55]. Especially changes in kinematics in opposite directions were often mentioned to result in a lack of significant findings on a group level. Siler and Martin [48] found that changes in maximal knee extension due to fatigue ranged from an increase of 7.8° to a decrease of 11.1°. Hence, already in 1991, it was proposed by Siler and Martin that future research should be sensitive to individual responses to fatigue. Running kinematics are unique for a runner, as well as the way they change with fatigue. Hence, it is recommended to investigate changes in running kinematics as a result of fatigue on a subject-specific level since group-level analysis might mask individual responses.

Limitations and future research

Studies often consisted of small sample sizes, had different fatigue protocols, and some kinematic quantities were investigated by a limited number of studies. All these factors increase heterogeneity and variability in the results. Many studies were likely underpowered, resulting in non-significant pooled findings. In multiple cases, conflicting significant changes for a quantity were reported. Part of the conflicting findings might be caused by confounding factors such as not reaching a subject-specific fatigue threshold, running surface, foot strike pattern, covered distance, experience level, or stopping criterium. For future studies, it is advised to investigate the possible influence of these factors or at least clearly report the fatigue protocol and subject characteristics. Heterogeneity of results was variable for the pooled significant findings that were found in this literature review, indicating some inconsistent results between studies. Hence, results of individual studies should be interpreted with caution, and results from this review should be treated carefully.

Multiple studies did not report exact p-values of statistical tests but only reported that the p-value was below or above a certain threshold, typically 0.05. The CI of MD was computed based on p-values when these were available. A conservative approach was used when p-values were reported to be below a defined threshold by assuming that the p-value was equal to that threshold. When p-values were actually lower than that threshold, this would result in a smaller standard error and CI and increase the weight of that particular study since the weight is based on the inverse variance. Hence, multiple studies finding significant differences without reporting the exact p-values were assigned lower weights in these meta-analyses, possibly underestimating the true effect of fatigue on multiple kinematic quantities.

There are many possible kinematic quantities to investigate when analyzing running gait, increasing the risk of reporting and publication bias. The risk of bias was minimized by performing a quality assessment and by estimating the heterogeneity between studies. The quality assessment showed that the mean quality was good, although studies scored poorly on questions related to external validity and power calculations. Heterogeneity was large for most kinematic quantities, indicating inconsistent findings based on I^2, supported by conflicting findings for multiple quantities. Results for kinematic quantities that did not significantly change with fatigue were often published, implying a small effect of reporting and publication bias. The effect of bias on this literature review was assumed to be limited and results were assumed to be valid for the investigated kinematic quantities.

The unfatigued and fatigued states were defined differently across studies. Some studies performed separate measurements before and after a fatigue protocol while others measured quantities during a fatigue protocol. Studies included different amounts of steps in their analyses and applied different filters to their data. Since this review focused on changes in kinematic quantities due to fatigue rather than the absolute values across studies, differences in data acquisition and processing are expected to have a similar influence on unfatigued and fatigued values and, therefore, a small influence on the result of this literature review.

To prevent general conclusions based on a small number of findings, only quantities that were investigated in a minimum of two studies were included. Hence, possible relevant findings mentioned in just one study were not taken into account, for example, studies investigating knee stiffness. Furthermore, $F_{z,max}$ and especially the impulse of $F_{z,max}$ were not included

in this review. Based on the results of this review, it is thought that ground reaction force variables in combination with shock attenuation, will provide additional insight into changes in shock attenuation mechanisms with fatigue and should be investigated in the future.

To limit the number of included kinematic quantities, joint angles in the frontal and transversal planes were not included in this review. Frontal and transversal plane joint angles have relatively large errors with respect to their ROM and their contribution to shock attenuation is expected to be smaller than for sagittal plane kinematics. However, Pratt [59] showed that ankle pronation also contributes to shock attenuation and it is therefore recommended to further investigate the effect of fatigue on frontal and transversal plane kinematics in future research.

Conclusions

This literature review showed that running kinematics change as a result of running-induced fatigue. As a consequence of fatigue, peak accelerations at the tibia increased, leg stiffness decreased, knee flexion at initial contact and maximum knee flexion increased and ΔCOM_z increased in novice but not in experienced runners. In addition, large inter-individual differences in responses to fatigue were found. Changes in running kinematics due to fatigue might be explained by a decrease in the tolerance of knee extensors to imposed stretch loads or a decrease in the neuromuscular control resulting in less spreading of the impact force impulse over time.

Recommendations

- Investigate kinematic changes due to fatigue on an individual instead of a group level
- Clearly report training history of subjects since results of runners with a certain experience level cannot be generalized to the total population of runners
- Investigate additional confounding factors to explain contradicting findings, especially concerning joint angles
- Investigate the effect of fatigue on joint angles in the frontal and transversal plane
- Investigate the effect of spreading of impact force impulses over time on peak accelerations

Acknowledgment

This study was supported by EFRO OP Oost (Grant number: 0784). The study sponsor had no involvement in the study design, data collection, analysis, interpretation, writing, or decision to submit the manuscript for publication. The authors would like to thank Bouke Scheltinga, Anne Haitjema, and Xanthe ter Wengel for their help with reviewing articles and Job van der Palen for his statistical advice.

References

1. Van Gent, R. N. et al. Incidence and determinants of lower extremity running injuries in long distance runners: A systematic review. Br. J. Sports Med. 41, 469–480 (2007).
2. Nielsen, R. O. et al. Training errors and running related injuries: a systematic review. Int J Sport. Phys Ther 7, 58–75 (2012).
3. Willems, T. M., Witvrouw, E., De Cock, A. & De Clercq, D. Gait-related risk factors for exercise-related lower-leg pain during shod running. Med. Sci. Sports Exerc. 39, 330–339 (2007).
4. Hreljac, A. Etiology, prevention, and early intervention of overuse injuries in runners: A biomechanical perspective. Phys. Med. Rehabil. Clin. N. Am. 16, 651–667 (2005).
5. Clansey, A. C., Hanlon, M., Wallace, E. S. & Lake, M. J. Effects of fatigue on running mechanics associated with tibial stress fracture risk. Med. Sci. Sports Exerc. 44, 1917–1923 (2012).
6. Gerritsen, K. G. M., Bogert, A. J. Van Den & Nigg, B. M. Direct dynamics simulation of the impact phase in heel-toe running. J. Biomech. 28, 661–666 (1995).
7. Derrick, T. R. The Effects of Knee Contact Angle on Impact Forces and Accelerations. Med. Sci. Sports Exerc. 36, 832–837 (2004).
8. Musgjerd, T., Anason, J., Rutherford, D. & Kernozek, T. W. Effect of Increasing Running Cadence on Peak Impact Force in an Outdoor Environment. Int. J. Sports Phys. Ther. 16, 1076–1083 (2021).
9. Breine, B. et al. Initial foot contact and related kinematics affect impact loading rate in running. J. Sports Sci. 35, 1556–1564 (2017).
10. Vanwanseele, B., Beéck, T. Op De, Schütte, K. & Davis, J. Accelerometer Based Data Can Provide a Better Estimate of Cumulative Load During Running Compared to GPS Based Parameters. 2, 1–7 (2020).

11. Sheerin, K. R., Reid, D. & Besier, T. F. The measurement of tibial acceleration in runners—A review of the factors that can affect tibial acceleration during running and evidence-based guidelines for its use. Gait Posture 67, 12–24 (2019).
12. Milner, C. E., Ferber, R., Pollard, C. D., Hamill, J. & Davis, I. S. Biomechanical Factors Associated with Tibial Stress Fracture in Female Runners. 323–328 (2006) doi:10.1249/01.mss.0000183477.75808.92.
13. Derrick, T. R., Dereu, D. & Mclean, S. P. Impacts and kinematic adjustments during an exhaustive run. Med. Sci. Sports Exerc. 34, 998–1002 (2002).
14. Lucas-Cuevas, A. G. et al. Effect of 3 Weeks Use of Compression Garments on Stride and Impact Shock during a Fatiguing Run. Int. J. Sports Med. 36, 826–831 (2015).
15. Mizrahi, J., Verbitsky, O., Isakov, E. & Daily, D. Effect of fatigue on leg kinematics and impact acceleration in long distance running. Hum. Mov. Sci. 19, 139–151 (2000).
16. Winter, S., Gordon, S. & Watt, K. Effects of fatigue on kinematics and kinetics during overground running : a systematic review. 57, 887–899 (2017).
17. Kim, H. K., Mirjalili, S. A. & Fernandez, J. Gait kinetics, kinematics, spatiotemporal and foot plantar pressure alteration in response to long-distance running : Systematic review. Hum. Mov. Sci. 57, 342–356 (2018).
18. Apte, S. et al. Biomechanical Response of the Lower Extremity to Running-Induced Acute Fatigue: A Systematic Review. Front. Physiol. 12, 1–16 (2021).
19. Valiant, G. A. Transmission and attenuation of heelstrike accelerations. (Human Kinetics Publishers, Champaign, IL, 1990).
20. Downs, S. H. & Black, N. The feasibility of creating a checklist for the assessment of the methodological quality both of randomised and non-randomised studies of health care interventions. J. Epidemiol. Community Health 52, 377–384 (1998).
21. Britannica, T. E. of E. Long-distance running. Brittanica https://www.britannica.com/sports/long-distance-running.
22. Hooper, P., Jutai, J. W., Strong, G. & Russell-Minda, E. Age-related macular degeneration and low-vision rehabilitation: A systematic review. Can. J. Ophthalmol. 43, 180–187 (2008).
23. McMahon, T. A. & Cheng, G. C. The mechanics of running: How does stiffness couple with speed? J. Biomech. 23, 65–78 (1990).
24. Farley, C. T. & González, O. Leg stiffness and stride frequency in human running. J. Biomech. 29, 181–186 (1996).

25. Della Croce, U., Leardini, A., Chiari, L. & Cappozzo, A. Human movement analysis using stereophotogrammetry Part 4: Assessment of anatomical landmark misplacement and its effects on joint kinematics. Gait Posture 21, 226–237 (2005).
26. Borg, G. A. V. Psychophysical bases of perceived exertion. Med. Sci. Sport. Exerc. 14, 377–381 (1982).
27. Higgins JPT, Li T, D. J. (editors). Chapter 6: Choosing effect measures and computing estimates of effect. in Cochrane Handbook for Systematic Reviews of Interventions version 6.3 (updated Febrauary 2022) (2022).
28. Deeks, J., Higgins, J. & Altman. Chapter 10: Analysing data and undertaking meta-analyses. in Cochrane Handbook for Systematic Reviews of Interventions version 6.3 (updated Febrauary 2022) (2022).
29. García-Pérez, J. A., Pérez-Soriano, P., Llana Belloch, S., Lucas-Cuevas, Á. G. & Sánchez-Zuriaga, D. Effects of treadmill running and fatigue on impact acceleration in distance running. Sport. Biomech. 13, 259–266 (2014).
30. Koblbauer, I. F., van Schooten, K. S., Verhagen, E. A. & van Dieën, J. H. Kinematic changes during running-induced fatigue and relations with core endurance in novice runners. J. Sci. Med. Sport 17, 419–424 (2014).
31. Higgins, J. P. T. & Thompson, S. G. Quantifying heterogeneity in a meta-analysis. Stat. Med. 21, 1539–1558 (2002).
32. Abt, J. P. et al. Running kinematics and shock absorption do not change after brief exhaustive running. J. Strength Cond. Res. 25, 1479–1485 (2011).
33. Avogadro, P., Dolenec, A. & Belli, A. Changes in mechanical work during severe exhausting running. Eur. J. Appl. Physiol. 90, 165–170 (2003).
34. Jewell, C., Boyer, K. A. & Hamill, J. Do footfall patterns in forefoot runners change over an exhaustive run? J. Sports Sci. 35, 74–80 (2017).
35. Maas, E., De Bie, J., Vanfleteren, R., Hoogkamer, W. & Vanwanseele, B. Novice runners show greater changes in kinematics with fatigue compared with competitive runners. Sport. Biomech. 17, 350–360 (2018).
36. Mizrahi, J., Verbitsky, O. & Isakov, E. Fatigue-induced changes in decline running. Clin. Biomech. 16, 207–212 (2001).
37. Mizrahi, J., Verbitsky, O. & Isakov, E. Fatigue-related loading imbalance on the shank in running: a possible factor in stress fractures. Ann. Biomed. Eng. 28, 463–469 (2000).
38. Mizrahi, J., Verbitsky, O. & Isakov, E. Shock accelerations and attenuation in downhill and level running. Clin. Biomech. 15, 15–20 (2000).

39. Murray, L., Beaven, C. M. & Hébert-Losier, K. The effects of running a 12-km race on neuromuscular performance measures in recreationally competitive runners. Gait Posture 70, 341–346 (2019).
40. Nicol, C., Komi, P. V. & Marconnet, P. Effects of marathon fatigue on running kinematics and economy. Scand. J. Med. Sci. Sports 1, 195–204 (1991).
41. Paquette, M. R., Milner, C. E. & Melcher, D. A. Foot contact angle variability during a prolonged run with relation to injury history and habitual foot strike pattern. Scand. J. Med. Sci. Sport. 27, 217–222 (2017).
42. Paquette, M. R. & Melcher, D. A. Impact of a long run on injury-related biomechanics with relation to weekly mileage in trained male runners. J. Appl. Biomech. 33, 216–221 (2017).
43. Rabita, G., Slawinski, J., Girard, O., Bignet, F. & Hausswirth, C. Spring-mass behavior during exhaustive run at constant velocity in elite triathletes. Med. Sci. Sports Exerc. 43, 685–692 (2011).
44. Bazett-Jones, D. M. et al. Effect of patellofemoral pain on strength and mechanics after an exhaustive run. Med. Sci. Sports Exerc. 45, 1331–1339 (2013).
45. Reenalda, J., Maartens, E., Buurke, J. H. & Gruber, A. H. Kinematics and shock attenuation during a prolonged run on the athletic track as measured with inertial magnetic measurement units. Gait Posture 68, 155–160 (2019).
46. Sanno, M., Willwacher, S., Epro, G. & Brüggemann, G. P. Positive work contribution shifts from distal to proximal joints during a prolonged run. Med. Sci. Sports Exerc. 50, 2507–2517 (2018).
47. Schütte, K. H. et al. Wireless tri-axial trunk accelerometry detects deviations in dynamic center of mass motion due to running-induced fatigue. PLoS One 10, (2015).
48. Siler, W. L. & Martin, P. E. Changes in Running Pattern during a Treadmill Run to Volitional Exhaustion: Fast versus Slower Runners. Int. J. Sport Biomech. 7, 12–28 (1991).
49. Strohrmann, C., Harms, H., Kappeler-Setz, C. & Tröster, G. Monitoring kinematic changes with fatigue in running using body-worn sensors. IEEE Trans. Inf. Technol. Biomed. 16, 983–990 (2012).
50. Voloshin, A. S., Mizrahi, J., Verbitsky, O. & Isakov, E. Dynamic loading on the human musculoskeletal system effect of fatigue. Clin. Biomech. 13, 515–520 (1998).
51. Verbitsky, O., Mizrahi, J., Voloshin, A., Treiger, J. & Isakov, E. Shock transmission and fatigue in human running. J. Appl. Biomech. 14, 300–311 (1998).

52. Bigelow, E. M. R., Elvin, N. G., Elvin, A. A. & Arnoczky, S. P. Peak impact accelerations during track and treadmill running. J. Appl. Biomech. 29, 639–644 (2013).
53. Dierks, T. A., Davis, I. S. & Hamill, J. The effects of running in an exerted state on lower extremity kinematics and joint timing. J. Biomech. 43, 2993–2998 (2010).
54. Dierks, T. A., Manal, K. T., Hamill, J. & Davis, I. Lower extremity kinematics in runners with patellofemoral pain during a prolonged run. Med. Sci. Sports Exerc. 43, 693–700 (2011).
55. Dutto, D. J. & Smith, G. A. Changes in spring-mass characteristics during treadmill running to exhaustion. Med. Sci. Sport. Exerc. 34, 1324–31 (2002).
56. Fuhr, D. P., Chiu, L. Z. F. & Kennedy, M. D. Compensatory changes in female running mechanics during a simulated 10 km race. J. Hum. Sport Exerc. 13, 89–98 (2018).
57. García-Pinillos, F. et al. Does fatigue alter step characteristics and stiffness during running? Gait Posture 76, 259–263 (2020).
58. Hanley, B. & Mohan, A. Changes in gait during constant pace treadmill running. J. Strength Cond. Res. 28, 1219–1225 (2014).
59. Pratt, D. J. Mechanisms of shock attenuation via the lower extremity during running. Clin. Biomech. 4, 51–57 (1989).
60. Pozzo, T., Berthoz, A. & Lefort, L. Head stabilization during various locomotor tasks in humans. Exp. Brain Res. 82, 97–106 (1990).
61. McMahon, T. A., Valiant, G. A. & Frederick, E. C. Groucho running. J. Appl. Physiol. 62, 2326–2337 (1987).
62. Anderson, T. Biomechanics and running economy. Sports Med. 22, 76–89 (1996).
63. Giandolini, M. et al. Fatigue associated with prolonged graded running. Eur. J. Appl. Physiol. 116, 1859–1873 (2016).
64. Williams, K. R., Snow, R. & Agruss, C. Changes in Distance Running Kinematics with Fatigue. Int. J. Sport Biomech. 7, 138–162 (1991).
65. Orendurff, M. S. et al. A little bit faster: Lower extremity joint kinematics and kinetics as recreational runners achieve faster speeds. J. Biomech. 71, 167–175 (2018).
66. Van Hooren, B. et al. Is Motorized Treadmill Running Biomechanically Comparable to Overground Running? A Systematic Review and Meta-Analysis of Cross-Over Studies. Sport. Med. 50, 785–813 (2020).

Appendix 2.A: Search strategy

This appendix provides an overview of search strings and additional limitations used for the different included databases (i.e., PubMed, Web of Science, Scopus). Note that “Marathon” was included in the search terms while other distances were not included in the search terms. Since “Marathon” is implicitly connected to running, the modality is not always mentioned together with “Marathon”. To be sure that articles investigating Marathon running wouldn’t be missed, “Marathon” was added to the search terms referring to the modality.

For PubMed, the MeSH term “Humans” was required and the full-text article needed to be available.

For Web of Science, titles, abstracts and keywords were searched. Additionally, results needed to be categorized as “article” and belong to one of the four following Web of Science categories; “Sport sciences”, ”Engineering biomedical”, ”Orthopaedics”, ”Biophysics”.

For Scopus, titles and abstracts were searched. Results needed to be categorized as “article” or “article in press”. The MedLine database was excluded from the Scopus search (MedLine was already included in the PubMed search). Furthermore, results needed to belong to one of the three following subject areas: “Engineering”, ”Medicine”, ”Health professions” and one of the following keywords needed to present; ”running”, ”exercise”, ”fatigue”, ”exertion”, ”athlete”, ”endurance”, ”biomechanics”. Results containing the keyword; “fatigue of materials” were excluded.

PubMed search string

(((((run[Title/Abstract] OR running[Title/Abstract] OR runner*[Title/Abstract] OR marathon[-Title/Abstract])) AND (exhaust*[Title/Abstract] OR exert*[Title/Abstract] OR prolong*[Title/Abstract] OR fatigue*[Title/Abstract])) AND (kinemat*[Title/Abstract] OR kinet*[Title/Abstract] OR biomechanic*[Title/Abstract] OR mechanic*[Title/Abstract] OR acceler*[Title/Abstract] OR centre-of-mass[Title/Abstract] OR center-of-mass[Title/Abstract] OR center-of-gravity[-Title/Abstract] OR centre-of-gravity [Title/Abstract] OR ground-reaction[Title/Abstract] OR angle[Title/Abstract] OR angular[Title/Abstract] OR force[Title/Abstract] OR moment*[Title/Abstract] OR impact[Title/Abstract] OR shock[Title/Abstract] OR inertia*[Title/Abstract] OR pressure[Title/Abstract]))) AND (full text[sb] AND Humans[Mesh])

Web of Science search string

(TS=((run OR running OR runner* OR marathon) AND (exhaust* OR exert* OR prolong* OR fatigue*) AND (kinemat* OR kinet* OR biomechanic* OR mechanic* OR acceler* OR centre-of-mass OR center-of-mass OR center-of-gravity OR centre-of-gravity OR ground-reaction OR angle OR angular OR force OR moment* OR impact OR shock OR inertia* OR pressure))) AND DOCUMENT TYPES: (Article)

Refined by: WEB OF SCIENCE CATEGORIES: (SPORT SCIENCES OR ENGINEERING BIOMEDICAL OR ORTHOPEDICS OR BIOPHYSICS)

Timespan: All years. Indexes: SCI-EXPANDED, SSCI, A&HCI, CPCI-S, CPCI-SSH, ESCI.

Scopus search string

TITLEABS ((run OR running OR runner* OR marathon) AND (exhaust* OR exert* OR prolong* OR fatigue*) AND (kinemat* OR kinet* OR biomechanic* OR mechanic* OR acceler* OR centre-of-mass OR center-of-mass OR center-of-gravity OR centre-of-gravity OR ground-reaction OR angle OR angular OR force OR moment* OR impact OR shock OR inertia* OR pressure)) AND KEY (running OR exercise OR fatigue OR exertion OR athlete OR endurance OR biomechanics) AND NOT KEY (fatigue-of-materials) AND NOT DBCOLL (medl) AND (LIMIT-TO (DOCTYPE , “ar”) OR LIMITTO (DOCTYPE , “ip”)) AND (LIMITTO (SUBJAREA , “MEDI”) OR LIMIT-TO (SUBJAREA , “ENGI”) OR LIMIT-TO (SUBJAREA , “HEAL”))

Appendix 2.B: Quality assessment

The quality assessment checklist (see Table 2.3 (short version) and Table 2.8) is based on 13 out of 27 items of the Downs and Black quality assessment checklist [20]. Fourteen items of the original Downs and Black quality assessment checklist were removed because they applied to intervention studies, comparison studies, follow-up measurements or adverse events and did not apply to the aim of this review. Three questions were adapted for the scope of this review. In question 3 of the original Downs and Black quality assessment checklist, “patients” was replaced by “subjects”. In question 4, “Interventions of interest” was replaced by “Fatigue protocol”. Question 13 (“were the staff, places, and facilities where the patients were treated, representative of the treatment the majority of patients receive?”) was replaced by “Was the setting of the fatiguing protocol representative for a typical run (i.e., overground and with a self-selected speed)?”. The adapted Downs and Black quality assessment checklist consists of 13 questions compared to the 27 questions from the original checklist.

In the original Downs and Black quality assessment checklist, question 27 is about the statistical power calculation. A study could score between zero and five points for their power calculation, out of a total of 32 possible points for the complete checklist. The weight factor of question 27 in the original checklist is therefore 16% (100*(5/32)). Since fourteen items were removed from the adapted quality checklist, a maximum of five points for question 27 would increase the weight of question 27 to 29% (100*(5/17)). Hence, the scoring of question 27 was adapted to keep the weight of question 27 around 15% by adjusting the maximum score for this question to two points instead of five (100*(2/14)=14%). Studies received 0 points if they had a power below 80% or when no power calculation was performed or reported. Studies with a power between 80% and 89% received 1 point. Studies with a power of 90% or higher received 2 points. Because of the new scoring of question 27, the maximum number of points that a study can score for the adapted Downs and Black quality assessment checklist is 14.

Quality labels were matched with quality scores based on the scoring of Hooper et al. [22]. This resulted in the following cut-off scores. A quality score between 0 and 7 points indicated a study of “Poor” quality, a score of 8 or 9 a study of “Fair” quality, a score of 10 till 12 a study of “Good” quality and a score of 13 or 14 a study of “Excellent” quality.”

Table 2.8: *Quality assessment checklist based on the Downs and Black quality assessment checklist [20]. UTD = Unable to determine.*

Quality assessment checklist		
#	Question	Scoring
Q1	**Is the hypothesis/aim/objective of the study clearly described?**	0/1
Q2	**Are the main outcomes to be measured clearly described in the Introduction or Methods section?** (If the main outcomes are first mentioned in the Results section, the question should be answered no)	0/1
Q3	**Are the characteristics of the subjects included in the study clearly described?** (Inclusion and/or exclusion criteria should be given. Some information regarding training history should be given (km/week, hr/week, years of training, 5k or 10k time))	0/1
Q4	**Is the fatigue protocol clearly described?** (Duration, distance and speed (two out of three) should be reported. Stopping criteria and setting of the fatigue protocol should be given)	0/1
Q6	**Are the main findings of the study clearly described?** (Simple outcome data (including denominators and numerators) should be reported for all major findings. This question does not cover statistical tests)	0/1
Q7	**Does the study provide estimates of the random variability in the data for the main outcomes?** (In non-normally distributed data the inter-quartile range of results should be reported. In normally distributed data the standard error, standard deviation or confidence intervals should be reported. If the distribution of the data is not described, it must be assumed that the estimates used were appropriate and the question should be answered yes)	0/1
Q10	**Have actual probability values been reported (e.g. 0.035 rather than <0.05) for the main outcomes except where the probability value is less than 0.001?**	0/1
Q11	**Were the subjects asked to participate in the study representative of the entire population from which they were recruited?** (The study must identify the source population/how subjects were recruited/how subjects were selected. The subject population that is included should be described (competitive, novice, experienced, marathon runners, etcetera))	0/1/UTD
Q13	**Was the setting of the fatiguing protocol representative for a typical run (i.e. overground and with a self-selected speed)?** (For the question to be answered yes the study should mimic a typical run (free to adapt running speed and running overground))	0/1/UTD
Q16	**If any of the results of the study were based on "data dredging", was this made clear?** Any analyses that had not been planned at the outset of the study should be clearly indicated. If no retrospective unplanned subgroup analyses were reported, then answer yes.	0/1/UTD

Quality assessment checklist		
#	Question	Scoring
Q18	**Were the statistical tests used to assess the main outcomes appropriate?** (The statistical techniques used must be appropriate to the data. For example, non-parametric methods should be used for small sample sizes. Where little statistical analysis has been undertaken but where there is no evidence of bias, the question should be answered yes. If the distribution of the data (normal or not) is not described it must be assumed that the estimates used were appropriate and the question should be answered yes)	0/1/UTD
Q20	**Were the main outcome measures used accurate (valid and reliable)?** (For studies where the outcome measures are clearly described, the question should be answered yes. For studies that refer to other work or that demonstrates the outcome measures are accurate, the question should be answered as yes)	0/1/UTD
Q27	**Did the study have sufficient power to detect a clinically important effect where the probability value for a difference being due to chance is less than 5%?** (Sample sizes have been calculated to detect a difference of x% and y%. 70% (power of 0.7) = 0 points, 80-89% (power of 0.8-0.89) = 1 point, 90-99% (power of 0.9-0.99) = 2 points)	0/1/2/ UTD

Chapter 3

Quantifying and correcting for speed and stride frequency effects on running mechanics in fatiguing outdoor running

Submitted for publication as:
Zandbergen, M.A., Buurke, J.H., Veltink, P.H., Reenalda, J. Quantifying and correcting for speed and stride frequency effects on running mechanics in fatiguing outdoor running

The data presented in this study will be openly available in 4TU.ResearchData.

Abstract

Background: Real-time feedback on impact-related quantities in running is of interest to prevent injuries. Many quantities are typically measured in a controlled laboratory setting, even though most runners run in uncontrolled outdoor environments. While monitoring running mechanics in an uncontrolled environment, a decrease in speed or stride frequency can mask fatigue-related changes in running mechanics.

Aim: This study aimed to quantify and correct for the subject-specific effects of running speed and stride frequency on changes in impact-related running mechanics during a fatiguing outdoor run.

Methods: Nine runners ran a competitive marathon while peak tibial acceleration and knee angles were measured with inertial measurement units. Running speed was measured through GPS-based sports watches. Median values over segments of 25 strides throughout the marathon were computed and used to create subject-specific multiple linear regression models. These models predicted peak tibial acceleration, knee angles at initial contact, and maximum stance phase knee flexion based on running speed and stride frequency. Data for all subjects were corrected for individual speed and stride frequency effects during the marathon. The speed and stride frequency corrected and uncorrected data were divided into ten stages to investigate the effect of marathon stage on mechanical quantities.

Results and significance: Running speed and stride frequency explained on average 20% to 30% of the variance in peak tibial acceleration, knee angles at initial contact, and maximum stance phase knee angles while running in an uncontrolled setting. Regression coefficients for speed and stride frequency varied strongly between subjects. Speed and stride frequency corrected peak tibial acceleration and maximum stance phase knee flexion increased throughout the marathon. At the same time, uncorrected values showed no significant differences between marathon stages due to a decrease in running speed. Hence, subject-specific effects of changes in speed and stride frequency on running mechanics should be corrected for when interpreting or providing feedback on the gait pattern in uncontrolled environments.

Introduction

Motion analysis in running provides objective information about running technique. This information can be used to improve running performance [1,2], monitor effects of fatigue on the gait pattern [3,4], and possibly reduce injury risk through real-time feedback on mechanical quantities [5,6]. The repetitiveness of impact forces during running is thought to be related to the development of running injuries [7,8]. Impact forces cause a rapid deceleration of the foot after initial contact, shortly followed by deceleration of the lower leg, upper leg, pelvis, and upper body [9]. Accelerometers can quantify the magnitude of deceleration at, for instance, the tibia (i.e., peak tibial acceleration (PTA)) and thereby reflect the effect of impact forces when force plates are unavailable. Impact forces can be modulated by controlling the knee angle [10], which makes PTA and knee angles interesting quantities to monitor with respect to injury risk.

Traditionally, running mechanics were measured in a gait laboratory. A laboratory setting allows researchers to control or minimize influences on the gait pattern from, for instance, running speed, inclination, running surface, and the weather. Simultaneously, a laboratory setting is restricted to an artificial environment that is not sport-specific. Multiple mechanical quantities concerning peak accelerations and shock attenuation showed important differences between overground and treadmill running [11–14]. Hence, running mechanics should be analyzed in a representative environment since findings from laboratory-based treadmill studies cannot easily be generalized to overground running [14–16].

One essential difference between treadmill and outdoor running is the ability to adapt running speed. Most runners lower their speed after prolonged running due to fatigue [17,18]. The influence of running speed and stride frequency on mechanical variables has extensively been studied in controlled environments and typically on a treadmill. PTA increases with an increase in running speed [19] or a decrease in stride frequency [20]. PTA showed a strong significant linear regression with speed in treadmill running [21,22]. Individual variances in these relationships were large, highlighting the need for subject-specific analysis [19,21]. Additionally, maximum stance phase knee flexion increased with an increase in speed or a decrease in stride frequency [23,24]. No speed effect on knee flexion angles at initial contact was found over a small range of running speeds in recreational runners [23]. Hence, running speed and stride frequency influence PTA and some measures related to knee angles in running. Two previous studies corrected mechanical quantities during running in an uncontrolled setting for speed

by computing individual ratios (i.e., dividing by speed) [17,18]. This correction assumes that the relationship between speed and quantities of interest is linear and crosses the origin for all subjects. In the case of PTA, the regression equation between speed and PTA differs between foot strike patterns [18], between subjects [19] and the intercepts of group-based analyses do not appear to cross the origin [18]. Thus, individual ratios likely oversimplify the relationship between speed and quantities of interest.

Inertial measurement units (IMUs) can measure running mechanics in a sport-specific setting and open up new possibilities for real-time feedback on running technique in a representative environment [16]. PTA is often used as bio-feedback quantity to improve running technique and prevent injuries by providing feedback on high PTA values, both in commercial devices and in research [25–29]. Additionally, algorithm development allows the estimation of knee angles based on a minimal sensor set [30]. Feedback on running technique is often based on an arbitrary fixed threshold independent of running speed and stride frequency which can mask fatigue-related changes in running biomechanics. Without correcting for the effects of speed and stride frequency, the origin of changes is unclear, preventing appropriate interpretation and feedback on running biomechanics. Hence, this study aims to quantify and correct for the subject-specific effect of running speed and stride frequency on changes in impact-related running mechanics during a fatiguing outdoor run.

A marathon was used as an uncontrolled setting to ensure that a wide range of external influences (e.g., fatigue, different surfaces, other runners) found in typical uncontrolled outdoor running were incorporated to improve the ecological validity of relationships. We hypothesized that:

- Running speed and stride frequency decrease toward the end of the marathon
- The influence of running speed and stride frequency on PTA, knee angles at initial contact, and maximum stance phase knee flexion angles differs between subjects
- Speed and stride frequency influence the interpretation of running mechanics in uncontrolled settings

Methods

Participants

Nine healthy recreational runners participated in this study. Technical errors resulted in missing data for two subjects. Therefore, data from three females and four males were included (mean (standard deviation); age: 36 (11) years, height: 181 (5) cm, mass: 74 (8) kg, running experience: 7 (4) years). All subjects gave written informed consent before participating in this study. The Ethics Committee Computer and Information Science of the University of Twente approved the study protocol.

Measurement systems

Subjects were equipped with eight IMUs (240 Hz, MVN Link, Xsens Technologies, Enschede, The Netherlands). IMUs were placed on the sternum, back of the pelvis, and bilaterally on the midportion of the lateral upper leg, proximally on the tibia, and on the midfoot. Hair on the skin was shaved to improve IMU attachment before IMUs were fixed to the skin with double-sided tape and covered with additional tape. IMUs on the midfoot were placed under the tongue of the shoes. Wires between IMUs were loosely taped to the skin to prevent entanglement, see Figure 3.1. IMUs were connected with a bodypack and battery pack. The bodypack delivered power from the battery pack to the IMUs and synchronized and stored data from the IMUs on internal memory. The bodypack and battery pack weighed 220 grams [31] and were placed in a neoprene storage belt around the waist of the runners. Subjects used their personal sports watches with a global positioning system (GPS), measuring GPS coordinates with different sampling frequencies (on average 0.7 (0.4) Hz).

Figure 3.1: *One of the runners a few meters before the finish line. The bodypack and battery pack are placed in the pink belt. White tape is visible, which covers the sensors and fixates sensor wires.*

Measurement protocol

Measurements were performed during the Enschede marathon (42.195 km) in the Netherlands on a typical Dutch spring day with temperatures around 10 °C. The course was relatively flat, with about 170 meters of elevation. Before the marathon, multiple anthropometric values were measured (body height, hip height, hip width, knee height, ankle height, and shoe length). Sensor-to-segment calibration was performed according to the manufacturer's recommendations [32]. Subjects were instructed to run their marathon as planned and not to worry about the equipment.

Data analysis

The data presented in this study will be openly available in 4TU.ResearchData.

Data extraction and computing speed

Sensor data was extracted from the internal memory of the bodypack. Proprietary filtering based on sensor acceleration, angular velocity, and magnetometer data was used to estimate sensor orientations in the software package Xsens MVN Analyze (version 2019.2.1). A scaled biomechanical model was created based on anthropometric measurements, raw sensor data (accelerations and angular velocities), and estimated sensor orientations. Knee flexion angles were obtained from this scaled biomechanical model [32]. Latitude and longitude coordinates were extracted from the GPS data. Missing latitude-longitude coordinates were linearly interpolated before speed was computed as the distance between two latitude-longitude coordinates based on the Haversine formula [33]. Speeds above 20 km/h were deemed extremely unlikely and replaced with spline interpolation. Speed was then resampled to 240 Hz to match the sampling frequency of the IMUs.

Temporal synchronization

GPS and IMU data were temporally aligned based on GPS speed and speed of the pelvis IMU. Pelvis IMU speed was computed as the resultant pelvis IMU velocity obtained from the scaled biomechanical model. GPS and IMU data were then synchronized by cross-correlating GPS speed with pelvis IMU speed. Temporal alignment between both systems was visually checked at the start and end of the marathon to ensure that possible differences in internal clocks would not influence temporal alignment. Visual misalignment was present in data of one subject, for which IMU data was resampled based on cross-correlation of the first and last 20% of the data points separately.

Removing walking parts and segmentation

Some participants walked for short periods during the marathon to drink something or due to fatigue. PTA is higher for running than for walking [9]. Walking parts were detected and removed based on a minimum of two adjacent outliers in PTA of the right leg. In this case, an outlier was defined as a PTA value of more than four scaled median absolute deviations below the median over the complete marathon [34]. Additionally, ten strides before and after a walking part were removed to omit the effect of slowing down and increasing speed. After removing the walking parts, data were segmented into time-normalized gait cycles starting with initial contact based on right foot accelerations [35].

Extracting quantities of interest and removing outliers

Quantities of interest were computed for the right legs from all subjects. PTA was defined as the positive acceleration peak in the axial direction of the tibia in a sensor-fixed coordinate system during the first 33% of the gait cycle. Accelerations in the axial direction compared to the resultant acceleration were chosen to better represent the main direction of impact forces in the body. Knee flexion angles were defined as 0° when the leg was fully extended, and flexion resulted in positive values. The knee angle at initial contact was extracted from the first sample of the time-normalized gait cycle. Maximum stance phase knee flexion was defined as the maximum knee angle during the first 33% of the gait cycle. Stride frequency (strides/minute) was based on the time between two right initial contacts. Speed was averaged over the complete gait cycle. The average foot strike angle (i.e., angle between the foot and horizon in the sagittal plane at initial contact) over the complete marathon was computed to determine the foot strike pattern of subjects [36]. Outliers in quantities of interest were defined as values deviating more than four scaled median absolute deviations from the moving median over a window of 500 strides. A relatively large deviation from the median value was chosen to classify outliers to prevent removal of a considerable amount of data and over-smoothing the data. All strides with an outlier in any of the quantities of interest were removed from further analyses.

Median values over segments of 25 strides were computed, and outliers were removed (>4 scaled median absolute deviation from moving median over a window of 500 segments) to improve data stability and reduce the amount of data [37]. The marathon was divided into ten stages to investigate the effect of marathon stage; each stage was roughly equal to 4 km of running data. Mean values for each stage of the marathon were computed from the earlier defined median values, see Figure 3.2.

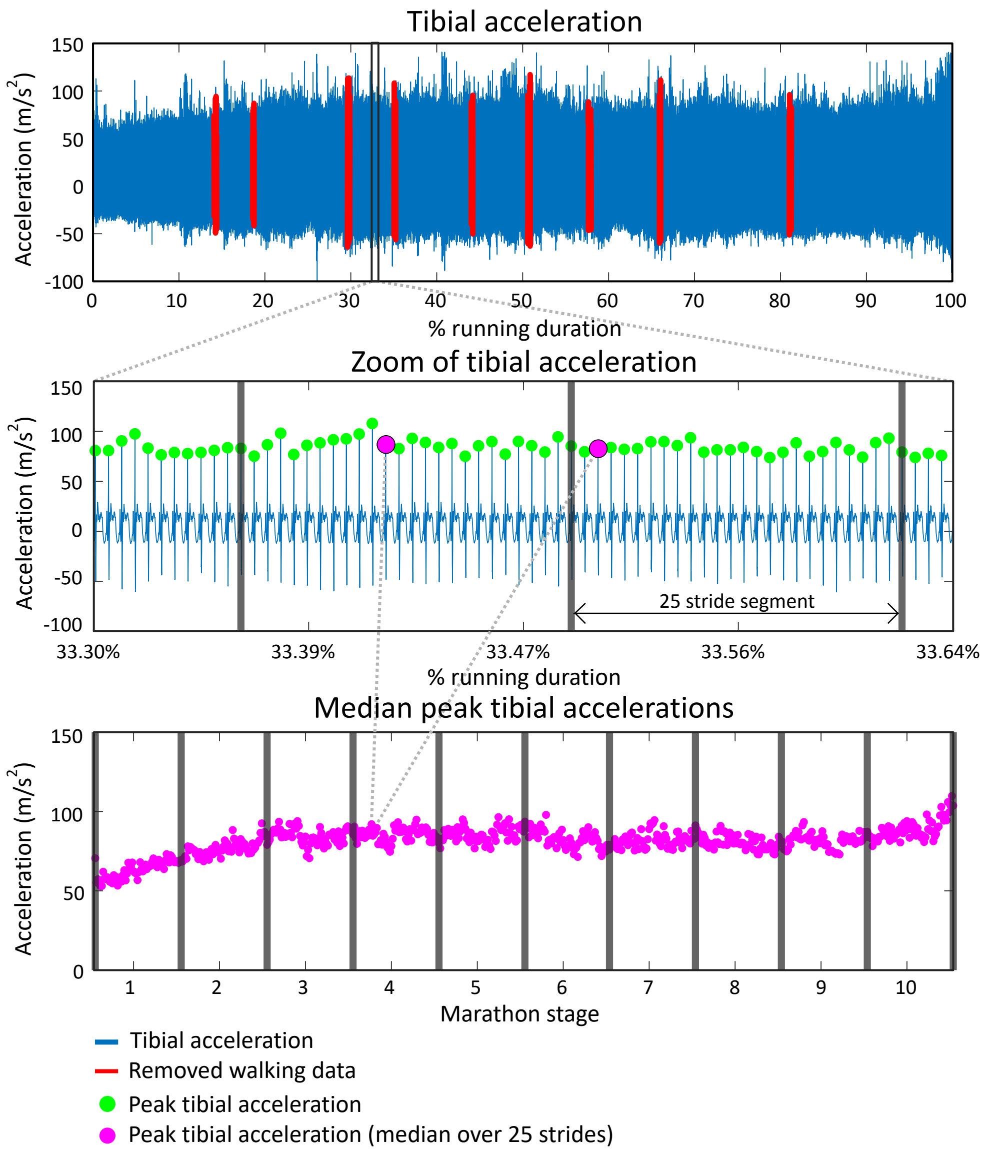

Figure 3.2: *Data extraction shown for peak tibial acceleration (PTA). The top figure shows the tibial acceleration of one subject during the full marathon. Walking parts are labeled red and removed from further analysis. The middle figure shows a snapshot of the tibial acceleration signal in which PTAs are shown with green dots. Vertical grey lines show segments of 25 strides from which the median PTA is computed and shown as a pink dot. The bottom figure shows all median PTA values during the marathon. The full marathon duration is divided into ten stages for group-based statistical analyses.*

Statistical analysis

Group-based one-way repeated measures ANOVAs were performed to test whether running speed, stride frequency, PTA, knee angles at initial contact, and maximum stance phase knee flexion changed over the different stages of the marathon. The ANOVAs had ten levels (stages of the marathon), and the mean values for each subject for all ten stages were used as input. When a significant effect of marathon stage on one of the quantities of interest was found, post hoc tests were used to test which marathon stages differed from each other.

Subject-specific multiple linear regression models were created to test if running speed and stride frequency could predict PTA, knee angles at initial contact, and maximum stance phase knee flexion angles. Median values for all 25 stride segments were used as input for the regression models, and no distinction for marathon stage was made. Intercepts and coefficients from the subject-specific regression equations were used to correct PTA and knee angles for the subject-specific effect of changes in speed and stride frequency.

Speed and stride frequency corrected quantities were computed by subtracting the product of the coefficient for speed with the deviation from the mean speed and by subtracting the product of the coefficient for stride frequency with the deviation from the mean stride frequency for all median values. Effectively, this creates a signal in which speed and stride frequency are equal to the average speed and stride frequency during the whole marathon. Group-based one-way repeated measures ANOVAs (10-levels) were repeated to test whether speed and stride frequency corrected PTA, knee angles at initial contact, and maximum stance phase knee flexion changed over the different stages of the marathon.

An alpha level of 0.05 was used to determine statistical significance. When applicable, Holm-Bonferroni corrections were applied for all possible 45 post hoc pairwise comparisons. Correlations were interpreted as very strong r = (0.90, 1.00), strong for r = (0.70, 0.89), moderate for r = (0.40, 0.69), weak for r = (0.20, 0.39) and very weak for r = (0.00, 0.19) [38].

Results

Subjects finished the marathon in 3 hours and 55 minutes (30 minutes), with an average speed of 11.0 (1.5) km/h and an average stride frequency of 85.6 (2.9) strides/minute. Walking parts resulted in the removal of 2.7 (2.1)% of all data points. An average of 19383 (2073) gait cycles were measured per runner, of which 8.8 (2.4)% was removed due to outliers. Runners 1 and 5 were classified as non-rearfoot strikers based on a foot contact angle smaller than 8° [36].

Speed and stride frequency

There was a statistically significant effect of marathon stage on speed on a group level, $F(9,54) = 5.766$, $p < 0.001$, see Figure 3.3. Running speed decreased from 11.5 (1.8) km/h to 10.3 (1.4) km/h between the first and last stages of the marathon. Post-hoc analyses showed that speed during the last two stages was lower than in the first four stages of the marathon. No significant effect of marathon stage on stride frequency was found on a group-level, $F(9,54) = 0.725$, $p = 0.684$. Speed and stride frequency were weakly correlated on a group level, $r = 0.21$ (0.18).

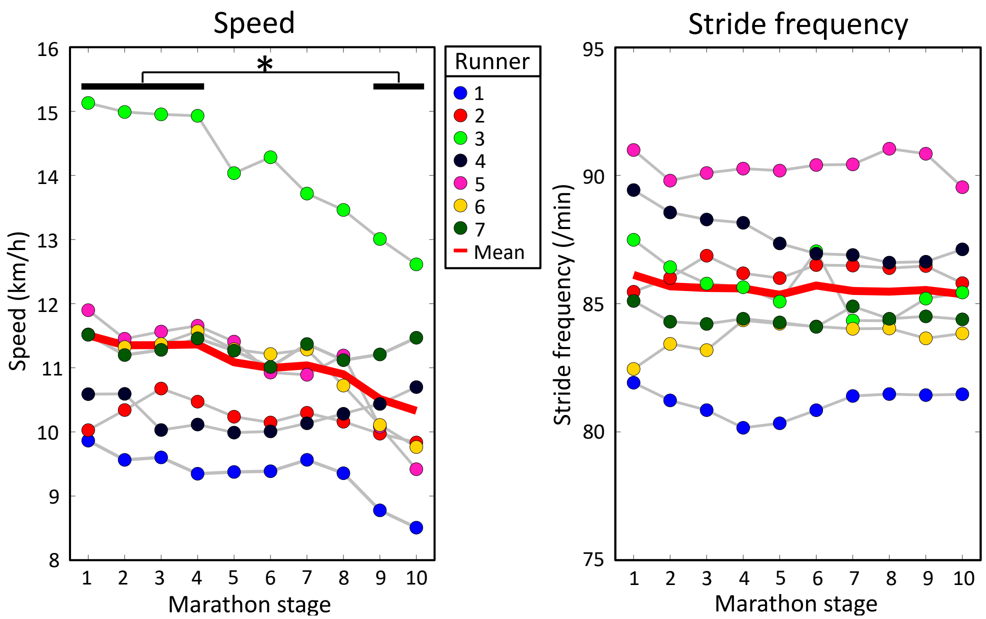

Figure 3.3: *Mean speed and stride frequency for every runner during all marathon stages. The solid red lines show the group means. A significant effect of marathon stage on speed was found. Significant results from post hoc analyses are shown by an asterisk at the top of the figure.*

Peak tibial acceleration

On a group level, PTA had a moderate positive correlation with speed (r = 0.40 (0.24)) and a very weak negative correlation with stride frequency (r = -0.09 (0.20)), see Table 3.1. Subject-specific multiple linear regression equations to predict PTA based on speed and stride frequency were significant for all subjects and explained 26 (18)% of the variance in PTA, see Figure 3.4. Speed was a significant predictor of PTA for all runners while stride frequency was a significant predictor for all but one runner. On a group level, there was a statistically significant effect of marathon stage on PTA both for uncorrected ($F(9,54) = 2.786$, $p = 0.009$) and speed and stride frequency corrected values ($F(9,54) = 2.316$, $p = 0.028$). However, post hoc analyses only showed significant differences in PTA between marathon stages after correcting for speed and stride frequency, see Figure 3.5. PTA corrected for speed and stride frequency was higher in the third (77.5 (17.3) m/s^2) compared to the first stage of the marathon (71.0 (17.5) m/s^2).

Table 3.1: *Left side of table: Individual correlations of peak tibial acceleration (PTA) with speed and stride frequency (SF). Right side of table: Individual regression equations to predict PTA based on speed and stride frequency together with the adjusted R-squared value (i.e., explained variance of regression equation). r = Pearson's correlation coefficient, SD = standard deviation, ns = non-significant finding, NRF = non-rearfoot striking subject.*

PTA	Correlation		Regression			
	Speed (r)	SF (r)	Intercept	Coefficient speed $\left(\frac{m/s^2}{km/h}\right)$	Coefficient SF $\left(\frac{m/s^2}{strides/min}\right)$	Adjusted R^2
Runner 1 NRF	0.48	-0.22	148.18	4.14	-1.37	0.31
Runner 2	0.33	0.11	65.78	3.75	-0.31 ns	0.11
Runner 3	0.55	0.11	106.14	4.83	-0.77	0.32
Runner 4	0.17	-0.21	115.32	1.45	-0.93	0.08
Runner 5 NRF	0.79	0.12	23.27 ns	7.76	-0.43	0.62
Runner 6	0.44	-0.17	114.41	2.00	-0.89	0.21
Runner 7	0.06 ns	-0.39	479.17	1.53	-4.92	0.16
Mean (SD)	0.40 (0.24)	-0.09 (0.20)	150.32 (150.50)	3.64 (2.26)	-1.37 (1.60)	0.26 (0.18)

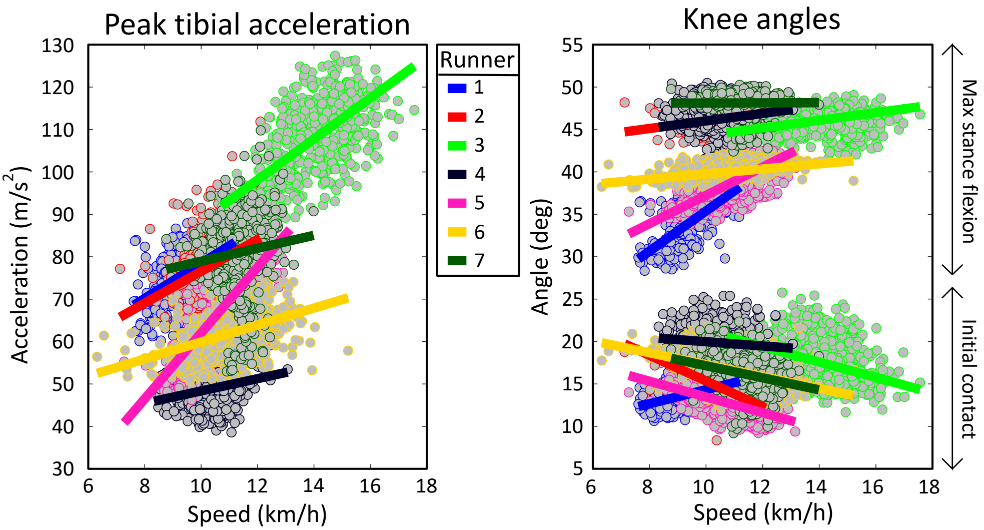

Figure 3.4: *Scatterplot of individual peak tibial acceleration and knee angle values as a function of speed. Each dot represents the median value over a segment of 25 strides during the marathon. Subject-specific linear regressions are shown as solid lines.*

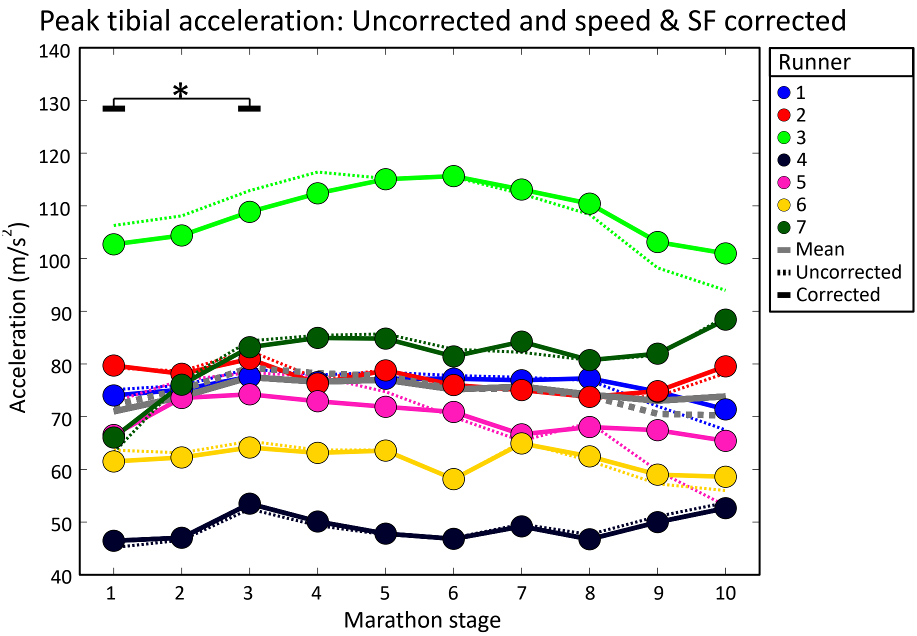

Figure 3.5: *Individual mean peak tibial accelerations during all marathon stages. Dotted lines show uncorrected PTA values (i.e., as measured during the marathon). Solid lines represent speed and stride frequency corrected PTA values. Grey lines show the group means. Significant effects of running duration are shown with an asterisk and black lines. Solid black lines represent significant differences in corrected PTA values.*

Knee angle at initial contact

On a group level, knee angles at initial contact showed a weak negative correlation with speed (r =-0.24 (0.30)) and a very weak negative correlation with stride frequency (r =-0.03 (0.28)), see Table 3.2. Subject-specific multiple linear regression equations to predict knee angles at initial contact based on speed and stride frequency were significant for all subjects and explained 20 (10)% of the variance in knee angles at initial contact, see Figure 3.6. Speed was a significant predictor of knee angles at initial contact for all runners while stride frequency was a significant predictor for all but two runners. On a group level, there was a statistically significant effect of marathon stage on both corrected ($F(9,54) = 5.136$, $p < 0.001$) and uncorrected knee angles at initial contact ($F(9,54) = 7.227$, $p < 0.001$). Knee angles at initial contact during later stages of the marathon were significantly higher than during the first stages of the marathon.

Table 3.2: *Left side of table: Individual correlations of knee angles at initial contact (IC) with speed and stride frequency (SF). Right side of table: Individual regression equations to predict knee angles at IC based on speed and stride frequency together with the adjusted R-squared value (i.e., explained variance of regression equation). r = Pearson's correlation coefficient, SD = standard deviation, ns = non-significant finding, NRF = non-rearfoot striking subject.*

Knee IC	**Correlation**		**Regression**			
	Speed (r)	SF (r)	Intercept	Coefficient speed $\left(\frac{deg}{km/h}\right)$	Coefficient SF $\left(\frac{deg}{strides/min}\right)$	Adjusted R^2
Runner 1 NRF	0.37	0.02 ns	10.08	0.83	-0.05 ns	0.13
Runner 2	-0.44	-0.24	44.34	-1.52	-0.16 ns	0.19
Runner 3	-0.29	0.06 ns	2.04 ns	-0.91	0.33	0.12
Runner 4	-0.15	-0.42	78.54	-0.25	-0.64	0.18
Runner 5 NRF	-0.51	0.19	-17.90	-0.93	0.45	0.36
Runner 6	-0.43	0.40	-45.22	-0.70	0.83	0.32
Runner 7	-0.25	-0.21	67.32	-0.71	-0.51	0.09
Mean (SD)	-0.24 (0.30)	-0.03 (0.28)	19.89 (45.40)	-0.60 (0.73)	0.04 (0.53)	0.20 (0.10)

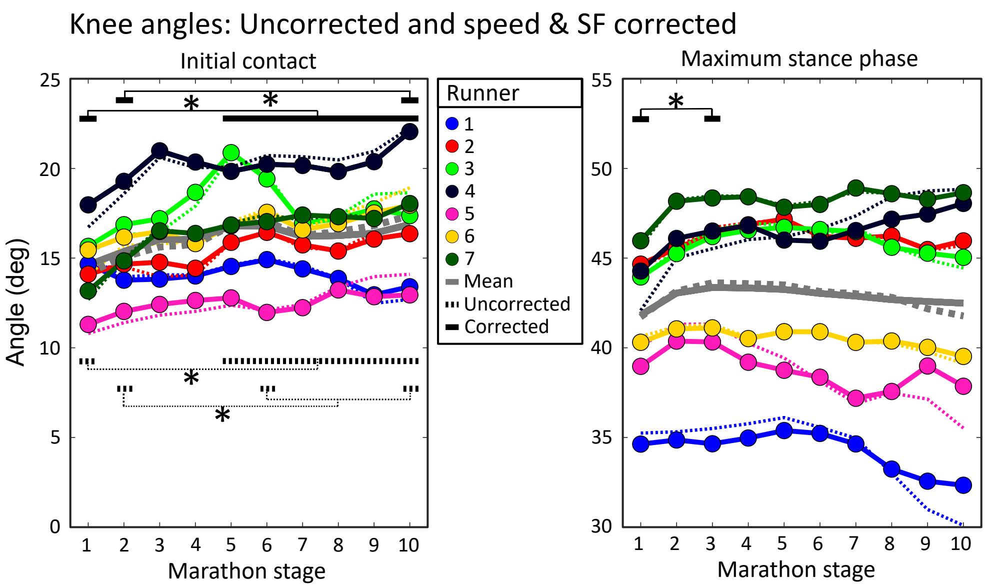

Figure 3.6: *Individual mean knee angles during all marathon stages. The left figure shows knee angles at initial contact, while the right figure shows maximum stance phase knee flexion angles. Dotted lines show uncorrected knee angles (i.e., as measured during the marathon). Solid lines represent speed and stride frequency corrected knee angles. Dotted black lines represent significant differences in uncorrected knee angles while solid black lines represent significant differences in knee angles corrected for the effect of changes in speed and stride frequency. Grey lines show the group means. Significant effects of marathon stage are shown with an asterisk and black lines.*

Maximum stance phase knee angles

On a group level, maximum stance phase knee angles had a weak positive correlation with speed (r = 0.32 (0.27)) and a weak negative correlation with stride frequency (r =-0.21 (0.28)), see Table 3.3. Subject-specific multiple linear regression equations to predict maximum stance phase knee angles based on speed and stride frequency were significant for all subjects and explained 30 (20)% of the variance in maximum stance phase knee angles, see Figure 3.6. Speed was a significant predictor for maximum stance phase knee angles for all runners while stride frequency was a significant predictor for all but one runner. On a group level, marathon stage had no statistically significant effect on maximum stance phase knee flexion ($F(9,54)$ = 1.770, p = 0.096). After correcting knee angles for subject-specific effects of speed and stride frequency, a significant effect of marathon stage on maximum stance phase knee flexion was found ($F(9,54)$ = 2.294, p = 0.029). Maximum stance knee flexion corrected for speed and stride frequency was significantly higher in the third (43.4 (4.9)) compared to the first stage of the marathon (41.8 (4.0)).

Table 3.3: *Left side of table: Individual correlations of maximum stance phase knee angles with speed and stride frequency (SF). Right side of table: Individual regression equations to predict maximum stance phase knee angles based on speed and stride frequency together with the adjusted R-squared value (i.e., explained variance of regression equation). r = Pearson's correlation coefficient, SD = standard deviation, ns = non-significant finding, NRF = non-rearfoot striking subject.*

Knee stance	Correlation		Regression			
	Speed (r)	SF (r)	Intercept	Coefficient speed $\left(\frac{deg}{km/h}\right)$	Coefficient SF $\left(\frac{deg}{strides/min}\right)$	Adjusted R^2
Runner 1 ^{NRF}	0.59	-0.27	76.58	2.37	-0.80	0.48
Runner 2	0.31	0.25	25.13	0.45	0.19	0.11
Runner 3	0.22	-0.22	62.92	0.45	-0.27	0.17
Runner 4	0.03 ^{ns}	-0.69	152.86	0.44	-1.27	0.49
Runner 5 ^{NRF}	0.69	-0.08	63.90	1.67	-0.48	0.54
Runner 6	0.42	-0.17	48.46	0.30	-0.14	0.20
Runner 7	-0.04 ^{ns}	-0.30	89.40	0.01 ^{ns}	-0.49	0.09
Mean (SD)	0.32 (0.27)	-0.21 (0.28)	74.18 (40.27)	0.81 (0.86)	-0.47 (0.47)	0.30 (0.20)

Discussion

This research aimed to quantify and correct for the subject-specific effect of changes in running speed and stride frequency on impact-related running mechanics during a fatiguing outdoor run. Mostly in line with our hypothesis, speed decreased throughout the marathon while no effect of marathon stage on stride frequency was found. PTA and maximum stance phase knee flexion corrected for changes in speed and stride frequency increased throughout the marathon, while uncorrected values showed no significant change. Running speed and stride frequency explained, on average 20 to 30% of the variance in PTA, knee angles at initial contact, and maximum stance phase knee flexion while running in an uncontrolled setting. Regression coefficients for speed and stride frequency varied strongly between subjects. Hence, the subject-specific effects of changes in speed and stride frequency on running mechanics should be corrected for when interpreting or providing feedback on the gait pattern in uncontrolled environments.

Speed and stride frequency

Running speed significantly decreased during the marathon. A decrease in speed during a marathon is typically found [17,18,39,40] and is likely caused by fatigue, although race strategy can also play a role. Stride frequency did not show a significant effect of marathon stage and was

weakly correlated with speed, indicating that, similar to previous studies, the speed reduction is generally caused by a decrease in stride length instead of stride frequency [17,41]. The significance of predictors, regression equations, and explained variances differed between subjects. Differences might be caused by differences in body weight, ankle angle at initial contact [10], foot strike pattern [18], individual differences in adaptations to speed by increasing step length versus stride frequency, differences in the tolerance to effects of fatigue and differences in the capacity to sustain a stable gait pattern over a range of speeds. Even though stride frequency did not change on a group level, adding stride frequency to the regression models resulted in significantly better predictions for almost all runners, emphasizing the benefits of subject-specific analysis versus group-based analysis.

Peak tibial acceleration

Average group-based PTA values showed a significant main effect of marathon stage, although post hoc analyses showed no differences between marathon stages for uncorrected values. PTA values were within the range found in literature [18,19,42]. The correlations between PTA and speed ($r = 0.40$ (0.24)) during a marathon were similar to the correlations between resultant PTA and speed in controlled settings ($r = 0.42$) [19]. Subject-specific multiple linear regressions showed that, on average, PTA increased with 3.6 m/s^2 for every 1 km/h increase in speed, although subject-specific coefficients ranged from 1.5 m/s^2 to 7.8 m/s^2. The speed coefficient of PTA was between 4.1 m/s^2 and 6.7 m/s^2 in controlled settings [19,22] . The speed coefficient to predict PTA in our study was generally lower than in laboratory-based studies, possibly due to the inclusion of stride frequency or external influences like fatigue. Foot strike pattern has been shown to influence the speed coefficient of PTA during a marathon. Rearfoot striking runners showed higher speed coefficients (12.8 m/s^2) than midfoot striking runners (7.0 m/s^2), while no significant speed coefficient was found for forefoot striking runners [18]. In our study, the two non-rearfoot striking runners (subjects 1 and 5) had amongst the highest speed coefficients, which is possibly an effect of group- versus subject-based analysis. The regression equation explained, on average, 26 (18)% of the variance in PTA. Although relatively low, it is higher than the 19% of explained variance in resultant PTA found in laboratory-based studies [19]. To accurately predict PTA in outdoor environments, more variables are needed in the multiple linear regression equation (e.g., knee angle at initial contact), but for the scope of this paper, we were solely interested in the explained variance by speed and stride frequency. After correcting PTA for the subject-specific effects of speed and stride frequency, a significant increase in PTA between the first and third stages of the marathon was found. An increase in PTA corrected for changes in speed and stride frequency could indicate a decrease in the runner's capacity to attenuate shocks. Alternatively, the effective mass (i.e., the portion of body mass that is decelerated upon ground contact [43]) can decrease with increased knee flexion at initial contact (as shown during the marathon), which results in higher leg accelerations when similar ground reaction forces are applied. To conclude, PTA and its interpretation are influenced by subject-specific effects of changes in speed and stride frequency during a fatiguing run.

Knee angles

Average knee angles at initial contact (16.1 (2.5)°) and maximum stance phase knee angles (42.9 (5.1)°) were within the range reported in literature [4,23,43–45]. Knee angles at initial contact showed a negative weak and very weak correlation with speed and stride frequency, indicating more knee extension with higher speeds and stride frequencies. Previously, the knee flexion angle at initial contact remained similar [23] or increased with speed [46], although the range of speeds included was drastically higher than those found during the marathon. A decrease in knee angle at initial contact with an increase in speed might be a strategy to increase stride length by increasing leg extension. Knee angles at initial contact corrected for subject-specific effects of changes in speed and stride frequency showed a similar increasing pattern during the marathon compared to uncorrected values. Knee angles at initial contact have been found to increase with fatigue in controlled settings [43,45,47], possibly to decrease vertical ground reaction forces [10] at a higher metabolic cost [48]. Hence, the increase in knee angles at initial contact during a marathon is not solely an effect of changes in speed and stride frequency but is likely a result of fatigue.

Maximum stance phase knee angles had a weak positive correlation with speed and a weak negative correlation with stride frequency, indicating that the stance phase shortens at higher stride frequencies, resulting in less knee flexion during stance [24]. An increase in knee flexion with an increase in speed has been shown previously [23] and might be caused by higher forces on the body that need to be absorbed at higher speeds. However, it seems counterintuitive since more flexion during the stance phase typically increases the stance phase, while shorter contact times are expected at higher speeds [23,40]. The average increase in maximum stance phase knee flexion of 0.8° for every 1 km/h increase in speed is similar to previous findings in controlled settings (0.7°) [23]. Maximum stance phase knee flexion angles corrected for changes in speed and stride frequency reveal a significant increase between the first and third stages of the marathon that is not present in uncorrected values. An increase in maximal stance knee flexion could indicate an increase in stride length [49], knee extensor

strength loss, or a reduced tolerance to imposed stretch loads with fatigue [40,50]. Despite relatively small explained variances of regression equations for knee angles, subject-specific corrections for changes in speed and stride frequency on knee angles significantly influenced the interpretation of mechanical changes during a marathon.

Fatigue

Subjects likely experienced high levels of fatigue toward the end of the marathon. Running-induced fatigue typically increases PTA [47], knee flexion at initial contact [47] and tends to increase maximal stance phase knee flexion [43,45,51]. Both speed and fatigue are positively associated with PTA and maximum stance phase knee angles. Fatigue might have caused lower speed coefficients for PTA and maximum stance phase knee angles than expected without the influence of fatigue. Since subjects generally ran slower at the end of the marathon, PTA and maximum knee angles possibly decreased less with a decrease in speed towards the end of the marathon due to fatigue. Therefore, the influence of speed and stride frequency on running mechanics in an uncontrolled environment might be larger than shown in this study. To omit the effect of fatigue, we could have taken data from the start of the marathon, defined linear regression equations from data in an unfatigued state, and applied a correction to the remainder of the data, similar to [52]. However, most runners will experience some level of fatigue during their runs, making relationships solely based on unfatigued data invalid. Hence, we deliberately included data from an unfatigued to a fully fatigued state to create subject-specific relationships with better ecological validity.

Limitations

Collecting data in an uncontrolled environment is both a benefit and a shortcoming of this study. The benefit is that runners were measured in the actual environment where they typically run without any constrictions that a laboratory setting or a treadmill would impose on their gait pattern. However, we investigated the effects of speed and stride frequency on multiple mechanical quantities. At the same time, many other external influences could have played a role, such as running surface, fatigue, other runners, or distractions. The explained variance of quantities of interest can be improved by incorporating additional variables into the regression equation. However, for the scope of this paper, we were only interested in how much of the variance in included quantities could be explained by changes in speed and stride frequency.

Practical implications

This study showed that running speed and stride frequency have a subject-specific relationship with PTA, knee angles at initial contact, and maximum stance phase knee flexion. Correcting for these relationships influences the interpretation of changes in mechanical quantities while running in an uncontrolled environment. Many wearable devices provide feedback on peak accelerations to reduce injury risk [25–27]. Since a decrease in speed or an increase in stride frequency can mask an increase in PTA due to fatigue, it would be relevant from an injury perspective to provide feedback on changes in quantities caused by fatigue rather than by changes in speed or stride frequency. We advise investigating and correcting for subject-specific regression equations for all quantities of interest when measuring and providing feedback on running mechanics in an uncontrolled environment.

Conclusions

In this study, we quantified and corrected for the subject-specific effect of changes in running speed and stride frequency on impact-related running mechanics during a fatiguing outdoor run. Subject-specific corrections through multiple linear regression equations revealed a significant effect of marathon stage on PTA and maximal stance phase knee flexion, which was previously masked by changes in speed and stride frequency. The effect of marathon stage on knee angles at initial contact changed after correcting for changes in speed and stride frequency. Hence, speed and stride frequency influence the interpretation of changes in mechanical quantities in a subject-specific manner when running in an uncontrolled environment. Subject-specific effects of speed and stride frequency on quantities of interest should be investigated and corrected when interpreting, or providing feedback on, running mechanics in an uncontrolled environment.

Data availability statement

The data presented in this study will be openly available in 4TU.ResearchData.

Acknowledgment

This study was supported by EFRO OP Oost (Grant number: 0784). The study sponsor had no involvement in the study design, data collection, analysis, interpretation, writing, or decision to submit the manuscript for publication. The authors would like to thank the organization of the Enschede Marathon and the runners who participated in this study for their time and dedication to increase our knowledge about running.

References

1. Saunders, P. U., Pyne, D. B., Telford, R. D. & Hawley, J. A. Factors affecting running economy in trained distance runners. Sport. Med. 34, 465–485 (2004).
2. Pizzuto, F. et al. Relationship between Running Economy and Kinematic Parameters in Long-Distance Runners. J. Strength Cond. Res. 33, 1921–1928 (2019).
3. García-Pinillos, F. et al. Does fatigue alter step characteristics and stiffness during running? Gait Posture 76, 259–263 (2020).
4. Maas, E., De Bie, J., Vanfleteren, R., Hoogkamer, W. & Vanwanseele, B. Novice runners show greater changes in kinematics with fatigue compared with competitive runners. Sport. Biomech. 17, 350–360 (2018).
5. Giraldo-Pedroza, A., Chiu-Chun Lee, W., Lam, W., Coman, R. & Alici, G. Effects of wearable devices with biofeedback on biomechanical performance of running - A systematic reveiw. Sensors (Switzerland) 20, (2020).
6. Van Hooren, B., Goudsmit, J., Restrepo, J. & Vos, S. Real-time feedback by wearables in running: Current approaches, challenges and suggestions for improvements. J. Sports Sci. 38, 214–230 (2020).
7. Milner, C. E., Ferber, R., Pollard, C. D., Hamill, J. & Davis, I. S. Biomechanical Factors Associated with Tibial Stress Fracture in Female Runners. 323–328 (2006) doi:10.1249/01.mss.0000183477.75808.92.
8. Hreljac, A. Etiology, prevention, and early intervention of overuse injuries in runners: A biomechanical perspective. Phys. Med. Rehabil. Clin. N. Am. 16, 651–667 (2005).
9. Lafortune, M. A. Three-dimensional acceleration of the tibia during walking and running. J. Biomech. 24, (1991).
10. Gerritsen, K. G. M., Bogert, A. J. Van Den & Nigg, B. M. Direct dynamics simulation of the impact phase in heel-toe running. J. Biomech. 28, 661–666 (1995).
11. Sinclair, J. et al. Three-dimensional kinematic comparison of treadmill and overground running. Sport. Biomech. 12, 272–282 (2013).
12. García-Pérez, J. A., Pérez-Soriano, P., Llana Belloch, S., Lucas-Cuevas, Á. G. & Sánchez-Zuriaga, D. Effects of treadmill running and fatigue on impact acceleration in distance running. Sport. Biomech. 13, 259–266 (2014).
13. Milner, C. E., Hawkins, J. L. & Aubol, K. G. Tibial acceleration during running is higher in field testing than indoor testing. Med. Sci. Sports Exerc. 52, 1361–1366 (2020).

14. Lafferty, L. et al. Clinical Indoor Running Gait Analysis May Not Approximate Outdoor Running Gait Based on Novel Drone Technology. Sports Health 1–7 (2021) doi:10.1177/19417381211050931.

15. Benson, L. C., Clermont, C. A. & Ferber, R. New Considerations for Collecting Biomechanical Data Using Wearable Sensors: The Effect of Different Running Environments. Front. Bioeng. Biotechnol. 8, 1–8 (2020).

16. Benson, L. C., Räisänen, A. M., Clermont, C. A. & Ferber, R. Is This the Real Life, or Is This Just Laboratory? A Scoping Review of IMU-Based Running Gait Analysis. Sensors 22, 1–38 (2022).

17. Chan-Roper, M., Hunter, I., Myrer, J. W., Eggett, D. L. & Seeley, M. K. Kinematic changes during a marathon for fast and slow runners. J. Sport. Sci. Med. 11, 77–82 (2012).

18. Ruder, M., Jamison, S. T., Tenforde, A., Mulloy, F. & Davis, I. S. Relationship of Foot Strike Pattern and Landing Impacts during a Marathon. Med. Sci. Sports Exerc. 51, 2073–2079 (2019).

19. Sheerin, K. R., Reid, D. & Besier, T. F. The measurement of tibial acceleration in runners—A review of the factors that can affect tibial acceleration during running and evidence-based guidelines for its use. Gait Posture 67, 12–24 (2019).

20. Busa, M. A., Lim, J., Van Emmerik, R. E. A. & Hamill, J. Head and tibial acceleration as a function of stride frequency and visual feedback during running. PLoS One 11, 1–13 (2016).

21. Clarke, T. E., Cooper, L. B., Clark, D. E. & Hamill, C. L. The effect of increased running speed upon peak shank deceleration during ground contact. Hum. Kinet. 101–105 (1985).

22. Mercer, J. A., Vance, J., Hreljac, A. & Hamill, J. Relationship between shock attenuation and stride length during running at different velocities. Eur. J. Appl. Physiol. 87, 403–408 (2002).

23. Orendurff, M. S. et al. A little bit faster: Lower extremity joint kinematics and kinetics as recreational runners achieve faster speeds. J. Biomech. 71, 167–175 (2018).

24. Heiderscheit, B. C., Chumanov, E. S., Michalski, M. P., Wille, C. M. & Ryan, M. B. Effects of step rate manipulation on joint mechanics during running. Med. Sci. Sports Exerc. 43, 296–302 (2011).

25. Moov now. https://welcome.moov.cc/.

26. Runscribe. https://runscribe.com/metrics/.

27. TgForce 3D. https://tgforce.com/about-tibial-shock/.

28. Crowell, H. P. & Davis, I. S. Gait retraining to reduce lower extremity loading in runners. Clin. Biomech. 26, 78–83 (2011).
29. Crowell, H. P., Milnert, C. E., Hamill, J. & Davis, I. S. Reducing impact loading during running with the use of real-time visual feedback. J. Orthop. Sports Phys. Ther. 40, 206–213 (2010).
30. Wouda, F. J. et al. Estimation of vertical ground reaction forces and sagittal knee kinematics during running using three inertial sensors. Front. Physiol. (2018) doi:10.3389/fphys.2018.00218.
31. Schepers, M., Giuberti, M. & Bellusci, G. Xsens MVN: Consistent Tracking of Human Motion Using Inertial Sensing. 1–8 (2018) doi:10.13140/RG.2.2.22099.07205.
32. Xsens Technologies B.V. MVN User Manual. MVN Man. 162 (2021).
33. Chopde, N. R. & Nichat, M. K. Landmark Based Shortest Path Detection by Using A* and Haversine Formula. Int. J. Innov. Res. Comput. Commun. Eng. 1, 298–302 (2013).
34. Leys, C., Ley, C., Klein, O., Bernard, P. & Licata, L. Detecting outliers: Do not use standard deviation around the mean, use absolute deviation around the median. J. Exp. Soc. Psychol. 49, 764–766 (2013).
35. Benson, L. C., Clermont, C. A., Watari, R., Exley, T. & Ferber, R. Automated accelerometer-based gait event detection during multiple running conditions. Sensors (Switzerland) 19, 1–19 (2019).
36. Altman, A. R. & Davis, I. S. A kinematic method for footstrike pattern detection in barefoot and shod runners. Gait Posture 35, 298–300 (2012).
37. Oliveira, A. S. & Pirscoveanu, C. I. Implications of sample size and acquired number of steps to investigate running biomechanics. Sci. Rep. 11, 1–15 (2021).
38. Evans, J. D. Straightforward statistics for the behavioral sciences. (Thomson Brooks/Cole Publishing Co., 1996).
39. Bertram, J. E. A., Prebeau-Menezes, L. & Szarko, M. J. Gait characteristics over the course of a race in recreational marathon competitors. Res. Q. Exerc. Sport 84, 6–15 (2013).
40. Nicol, C., Komi, P. V. & Marconnet, P. Effects of marathon fatigue on running kinematics and economy. Scand. J. Med. Sci. Sports 1, 195–204 (1991).
41. Cavanagh, P. R. & Kram, R. Stride length in distance running: velocity, body dimensions, and addes mass effects. Med. Sci. Sport. Exerc. 21, 467–479 (1989).
42. Reenalda, J., Maartens, E., Buurke, J. H. & Gruber, A. H. Kinematics and shock attenuation during a prolonged run on the athletic track as measured with inertial magnetic measurement units. Gait Posture 68, 155–160 (2019).

43. Derrick, T. R., Dereu, D. & Mclean, S. P. Impacts and kinematic adjustments during an exhaustive run. Med. Sci. Sports Exerc. 34, 998–1002 (2002).

44. Reenalda, J., Maartens, E., Homan, L. & Buurke, J. H. Continuous three dimensional analysis of running mechanics during a marathon by means of inertial magnetic measurement units to objectify changes in running mechanics. J. Biomech. 49, 3362–3367 (2016).

45. Sanno, M., Willwacher, S., Epro, G. & Brüggemann, G. P. Positive work contribution shifts from distal to proximal joints during a prolonged run. Med. Sci. Sports Exerc. 50, 2507–2517 (2018).

46. Nigg, B. M., Bahlsen, H. A., Luethi, S. M. & Stokes, S. The influence of running velocity and midsole hardness on external impact forces in heel-toe running. J. Biomech. 22, 963–965 (1989).

47. Apte, S. et al. Biomechanical Response of the Lower Extremity to Running-Induced Acute Fatigue: A Systematic Review. Front. Physiol. 12, 1–16 (2021).

48. Valiant, G. A. Transmission and attenuation of heelstrike accelerations. (Human Kinetics Publishers, Champaign, IL, 1990).

49. Schubert, A. G., Kempf, J. & Heiderscheit, B. C. Influence of Stride Frequency and Length on Running Mechanics: A Systematic Review. Sports Health 6, 210–217 (2014).

50. Giandolini, M. et al. Fatigue associated with prolonged graded running. Eur. J. Appl. Physiol. 116, 1859–1873 (2016).

51. Jewell, C., Boyer, K. A. & Hamill, J. Do footfall patterns in forefoot runners change over an exhaustive run? J. Sports Sci. 35, 74–80 (2017).

52. Clermont, C. A., Benson, L. C., Edwards, W. B., Hettinga, B. A. & Ferber, R. New Considerations for wearable Technology Data: Changes in Running Biomechanics during a Marathon. J. Appl. Biomech. 35, 401–409 (2019).

Chapter 4

Peak tibial acceleration should not be used as indicator of tibial bone loading during running

Accepted for publication as:
Zandbergen, M.A., ter Wengel, X.J., van Middelaar, R.P., Buurke, J.H., Veltink, P.H., Reenalda, J. Peak tibial acceleration should not be used as indicator of tibial bone loading during running. Sports Biomechanics.

Abstract

Peak tibial acceleration (PTA) is a widely used indicator for tibial bone loading. Indirect bone loading measures are of interest to reduce the risk of stress fractures during running. However, tibial compressive forces are caused by both internal muscle forces and external ground reaction forces. PTA might reflect forces from outside the body, but likely not the compressive force from muscles on the tibial bone. Hence, the strength of the relationship between PTA and maximum tibial compression forces in rearfoot-striking runners was investigated. Twelve runners ran on an instrumented treadmill while tibial acceleration was captured with accelerometers. Force plate and inertial measurement unit data were spatially aligned with a novel method based on the center of pressure crossing a virtual toe marker. With spatially aligned data, the ground reaction force moment arm with respect to the ankle joint center, the sagittal plane ankle moment, and maximum tibial compression forces were computed. The correlation coefficient between maximum tibial compression forces and PTA was 0.04 ± 0.14 with a range of -0.15 to +0.28. On a group level, this study showed a very weak and non-significant correlation between PTA and maximum tibial compression forces while running on a level treadmill at a single speed. Hence, PTA as an indicator for tibial bone loading should be reconsidered, as PTA does not provide a complete picture of both internal and external compressive forces on the tibial bone.

Introduction

Runners are at high risk of developing bone stress fractures. Stress fractures account for 3% to 14% of running injuries [1–3] and are most prevalent in the distal part of the tibial bone (20% to 53%) [4,5]. Stress fractures are the result of prolonged and repetitive forces on the bone without enough rest for bone remodelling [6,7]. Stress fracture risk is influenced by both fixed factors, such as sex, skeleton alignment, bone geometry, bone remodelling, and bone mineral density, and variable factors, such as training intensity, training frequency, training surface, footwear, running incline, and running kinematics [6–10]. Forces on the tibia and subsequent tibial bone deformation can only be directly measured in vivo after an invasive surgery [11–13]. Hence, there is a lot of interest in indirect measures of tibial bone forces.

Ground reaction forces (GRFs) and peak tibial accelerations (PTAs) are often used as surrogate measures for tibial bone loading and injury risk in running [14–21]. GRF is the force exerted by the ground on the body to support the body weight (BW) and, in addition, results in acceleration and deceleration of the body's center of mass during the stance phase of running. The collision of the foot with the ground causes an impact shock that travels through the body [20]. PTA reflects this impact shock at the surface of the skin near the tibia bone [22]. PTA occurs shortly after initial contact and negligibly to moderately correlates with the slope of the vertical GRF and GRF impact peak shortly after initial contact [23,24]. The benefit of PTA compared to GRF metrics is that PTA can be easily measured outside of the lab with a wearable accelerometer. Multiple studies link high PTA values to retrospective running injuries [10,14,25]. Prospective preliminary data of five runners suggest that runners with a tibial stress fracture tended to have higher PTA values (9.1 g) compared to matched controls (4.7 g; $p = 0.06$) before they sustained an injury [26]. PTA is often used as a biofeedback variable to decrease impacts and risk of tibial stress fractures in runners [27–29] and is even applied in commercially available sensors as an indicator of running injury risk [30]. Hence, many findings support the idea of using PTA as a surrogate measure for tibial bone forces in running.

Compression forces acting on the tibial bone (F_{tibia}) can be divided into external forces (F_{ext}) caused by the foot contacting the ground and internal forces (F_{int}) caused by the pull of muscles [5,31]. F_{tibia} in the distal tibia can reach values of 10.3 up to 14.3 times BW during running, of which only 18% is caused by F_{ext} [31]. Most of F_{tibia} is therefore caused by internal forces which reach their maximum compressive action around midstance during running [24,31–34]. Matijevich and colleagues investigated the commonly assumed relationship

between GRF metrics (peak vertical GRF around impact and midstance, slope of vertical GRF and GRF impulse) and maximum tibial compression forces ($F_{tibia,max}$) during running [24]. Since GRF does not account for compressive muscle forces, no strong group-level correlation with F_{tibia} was found, although there was high inter-subject variability. Hence, GRF metrics should not be used as indicator of tibial bone forces in running.

Despite the widespread use of PTA as a measure for tibial bone loading and injury risk, PTA (occurring shortly after initial contact) and $F_{tibia,max}$ (occurring around midstance) do not coincide in time. PTA is expected to reflect the contribution of GRF around initial contact to F_{tibia}, however, F_{ext} is only 18% of $F_{tibia,max}$ [31]. Hence, there is reason to doubt the commonly used PTA as a surrogate for tibial bone loading in running. Therefore, the research question of this study is: How strong is the relationship between PTA and $F_{tibia,max}$ in rearfoot-striking runners during level running at a single speed? It is hypothesized that PTA does not reflect the contribution of F_{int} (i.e., muscle contractions) to $F_{tibia,max}$ and therefore that there are no statistically significant correlations between PTA and $F_{tibia,max}$.

Methods

Participants

Thirteen recreational runners participated in this study. Since internal forces tend to be different for non-rearfoot striking runners, only rearfoot striking runners were included in this study [35–37]. Inclusion criteria were: 1) Able to run for 5 minutes at 14 km/h to prevent possible effects of fatigue; 2) Injury-free for at least six months; 3) Self-reported rear-foot strike pattern. One subject was retrospectively excluded from analysis because of a non-rearfoot strike pattern. Data from 4 females and 8 males were included (age: 36.7±12.2 years, height: 178.7±9.6 cm, mass: 74.2±17.7 kg). Subjects ran on average 29.9±19.9 km per week with 15.0±14.9 years of running experience. All participants gave written informed consent before participating in this study. The study protocol was approved by the Ethics Committee Computer and Information Science of the University of Twente (EC-CIS, ref.:RP2021-117).

Measurement systems

Subjects ran on one belt of a dual-belt treadmill with an integrated three-dimensional (3D) force plate (custom Y-mill, Motekforce-Link, Culemborg, The Netherlands). 3D GRFs and ground reaction moments were captured at 2048 Hz. Subjects were equipped with eight IMU sensors (MVN Link, Xsens, Enschede, The Netherlands) capturing at 240 Hz, measuring acceleration (±16 g), angular velocity (±2000 deg/s), and the Earth magnetic field (±1.9 Gauss).

Sensors were placed on the sternum and pelvis and bilaterally on the lateral midportion of the thigh, medial surface of the proximal tibia, and on top of the midfoot in the shoes. All sensors had one axis aligned with the longitudinal direction of the associated segment. Sensors were attached to the skin with double-sided tape and covered with stretchable tape [19]. Subjects wore slightly compressing sleeves to firmly fix the sensors on the tibia to the lower leg.

Measurement protocol

Multiple anthropometric values were measured (body height, hip height, hip width, knee height, ankle height, and shoe length). Subjects wore their own running shoes throughout the experiment. Subjects performed a five-minute warming-up at a self-selected speed on an instrumented treadmill. After the warming-up, an IMU sensor-to-segment calibration was performed according to the manufacturer's instructions [38].

Subjects performed a ninety-second running trial at their self-selected step frequency at 12 km/h. Trials started and ended with three jumps on the treadmill to time-synchronize the force plate and IMU data (see section: "Temporal synchronization and spatial alignment") [39]. Since this study was part of a larger experiment, each subject performed a total of nine running trials of ninety seconds at different speeds (10, 12, and 14 km/h) in random order and with different step frequencies (self-selected and imposed), of which data was not included in further analysis. Subjects had a three-minute break after every trial to minimize possible effects of fatigue.

Data processing

Unless stated otherwise, data were expressed in the global force plate coordinate system ($\psi^{gl,fp}$) with the X-axis pointing in the running direction, the Y-axis upwards, and the Z-axis to the right. The stance phase of running was defined as the period where the vertical GRF was larger than 20 N [40]. The stance phase started with initial contact and ended with toe-off. Data were normalized for BW and expressed as a percentage of the stance phase. To exclude effects of adapting to the treadmill speed, 50 right leg stance phases between the 40th and 80th second of the running trial were used for analysis. To check if all runners had a rearfoot striking pattern, the mean foot contact angle (i.e., angle between sagittal plane orientation of the foot and the global vertical axis as provided by the IMU-based biomechanical model) at initial contact was computed for each subject. A mean foot contact angle smaller than 8 degrees (less dorsiflexion results in a smaller angle) was interpreted as a non-rearfoot strike pattern, and these subjects were excluded from further analysis [41]. Data processing and statistics were performed in MATLAB (MathWorks Inc., MA, USA, version 2022a).

IMU data

Sensor orientations were estimated with proprietary filtering based on acceleration, angular velocity, and magnetometer data from the IMUs in the software package Xsens MVN Analyze (version 2020.0.2). Sensor orientations, together with anthropometric measurements, were used to create a scaled biomechanical model of each subject in the same software. Lower body kinematics, 3D coordinates of joint centers, and locations of virtual anatomical landmarks with respect to joint centers were obtained from the scaled biomechanical model [38]. These IMU-derived data were expressed in either a global IMU-based coordinate system ($\psi^{gl,imu}$) or a sensor-fixed coordinate system (ψ^{s}). The forward direction (X-axis) of $\psi^{gl,imu}$ was determined during the sensor-to-segment calibration and was roughly similar to the running direction in $\psi^{gl,fp}$.

Force plate data

GRF, ground reaction moments, and center of pressure (COP) as measured by the force plate (in $\psi^{gl,fp}$) were low-pass filtered with a third-order recursive Butterworth filter of 15 Hz [24]. Force plate data were then linearly downsampled to 240 Hz to match the sampling frequency of IMU data.

Temporal synchronization and spatial alignment

A rough estimate of the vertical ground reaction force in running can be made by multiplying vertical pelvis acceleration with BW [39]. Force plate and IMU data can then be time-synchronized by cross-correlating the vertical acceleration of the pelvis segment with the vertical GRF during the first three jumps on the treadmill [39]. Note that BW only functions as a scaling factor and is not necessary for time synchronization.

To compute F_{tibia}, the sagittal plane ankle moment (M_{ankle}) and the GRF moment arm with respect to the ankle joint center was required (see Section "Tibial compression force"). To compute the GRF moment arm, IMU-derived data (expressed in $\psi^{gl,imu}$) needed to be transformed to $\psi^{gl,fp}$. First, the orientation of $\psi^{gl,imu}$ was rotated to match the orientation of $\psi^{gl,fp}$ using the running direction (positive X-axis). The IMU-based biomechanical model cannot distinguish between stationary (i.e., on a treadmill) and overground running, which resulted in a displacement of the pelvis segment in $\psi^{gl,imu}$ of about 250 m during each trial, predominantly in the X-axis. A least-squares line was fitted through the forward and sideward pelvis displacement in $\psi^{gl,imu}$ and the angle between these lines was used to rotate all IMU-derived data from $\psi^{gl,imu}$ to $\psi^{gl,fp}$.

The origin of $\psi^{gl,imu}$ was then translated to match $\psi^{gl,fp}$ during each step to be able to estimate the GRF moment arm and compute M_{ankle}. Since F_{tibia} is computed with a 2D model, only spatial alignment of data in the forward direction (X-axis) was required. The COP trajectory was provided by the force plate in $\psi^{gl,fp}$. In rearfoot striking runners on a treadmill, the forward trajectory of COP (COP_x) over the surface of the foot was expected to be similar. Therefore, it was assumed that the percentage of the stance phase at which COP_x crossed the fifth metatarsal marker ($MT5_x$) would be similar between strides and subjects. The IMU-based scaled biomechanical model provided virtual marker locations of the heel and MT5 with respect to the ankle joint center. These virtual marker locations were modeled based on the foot length of participants. The mean percentage of the stance phase at which COP_x crossed $MT5_x$ in rearfoot runners was then used to spatially align $\psi^{gl,imu}$ with $\psi^{gl,fp}$ in the X-direction during each stride, see Figure 4.1. A published dataset of six rearfoot striking runners running at eight different speeds was used to test this method and to obtain the mean percentage of the stance phase at which COP_x crossed $MT5_x$ [24]. This mean percentage at which COP_x crossed $MT5_x$ was then applied to all steps from all subjects from the online dataset. The error of this alignment method was quantified by computing the absolute distance between $MT5_x$ and COP_x at the group-mean percentage of the stance phase were $MT5_x$ crossed COP_x. A full description of the analyses of the online dataset can be found in Appendix 4.

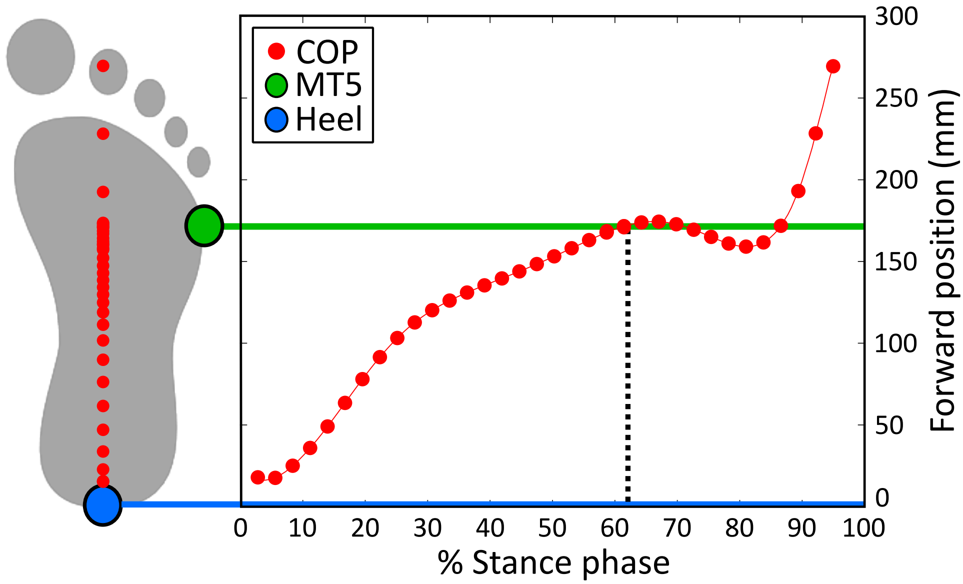

Figure 4.1: *Visualization of spatial alignment method for $\psi^{gl,imu}$ and $\psi^{gl,fp}$ for a representative subject. The mean percentage of the stance phase at which the center of pressure (COP) crosses the fifth metatarsal marker (MT5) in the forward direction (X-axis) is used to align $\psi^{gl,imu}$ and $\psi^{gl,fp}$. COP and MT5 positions with respect to the heel marker are shown. COP data was downsampled for visualization purposes and only the forward position of COP is aligned and shown. This figure was inspired by Figure 1 of* [58].

Tibial compression force

F_{tibia} was defined as the axial compression force on the distal end of the tibia and is equal to the ankle compression force [24,31,32,42], see Figure 4.2. F_{tibia} is computed according to a 2D (sagittal plane) lower limb model which sums the ankle joint reaction force caused by GRF (F_{ext}) and an estimate of compression forces on the tibia exerted by the soleus, gastrocnemius medialis, and lateralis plantar flexor muscles (F_{int}) while ignoring contributions of other muscles [31].

$$F_{tibia}(t) = F_{ext}(t) + F_{int}(t) \tag{4.1}$$

The mass and inertia of the foot were assumed to be negligible [24,31,42]. F_{ext} was therefore set equal to GRF in the axial direction of the tibia, but GRF was low-pass filtered with a 45 Hz ($\overrightarrow{GRF}^{*}$) instead of a 15 Hz cut-off frequency to allow representation of the heel impact in F_{ext} [24,31]:

$$F_{ext}(t) = \left|\overrightarrow{GRF}^{*}(t)\right| * cos\beta(t) \tag{4.2}$$

Where β represents the angle between $\overrightarrow{GRF}^{*}$ and the orientation of the tibial segment (obtained from IMU-based biomechanical model) in the sagittal plane. F_{int} is computed as M_{ankle} divided by the Achilles tendon moment arm relative to the ankle joint center (r_{at}), which was assumed to be constant and 0.05 m [24,42–44]:

$$F_{int}(t) = \frac{M_{ankle}}{r_{at}} = \frac{COP_{x,ankle} * GRF_z(t)}{0.05} \tag{4.3}$$

Where $COP_{x,ankle}$ represent the forward COP position with respect to the ankle joint center obtained from the scaled biomechanical model and is an estimate of the GRF moment arm relative to the ankle joint center. M_{ankle} was estimated by multiplying $COP_{x,ankle}$ with the vertical GRF (GRF_z). This computation of M_{ankle} assumes that solely the plantar flexors contribute to F_{int} during the stance phase and that there is no co-contraction between plantar and dorsi flexors during the stance phase [24,31,42].

Peak tibial acceleration

The acceleration of the tibial sensor, including gravity ($\vec{a}_{tibia}$) expressed in ψ^{s}, was filtered with a fourth-order Butterworth recursive lowpass filter of 60 Hz to minimize noise [22]. PTA was defined as the peak acceleration in the axial direction of the tibial sensor in the local tibial sensor coordinate system, similar to [18,29,45].

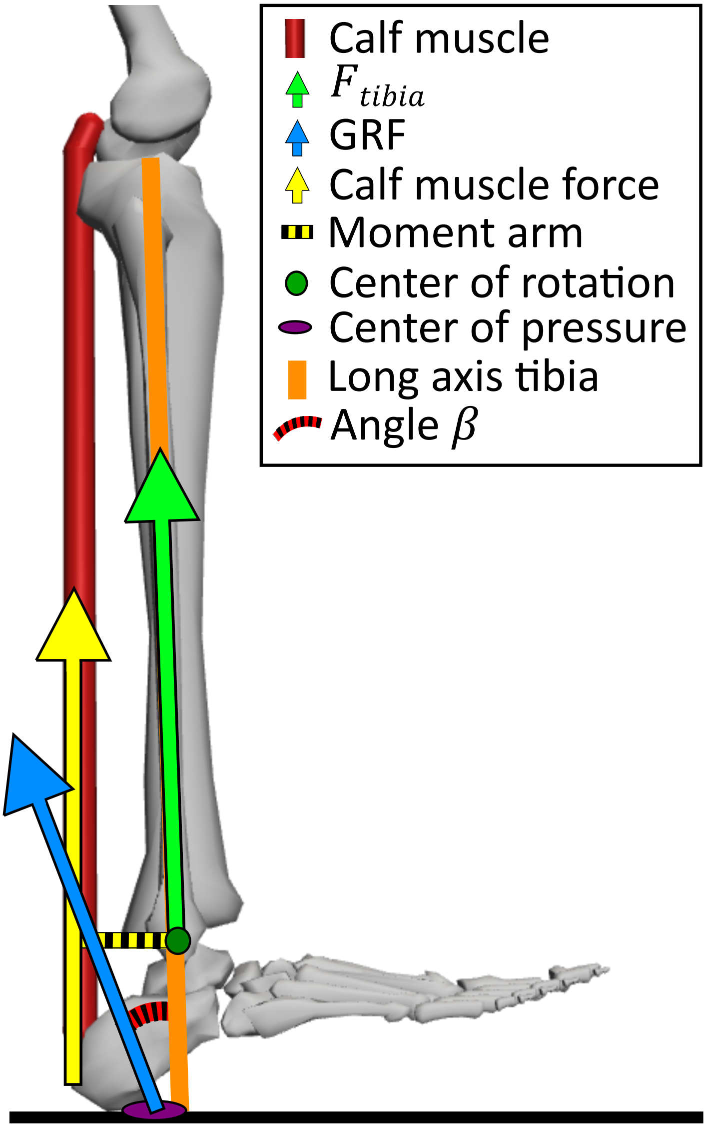

Figure 4.2: *Visualization of the 2D lower leg model to estimate tibial compression forces. Calf muscle = combination of the soleus, gastrocnemius medialis and lateralis muscles; r_{at} = Achilles tendon moment arm relative to the ankle joint center; GRF = ground reaction force; Center of rotation = center of rotation of the ankle joint; Angle β = Angle between long axis of tibia and ground reaction force vector in the sagittal plane.*

Statistical analysis

To test if PTA correlates with $F_{tibia,max}$ in running on level ground at a single speed, Pearson's correlation coefficients (r) were computed for each participant independently, after which the group mean correlation was computed. Correlation coefficients were based on 50 right leg PTA and $F_{tibia,max}$ values for each subject. Correlations were interpreted as very strong r = ±(0.90, 1.00), strong for r = ±(0.70, 0.89), moderate for r = ±(0.40, 0.69), weak for r = ±(0.20, 0.39) and very weak for r = ±(0.00, 0.19) [46]. The level of statistical significance was set to an alpha of 0.05. The influence of an offset in aligning $\psi^{gl,imu}$ with $\psi^{gl,fp}$ on the conclusion of this study was assessed by introducing an additional error of 10, 20, and 30 mm to the alignment of $\psi^{gl,imu}$ and $\psi^{gl,fp}$ and recomputing the correlation between PTA and $F_{tibia,max}$ with these offsets.

Results

$F_{tibia,max}$ was estimated to be, on average 7.6 ± 0.6 BW with a range of 6.5 to 8.7 BW, see Table 4.1 and Figure 4.3. The within-subject range of $F_{tibia,max}$ was on average 1.6 BW. Mean PTA was 7.8 ± 1.6 g and ranged from 4.9 up to 10.1 g. The within-subject range of PTA was on average 3.3 g. On a group level, PTA and $F_{tibia,max}$ showed a very weak correlation coefficient of 0.04 ± 0.14 with a range of -0.15 up to 0.28 (very weak to weak). No significant correlations between PTA and $F_{tibia,max}$ were found for any of the runners, see Figure 4.4.

Table 4.1: *Mean maximum values. Range refers to the minimum and maximum average subject values (coloured dots in Figure 4.4). GRF_{max} = Maximum vertical ground reaction force; $M_{ankle,max}$ = Maximum ankle moment; $F_{ext,max}$ = Maximum external force; $F_{int,max}$ = Maximum internal force; $F_{tibia,max}$ = Maximum tibial force; PTA = Peak tibial acceleration; r = correlation coefficient; BW = body weight; g = gravitational acceleration; SD = standard deviation.*

	Mean±SD	Range
GRF_{max} (BW)	2.4 ± 0.2	2.1- 2.7
$M_{ankle,max}$ $\left(\frac{Nm}{kg}\right)$	0.3 ± 0.0	0.2- 0.3
$F_{ext,max}$ (BW)	2.4 ± 0.2	2.1- 2.8
$F_{int,max}$ (BW)	5.3 ± 0.6	4.5- 6.2
$F_{tibia,max}$ (BW)	7.6 ± 0.6	6.5 – 8.7
PTA (g)	7.8 ± 1.6	4.9- 10.1
Correlation *PTA*- F_{tibia} (r)	0.04 ± 0.14	-0.15- +0.28

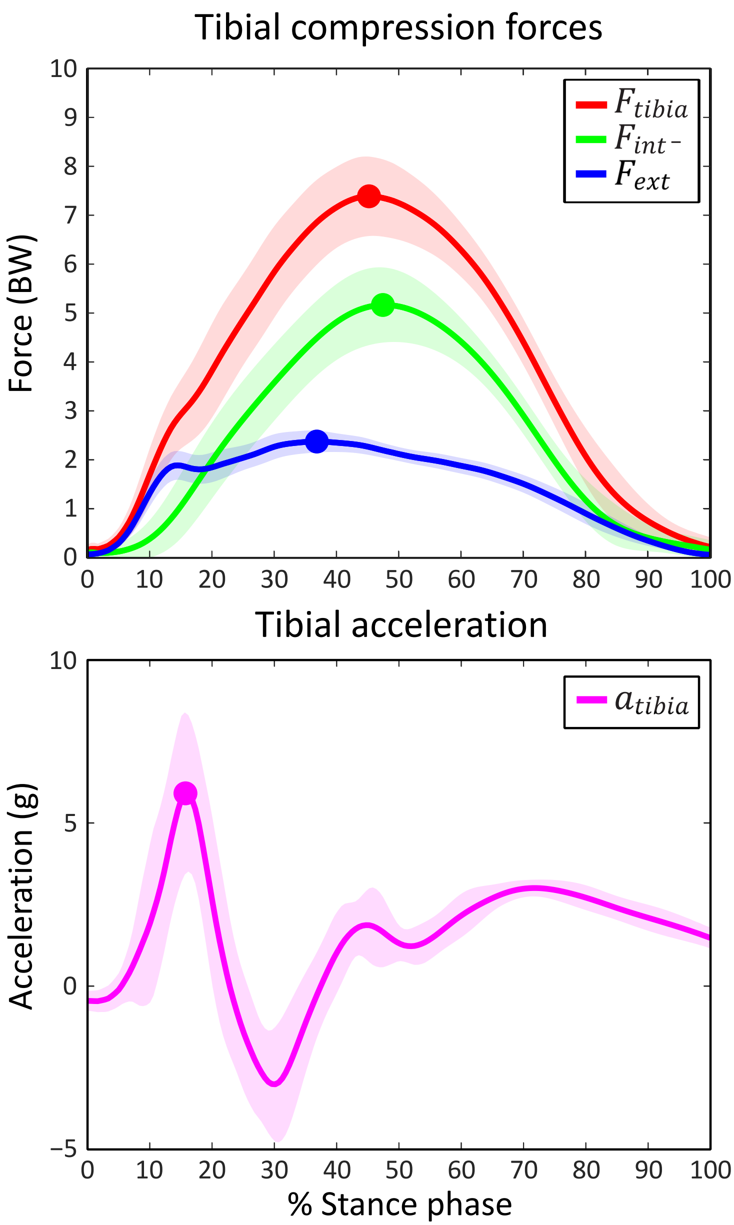

Figure 4.3: *Group average estimated tibial forces (top figure) and axial tibial acceleration (bottom figure) as a percentage of the stance phase. Dots represent maximum values for estimated tibial forces and tibial acceleration during the stance phase. Shaded areas represent the standard deviation around the group mean.* F_{tibia} *= tibial compression force;* F_{int} *= Internal component of tibial compression force (i.e., caused by muscle contractions);* F_{ext} *= external component of tibial compression force (i.e., caused by ground reaction force);* a_{tibia} *= tibial acceleration in the axial direction of the tibial sensor; BW = body weight; g = gravitational acceleration.*

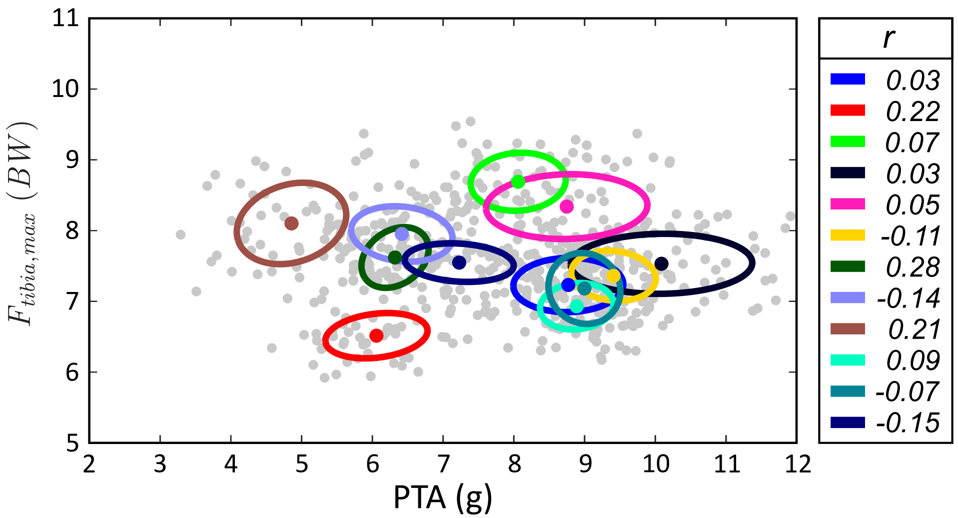

Figure 4.4: *scatterplot of PTA and estimated $F_{tibia,max}$ values for all 50 strides of all subjects (light grey dots). Coloured dots represent the mean PTA and $F_{tibia,max}$ for each subject. Coloured ellipses represent the standard deviation ellipse for all individual runners. The legend shows the correlation coefficients (r) between PTA and $F_{tibia,max}$.*

To validate the method to spatially align $\psi^{gl,imu}$ with $\psi^{gl,fp}$ during each step, to be able to compute the GRF moment arm, an online dataset was used [24]. On average, COP crossed the MT5 marker in the forward direction at 62 ± 12% of the gait cycle with a range of 47% to 85%, see Table 4.2. Within-subject variability was small, while between-subject variability was larger. The mean absolute error introduced by this alignment method was 12 ± 15 mm with a range of 4 to 28 mm.

The effect of a possible error in tibial force estimates caused by the alignment method of $\psi^{gl,imu}$ with $\psi^{gl,fp}$ on the conclusion of this study was investigated by applying an additional alignment offset in the forward direction impacting the GRF moment arm estimate, see Table 4.3. An additional alignment offset influenced the estimation of F_{int} and $F_{tibia,max}$, however the correlation between $F_{tibia,max}$ and PTA remained very weak for all imposed offsets.

Table 4.2: *Results from validating the spatial alignment method on an online dataset. The second column shows the percentage of the stance phase at which the center of pressure in the forward direction (COP_x) crossed the marker of the fifth metatarsal $(MT5_x)$. The third column shows the absolute mean error in spatial alignment introduced by assuming that COP_x always crossed $MT5_x$ at 62% of the stance phase.*

Subject	COP crossing MT5 (% stance phase)	Absolute mean error (mm)
1	47 ± 2	28 ± 3
2	59 ± 3	4 ± 3
4	85 ± 10	16 ± 3
5	56 ± 4	9 ± 5
6	68 ± 3	5 ± 2
7	68 ± 6	14 ± 9
10	56 ± 2	8 ± 3
Group mean	62 ± 12	12 ± 15

Table 4.3: *Influence of additional alignment offset between $\psi^{gl,imu}$ and $\psi^{gl,fp}$ on estimated tibial forces and the correlation between PTA and $F_{tibia,max}$. Columns represent the introduced translation error in the forward direction of $\psi^{gl,imu}$ with respect to $\psi^{gl,fp}$ for each step.*

	-30 mm	-20 mm	-10 mm	0 mm	+10 mm	+20 mm	+30 mm
$F_{ext,max}$ (BW)	2.4 ± 0.2	2.4 ± 0.2	2.4 ± 0.2	2.4 ± 0.2	2.4 ± 0.2	2.4 ± 0.2	2.4 ± 0.2
$F_{int,max}$ (BW)	4.0 ± 0.5	4.4 ± 0.5	4.9 ± 0.6	5.3 ± 0.6	5.8 ± 0.6	6.3 ± 0.6	6.8 ± 0.6
$F_{tibia,max}$ (BW)	6.2 ± 0.6	6.6 ± 0.6	7.1 ± 0.6	7.6 ± 0.6	8.1 ± 0.6	8.5 ± 0.6	9.0 ± 0.7
Correlation PTA- $F_{tibia,max}$ (r)	0.04 ± 0.14	0.04 ± 0.14	0.04 ± 0.14	0.04 ± 0.14	0.04 ± 0.15	0.04 ± 0.15	0.05 ± 0.15

Discussion and implications

This research aimed to investigate the strength of the relationship between PTA, a commonly used measure for tibial bone loading, and estimated $F_{tibia,max}$ during treadmill running. This study showed a very weak correlation (r = 0.04 ± 0.14) between PTA and $F_{tibia,max}$ in rearfoot striking runners on a treadmill at a single running speed. The hypothesis that there would be no statistically significant correlations between PTA and $F_{tibia,max}$ was accepted. On a group level, the very weak correlation between PTA and $F_{tibia,max}$ cannot be considered relevant for estimating tibial bone loading based on PTA. The weak correlations between PTA and $F_{tibia,max}$ are expected to be caused by the inability of PTA to reflect internal compressive forces from muscle contractions and the mis-timing between PTA (shortly after initial contact) and $F_{tibia,max}$ (around midstance). The use of PTA as a surrogate measure for $F_{tibia,max}$ during treadmill running is therefore not supported by the findings of this study.

PTA and GRF reflect the effect of external forces on the body during running. GRF represents the effect of external forces during the complete stance phase, while PTA mostly reflects the impact peak that travels up the leg caused by the foot hitting the ground at the start of the stance phase. The contribution of F_{ext} to $F_{tibia,max}$ is only about 18% - 30%, while the remainder is caused by F_{int} [31]. PTA, GRF loading rate, and GRF impact peak are often used as surrogate measures for each other and for tibial bone loading [14–21]. Previously, Matijevich et al. [24] showed that the slope of the vertical GRF and impact peak did not strongly correlate with F_{tibia}. Hence, the contribution of the high impact peak shortly after initial contact towards tibial stress fracture injury risk has been challenged before [47,48] but not in relation to PTA assessed using an IMU on the tibia, although this relation has been often assumed [14–21]. No strong correlations between the slope of the vertical GRF, GRF impact peak, PTA, and tibial bone loading have been found in this study or in other literature [23,24], indicating that these metrics should not be used as surrogate measures for each other.

A group mean value for PTA of 7.8 ± 1.6 g was found, which is well within the expected range when running at 12 km/h [22,23,49]. $F_{tibia,max}$ in this study was estimated to be 7.6 ± 0.6 BW on average, which is similar to studies in which subjects ran at a similar speed [42] and falls between values reported for lower [36] and higher speeds [31–33]. $F_{tibia,max}$ increases with running speed [50]. Values for $F_{int,max}$, also called plantar flexor forces or Achilles tendon forces, reported in literature were similar to our findings, respectively 5.7 ± 1.5 versus 5.3

± 0.6 BW [51]. Comparable values for F_{int} of 5.1 ± 0.9 BW [52] when running at 14.4 km/h and 6.1 ± 0.6 [35] when running at 13 km/h were found in literature. In vivo values for $F_{int,max}$ of 3750 N at 14 km/h were found with a buckle transducer [11]. These findings are only slightly lower than what we found (3914 ± 1094 N). Values for $F_{ext,max}$ from our study (2.4 ± 0.2 BW) where higher than found in literature (1.6 - 2.0 BW) [31,32] at similar speeds. Overall, PTA and estimated tibial force values of this study are in line with literature.

A simple 2D lower leg model was used to estimate F_{tibia} of the distal third of the tibial bone [31]. This model assumes that only the gastrocnemius medialis, lateralis, and soleus contribute to F_{int} , that there is no co-activation of dorsiflexor muscles or other plantarflexor muscles, no influence of bi-articular muscles and neglects the mass and inertia of the foot. These assumptions likely result in an underestimation of true F_{int} at similar speeds due to co-activation of dorsiflexor muscles and contribution of smaller plantarflexor muscles. F_{ext} is likely overestimated in the simple 2D lower leg model since the mass and inertia of the foot dampens GRF while the model assumes that the full GRF acts on the ankle joint. Multiple studies used more elaborate models to estimate F_{tibia} that included dorsiflexor muscles and smaller plantarflexor muscles [32,33,51]. They found that during 20% - 90% of the stance phase, mostly the gastrocnemius medialis, lateralis, and soleus were active with only little contributions (max 0.3 BW per muscle) from other plantar or dorsiflexor muscles [32]. When co-activation occurred, this was mostly during the start and end of the stance phase while $F_{tibia,max}$ occurs around midstance. The simple 2D lower leg model has been shown to provide $F_{int,max}$ in running that were similar to an extensive musculoskeletal model using 300 muscles with static optimization, respectively 5.7 ± 0.6 and 5.5 ± 1.4 BW [51]. A 2D versus a 3D lower leg model to compute $F_{tibia,max}$ and $F_{int,max}$ provided similar results for both models [33]. Hence, using a simple or more elaborate model of the lower leg to estimate F_{tibia} is not expected to influence the conclusion of this study.

A new method was developed, validated, and applied to spatially align force plate and IMU data in the forward direction to be able to estimate the GRF moment arm relative to the ankle joint center. Validation was performed on an online dataset and showed an absolute misalignment error of 12 ± 15 mm in the forward direction [24]. To ascertain that an error of this magnitude would not affect the conclusion of this study, an additional offset between $\psi^{gl,imu}$ and $\psi^{gl,fp}$ was added (i.e., affecting the GRF moment arm relative to the ankle joint center and thus M_{ankle}, F_{int} and F_{tibia} and the correlation between PTA and $F_{tibia,max}$

was computed. This analysis showed that despite some uncertainty regarding the exact alignment of $\psi^{gl,imu}$ and $\psi^{gl,fp}$, all alignment offsets (of up to 30 mm) resulted in a very weak correlation (r = 0.04- 0.05) and did not influence the conclusion of this study.

This study focussed on the relationship between tibial compression forces and 1-dimensional axial tibial sensor acceleration. Besides compression forces, bending and shear forces on the tibia might play a role in the development of stress fractures [31–34]. However, there is no reason to expect that PTA, measured in the axial direction of the tibial bone, would correlate better with bending or shear forces than with axial compression forces. Additionally, these bending and shear forces are of a smaller magnitude (max 1.2 BW) and work in different directions than maximum axial compression forces [32]. The axial compared to the resultant tibial acceleration was investigated in this study due to its demonstrated relationship with injuries [22] and possibly a stronger correlation with tibial compression forces. The difference between axial and resultant PTA is caused by acceleration components in the forward and sideward direction, while these are not expected to contribute to axial compression forces. Hence, the correlation between the resultant PTA and $F_{tibia,max}$ is expected to be lower than between the axial PTA and $F_{tibia,max}$.

The results of this study are based on a relatively small sample of twelve subjects. None of the runners showed a significant correlation between PTA and $F_{tibia,max}$. Increasing the sample size of this study would likely not affect the conclusion that there is no clinically relevant correlation between PTA and $F_{tibia,max}$ on a group level.

Measurements were performed on an indoor instrumented treadmill. However, the effect of running surface on PTA is unclear [17,49, 53,54]. In-vivo axial tibial compression strains were lower [55] while modeled F_{int} were higher in treadmill versus overground running [56]. Without further understanding of the effect of running surface on PTA and tibial forces, the results of this study cannot be generalized to overground running without additional validation.

This study showed that there is only a very weak and non-significant correlation between PTA and $F_{tibia,max}$ during treadmill running in rearfoot-striking runners, which cannot be considered relevant for estimating tibial bone loading based on PTA. Hence, PTA as an indicator for $F_{tibia,max}$ and tibial stress fractures, as often used in literature and commercial products, is not supported by scientific data. PTA might be an indicator of other running-related injuries, although the relation between PTA and tibial stress fracture risk is

most referred to in literature [14,27,29]. Future research should focus on a surrogate measure for tibial bone loading, which includes the contribution of F_{int} . The plantar flexor muscles are the largest contributors to F_{tibia}[51] and the magnitude of ankle power generation is directly related to running speed [57]. Therefore, 3D acceleration of the pelvis (i.e., close to the center of mass) might reflect plantar flexor forces during running, and thus the contribution of F_{int} to F_{tibia}.

Conclusion

A very weak but non-relevant correlation between PTA and $F_{tibia,max}$ in treadmill running at a single speed on level ground was found for rearfoot-striking runners. Compression forces on the tibia are composed of both F_{int} (i.e., muscle contractions) and F_{ext} (i.e., GRF). PTA is unable to reflect the contribution of muscle contractions to F_{tibia}. Hence, the assumed link between PTA and tibial bone loading $F_{tibia,max}$, and between PTA and the risk of tibial stress fractures during treadmill running is not supported by the results of this study. Further research should focus on validating these findings in overground running and the development of a surrogate measure for F_{tibia} which reflects both F_{int} and F_{ext} .

Acknowledgment

This study was supported by EFRO OP Oost under Grant 0784. The authors would like to thank Bouke Scheltinga and Hazal Usta for their assistance during the data collection process. Furthermore, the authors would like to thank all participants for their willingness and enthusiasm to participate in this study.

References

1. McBryde, A. M. Stress fractures in runners. Am. J. Sport. Med. 4, (1985).
2. Taunton, J, E. et al. A retrospective case-control analysis of 2002 running injuries. Br. J. Sports Med. 36, 95–101 (2002).
3. James, S., Bates, B. & Osternig, L. Injuries to runners. Am. J. Sport. Med. 6, 40–50 (1978).
4. Wall, J. & Feller, J. F. Imaging of Stress Fractures in Runners. Clin. Sports Med. 25, 781–802 (2006).
5. Romani, W. A., Gieck, J. H., Perrin, D. H., Saliba, E. N. & Kahler, D. M. Mechanisms and management of stress fractures in physically active persons. J. Athl. Train. 37, 306–314 (2002).
6. Umans, H. & Pavlov, H. Stress fractures of the lower extremities. Semin. Roentgenol. 29, 176–193 (1994).
7. Harrast, M. A. & Colonno, D. Stress fractures in runners. Clin. Sports Med. 29, 399–416 (2010).
8. Edwards, W. B. Modeling Overuse Injuries in Sport as a Mechanical Fatigue Phenomenon. Exerc. Sport Sci. Rev. 46, 224–231 (2018).
9. Saunier, J. & Chapurlat, R. Stress fracture in athletes. Jt. Bone Spine 85, 307–310 (2018).
10. Pohl, M. B., Mullineaux, D. R., Milner, C. E., Hamill, J. & Davis, I. S. Biomechanical predictors of retrospective tibial stress fractures in runners. 41, 1160–1165 (2008).
11. Komi, P. V. Relevance of in vivo force measurements to human biomechanics. J. Biomech. 23, (1990).
12. Lanyon, L. E., Hampson, W. G. J., Goodship, A. E. & Shah, J. S. Bone deformation recorded in vivo from strain gauges attached to the human tibial shaft. Acta Orthop. 46, 256–268 (1975).
13. Milgrom, C. et al. Do high impact exercises produce higher tibial strains than running? Br. J. Sports Med. 34, 195–199 (2000).
14. Milner, C. E., Ferber, R., Pollard, C. D., Hamill, J. & Davis, I. S. Biomechanical Factors Associated with Tibial Stress Fracture in Female Runners. 323–328 (2006) doi:10.1249/01.mss.0000183477.75808.92.
15. Mizrahi, J., Verbitsky, O. & Isakov, E. Fatigue-related loading imbalance on the shank in running: a possible factor in stress fractures. Ann. Biomed. Eng. 28, 463–469 (2000).

16. Bigelow, E. M. R., Elvin, N. G., Elvin, A. A. & Arnoczky, S. P. Peak impact accelerations during track and treadmill running. J. Appl. Biomech. 29, 639–644 (2013).
17. García-Pérez, J. A., Pérez-Soriano, P., Llana Belloch, S., Lucas-Cuevas, Á. G. & Sánchez-Zuriaga, D. Effects of treadmill running and fatigue on impact acceleration in distance running. Sport. Biomech. 13, 259–266 (2014).
18. Lucas-Cuevas, A. G. et al. Effect of 3 Weeks Use of Compression Garments on Stride and Impact Shock during a Fatiguing Run. Int. J. Sports Med. 36, 826–831 (2015).
19. Chadefaux, D., Gueguen, N., Thouze, A. & Rao, G. 3D propagation of the shock-induced vibrations through the whole lower-limb during running. J. Biomech. 96, 109343 (2019).
20. Lafortune, M. A., Lake, M. J. & Hennig, E. M. Differential shock transmission response of the human body to impact severity and lower limb posture. J. Biomech. 29, 1531–1537 (1996).
21. Zadpoor, A. A. & Nikooyan, A. A. The relationship between lower-extremity stress fractures and the ground reaction force: A systematic review. Clin. Biomech. 26, 23–28 (2011).
22. Sheerin, K. R., Reid, D. & Besier, T. F. The measurement of tibial acceleration in runners—A review of the factors that can affect tibial acceleration during running and evidence-based guidelines for its use. Gait Posture 67, 12–24 (2019).
23. Van den Berghe, P., Six, J., Gerlo, J., Leman, M. & De Clercq, D. Validity and reliability of peak tibial accelerations as real-time measure of impact loading during over-ground rearfoot running at different speeds. J. Biomech. 86, 238–242 (2019).
24. Matijevich, E. S., Branscombe, L. M., Scott, L. R. & Zelik, K. E. Ground reaction force metrics are not strongly correlated with tibial bone load when running across speeds and slopes: Implications for science, sport and wearable tech. PLoS One 14, 1–19 (2019).
25. Zifchock, R. A., Davis, I., Higginson, J., McCaw, S. & Royer, T. Side-to-side differences in overuse running injury susceptibility: A retrospective study. Hum. Mov. Sci. 27, 888–902 (2008).
26. Davis, I., Milner, C. E. & Hamill, J. Does increased loading during running lead to tibial stress fractures? A prospective study. S58 (2004).
27. Crowell, H. P. & Davis, I. S. Gait retraining to reduce lower extremity loading in runners. Clin. Biomech. 26, 78–83 (2011).

28. Crowell, H. P., Milnert, C. E., Hamill, J. & Davis, I. S. Reducing impact loading during running with the use of real-time visual feedback. J. Orthop. Sports Phys. Ther. 40, 206–213 (2010).
29. Clansey, A. C., Hanlon, M., Wallace, E. S., Nevill, A. & Lake, M. J. Influence of Tibial shock feedback training on impact loading and running economy. Med. Sci. Sports Exerc. 46, 973–981 (2014).
30. Runscribe. https://runscribe.com/metrics/.
31. Scott, S. H. & David, A. W. Internal forces at chronic running injury sites. Med. sci 22, 357–369 (1990).
32. Sasimontonkul, S., Bay, B. K. & Pavol, M. J. Bone contact forces on the distal tibia during the stance phase of running. J. Biomech. 40, 3503–3509 (2007).
33. Burdett, R. G. Forces predicted at the ankle during running. Med. Sci. Sport. Exerc. 14, 308–316 (1982).
34. Glitsch, U. & Baumann, W. The three-dimensional determination of internal loads in the lower extremity. J. Biomech. 30, 1123–1131 (1997).
35. Almonroeder, T., Willson, J. D. & Kernozek, T. W. The effect of foot strike pattern on achilles tendon load during running. Ann. Biomed. Eng. 41, 1758–1766 (2013).
36. Chen, T. L. et al. Immediate effects of modified landing pattern on a probabilistic tibial stress fracture model in runners. Clin. Biomech. 33, 49–54 (2016).
37. Rooney, B. D. & Derrick, T. R. Joint contact loading in forefoot and rearfoot strike patterns during running. J. Biomech. 46, 2201–2206 (2013).
38. Xsens Technologies B.V. MVN User Manual. MVN Man. 162 (2021).
39. Day, E. M., Alcantara, R. S., McGeehan, M. A., Grabowski, A. M. & Hahn, M. E. Low-pass filter cutoff frequency affects sacral-mounted inertial measurement unit estimations of peak vertical ground reaction force and contact time during treadmill running. J. Biomech. 119, 110323 (2021).
40. Milner, C. E. & Paquette, M. R. A kinematic method to detect foot contact during running for all foot strike patterns. J. Biomech. 48, 3502–3505 (2015).
41. Altman, A. R. & Davis, I. S. A kinematic method for footstrike pattern detection in barefoot and shod runners. Gait Posture 35, 298–300 (2012).
42. Matijevich, E. S., Scott, L. R., Volgyesi, P., Derry, K. H. & Zelik, K. E. Combining wearable sensor signals, machine learning and biomechanics to estimate tibial bone force and damage during running. Hum. Mov. Sci. 74, 102690 (2020).

43. Honert, E. C. & Zelik, K. E. Inferring muscle-tendon unit power from ankle joint power during the push-off phase of human walking: Insights from a multiarticular EMG-Driven model. PLoS One 11, 1–16 (2016).
44. Farris, D. J. & Sawicki, G. S. Human medial gastrocnemius force-velocity behavior shifts with locomotion speed and gait. Proc. Natl. Acad. Sci. U. S. A. 109, 977–982 (2012).
45. Reenalda, J., Maartens, E., Buurke, J. H. & Gruber, A. H. Kinematics and shock attenuation during a prolonged run on the athletic track as measured with inertial magnetic measurement units. Gait Posture 68, 155–160 (2019).
46. Evans, J. D. Straightforward statistics for the behavioral sciences. (Thomson Brooks/Cole Publishing Co., 1996).
47. Loundagin, L. L., Schmidt, T. A. & Brent Edwards, W. Mechanical Fatigue of Bovine Cortical Bone Using Ground Reaction Force Waveforms in Running. J. Biomech. Eng. 140, 1–5 (2018).
48. Hamill, J., Boyer, K. A. & Weir, G. A paradigm shift is necessary to relate running injury risk and footwear design – comment on Nigg et al. Curr. Issues Sport Sci. 3, 1–3 (2018).
49. Milner, C. E., Hawkins, J. L. & Aubol, K. G. Tibial acceleration during running is higher in field testing than indoor testing. Med. Sci. Sports Exerc. 52, 1361–1366 (2020).
50. Brent Edwards, W., Taylor, D., Rudolphi, T. J., Gillette, J. C. & Derrick, T. R. Effects of running speed on a probabilistic stress fracture model. Clin. Biomech. 25, 372–377 (2010).
51. Kernozek, T., Gheidi, N. & Ragan, R. Comparison of estimates of Achilles tendon loading from inverse dynamics and inverse dynamics-based static optimisation during running. J. Sports Sci. 35, 2073–2079 (2017).
52. Sinclair, J. Effects of barefoot and barefoot inspired footwear on knee and ankle loading during running. Clin. Biomech. 29, 395–399 (2014).
53. Montgomery, G., Abt, G., Dobson, C., Smith, T. & Ditroilo, M. Tibial impacts and muscle activation during walking, jogging and running when performed overground, and on motorised and non-motorised treadmills. Gait Posture 49, 120–126 (2016).
54. Fu, W. et al. Surface effects on in-shoe plantar pressure and tibial impact during running. J. Sport Heal. Sci. 4, 384–390 (2015).
55. Milgrom, C. et al. Are overground or treadmill runners more likely to sustain tibial stress fracture? Br. J. Sports Med. 37, 160–163 (2003).

56. Willy, R. W., Halsey, L., Hayek, A. & Willson, J. D. Overground and treadmill comparison of patellofemoral joint and achilles tendon loads. J Orthop Sport. Phys Ther 1–31 (2016).
57. Novacheck, T. F. The biomechanics of running. Gait Posture 7, 77–95 (1998).
58. Fuchioka, S. et al. The Forward Velocity of the Center of Pressure in the Midfoot is a Major Predictor of Gait Speed in Older Adults. Int. J. Gerontol. 9, 119–122 (2015).

Appendix 4

This appendix describes the analysis of an online dataset [24] to develop and validate a method to spatially align IMU-derived data expressed in a global IMU-based coordinate system ($\psi^{gl,imu}$), with force plate data expressed in a global force plate-based coordinate system ($\psi^{gl,fp}$).

Force plate and optical motion analysis data of ten runners running at eight different speeds (ranging from 9.4-14.4 km/h) on a level treadmill were extracted from an online dataset [24]. More details about the study protocol can be found in the original article accompanying the online dataset [24].

The stance phase of running was defined as the period where the vertical GRF was larger than 20 N [40]. The stance phase started with initial contact and ended with toe-off. To be representative of the population used in the main study, only rearfoot striking runners were included. A rearfoot strike was defined as a mean foot contact angle at initial contact of 8 degrees or more [41]. The mean foot contact angle was defined as the sagittal plane angle between a line from the right heel to the right toe marker and the horizontal at initial contact [41]. Four out of ten runners had a foot contact angle smaller than 8 degrees and were classified as non-rearfoot strikers and excluded from further analysis.

Ground reaction forces (GRF) and ground reaction moments (GRM) were filtered with a third-order recursive Butterworth filter of 15 Hz [24]. The center of pressure (COP) in the running direction (COP_x) was computed:

$$COP_x = \frac{GRM_z}{GRF_y} \tag{4.4}$$

Where GRM_z represents GRM around the Z-axis (sidewards) of $\psi^{gl,fp}$ and where GRF_y represents the vertical GRF in $\psi^{gl,fp}$.

Positions of the right heel, right toe, and fifth metatarsal marker (MT5) marker were extracted and filtered with a third-order recursive Butterworth filter of 10 Hz [24]. In one subject, the right toe marker was not present; in this case, the position of the right first metatarsal marker (MT1) was extracted and filtered instead of MT5 to compute the foot contact angle.

The first 24 strides for each speed of all included subjects were used for analysis since each trial consisted of at least 24 strides. COP_x and the forward position of the MT5 marker $(MT5_x)$ were normalized to the percentage of the stance phases. The percentage of the stance phase at which COP_x crossed $MT5_x$ was computed and averaged for all steps. On average, COP_x crossed $MT5_x$ at 62 ± 12% of the stance phase, see Table 2 of the manuscript.

To quantify the error introduced by assuming that COP_x crossed $MT5_x$ at 62% of the stance phase in all rearfoot striking runners, the positional difference between COP_x and $MT5_x$ for all subjects, and speeds at 62% of the stance phase were computed. This error was, on average 12 ± 15 mm, see Table 4.2.

Chapter 5

Estimating 3D orientation of a body segment during running using a single gyroscope

Published as:
Zandbergen, M.A., Ferla, R.I., Buurke, J.H., Veltink, P.H., Reenalda, J. Estimating 3D orientation of a body segment during running using a single gyroscope. Abstract booklet of 16th International symposium on 3D-analysis of human movement (3D-AHM) 2020.

Abstract

Long distance running has a high incidence of injuries. Wearable sensors are suitable to monitor running technique (i.e., joint angles based on segment orientations) and provide feedback to runners, potentially contributing to reducing injury risk. Wearable sensors often consist of accelerometers, gyroscopes and are typically combined with magnetometers. Three-dimensional (3D) orientation estimation of a body segment based on just a single gyroscope could limit computational load and increase battery life but is prone to errors. Currently, there is no drift-free 3D orientation estimation for running based on a single gyroscope. The aim of this study was to test two new methods for 3D orientation drift reduction, based on the assumption that running is quasi-cyclical. Method 1 is based on zero-mean corrected angular velocities before estimating orientation. Method 2 is based on a coordinate transformation, reducing tibia rotations to a quasi-1D rotation in a new coordinate system. These methods were tested during treadmill running. Zero-mean correction did not reduce drift; however, a coordinate transformation reducing tibia rotations to a quasi-1D rotation in a new coordinate system strongly reduced drift in 3D orientation estimation.

Introduction

Long distance running is associated with high risks of lower extremity injuries [1]. Improper running technique and changes in running technique due to fatigue are expected to contribute to the aetiology of these injuries. When the running technique can be measured easily in real-life settings, runners can be informed in real-time about their current technique and can make corrections to their technique or training to reduce injury risk.

There are a number of sensor systems that can be used to measure running technique (e.g., joint angles based on segment orientations) in a real-life setting. Such sensor systems frequently consist of inertial measurement units (IMUs), which are composed of accelerometers, gyroscopes and often combined with magnetometers. Previous research from our group showed the possibility of an 8 IMU sensor setup to track changes in running technique during a marathon [2]. This required heavy computations afterwards. In order to reduce computational load, a single IMU can be used to calculate 3D orientation, acceleration, velocity and position of selected body segments based on a strapdown inertial navigation algorithm (i.e., sensor fusion) [3]. This algorithm uses the angular velocity to estimate 3D orientation based on numerical integration, although this is prone to integration drift. Gyroscopes are also subject to errors (e.g., bias and thermo-mechanical white noise) [3]. When integrated, most errors become significant as they add up over time [4]. Drift in the estimated 3D orientation should be minimized as it affects the estimated acceleration rotated to the global coordinate system. Orientation drift corrections can be based on sensor fusion or domain-specific assumptions. Downsides of sensor fusion include; requiring multiple sensors, computationally heavy algorithms, and (often) an extensive calibration procedure. All of these can be a burden to runners. A domain-specific assumption often used during walking is the zero velocity update, which assumes the velocity of the foot to be zero during the stance phase [5,6]. This method is less suitable for running at higher velocities, as the stance phase is too short. A domain-specific assumption for orientation drift reduction in running based on a single gyroscope would equip us with a small sensor and a relatively simple algorithm to provide drift-free 3D orientation of a body segment during running without the need for an extensive calibration procedure.

Hence, the aim of this study was to investigate if the quasi-cyclical nature of running can be used to acquire drift-free 3D orientation of a body segment using a single gyroscope. Two methods for drift reduction are proposed and tested. Both methods depend on the assumption that constant speed running in a straight line is quasi-cyclical and that consecutive gait cycles and their parameters (e.g., orientation) are therefore similar. Method 1 corrects the angular velocity to have a zero-mean before estimating orientation. Method 2 rotates angular velocities to a partly functional coordinate system, which reduces the motion of the tibia to a quasi-1D rotation before estimating orientation. We hypothesize that Method 2 will work best because 3D orientations are non-commutative and, therefore, the mean angular velocity does not need to be zero for a cyclical 3D movement.

Material and Methods

Orientation estimation

The orientation of the sensor coordinate system (ψ^s) at any time with respect to the initial sensor coordinate system ($\psi^{s,init}$) depends on the previous sensor orientation and the angular velocities measured in all three axes (Equation 5.1) [7]. The time-dependent rotation matrix $R_s^{s,init}$ expresses the rotation from ψ^s to $\psi^{s,init}$. $\dot{R}_s^{s,init}$ is the time derivative of $R_s^{s,init}$. $\tilde{\omega}_s$ is a skew-symmetric matrix consisting of the components of the angular velocity vector as measured in the sensor coordinate system ψ^s (Equation 5.2) [7]. $R_s^{s,init}$ can then be transformed to quaternions to visualize orientations.

$$\dot{R}_s^{s,init} = R_s^{s,init} * \tilde{\omega}_s \tag{5.1}$$

$$\tilde{\omega}_s = \begin{bmatrix} 0 & -\omega_z & \omega_y \\ \omega_z & 0 & -\omega_x \\ -\omega_y & -\omega_x & 0 \end{bmatrix} \tag{5.2}$$

Errors and drift

A gyroscope can be modeled as Equation 5.3, where the relation between the estimated angular velocity $\hat{\omega}_s$ is based on the measurement of its actual value ω_s and is influenced by an estimated bias $\hat{b}$ and stochastic component σ, assuming that the gain is correct. The estimated bias $\hat{b}$ is assumed to be the actual bias b plus a bias error b_e (Equation 5.4).

$$\hat{\omega}_s = \omega_s + \hat{b} + \sigma \tag{5.3}$$

$$\hat{b} = b + b_e \tag{5.4}$$

It is expected that b_e has the largest influence on orientation estimation drift since its effect grows linearly over time if the actual orientation is not changing. The effect of the stochastic component σ is assumed to be minimal. If b_e is the only major influence on the drift in the orientation estimation, the effect of b_e on the orientation can be analyzed using Equation 5.2 and 5.1. Please note that errors in angular velocity components impact the derivative of the orientation matrix $\dot{R}_s^{s,init}$ in other axes (Equation 5.2).

Method 1: Zero-mean

We assume that during constant speed running in a straight line, consecutive gait cycles and their parameters (e.g., orientation) are similar, and that b_e would result in a drift in the orientation estimation. Furthermore, we assume that the quasi-cyclical movement is such that the mean angular velocity in each axis over a complete number of gait cycles is zero. Therefore, Method 1 consists of correcting for drift in orientation estimation by subtracting the mean angular velocity (assumed to be equal to b_e) of a complete number of gait cycles in each axis to acquire a zero-mean angular velocity $\omega_{s(zero-mean)}$.

Method 2: Transformed coordinate system

Furthermore, we assume that rotations of the tibia during running are quasi-1D since they predominantly occur around the flexion/extension rotation axis perpendicular to the sagittal plane. Hence, Method 2 first rotates ψ^s to a partly functional coordinate system ψ^{pf}, of which one axis is approximately perpendicular to the sagittal plane. Thereby we ensure that the angular velocity around this axis is considerably larger than the angular velocities around the other axes, thus, creating quasi-1D angular velocities. Principal component analysis is used to determine the axis around which most rotation occurs (Equation 5.5). This axis, the first principal component (*PC1*), is used to create the rotation matrix R_s^{pf} (Equations 5.6 and 5.7)[7]. In Method 2, R_s^{pf} is used to rotate the angular velocity from ψ^s to ψ^{pf}, resulting in ω_{pf}.

$$z_s^{pf} = PC1 \times \begin{bmatrix} 0 & 1 & 0 \end{bmatrix} \tag{5.5}$$

$$y_s^{pf} = z_s^{pf} \times PC1 \tag{5.6}$$

$$R_s^{pf} = \left[PC1; \quad \frac{y_s^{pf}}{\left\| y_s^{pf} \right\|}; \quad \frac{z_s^{pf}}{\left\| z_s^{pf} \right\|} \right] \tag{5.7}$$

For both methods, orientations are estimated with Equations 5.2 and 5.1. Orientations estimates of Method 1 are rotated to ψ^{pf} with R_s^{pf} to be able to compare them with the results of Method 2. Additionally, Methods 1 and 2 are combined by zero-mean correction of ω_{pf}, resulting in $\omega_{pf(zero-mean)}$, before orientation estimation with Equations 5.2 and 5.1.

Participants and measurement setup

The measurement was performed with one healthy male subject with running experience (age: 22 years, mass: 70.0 kg, height: 1.76 m). The subject signed informed consent and the measurements were conducted in accordance with the Declaration of Helsinki. The subject ran for 90 seconds at 12 km/h on a treadmill (ForceLink, Culemborg, the Netherlands). Angular velocities were collected with a wireless IMU (MTw Awinda, Xsens Technologies B.V., the Netherlands) with a sampling frequency of 100 Hz. The weight of the sensor was 16 grams and the signal range of the gyroscope ±2000 deg/s. The IMU was placed on the medial proximal side of the right tibia and fixated with double-sided tape between the skin and the sensor and adhesive tape over the sensor.

Data analysis

Complete trials were cut into time-normalized gait cycles. Gait cycles started and ended with a falling edge zero crossing of $\omega_{s,y}$. This moment occurs just before initial contact. Quaternions were used to visualize rotations with respect to the initial orientation (i.e., first falling edge zero crossing of $\omega_{s,y}$ during the trial). A quaternion consists of a scalar q_0 and a vector part $\mathbf{q}$ (Equation 5.8) [8]. With the scalar part, the magnitude of the rotation between the initial orientation and another orientation can be shown. If q_0 = 1 this indicates that there is no orientation difference while q_0 = 0 indicates a rotation of 180° with respect to the initial orientation. The amount of orientation drift for the different methods is visually compared based on the scalar part of the quaternion and the (mean) standard deviation of the vector part of the quaternion. Data were analyzed offline in MATLAB R2016b.

$$q = q_0 + \mathbf{q} = q_0 + (iq_1 + jq_2 + kq_3) \tag{5.8}$$

Results

The angular velocity without drift reduction shows a small standard deviation (Figure 5.1). Scalar and vector parts of the quaternions for the drift reduction methods are shown in Figure 5.2 and Figure 5.3. If the estimated 3D rotations were exactly cyclical, the quaternion scalar part would reach a value of approximately 1 during each gait cycle and the standard deviation of the vector part of the quaternion would be small. Mean standard deviations of the quaternion vector parts are shown in Table 5.1.

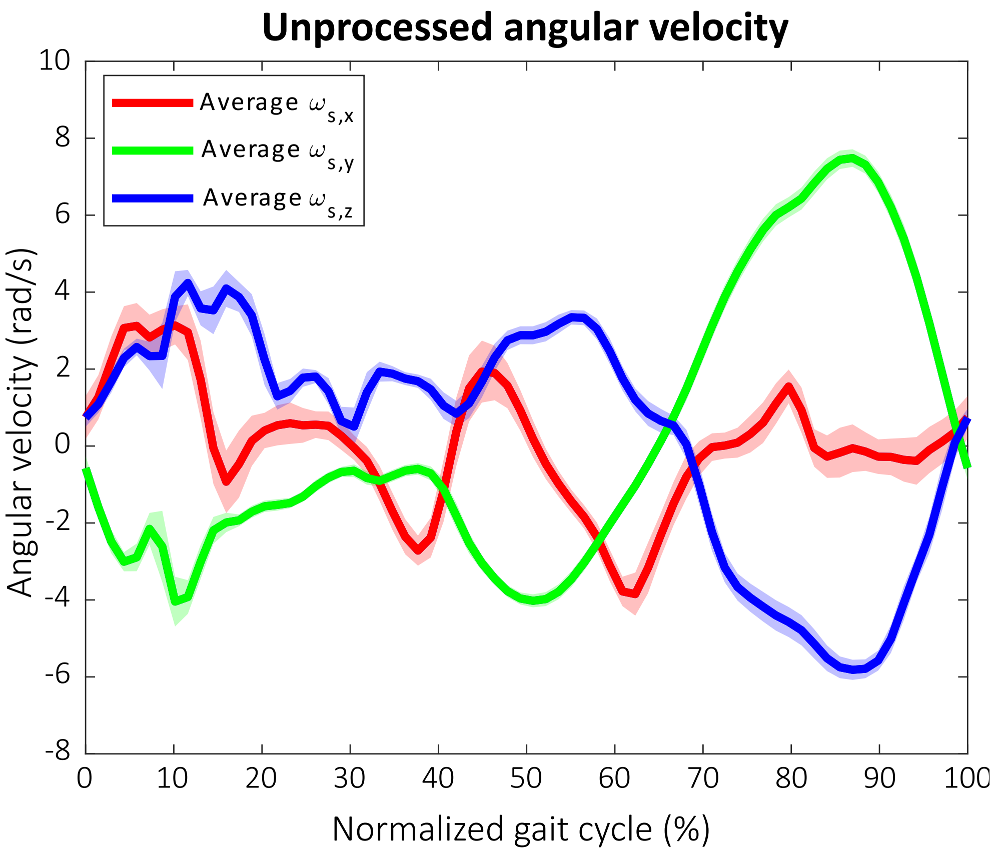

Figure 5.1: *Mean angular velocity in ψ^s as a function of the gait cycle. Shaded areas represent standard deviations around the mean.*

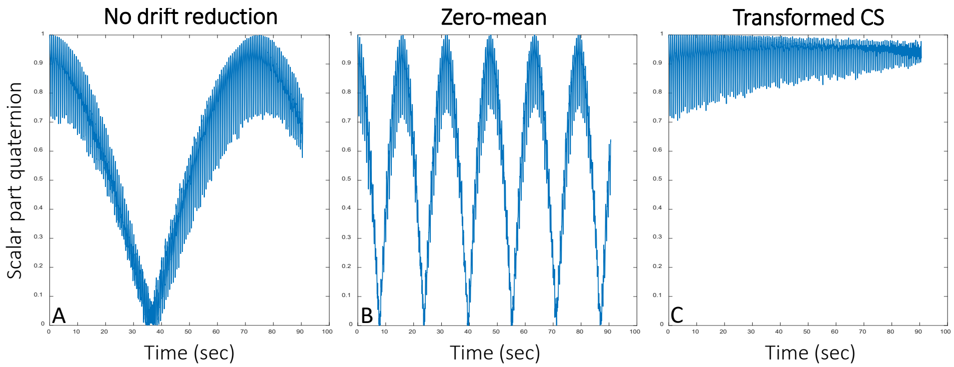

Figure 5.2: *The scalar part of the quaternions as a function of time. A, B and C show respectively the results with no drift reduction, zero-mean (Method 1), and transformation to a partly functional coordinate system (CS) ψ^{f} (Method 2).*

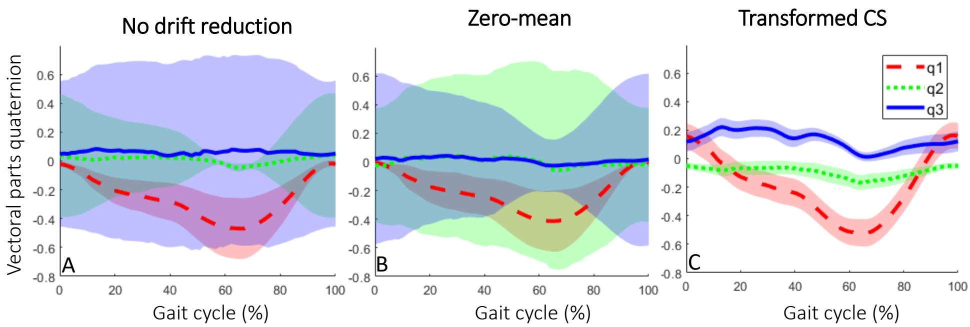

Figure 5.3: *The vector parts of the quaternions in ψ^{pf} as a function of the gait cycle. A, B and C show respectively the results with no drift reduction, zero-mean (Method 1), and transformation to a partly functional coordinate system (CS) ψ^{pf}*

Table 5.1: *Mean standard deviation of the quaternion vector parts for the different drift reduction methods, including the combination of Method 1 and 2 (i.e., transformed coordinate system and zero-mean). CS = Coordinate system.*

	No drift reduction	Method 1: Zero-mean	Method 2: Transformed CS	Method 1+2
q1	0.12	0.12	0.10	0.12
q2	0.22	0.57	0.04	0.63
q3	0.61	0.41	0.05	0.29

Discussion

The aim of this study was to investigate if the quasi-cyclical nature of running can be used for drift-free 3D orientation of a body segment using a single gyroscope. This study showed that orientation drift could be drastically reduced by transforming angular velocities to a different coordinate system (i.e., Method 2) before estimating 3D orientations. The assumption that running at a constant speed and in a straight line is a quasi-cyclical motion is strengthened by the small standard deviation in the angular velocity (Figure 5.1).

Method 1 assumes that the mean angular velocity during quasi-cyclical running motion should be approximately zero. Therefore, Method 1 subtracts the mean of the angular velocity from each axis over a complete number of gait cycles before estimating 3D orientation. Method 1 did not result in an orientation drift reduction, as shown by the scalar part of the quaternion moving away from 1 (Figure 5.2b) and no reduction in the standard deviation of the vector part of the quaternion compared to no drift reduction (Table 5.1, Figure 5.3b). The angular velocity contains two dominant axes $\omega_{s,y}$ and $\omega_{s,z}$ (Figure 5.1), indicating that the quasi-1D rotation of the tibia is not around a single axis in the sensor coordinate system. Since 3D rotations are non-commutative, rotations in both dominant axes influence the orientation of the sensor coordinate system, resulting in Method 1 failing to decrease drift in orientation. Please note that the errors in cyclical orientation estimation without subtraction of mean angular velocities (Figure 5.2a and Figure 5.3a) may already reduce by increasing the sampling rate of the angular velocity.

To avoid the problem with non-commutative 3D orientations, Method 2 rotates the angular velocity to a partly functional coordinate system, in which the rotation of the tibia occurs mainly around a single axis (flexion/extension). Therefore, a quasi-1D situation is created before 3D orientations are estimated. Method 2 drastically decreased the drift in orientation estimation, as shown by the quaternion scalar part remaining closer to 1 (Figure 5.2c) and the standard deviation of the quaternion vector part being smaller than with no drift reduction or with Method 1 (Table 5.1, Figure 5.3c). However, there is still drift present in the 3D orientation estimation, as shown by the tendency of the scalar part of the quaternion to move away from 1 over the duration of the trial. Additional subtraction of the mean angular velocity in ψ^{pf} before integration (combination of Method 1 and 2) did not improve drift reduction but resulted in larger standard deviations of the vector parts of the quaternions (Table 5.1). This indicates that transforming to a quasi-1D situation helped in reducing orientation drift

but residual rotations around the other two axes are still present. Therefore subtraction of mean angular velocities according to Method 1 does not result in further improvement in estimating cyclical 3D rotations.

The reason for the errors in cyclical orientation estimation in Method 1 is clearly not due to an error in angular velocity bias but to the interactions of angular velocities around different axes according to Equations 5.2 and 5.1, which may reduce if a higher sampling rate would be used. This would need to be further tested. Please note that this interaction can be effectively reduced at the currently applied sampling rate by rotation to a partly functional coordinate system ψ^{pf} with one axis being the principle component of the rotation, directed approximately perpendicular to the sagittal plane (Method 2). This reduced interaction is clearly seen in Equation 5.2 if only ω_x is assumed to be non-zero.

This study showed that transforming angular velocities to a partly functional coordinate system before integration seems to be a promising method for reducing drift in 3D orientation based on a single gyroscope in running. As such, partly functional body segment orientations can be used to define running technique with a single gyroscope instead of using an IMU consisting of an accelerometer, gyroscope, and magnetometer, and eventually contribute to reducing injury risk. In future work, the drift reduction method should be adapted such that accurate 3D orientation estimates can be made for a longer duration, and this method should be validated in a larger group of runners.

References

1. Van Gent, R. N. et al. Incidence and determinants of lower extremity running injuries in long distance runners: A systematic review. Br. J. Sports Med. 41, 469–480 (2007).
2. Reenalda, J., Maartens, E., Homan, L. & Buurke, J. H. Continuous three dimensional analysis of running mechanics during a marathon by means of inertial magnetic measurement units to objectify changes in running mechanics. J. Biomech. 49, 3362–3367 (2016).
3. Woodman, O. J. An introduction to inertial navigation. Tech. Rep. Univ. Cambridge (2007) doi:10.4271/2000-01-0305.
4. Luttwak, A. Human Motion Tracking and Orientation Estimation using inertial sensors and RSSI measurements. (2011).
5. Park, S. K. & Suh, Y. S. A zero velocity detection algorithm using inertial sensors for pedestrian navigation systems. Sensors 10, 9163–9178 (2010).
6. Yun, X., Bachmann, E. R., Moore IV, H. & Calusdian, J. Self-contained position tracking of human movement using small inertial/magnetic sensor modules. Proc.- IEEE Int. Conf. Robot. Autom. 2526–2533 (2007) doi:10.1109/ROBOT.2007.363845.
7. Bortz, J. E. A new mathematical formulation for strapdown inertial navigation. 61–66 (1971).
8. Kuipers, J. B. Quaternions and rotation sequences. Princet. Univ. Press Fifth prin, (2002).

Chapter 6

Drift-free 3D orientation and displacement estimation for quasi-cyclical movements using one inertial measurement unit

Application to running

Published as:
Zandbergen, M.A., Reenalda, J., van Middelaar, R.P., Ferla, R.I., Buurke, J.H., Veltink, P.H. Drift-free 3D orientation and displacement estimation for quasi-cyclical movements using one inertial measurement unit: Application to running. Sensors, 22(3), 956 (2022).

The data presented in this study are openly available in 4TU.ResearchData.

Abstract

A Drift-Free 3D Orientation and Displacement estimation method (DFOD) based on a single inertial measurement unit (IMU) is proposed and validated. Typically, body segment orientation and displacement methods rely on a constant- or zero-velocity point to correct for drift. Therefore, they are not easily applicable to more proximal segments than the foot. DFOD uses an alternative single sensor drift reduction strategy based on the quasi-cyclical nature of many human movements. DFOD assumes that the quasi-cyclical movement occurs in a quasi-2D plane and with an approximately constant cycle average velocity. DFOD is independent of a constant- or zero-velocity point, a biomechanical model, Kalman filtering or a magnetometer. DFOD reduces orientation drift by assuming a cyclical movement, and by defining a functional coordinate system with two functional axes. These axes are based on the mean acceleration and rotation axes over multiple complete gait cycles. Using this drift-free orientation estimate, the displacement of the sensor is computed by again assuming a cyclical movement. Drift in displacement is reduced by subtracting the mean value over five gait cycles from the free acceleration, velocity, and displacement. Estimated 3D sensor orientation and displacement for an IMU on the lower leg were validated with an optical motion capture system (OMCS) in four runners during constant velocity treadmill running. Root mean square errors for sensor orientation differences between DFOD and OMCS were 3.1 ± 0.4° (sagittal plane), 5.3 ± 1.1° (frontal plane), and 5.0 ± 2.1° (transversal plane). Sensor displacement differences had a root mean square error of 1.6 ± 0.2 cm (forward axis), 1.7 ± 0.6 cm (mediolateral axis), and 1.6 ± 0.2 cm (vertical axis). Hence, DFOD is a promising 3D drift-free orientation and displacement estimation method based on a single IMU in quasi-cyclical movements with many advantages over current methods.

Introduction

Activities like walking, running, swimming, rowing, and skating are all quasi-cyclical in nature. The repetitiveness of these movements, and their associated loads on the human body, can result in overuse injuries [1]. Repetitive movements are often studied inside movement analysis laboratories for insight into overloading of the human body and performance enhancement, among other applications. With the introduction of wearable systems, motion analysis is no longer restricted to a controlled lab setting [2,3]. This opens up new possibilities of analyzing movements that are difficult to measure in a lab, due to technical constraints of optical motion capture systems (OMCS).

Inertial measurement units (IMUs) are widely used in wearable motion capture systems due to their small size and ease of use [4]. IMUs are composed of accelerometers, gyroscopes, and are often combined with magnetometers. The acceleration, orientation, and displacement of a sensor are of interest for many motion analysis applications such as impact analyses, monitoring the range of motion (ROM), or inclination of a body segment, e.g., the lower leg [5,6]. To obtain orientation and displacement from sensor accelerations and angular velocities, the orientation of the sensor in the global coordinate system (CS) (ψ^{gl}) is required. Displacement can then be obtained via strapdown inertial navigation, although this process is prone to errors [7]. Drift in estimated 3D orientations should be minimized as it strongly influences the estimated displacement in ψ^{gl} . Drift can be compensated for by incorporating other sensors (i.e., magnetometer). However, drift reduction and 3D orientation estimation become more challenging during highly dynamic movements, prolonged measurements, or when magnetic distortions are present [8]. Drift can alternatively be reduced by applying domain-specific assumptions, such as the zero-velocity update method [9,10].

The zero-velocity update method assumes that the velocity of the foot is zero and the orientation of the foot is known during the stance phase. This information is used to reset drift in orientation, velocity, and position during each gait cycle [9,10]. Similar assumptions have been used in running in specific conditions. Bailey and Harle corrected for positional drift of an IMU on the foot by using a constant-velocity update in runners with a heel strike [11]. However, constant- or zero-velocity assumptions are not suitable for more proximal segments or runners with a forefoot strike, since a constant- or zero-velocity point is often not present[12].

To estimate orientation and displacement using a single IMU placed on body segments without a constant- or zero-velocity point, the quasi-cyclical nature of numerous movements can be used. Kalman filtering or analytical integration of acceleration in combination with assumptions about the quasi-cyclical nature of movements have been used to estimate displacements of, for example, the pelvis during walking [13–15]. These studies involved relatively slow movements, required multiple sensors, a calibration procedure, or prior information about the movements. As a solution to many of these drawbacks, we propose to directly use the quasi-cyclical nature of movements to estimate 3D orientation and displacement using a single IMU without the need for Kalman filtering. Hence, the research question of this study was: How to estimate 3D orientation and displacement of a single IMU on the lower leg using the quasi-cyclical nature of running?

To answer this research question, a method is proposed in which drift-free 3D orientation and displacement of a single IMU are estimated using the quasi-cyclical nature of numerous human movements. We call this method Drift-Free Orientation and Displacement estimation (DFOD). DFOD assumes that the movement is quasi-cyclical, occurs in a quasi-2D plane, and has an approximately constant cycle average velocity. DFOD will be demonstrated in treadmill running, although it is expected to generalize to many quasi-cyclical quasi-2D movements.

Materials and methods

Validation of DFOD was part of a larger study. For sake of clarity, only measurement systems and trials required for validation of DFOD will be described.

Participants

Four healthy recreational runners participated in this study (2M/2F, age: 30.6 ± 9.2 years, height: 181 ± 4 cm, body mass: 65.0 ± 5.4 kg). The study was conducted according to the guidelines of the Declaration of Helsinki, and approved by the Ethics Committee of METC Twente. All participants gave written informed consent before participating in the study.

Protocol

Subjects ran for 2 min on a level treadmill at 3.6 m/s. To validate DFOD with OMCS, a calibration procedure was performed in which subjects stood still in a neutral pose and flexed and extended their leg four times while keeping their upper leg horizontal. This calibration procedure was not required for DFOD but was used to convert the OMCS orientation and displacement estimates to the same CS as used in DFOD for comparison purposes.

Measurement systems

Subjects ran on a treadmill (C-Mill, ForceLink, Culemborg, The Netherlands) while 3D angular velocities and accelerations were captured by a single IMU on the lower leg at 240 Hz (MVN Link, Xsens, Enschede, The Netherlands). The ranges of the accelerometer and angular velocity sensor were ±16 g and ±2000°/s, respectively. Positional data from a cluster marker set on the lower leg were captured for reference measurements with an eight-camera optical motion capture system (OMCS) at 100 Hz (Vantage, Vicon, Oxford, UK). The cluster marker set consisted of four individual markers attached to a rigid plate. The IMU was placed medially to the tibial tuberosity and the cluster marker set was placed below the IMU, both on the flat surface of the tibia to ensure measurements of tibia motion, see Figure 6.1. Both systems were attached to the skin with double-sided tape and covered with stretched strapping tape.

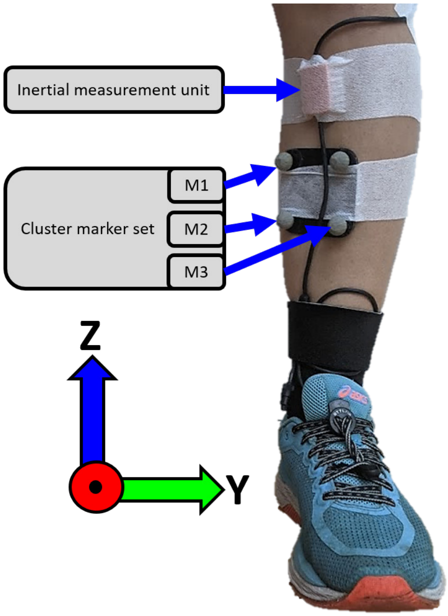

Figure 6.1: *Overview of IMU and cluster marker set placement. "M1", "M2", and "M3" refer to the individual markers of the cluster marker set. The shown coordinate system is the functional coordinate system ψ^f. The X-axis points forward (running direction), the Y-axis mediolateral, and the Z-axis upward.*

Data preparation

Optical and inertial data of the left or right lower leg were selected based on minimal OMCS marker occlusion. Optical data were upsampled to 240 Hz with linear interpolation and low-pass filtered with a recursive fourth-order 20 Hz Butterworth filter [16]. Inertial data were not filtered.

Data were segmented into gait cycles based on falling edge angular velocity zero-crossings in the sensor CS (ψ^s) Y-axis, which was directed in the global CS (ψ^{gl}) forward/mediolateral direction. These zero-crossings occur shortly before initial contact. Data were cropped to include all complete gait cycles during one minute of running, hereby excluding around 30–45 s of data in which the subject increased their running speed from standing still up

to 3.6 m/s. Sensor acceleration and angular velocity in ψ^s (i.e., input signals for DFOD) as a function of the time-normalized gait cycle for a representative subject are shown in Figure 6.2. Data analysis was performed in MATLAB R2021a.

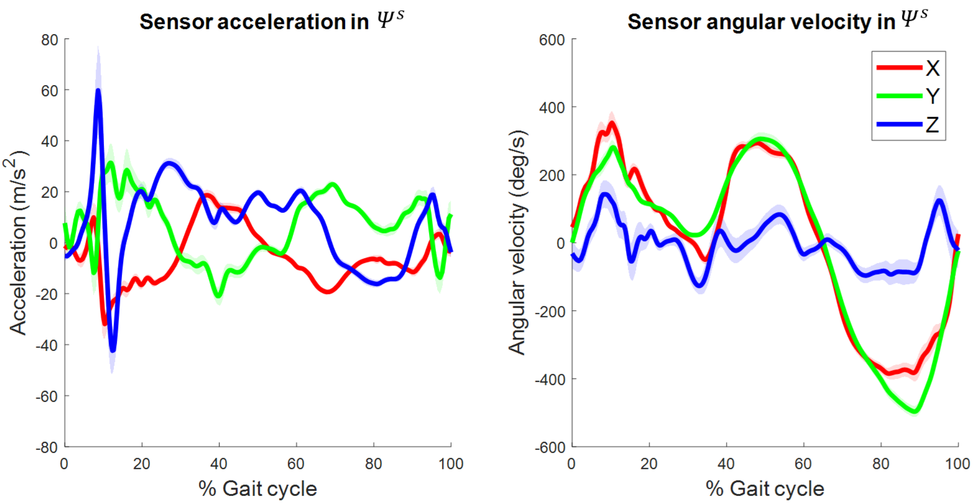

Figure 6.2: *Three-dimensional sensor acceleration (i.e., including gravity) (left figure) and sensor angular velocity (right) in ψ^s as a function of the time-normalized gait cycle for a representative subject. Solid lines represent the mean while shaded areas represent the standard deviation around the mean over one minute of running. Note that these two signals are the input for the orientation and displacement estimation algorithm. Positive acceleration values represent an acceleration into the upward, sideward (left), and forward direction of ψ^s. Positive angular velocity values represent anti-clockwise rotations in ψ^s.*

Estimate sensor orientation in a functional CS (ψ^f)

The aim of DFOD is to estimate 3D orientation and displacement of a single sensor in a functional CS (ψ^f) of which the vertical and mediolateral axes are fixed and the origin moves with the body at the cycle average velocity. ψ^f is defined in Figure 6.1 and Figure 6.3. DFOD assumes that the body segment on which the sensor is placed:

- moves quasi-cyclical (i.e., cycles are similar)
- moves in a quasi-2D plane (i.e., most movement occurs in a 2D plane)
- has an approximately constant cycle average velocity

The time- and gait cycle-dependent rotation matrix $R^f_{s,i}(t)$ from ψ^s to ψ^f, representing the sensor orientation in a functional drift-free CS of which the vertical and mediolateral axes are fixed and the origin moves with the body at the cycle average velocity, can be written as three subsequent rotations as in Equation 6.1:

$$R^{f}_{s,i}(t) = R^{f}_{df,i} R^{df}_{pf}(t) R^{pf}_{s} \tag{6.1}$$

where the sensor CS (ψ^{s}) is first rotated to a sensor-fixed partly functional CS (ψ^{pf}) with the time-independent rotation matrix from ψ^{s} to ψ^{pf} (R^{pf}_{s}). Then, ψ^{pf} is rotated to a drifting partly functional CS (ψ^{df}) with the time-dependent rotation matrix from ψ^{pf} to ψ^{df} ($R^{df}_{pf}(t)$). ψ^{df} has an origin that moves with the cycle average velocity. Lastly, drift in ψ^{df} is corrected for each gait cycle i by rotating to a functional drift free CS (ψ^{f}) with the gait cycle-dependent rotation matrix from ψ^{df} to ψ^{f} ($R^{f}_{df,i}$). All rotations are visualized in Figure 6.3.

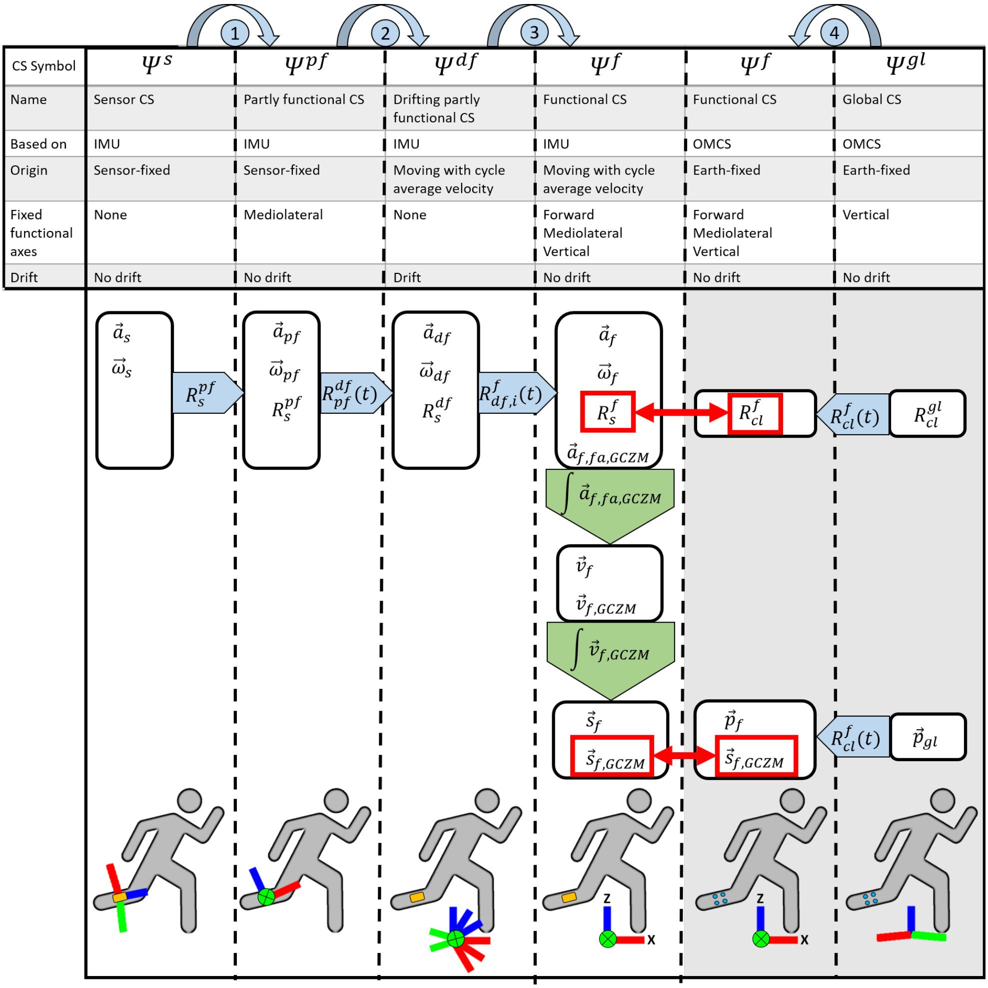

Figure 6.3: *Summary of DFOD (left four columns) and the validation of DFOD (right two columns). Columns represent different coordinate systems (CS). For each CS some basic information is stated: symbol, name, measurement system on which the CS is based, origin, fixed functional axes (i.e., which axes have functional meaning), and the presence of drift. Available quantities in each CS are shown in white squares (all time-dependent), rotation matrices from one CS to another are shown in blue arrows, curved arrows at the top represent the different rotations which are referred to in the text, integrations over time are shown as green arrows. At the bottom of the figure, a schematic representation of the CS with respect to the lower leg of a runner is shown, orange boxes represent the IMU, and blue dots represent the cluster marker set. DFOD is validated against an OMCS based on the quantities in the red squares. Note that the CSs in grey (two right columns) are only used for validation of DFOD and are not a part of DFOD. IMU = inertial measurement unit; OMCS = optical motion capture system; GCZM = gait cycle zero mean (mean value over each gait cycle is subtracted from the gait cycle); CS = coordinate system; $\vec{a}_{CS}$ = acceleration expressed in the CS in the subscript; $\vec{\omega}_{CS}$ = angular velocity expressed in the CS in the subscript; $\vec{a}_{f,fa,GCZM}$ = free acceleration (fa) with a gait cycle zero mean average (GCZM) expressed in the functional CS (f); R_{CS1}^{CS2} = rotation matrix from CS 1 to CS 2; $\vec{v}$ = velocity; $\vec{s}$ = displacement; $\vec{p}$ = position, i = index of gait cycle.*

Rotation 1
From sensor CS (ψ^s) to partly functional CS (ψ^{pf})

Integration error accumulation can be reduced by aligning the rotation axis of a quasi-2D movement with one axis in 3D space to create a partly functional CS (ψ^{pf}) [17]. One axis has functional and anatomical meaning in ψ^{pf}. The functional axis ($\vec{y}^{s}_{pf}$, the y-axis of the sensor-fixed partly functional CS (ψ^{pf}) expressed in the sensor CS (ψ^s)) is perpendicular to the plane of movement. Therefore, this axis is described by the first principal component of the angular velocity in ψ^s ($\vec{\omega}_s$), measured by the 3D angular velocity sensor of the IMU, over one minute of running [18]:

$$\vec{y}^{s}_{pf} = PCA1(\vec{\omega}_s) \tag{6.2a}$$

To create a rotation matrix from ψ^{pf} to ψ^s, a temporary X-axis is defined by arbitrarily setting the X-axis of ψ^{pf} ($\vec{x}'^{\,s}_{pf}$) to the X-axis of ψ^s:

$$\vec{x}'^{\,s}_{pf} = \begin{bmatrix} 1, & 0, & 0 \end{bmatrix} \tag{6.2b}$$

The Z-axis of ψ^{pf} ($\vec{z}^{s}_{pf}$) was computed and $\vec{x}'^{\,s}_{pf}$ updated to ensure an orthogonal CS according to the TRIAD algorithm [19]:

$$\vec{z}^{s}_{pf} = \vec{x}'^{\,s}_{pf} \times \vec{y}^{s}_{pf} \tag{6.2c}$$

$$\vec{x}^{s}_{pf} = \vec{y}^{s}_{pf} \times \vec{z}^{s}_{pf} \tag{6.2d}$$

The time-invariant orthonormal rotation matrix from ψ^{pf} to ψ^s was:

$$R^{s}_{pf} = \left[\frac{\vec{x}^{s}_{pf}}{\left\|\vec{x}^{s}_{pf}\right\|}; \quad \frac{\vec{y}^{s}_{pf}}{\left\|\vec{y}^{s}_{pf}\right\|}; \quad \frac{\vec{z}^{s}_{pf}}{\left\|\vec{z}^{s}_{pf}\right\|} \right] \tag{6.2e}$$

The time-invariant rotation matrix from ψ^s to ψ^{pf} (R^{pf}_{s}) was obtained by taking the inverse of R^{s}_{pf} (Equation 6.2e):

$$R^{pf}_{s} = {R^{s}_{pf}}^{-1} \tag{6.2f}$$

Rotation 2
From partly functional CS (ψ^{pf}) to drifting partly functional CS (ψ^{df})

To go from a sensor-fixed CS to a drifting CS in which axes do not depend on the sensor orientation, the angular velocity in ψ^{pf} ($\vec{\omega}_{pf}$) was integrated according to Bortz [20,21]. $\vec{\omega}_{pf}$ was expressed as a skew-symmetric matrix ($\tilde{\omega}_{pf}$), and the differential equation was solved and used to obtain the rotation matrix from ψ^{pf} to ψ^{df} (R^{df}_{pf}):

$$\tilde{\omega}_{pf}(t) = \begin{pmatrix} 0 & -\omega_{pf,z}(t) & \omega_{pf,y}(t) \\ \omega_{pf,z}(t) & 0 & -\omega_{pf,x}(t) \\ -\omega_{pf,y}(t) & -\omega_{pf,x}(t) & 0 \end{pmatrix} \tag{6.3a}$$

$$\dot{R}^{df}_{pf}(t) = R^{df}_{pf}(t)\tilde{\omega}_{pf}(t) \tag{6.3b}$$

$\dot{R}^{df}_{pf}(t)$ is the time-derivative of $R^{df}_{pf}(t)$, and $R^{df}_{pf}(t)$ at $t = 0$ is the identity matrix. Note that ψ^{df} drifts, predominantly around the y-axis (ψ^{df}_{y}), due to accumulated integration errors from Equations 6.3a and 6.3b. This drift needs to be corrected to get a useful orientation estimate of the sensor (rotation 3 in Figure 6.3).

Rotation 3
From drifting partly functional CS (ψ^{df}) to drift-free functional CS (ψ^{f})

Following an assumption of quasi-cyclical running, the lower leg keeps rotating around the same mediolateral axis. By continuously calculating this rotation axis we can correct for integration drift from Equation 6.3a and 6.3b. The rotation axis was again based on the first principal component of the 3D angular velocity, now in ψ^{df} ($\vec{\omega}_{df}$), over five complete gait cycles (Equation 6.4a). Multiple gait cycles were included to obtain a more robust estimate of $\vec{y}^{f}_{df,i}$ (see section "Algorithm characteristics"):

$$\vec{y}^{f}_{df,i} = PCA1(\vec{\omega}_{df}(t)) \qquad t_{0_i} - T_{i-1} - T_{i-2} < t < t_{0_i} + Ti + T_{i+1} + T_{i+2} \tag{6.4a}$$

Where $t_{0_i} - T_{i-1} - T_{i-2} < t < t_{0_i} + Ti + T_{i+1} + T_{i+2}$ represents the interval of five complete gait cycles, t_{0_i} stands for the first time point of gait cycle i, T_i stands for the duration of gait cycle i, and is obtained from the earlier described falling edge angular velocity zero-crossings in ψ_y^s (See section "Data preparation"). Note that the first principal component of the angular velocity is obtained twice (Equation 6.2a and Equation 6.4a). In Equation 6.2a, $\vec{y}_s^{\,pf}$ has a constant value over a longer period of time since there is no drift in ψ^s. In Equation 6.4a, the angular velocity ($\vec{\omega}_{df}$) is expressed in a drifting CS (ψ^{df}). Therefore, $\vec{y}^{\,f}_{df,i}$ differs for each gait cycle to correct for the drift in ψ^{df}.

Following an assumption of approximately constant cycle average velocity running, the free acceleration in ψ^f will be approximately zero-mean over a complete gait cycle. Hence, the mean total acceleration (i.e., including gravity) over a complete number of gait cycles represents the gravitational acceleration and is directed vertically. Therefore, the temporary Z-axis of the functional CS ψ^f ($\vec{z}\,'^{\,f}_{df}$) was based on the average total acceleration (i.e., including gravity) in ψ^{df} ($\vec{a}_{df}$), over five complete gait cycles (Equation 6.4b). Multiple gait cycles were included to obtain a more robust estimate of $\vec{z}\,'^{\,f}_{df}$ (see section "Algorithm characteristics"):

$$\vec{z}\,'^{\,f}_{df,i} = \frac{1}{\sum_{j=-2}^{+2} T_{i+j}} \int_{t_{0_i}-T_{i-1}-T_{i-2}}^{t_{0_i}+T_i+T_{i+1}+T_{i+2}} \vec{a}_{df}(\tau)\,d\tau \qquad (6.4b)$$

where j is an index to define included gait cycles. The x-axis of ψ^{df} ($\vec{x}^{\,f}_{df}$) was computed and $\vec{z}\,'^{\,f}_{df,i}$ updated to ensure an orthogonal CS according to the TRIAD algorithm [19]:

$$\vec{x}^{\,f}_{df,i} = \vec{y}^{\,f}_{df,i} \times \vec{z}\,'^{\,f}_{df,i} \qquad (6.4c)$$

$$\vec{z}^{\,f}_{df,i} = \vec{x}^{\,f}_{df,i} \times \vec{y}^{\,f}_{df,i} \qquad (6.4d)$$

The orthonormal drift-correcting rotation matrix from ψ^{df} to ψ^f was:

$$R^f_{df,i} = \left[\frac{\vec{x}^{\,f}_{df,i}}{\left\|\vec{x}^{\,f}_{df,i}\right\|};\quad \frac{\vec{y}^{\,f}_{df,i}}{\left\|\vec{y}^{\,f}_{df,i}\right\|};\quad \frac{\vec{z}^{\,f}_{df,i}}{\left\|\vec{z}^{\,f}_{df,i}\right\|} \right] \qquad (6.4e)$$

where $R^f_{df,i}$ has a constant value within each cycle but varies over cycles to correct for drift. The drift-free 3D rotation matrix of the sensor in a functional CS ($R^f_{s,i}$) of which the vertical and mediolateral axes are fixed, and the origin moves with the body at the cycle average velocity was then computed with Equation 6.1.

From sensor orientation to sensor displacement

Three-dimensional angular velocity and total (i.e., including gravity) acceleration in ψ^f ($\vec{\omega}_f$ and $\vec{a}_f$) were obtained with Equation 6.1. Free acceleration in ψ^f ($\vec{a}_{f,fa}$) was obtained by subtracting the modulus of the gravitational acceleration ($\vec{g}_f$) from the total acceleration ($\vec{a}_f$):

$$\vec{a}_{f,fa}(t) = \vec{a}_f(t) - \begin{bmatrix}0, & 0, & \|\vec{g}_f\|\end{bmatrix} \tag{6.5a}$$

Following an assumption of approximately constant cycle average velocity, the free acceleration in ψ^f will be approximately zero-mean over a complete number of gait cycles. Hence, the mean free acceleration value over a window of five gait cycle was subtracted to correct for drift:

$$\vec{a}_{f,fa,GCZM}(t) = \vec{a}_{f,fa}(t) - \frac{1}{T_i}\int_{t_{0_i}-T_{i-1}-T_{i-2}}^{t_{0_i}+T_i+T_{i+1}+T_{i+2}} \vec{a}_{f,fa}(\tau)d\tau \qquad t_{0_i} \leq t \; and \; t_{0_i} + T_i > t \tag{6.5b}$$

where $\vec{a}_{f,fa,GCZM}$ is the free acceleration with a gait cycle zero-mean (GCZM). $\vec{a}_{f,fa,GCZM}$ was numerically integrated (Figure 6.3, Column ψ^f, upper green arrow) with the trapezoidal rule to obtain the velocity ($\vec{v}_f$):

$$\vec{v}_f(t) = \int_{t_{0_i}}^{t} \vec{a}_{f,fa,GCZM}(\tau)d\tau \tag{6.6a}$$

Following an assumption of approximately constant cycle average velocity, the mean velocity in ψ^f over a complete number of gait cycles is approximately zero in all axes since the origin of ψ^f moves with the body at the cycle average velocity. Hence, the drift-corrected GCZM velocity was computed by subtracting the mean velocity over a window of five gait cycles:

$$\vec{v}_{f,GCZM}(t) = \vec{v}_f(t) - \frac{1}{T_i}\int_{t_{0_i}-T_{i-1}-T_{i-2}}^{t_{0_i}+T_i+T_{i+1}+T_{i+2}} \vec{v}_f(\tau)d\tau \tag{6.6b}$$

$$t_{0_i} \leq t \; and \; t_{0_i} + T_i > t$$

Sensor displacement in ψ^f ($\vec{s}_f$) was obtained with the trapezoidal rule and numeric integration of $\vec{v}_{f,GCZM}$ (Figure 6.3, Column ψ^f, lower green arrow):

$$\vec{s}_f(t) = \int_{t_{0_i}}^{t} \vec{v}_{f,GCZM}(\tau)d\tau \tag{6.7a}$$

Following an assumption of approximately constant cycle average velocity, the mean displacement in ψ^f approximates zero is all directions over a complete number of gait cycles. Hence, the mean displacement over five gait cycles was subtracted and GCZM displacement ($\vec{s}_{f,GCZM}$) was computed and used as outcome measure:

$$\vec{s}_{f,GCZM}(t) = \vec{s}_f(t) - \frac{1}{T_i}\int_{t_{0_i}-T_{i-1}-T_{i-2}}^{t_{0_i}+T_i+T_{i+1}+T_{i+2}} \vec{s}_f(\tau)d\tau \tag{6.7b}$$

$$t_{0_i} \leq t \; and \; t_{0_i} + T_i > t$$

Validation of orientation and displacement estimates

The steps described below are used to validate DFOD and are not part of DFOD. To compare the results of DFOD against OMCS, the orientation of the cluster marker set was computed and both the orientation and displacement were transformed to ψ^f.

Rotation 4
From optical motion capture CS (ψ^{cl}) to functional CS (ψ^f)

The orientation of the OMCS cluster marker set in (ψ^{gl}) was based on the relative positions of three of its individual markers according to the TRIAD algorithm [19]:

$$\vec{z}_{cl}^{\,gl}(t) = \vec{p}_{gl,m2}(t) - \vec{p}_{gl,m1}(t) \tag{6.8a}$$

$$\vec{y}'^{\,gl}_{cl}(t) = \vec{p}_{gl,m3}(t) - \vec{p}_{gl,m1}(t) \tag{6.8b}$$

where $\vec{p}_{gl,m}$ refers to the position of the individual markers of the cluster marker set in ψ^{gl}, see Figure 6.1. $\vec{z}\,^{gl}_{cl}$ and $\vec{y}\,'\,^{gl}_{cl}$ represent the Z-axis and temporary Y-axis of the cluster marker CS (ψ^{cl}) in ψ^{gl}. The X-axis of ψ^{cl} ($\vec{x}^{gl}_{cl}$) was computed and $\vec{y}\,'\,^{gl}_{cl}$ updated to ensure an orthogonal CS:

$$\vec{x}\,^{gl}_{cl}(t) = \vec{y}\,'\,^{gl}_{cl}(t) \times \vec{z}\,^{gl}_{cl}(t) \tag{6.8c}$$

$$\vec{y}\,^{gl}_{cl}(t) = \vec{z}\,^{gl}_{cl}(t) \times \vec{x}\,^{gl}_{cl}(t) \tag{6.8d}$$

The orthonormal rotation matrix of ψ^{cl} to ψ^{gl} (R^{gl}_{cl}) was:

$$R^{gl}_{cl}(t) = \left[\frac{\vec{x}^{gl}_{cl}(t)}{\left\|\vec{x}^{gl}_{cl}(t)\right\|};\quad \frac{\vec{y}^{gl}_{cl}(t)}{\left\|\vec{y}^{gl}_{cl}(t)\right\|};\quad \frac{\vec{z}^{gl}_{cl}(t)}{\left\|\vec{z}^{gl}_{cl}(t)\right\|}\right] \tag{6.8e}$$

To be comparable, the 3D orientation and position of the OMCS cluster marker set need to be expressed in the same functional CS as used for the sensor orientation and displacement estimate of DFOD. Therefore, the OMCS functional Y-axis (ψ^{f}_{y}) in ψ^{gl} ($\vec{y}\,^{gl}_{f}$) should be based on the same functional axis as in Equation 6.4a. However, differentiating $R^{gl}_{cl}(t)$ and computing the first principal component is prone to stochastic errors induced by differentiating 3D orientations. Alternatively, we estimated the rotation axis of the lower leg ($\vec{y}\,^{gl}_{f}$) during the flexion–extension movements of the calibration trial, described in the section "Protocol" . During the flexion–extension movements, the lower leg moves approximately around the same rotation axis. This rotation axis ($\vec{y}\,^{gl}_{f}$) was estimated by first dividing each of the four flexion–extension movements into seven intervals of equal duration ($\frac{T_i}{7}$), T_i being the duration of cycle i. See Section about algorithm characteristics. By using a larger time interval, the change in rotation during this interval is relatively large compared to the errors. The rotation matrix from time point $t_j = t_i + j \times \dfrac{T_i}{7}$ to the next was then computed as follows:

$$R^{t_{j+1}}_{t_j} = R^{gl}_{cl}(t_j)^{-1} R^{gl}_{cl}(t_{j+1}) \tag{6.9a}$$

Subsequently, $R_{t_j}^{t_{j+1}}$ of cycle i was transformed to a rotation axis ($\vec{v}_{rot,i,j}$) which corresponds to the vector part of a quaternion that can be derived from a rotation matrix [22]. $\vec{v}_{rot,i,j}$ was multiplied by a factor −1 for the extension part of each calibration movement cycle to ensure that the rotation axes were approximately equally directed for all intervals. The functional coordinate axis ($\vec{y}_f^{gl}$) (i.e., the rotation axis of the lower leg during the flexion–extension movements) was subsequently determined by averaging all resulting rectified rotation axes ($\vec{v}'_{rot,i,j}$) for all intervals j and all cycles i:

$$\vec{y}_f^{gl} = \frac{1}{4 \times 7} \sum_{i=1}^{4} \sum_{j=1}^{7} \vec{v}'_{rot,i,j} \tag{6.9b}$$

The temporary Z-axis of ψ^f ($\vec{z}'^{gl}_f$) was chosen to be equal to ψ_z^{gl}:

$$\vec{z}'^{gl}_f = \begin{bmatrix} 0, & 0, & 1 \end{bmatrix} \tag{6.9c}$$

The X-axis of ψ^f ($\vec{x}_f^{gl}$) was computed and $\vec{z}'^{gl}_f$ corrected to create an orthogonal CS:

$$\vec{x}_f^{gl} = \vec{y}_f^{gl} \times \vec{z}'^{gl}_f \tag{6.9d}$$

$$\vec{z}_f^{gl} = \vec{x}_f^{gl} \times \vec{y}_f^{gl} \tag{6.9e}$$

The orthonormal time-invariant rotation matrix from ψ^f to ψ^{gl} (R_f^{gl}) was:

$$R_f^{gl} = \left[\frac{\vec{x}_f^{gl}}{\left\| \vec{x}_f^{gl} \right\|}; \quad \frac{\vec{y}_f^{gl}}{\left\| \vec{y}_f^{gl} \right\|}; \quad \frac{\vec{z}_f^{gl}}{\left\| \vec{z}_f^{gl} \right\|} \right] \tag{6.9f}$$

The time-dependent rotation matrix of ψ^{cl} in ψ^f (R_{cl}^f) was then computed and represented the orientation of the cluster marker set in ψ^f (rotation 4 in Figure 6.3):

$$R_{cl}^f(t) = R_f^{gl^{-1}} R_{cl}^{gl}(t) \tag{6.10}$$

Orientation and displacement validation

The sensor and cluster orientation estimates in ψ^f of DFOD and OMCS were expressed in Euler angles (rotation order: YZX) for visualization purposes. To show the added drift-reducing benefit of DFOD in estimating sensor orientation, sensor orientation was also computed by integrating the sensor angular velocity in ψ^s, similar to Equations 6.3a and 6.3b without any drift reducing methods. This resulted in the sensor orientation with respect to the initial sensor orientation ($\psi^{s,init}$) at the start of the first gait cycle. The position of the marker closest to the IMU was selected and displacement during each gait cycle was computed (similar procedure to Equation 6.7b). OMCS and IMU data were time-synchronized based on the GCZM displacement in the forward direction of the sensor and cluster marker set ($\vec{s}_{f,GCZM,x}$). Three-dimensional differences in Euler angles and displacement between DFOD and OMCS over time-normalized gait cycles were quantified as root mean square errors (RMSE) and absolute mean differences. A 1D orientation error was computed by transforming the difference in orientation between DFOD and OMCS to an axis-angle representation and using the rotation angle as an outcome [23]. This 1D angle represents the rotation that is necessary to align R_s^f and R_{cl}^f. A 1D displacement error was defined as the root mean square of the 3D displacement errors. Additionally, differences at the first and last sample of each gait cycle, differences in minimum and maximum values, and the ROM between DFOD and OMCS for each gait cycle were computed and correlations between extrema and ROM were quantified with Pearson correlation coefficients. Correlations are interpreted as very strong for r = (0.90, 1.00), strong for r = (0.70, 0.89), moderate for r = (0.40, 0.69), weak for r = (0.20, 0.39), and very weak for r = (0.00, 0.19) [24]. The mediolateral and vertical axis of DFOD (Equations 6.4a and 6.4b) were based on five gait cycles unless stated otherwise.

Algorithm characteristics

DFOD assumes that the sensor on the lower leg moves quasi-cyclically and in a quasi-2D plane. To quantify how valid these assumptions are for the lower leg motion during treadmill running, respectively the mean cycle time and standard deviation and the explained variance of the first principal component of the angular velocity in ψ^s over one minute of running were computed.

The mediolateral (Equation 6.4a: $\vec{y}^{\,f}_{df,i}$) and vertical axes (Equation 6.4b: $\vec{z}^{\,f}_{df,i}$) of ψ^f can be computed independently of each other and are not necessarily based on data of the same number of gait cycles. The effect of using data of different numbers of gait cycles to determine these axes of ψ^f and its error with respect to an OMCS was tested. Data of 1 up to 15 gait cycles were used to define the mediolateral and vertical axes of ψ^f, resulting in a total of 225 combinations which were tested. The outcome measure of this analysis was the 1D orientation and displacement estimate.

Full trust in the TRIAD algorithm [19] was given to the mediolateral functional axis (Equation 6.4a) since this axis is not influenced by the violation of the approximately constant cycle average velocity assumption. The number of points used to estimate the rotation axis of Equations 6.9a and 6.9b was based on a trial and error procedure to obtain a small variation in the obtained axes while using as few intervals as possible. Note that the results of this trial and error process were only used to validate DFOD and were not part of DFOD.

To investigate the effect of sampling frequency on the performance of DFOD, IMU data were resampled from 240 Hz to 120 Hz and 60 Hz before DFOD was used to estimate orientation and displacement. For this analysis, the vertical and mediolateral axis of DFOD were both based on five gait cycles and the 1D orientation and displacement estimates were used as outcome measures.

Results

An average of 79 gait cycles (range: 66–94) per subject were analyzed. When not stated otherwise, the mediolateral and vertical axes of DFOD (Equations 6.4a and 6.4b) were based on data of five gait cycles.

Estimation of orientation

Estimated lower leg sensor orientations without drift reduction, with drift reduction according to DFOD and from an OMCS are shown in Figure 6.4. Estimated lower leg sensor orientations of DFOD were compared to an OMCS in treadmill running. Mean RMSE for orientations in the sagittal plane were 3.1 ± 0.4° while they were larger in the frontal (5.3 ± 1.1°) and transversal plane (5.0 ± 2.1°). The mean 1D rotation error (i.e., angle over which R_s^f needs to be rotated to coincide with R_{cl}^f was 7.5 ± 1.7°. The 3D mean difference at the start and end of the gait cycle, absolute difference, and maximum and minimum difference in orientation together with the difference in ROM of DFOD and OMCS are shown in Table 6.1. Correlations between the 3D maximal angle, minimal angle, and ROM from DFOD and OMCS ranged from strong (0.77) to very strong (0.99). Mean 3D orientations of DFOD and OMCS for a representative subject are shown in Figure 6.5.

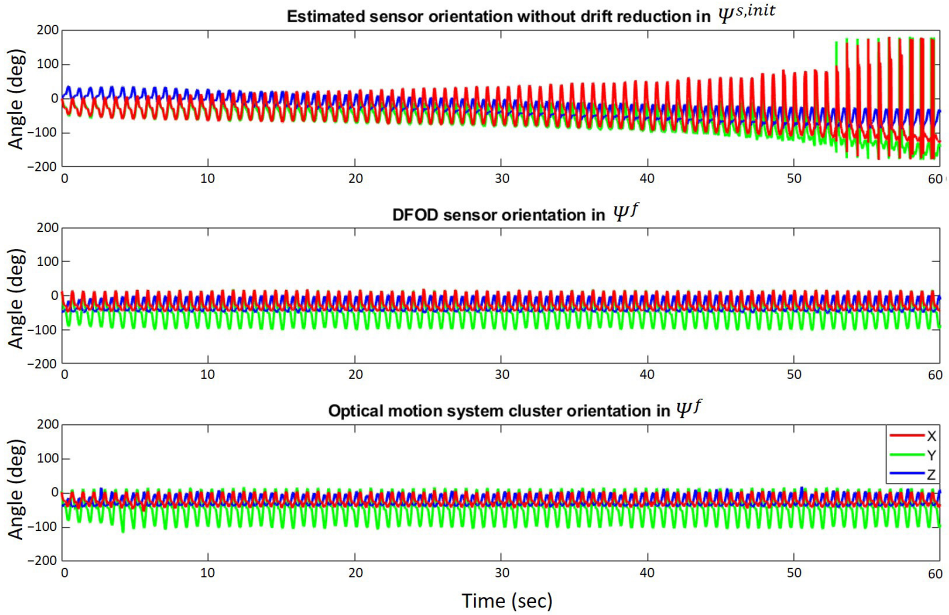

Figure 6.4: *Estimated sensor (inertial) and cluster marker set (optical) orientation for a representative subject. The top figure shows estimated sensor orientation without drift reduction with respect to the initial orientation of the sensor at the start of the first gait cycle ($\psi^{s,init}$). The middle figure shows the estimated sensor orientation obtained with DFOD in ψ^{f}. The bottom figure shows the actual cluster orientation according to an optical motion capture system in ψ^{f}. Note that data of the top graph are shown in a different coordinate system. This figure shows the added drift-reducing benefit of DFOD compared to orientation estimation without drift reduction. Anti-clockwise rotations in $\psi^{s,init}$, (top figure), and ψ^{f} (middle and bottom figure) correspond to positive angles. An angle of zero corresponds to the initial sensor orientation just before initial contact of the first gait cycle in $\psi^{s,init}$ (top figure) or ψ^{f} (middle and bottom figure).*

Table 6.1: *Mean orientation differences between DFOD and OMCS for all subjects combined. RMSE refers to the root mean square difference in 3D orientation. "Difference start cycle" and "Difference end cycle" refer to the difference between DFOD and OCMS (OMCS-DFOD) at the first and last sample of the gait cycle. "Δ Maximal angle" and "Δ Minimal angle" refer to the differences in the estimated maximal and minimal orientation during each gait cycle between DFOD and OMCS (OMCS-DFOD). "Δ ROM" refers to the mean differences in the estimated range of motion during each gait cycle for DFOD and OMCS. Pearson correlation coefficients (r) are provided between brackets.*

Orientation (ψ^f)	RMSE	Mean absolute difference	Difference start cycle	Difference end cycle	Δ Maximal angle	Δ Minimal angle	Δ ROM
Frontal plane (X-axis)	5.3±1.1°	4.3±0.7°	-6.1±5.0°	-6.2±5.1°	-4.7±6.1° (r = 0.78)	3.0±2.2° (r = 0.81)	-7.6±4.4° (r = 0.89)
Sagittal plane (Y-axis)	3.1±0.4°	2.6±0.3°	0.3±3.7°	0.4±4.0°	-0.4±3.4° (r = 0.95)	-2.1±1.7° (r = 0.99)	1.7±3.1° (r = 0.96)
Transversal plane (Z-axis)	5.0±2.1°	4.5±2.1°	-3.5±3.4°	3.4±3.7°	-3.3±3.2° (r = 0.96)	2.3±5.0° (r = 0.97)	-5.6±2.1° (r = 0.81)

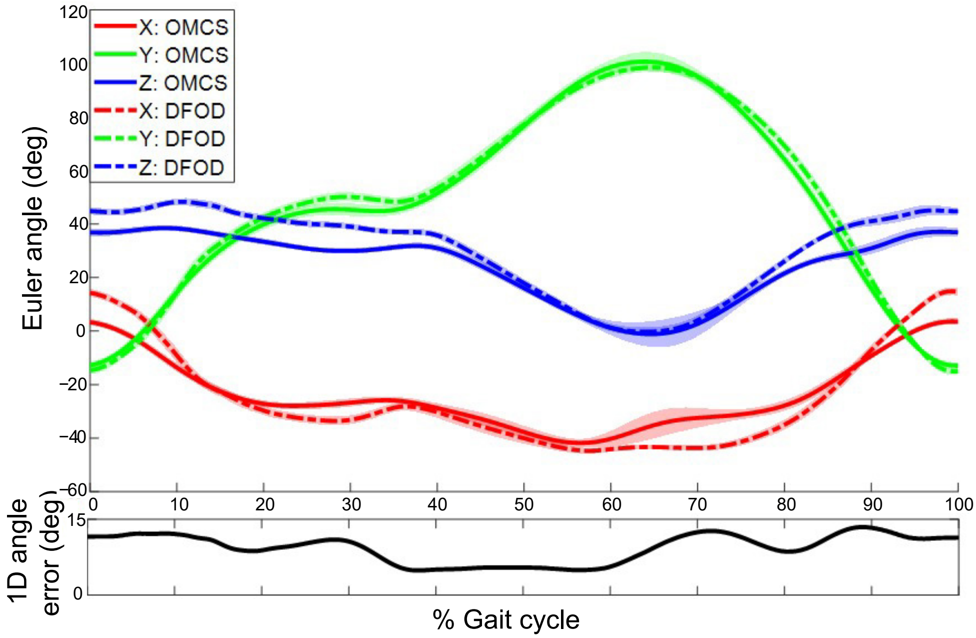

Figure 6.5: *Top figure: Mean time-normalized orientation of a sensor (DFOD, dashed line) and cluster marker (OMCS, solid line) on the lower leg (in ψ^f) as a function of the gait cycle. Shaded areas represent the standard deviation around the mean. Bottom figure: 1D orientation error as a function of the gait cycle. The 1D orientation error is the angle of the axis-angle representation of the difference in orientation between DFOD and OMCS [23]. Data are shown for a representative subject during one minute of running. Positive orientations represent anti-clockwise rotations in ψ^f.*

Estimation of displacement

Estimated lower leg sensor displacements of DFOD were compared to an OMCS in treadmill running. Mean RMSE for displacements in the forward direction were 1.6 ± 0.2 cm and similar for the mediolateral (1.7 ± 0.6 cm) and vertical direction (1.6 ± 0.2 cm). The mean 1D displacement error (i.e., length of the vector between the estimated sensor position of DFOD and OMCS) was 2.7 ± 0.4 cm. The 3D mean difference at the start and end of the gait cycle, absolute difference, maximum difference, and minimum difference in displacement, together with the difference in ROM of DFOD and OMCS, are shown in Table 6.2. Correlations between the 3D maximal displacement, minimal displacement, and ROM were moderate (r = 0.50) to strong (r = 0.82). Mean 3D displacements of DFOD and OMCS for a representative subject are shown in Figure 6.6.

Table 6.2: *Mean displacement differences between DFOD and OMCS for all subjects combined. RMSE refers to the root mean square difference in 3D sensor and cluster displacement. "Difference start cycle" and "Difference end cycle" refer to the difference between DFOD and OCMS (OMCS-DFOD) at the first and last sample of the gait cycle. "Δ Maximal displacement" and "Δ Minimal displacement" refer to the differences in the estimated maximal and minimal displacement during each gait cycle between DFOD and OMCS (OMCS-DFOD). "Δ ROM" refers to the mean differences in the estimated range of motion during each gait cycle for DFOD and OMCS. Pearson correlation coefficients (r) are provided between brackets.*

Displacement (ψ^f)	RMSE	Mean absolute difference	Difference start cycle	Difference end cycle	Δ Maximal displacement (cm)	Δ Minimal displacement (cm)	Δ ROM
Forward (X-axis)	1.6±0.2 cm	1.4±0.2 cm	2.7±0.7 cm	2.8±0.6 cm	2.4±0.7 cm (r = 0.72)	-1.1±0.4 cm (r = 0.79)	3.5±0.9 cm (r = 0.81)
Mediolateral (Y-axis)	1.7±0.6 cm	1.5±0.5 cm	-0.3±2.1 cm	-0.2±2.2 cm	-0.5±1.6 cm (r = 0.51)	0.6±1.5 cm (r = 0.65)	-1.1±3.1 cm (r = 0.59)
Vertical (Z-axis)	1.6±0.2 cm	1.3±0.2 cm	1.9±0.2 cm	2.0±0.3 cm	0.0±1.0 cm (r = 0.50)	-0.4±0.2 cm (r = 0.82)	0.4±1.1 cm (r = 0.71)

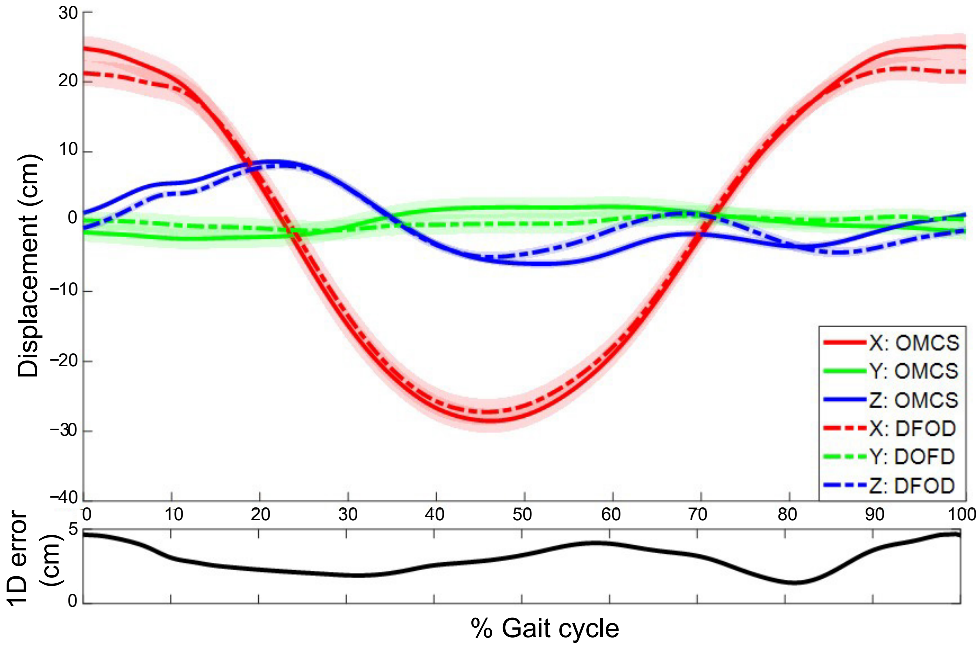

Figure 6.6: *Top figure: Mean time-normalized orientation of a sensor (DFOD, dashed line) and cluster marker (OMCS, solid line) on the lower leg (in ψ^f) as a function of the gait cycle. Shaded areas represent the standard deviation around the mean. Bottom figure: 1D orientation error as a function of the gait cycle. The 1D orientation error is the angle of the axis-angle representation of the difference in orientation between DFOD and OMCS [23]. Data are shown for a representative subject during one minute of running. Positive orientations represent anti-clockwise rotations in ψ^f.*

Algorithm characteristics

Two metrics were computed to show how valid the assumptions of a quasi-cyclical and quasi-2D movements were for treadmill running. The average cycle time was 0.68 ± 0.03 s/stride and the standard deviation ranged from 0.8–1.9% of the average cycle time. The first principal component of the angular velocity explained on average 90.2 ± 5.7% (range: 84.6–95.8%) of the variance.

The mediolateral and vertical axes of ψ^f (Equations 6.4a and 6.4b) are based on data of five complete gait cycles. The effect of using data of more or less gait cycles to define these axes on the mean 1D orientation error is investigated and shown in Figure 6.7. The lowest mean 1D orientation error was found when the vertical axis was based on data of 11 gait cycles and the mediolateral axis on data of 8 gait cycles (mean error: 7.5°). The highest mean orientation error was found when the vertical and mediolateral axes were both based on data of 1 gait cycle (mean error: 7.7°).

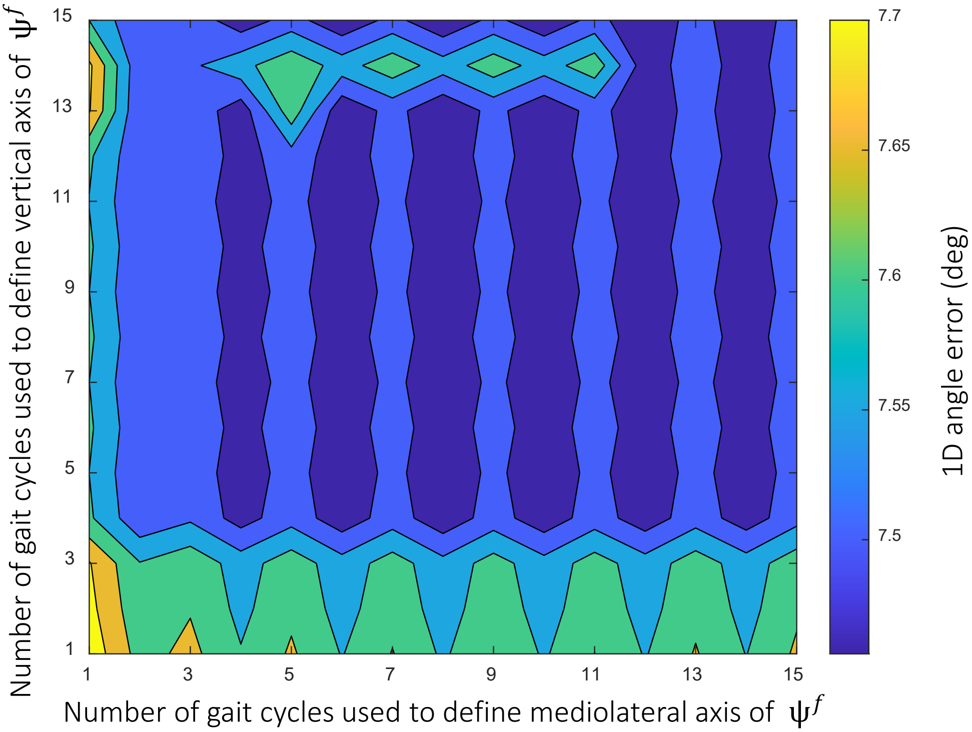

Figure 6.7: *Effect of the number of gait cycles used to determine the mediolateral (Equation 6.4a) and vertical axis (Equation 6.4b) of ψ^f on the 1D angle error. The 1D angle error represents the angle of the axis-angle representation of the difference in orientation between DFOD and OMCS.*

The effect of the number of gait cycles on the mean 1D displacement error is shown in Figure 6.8. The lowest mean displacement error was found when the vertical axis was based on data of 10 gait cycles and the mediolateral axis on data of 15 gait cycles (mean error: 2.6 cm). The highest mean displacement error was found when the vertical and mediolateral axes were both based on data of 1 gait cycle (mean error: 4.5 cm).

To investigate the effect of sampling frequencies on DFOD, inertial data were resampled from 240 Hz to 120 Hz and 60 Hz before applying DFOD. Compared to a sampling frequency of 240 Hz, the 1D orientation error increased with 0.3° for 120 Hz and 2.2° for 60 Hz. The 1D displacement error increased with 1.2 cm for 120 Hz and 12.7 cm for 60 Hz.

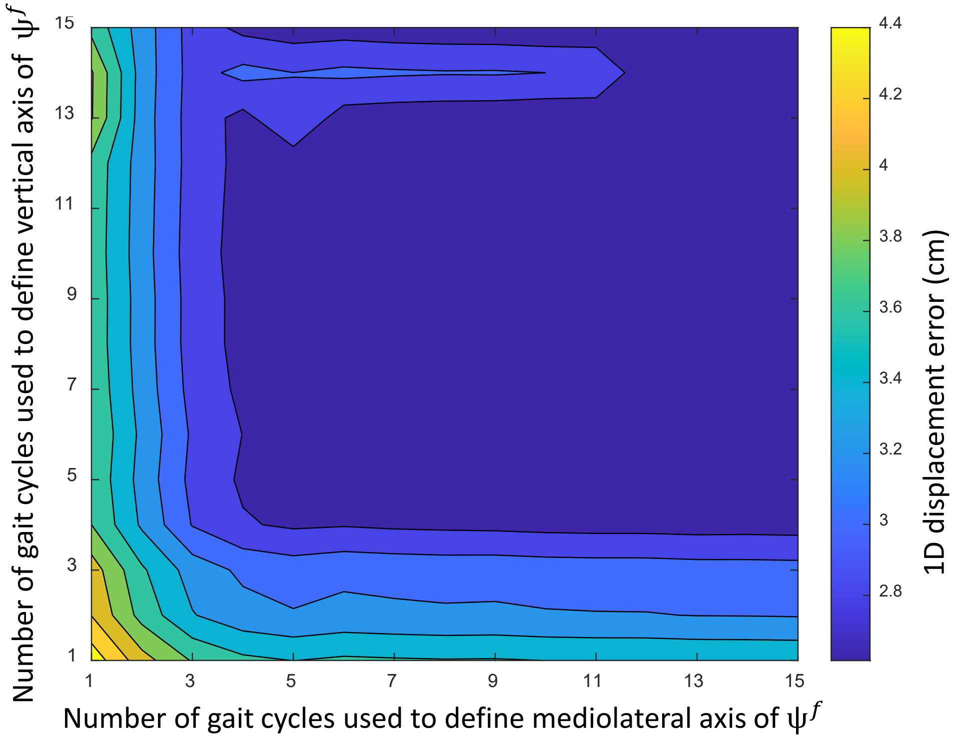

Figure 6.8: *Effect of the number of gait cycles used to determine the mediolateral (Equation 6.4a) and vertical axis (Equation 6.4b) of* ψ^f *on the 1D displacement error between DFOD and OMCS.*

Discussion

A new method, called Drift-Free Orientation and Displacement estimation (DFOD), is proposed to estimate drift-free 3D sensor orientation and displacement based on a single IMU. DFOD uses the quasi-cyclical behavior of human movements and assumes a quasi-2D movement with an approximately constant cycle average velocity. The performance of DFOD for a sensor on the lower leg was validated with an optical motion capture system (OMCS) in treadmill running. Errors in estimated sensor orientation and displacement between DFOD and OMCS were comparable to errors of other orientation and displacement algorithms. However, DFOD is independent of a constant- or zero-velocity point, a biomechanical model, a magnetometer, Kalman filtering, or a calibration procedure. Hence, DFOD is a promising method for quasi-cyclical motion analysis with a single IMU and has many advantages over current methods.

Estimation of orientation

Estimated lower leg sensor orientations of DFOD were compared to an OMCS in treadmill running. DFOD performs best for orientation estimation in the sagittal plane, possibly because the largest ROM occurs around the axis perpendicular to this plane (Equation 6.4a) in running.

To reduce drift in orientation estimation, a drift reducing rotation which was constant within each cycle, but varied over cycles, was applied (rotation 3, Figure 6.3). Orientation drift is relatively slow compared to the duration of a gait cycle (i.e., two min before ψ^{df} drifts 90°, or ±0.5°/stride, around ψ_y^f). Hence, a constant drift reducing rotation for each gait cycle seemed sufficient, although this did result in small discontinuities between gait cycles. In future work, a continuous drift reducing rotation could improve the performance of DFOD.

Since we are not aware of studies that estimated lower leg orientations during running, the results of DFOD can only be compared with studies estimating foot and thigh orientations during running and walking. Foot orientations during running have mostly been based on constant- or zero-velocity updates with an additional drift reducing component (e.g., based on joint center accelerations, filtering, or an orientation reset). At speeds similar to our study, sagittal plane foot orientations could be estimated with errors varying between 2.0° and 20.8° [11,12,25]. Frontal plane foot orientation errors differed from 2.6° to 4.4° [12,25]. Upper leg orientations during walking have been estimated with an RMSE of 1.9 ± 0.5°, although the zero acceleration and angular velocity update used in that study does not apply to continuous quasi-cyclical movements like running [26]. Orientation errors in our study are similar or slightly larger than found in literature for other body segments, although these studies used drift reducing methods unsuitable for a sensor on the lower leg in running (i.e., based on a constant- or zero-velocity point).

Tibial orientations in the sagittal and transversal plane are commonly studied with regard to running injuries [27–29]. The sagittal plane orientation of the tibia at initial contact has been shown to be 4.9° larger in injured than in uninjured runners and the tibia ROM in the transverse plane is around 15° in running [30]. With a mean difference of -0.3 ± 3.7° at the start of the gait cycle (just before initial contact) and -5.6 ± 2.1° in the transversal plane ROM, DFOD is capable to detect meaningful changes in tibia orientations during running.

Estimation of displacement

Estimated lower leg sensor displacements of DFOD were compared to an OMCS in treadmill running. OMCS cluster marker placement can explain some of the errors in the forward and vertical directions. The OMCS cluster marker set is placed below the IMU (see Figure 6.1). Lower placement of the cluster marker set results in a larger ROM for OMCS compared to DFOD in the forward and vertical direction. Hence, actual displacement errors in the forward and vertical direction are expected to be smaller than those reported in this study.

Since we are not aware of studies that estimated lower leg displacements during running, the results of DFOD can only be compared with studies estimating foot displacements and stride length based on IMU data during running. In literature, estimates of sagittal plane foot displacement during running at a speed similar to the speed in this study had an absolute 1D positional error of 5 ± 2 cm at maximal foot height and initial contact [11]. The absolute 1D positional error in our study was 2.7 ± 0.4 cm. Previously, stride length based on an IMU in a shoe could be estimated with a mean absolute error of 7.6 cm [31]. DFOD has a mean absolute displacement error of 1.4 ± 0.2 cm in the forward direction. Hence, displacement errors of DFOD for the tibia sensor are smaller than those reported by literature for the foot segment in running.

DFOD estimates the displacement of a sensor on the lower leg. However, the displacement of each point on the tibia can be estimated based on the orientation of the sensor and the distance from the sensor to the point of interest. When the distance from the sensor to the ankle joint is known, the forward (step length) and upward (step height) displacement of the ankle can be estimated. Running velocity can then be obtained with the step length and cycle time. Hence, DFOD provides insight into the 3D trajectory of the lower leg during running and can be used to estimate step length, step height, and running velocity based on a single IMU on the lower leg.

Algorithm characteristics

The assumptions that treadmill running is a quasi-cyclical and quasi-2D movement seem to hold based on the standard deviation of the cycle times (0.8–1.9% of the cycle time) and the explained variance of the first principal component for the angular velocity in ψ^s (84.6–95.8%). The explained variance shows that DFOD is capable of accurately estimating orientation and displacement even when 15% of the angular velocity in ψ^s occurs outside the 2D plane of a movement.

The effect of computing the functional mediolateral (Equation 6.4a) and vertical (Equation 6.4b) axes based on different numbers of gait cycles was found to be very small. The 1D orientation and displacement errors differed only 0.2° and 1.9 cm between the best- and worst-performing combination of the number of included gait cycles. Hence, during indoor treadmill running at a constant velocity, the number of gait cycles for the vertical and mediolateral axes has a limited influence on the results of DFOD.

However, the goal is to apply DFOD in less controlled environments such as outdoor running. Outdoor running is likely to result in a less cyclical running pattern [32]. It is hypothesized that for outdoor running, a smaller number of gait cycles to compute the functional mediolateral (Equation 6.4a) and vertical (Equation 6.4b) axes is favoured over a larger number since assumptions are less likely to be violated over shorter periods. Five gait cycles to define the vertical and mediolateral axes is expected to be a reasonable trade-off between including more data to compensate for the increased variability in outdoor running while still being able to adapt to sudden changes in the gait pattern and reduce violations of assumptions. Hence, five gait cycles for both the mediolateral and vertical axes (Equations 6.4a and 6.4b) were used in this study as the default setting for DFOD.

To investigate the effect of sampling frequencies on DFOD, inertial data were resampled from 240 Hz to 120 Hz and 60 Hz before applying DFOD. Orientation and displacement errors drastically increased when IMU data resampled to 60 Hz were used as input for DFOD. These results indicate that DFOD provides satisfactory results for a sampling frequency of 240 Hz and 120 Hz, but not for 60 Hz.

Limitations

Multiple assumptions were made to create DFOD, which can be violated by running outdoors. When runners run outside, they have a less constrained gait pattern than on a treadmill [32], and can freely change their running velocity and run up or downhill, thereby violating some assumptions of DFOD. Violation of the assumption of an approximately constant cycle average velocity does not influence the mediolateral axis of ψ^f (Equation 6.4a) since this axis is based on the first principal component of the angular velocity of the lower leg sensor. Additionally, this axis is not influenced by taking a turn or running in circles, since it moves with the body. However, the vertical axis of ψ^f (Equation 6.4b) is influenced by a violation of the approximately constant cycle average velocity assumption. This axis is equal to the direction of the total acceleration (i.e., including gravity) over a complete number of gait cycles when the cycle average velocity is constant. When a runner accelerates or decelerates, the free acceleration will not have a zero-mean over a complete number of gait cycles and will result in an offset in the estimated vertical axis proportional to the magnitude of the acceleration or deceleration. Since five gait cycles are included to estimate both functional axes, DFOD minimizes the effect of violated assumptions and is expected to recover from a short violation of assumptions within five gait cycles.

Similarly, the assumption of a quasi-cyclical 2D movement might be violated more often in running outdoors since impact accelerations are higher when running overground compared to a treadmill [33], due to uneven terrain, stumbling, or taking a turn. DFOD will recover from short violations of the quasi-cyclical 2D movement assumption within five gait cycles. Running-induced fatigue has been shown to increase variability in the gait pattern [34]. This increased variability and less cyclicity might cause the assumptions of DFOD to be less valid in fatigued running, resulting in larger orientation and displacement errors. Since DFOD has an origin that moves with the body at the cycle average velocity, a change in elevation caused by running on a sloped surface will cause the origin of DFOD to move up or down with the body. An elevation change will be visible over time; however, the average displacement will still be zero.

This study aimed to propose and validate a new algorithm that makes use of the quasi-cyclical nature of many movements. The algorithm was tested on treadmill running data of four runners and provided satisfactory results for all runners. Hence, to test the idea of using the quasi-cyclical nature of many human movements to estimate orientation and displacement, a limited number of subjects is appropriate. However, before DFOD can be used to study running kinematics it should be validated in more runners and different conditions.

This study estimated sensor orientation and displacement during running while segment orientations might provide more insight for motion analysis. For a sensor to segment calibration, two axes that relate to both CSs are required. One of these axes is already defined in DFOD (Equation 6.2a). The other axis could be based on the direction of the gravitational acceleration during neutral standing, in which the tibia is assumed to be vertical. However, this sensor to segment calibration does require an additional calibration procedure.

Future research

In future work, DFOD should be validated in a less controlled setting, such as outdoor running, in multiple body segments, and different quasi-2D movements like cycling and skating. The influence of short violations of the assumptions of DFOD, increased variability in the gait pattern (i.e., caused by fatigue), less cyclical movements, and different speeds on estimated orientations and displacement should be assessed in (outdoor) running. Additionally, the effect of continuous drift reduction instead of a drift reduction during each gait cycle (Equation 6.4e) could be evaluated to improve the performance of DFOD. As long as two functional axes can be defined, DFOD should be able to estimate sensor orientation and displacement. Hence, the generalized idea of DFOD could also be applied to quasi-cyclical 3D movements like swimming. For 3D movements, the validity of the functional mediolateral axis (Equation 6.4a) based on the first principal component of the angular velocity should be assessed. This component is expected to be less pronounced in 3D versus 2D movements. Finally, a sensor to segment calibration procedure could be added to enable DFOD to calculate segment orientations instead of sensor orientations.

Conclusions

The Drift-Free Orientation and Displacement estimation method (DFOD) is proposed and validated. DFOD estimates drift-free 3D sensor orientation and displacement with a single IMU in quasi-cyclical quasi-2D plane movements with an approximately constant cycle average velocity. DFOD does not require a calibration procedure, biomechanical model, constant- or zero-velocity point, Kalman filtering, or magnetometer. Small errors in lower leg sensor orientation and displacement were found when DFOD was validated against an optical reference system in treadmill running. Hence, DFOD is a promising method for quasi-cyclical motion analysis, especially when using a minimal sensor setup.

Data availability statement

The data presented in this study are openly available in 4TU.ResearchData. The data can be found here: [https://doi.org/10.4121/18394190] accessed on 13 December 2021.

References

1. Hreljac, A. Etiology, prevention, and early intervention of overuse injuries in runners: A biomechanical perspective. Phys. Med. Rehabil. Clin. N. Am. 16, 651–667 (2005).
2. Ruder, M., Jamison, S. T., Tenforde, A., Mulloy, F. & Davis, I. S. Relationship of Foot Strike Pattern and Landing Impacts during a Marathon. Med. Sci. Sports Exerc. 51, 2073–2079 (2019).
3. Reenalda, J., Maartens, E., Homan, L. & Buurke, J. H. Continuous three dimensional analysis of running mechanics during a marathon by means of inertial magnetic measurement units to objectify changes in running mechanics. J. Biomech. 49, 3362–3367 (2016).
4. Camomilla, V., Bergamini, E., Fantozzi, S. & Vannozzi, G. Trends supporting the in-field use of wearable inertial sensors for sport performance evaluation: A systematic review. Sensors (Switzerland) vol. 18 (2018).
5. Reenalda, J., Maartens, E., Buurke, J. H. & Gruber, A. H. Kinematics and shock attenuation during a prolonged run on the athletic track as measured with inertial magnetic measurement units. Gait Posture 68, 155–160 (2019).
6. Maas, E., De Bie, J., Vanfleteren, R., Hoogkamer, W. & Vanwanseele, B. Novice runners show greater changes in kinematics with fatigue compared with competitive runners. Sport. Biomech. 17, 350–360 (2018).
7. Woodman, O. J. An introduction to inertial navigation. Tech. Rep. Univ. Cambridge (2007) doi:10.4271/2000-01-0305.
8. Sabatini, A. M. Estimating three-dimensional orientation of human body parts by inertial/magnetic sensing. Sensors 11, 1489–1525 (2011).
9. Park, S. K. & Suh, Y. S. A zero velocity detection algorithm using inertial sensors for pedestrian navigation systems. Sensors 10, 9163–9178 (2010).
10. Yun, X., Bachmann, E. R., Moore IV, H. & Calusdian, J. Self-contained position tracking of human movement using small inertial/magnetic sensor modules. Proc.- IEEE Int. Conf. Robot. Autom. 2526–2533 (2007) doi:10.1109/ROBOT.2007.363845.
11. Bailey, G. P. & Harle, R. Assessment of foot kinematics during steady state running using a foot-mounted IMU. Procedia Eng. 72, 32–37 (2014).
12. Falbriard, M., Meyer, F., Mariani, B., Millet, G. P. & Aminian, K. Drift-Free Foot Orientation Estimation in Running Using Wearable IMU. Front. Bioeng. Biotechnol. 8, 1–11 (2020).

13. Sabatini, A. M., Ligorio, G. & Mannini, A. Fourier-based integration of quasi-periodic gait accelerations for drift-free displacement estimation using inertial sensors. Biomed. Eng. Online 14, 1–18 (2015).
14. Cardarelli, S. et al. Single IMU Displacement and Orientation Estimation of Human Center of Mass: A Magnetometer-Free Approach. IEEE Trans. Instrum. Meas. 69, 5629–5639 (2020).
15. Tan, U. et al. Estimating displacement of periodic motion with inertial sensors. Sensors 8, 1385–1388 (2008).
16. Sanno, M., Willwacher, S., Epro, G. & Brüggemann, G. P. Positive work contribution shifts from distal to proximal joints during a prolonged run. Med. Sci. Sports Exerc. 50, 2507–2517 (2018).
17. Zandbergen, M. A., Ferla, R. I., Buurke, J. H., Reenalda, J. & Veltink, P. H. Estimating 3D orientation of a body segment during running using a single gyroscope. 3DAHM 1–4 (2020).
18. Smith, L. I. A tutorial on Principal Components Analysis Introduction. Statistics (Ber). 51, 52 (2002).
19. Black, H. D. A passive system for determining the attitude of a satellite. AIAA J. 2, 1350–1351 (1964).
20. Bortz, J. E. A new mathematical formulation for strapdown inertial navigation. 61–66 (1971).
21. Schepers, H. M., Roetenberg, D. & Veltink, P. H. Ambulatory human motion tracking by fusion of inertial and magnetic sensing with adaptive actuation. Med. Biol. Eng. Comput. 48, 27–37 (2010).
22. Kuipers, J. B. Quaternions and rotation sequences. Princet. Univ. Press Fifth prin, (2002).
23. Luinge, H. J. & Veltink, P. H. Measuring orientation of human body segments using miniature gyroscopes and accelerometers. Med. Biol. Eng. Comput. 43, 273 – 282 (2005).
24. Evans, J. D. Straightforward statistics for the behavioral sciences. (Thomson Brooks/Cole Publishing Co., 1996).
25. Koska, D., Gaudel, J., Hein, T. & Maiwald, C. Validation of an inertial measurement unit for the quantification of rearfoot kinematics during running. Gait Posture 64, 135–140 (2018).

26. Abhayasinghe, N., Murray, I. & Bidabadi, S. S. Validation of thigh angle estimation using inertial measurement unit data against optical motion capture systems. Sensors (Switzerland) 19, 596 (2019).
27. Sugimoto, D. et al. Running propensities of athletes with hamstring injuries. Hip Pelvis Inj. Sport. Med. 181–190 (2012).
28. Fisher, R., Nye, N. S., Soles, J., Waldhelm, A. & Gottfredson, R. Overstride-induced medial knee desmopathy: An exploration case series. J. Athl. Train. 55, 1255–1261 (2020).
29. Bellchamber, T. L. & Van Den Bogert, A. J. Contributions of proximal and distal moments to axial tibial rotation during walking and running. J. Biomech. 33, 1397–1403 (2000).
30. Nigg, B. M., Cole, G. K. & Nachbauer, W. Effects of arch height of the foot on angular motion of the lower extremities in running. J. Biomech. 26, 909–916 (1993).
31. Zrenner, M., Gradl, S., Jensen, U., Ullrich, M. & Eskofier, B. M. Comparison of different algorithms for calculating velocity and stride length in running using inertial measurement units. Sensors (Switzerland) 18, (2018).
32. Lindsay, T. R., Noakes, T. D. & Mcgregor, S. J. Effect of treadmill versus overground running on the structure of variability of stride timing. Percept. Mot. Skills 118, 331–346 (2014).
33. García-Pérez, J. A., Pérez-Soriano, P., Llana Belloch, S., Lucas-Cuevas, Á. G. & Sánchez-Zuriaga, D. Effects of treadmill running and fatigue on impact acceleration in distance running. Sport. Biomech. 13, 259–266 (2014).
34. Schütte, K. H. et al. Wireless tri-axial trunk accelerometry detects deviations in dynamic center of mass motion due to running-induced fatigue. PLoS One 10, (2015).

Chapter 7

General discussion

The overarching aim of this thesis was to increase our understanding of running biomechanics as measured in and outside the laboratory, and to explore challenges regarding wearable motion analysis during running in a sport-specific setting. Where the previous chapters focused on specific research questions which individually contributed to this aim, the current chapter will place the combined findings in a broader perspective and critically discuss them. This chapter will start with a summary of the main findings from the individual chapters, after which a set of overarching topics about variability, moving outside the laboratory, and the future of monitoring running biomechanics will be discussed. This chapter will end with the strengths and limitations of the work presented in this thesis, general conclusions and recommendations.

Main findings

Increasing our understanding of running biomechanics

A systematic literature review with meta-analyses about the effect of fatigue on level-running induced fatigue showed that runners change their gait patterns due to fatigue by moving to a more compliant but less efficient gait pattern (**Chapter 2**). This gait pattern is characterized by decreased leg stiffness, increased knee flexion, and increased peak tibial accelerations. Interestingly, novice runners showed an increase in ΔCOM_z after a fatiguing protocol, while experienced runners did not. This suggests that experience level plays a role in changes in running biomechanics due to fatigue. Large differences between subjects were found, highlighting the need for subject-specific compared to group-based analyses of running biomechanics. In **Chapter 3**, subject-specific corrections for the effect of changes in speed and stride frequency on running mechanics were made during a fatiguing marathon. The effect of marathon stage on peak tibial acceleration and knee angles changed after correcting for speed and stride frequency changes. Hence, subject-specific effects of changes in speed and stride frequency on quantities of interest should be investigated and corrected when interpreting, or providing feedback on, running mechanics in an uncontrolled environment. The assumed link between peak tibial acceleration and tibial bone loading was tested in **Chapter 4**. A very weak non-significant correlation was found in rearfoot striking runners, indicating that an increase in peak tibial acceleration is not necessarily associated with an increase in tibial bone load. This non-significant correlation is caused by the inability of PTA to reflect internal compressive forces from muscle contractions and the disagreement in timing between PTA and peak tibial compression forces. Hence, the assumed link between PTA and maximal tibial compression forces and the expected associated risk of tibial stress fractures during treadmill running is not supported.

Exploring challenges regarding wearable motion analysis

Using IMUs for wearable motion analysis in a sport-specific setting introduces challenges regarding to external influences on the gait pattern (**Chapter 3**) but also on how we obtain quantities of interest from raw sensor data. Laboratory based motion analysis is often based on joint angles, segment orientations and positions while these are not provided by raw IMU data. Additionally, wearable motion analysis in a sport specific setting should not form a burden to runners by relying on an extended number of sensors or on extensive sensor-to-segment calibration procedures.

In **Chapter 5 and Chapter 6**, we showed that the quasi-cyclical nature of running can be used to correct for drift in 3D orientation estimates of the tibia during treadmill running. **Chapter 5** showed that drift could be drastically reduced by rotating angular velocities to a partly functional coordinate system in which flexion and extension of the lower leg occurred around one of the coordinate axes. However, not all drift in 3D orientation could be removed by rotating to a partly functional coordinate system. Therefore, based on the work performed in **Chapter 5**, additional characteristics of the quasi-cyclical nature of running were used in **Chapter 6** to estimate drift-free 3D sensor orientation and displacement. An algorithm was developed to create a fully functional coordinate system based on the mean acceleration and rotation axes over multiple gait cycles. Minor errors in lower leg sensor orientation and displacement were found when the algorithm was validated against an optical reference system in treadmill running. In comparison to current methods, this new method does not require a calibration procedure, biomechanical model, constant or zero-velocity point, Kalman filtering, or magnetometer. These findings suggest that the algorithm is promising for quasi-cyclical motion analysis, especially when using a minimal sensor setup, and reduces burdens for runners to monitor their gait pattern with IMUs.

Variability between subjects and studies

Variability between subjects

Large differences exist in running patterns between runners performing the same task [1–3]. Natural within-subject variability in stride duration and PTA correspond to coefficients of variation of 3% and 7%, respectively [4,5]. Stride time variability is highest for the preferred running speed since a given speed can be achieved by adapting both stride length and stride time. At higher and lower speeds, fewer dynamical degrees of freedom decrease stride time variability [4]. Less variability might reflect less flexibility to adapt to the environment

and promote repetitive overloading of specific structures or tissues [6]. By imposing a generic running speed on a group of runners, some might run above or below their preferred running speed, affecting their gait pattern. Individual differences in running patterns become even more prominent when runners get fatigued [1–3,7–10]. Fatigue-induced changes in running patterns depend, amongst others, on experience level (**Chapter 2**), running surface [11,12], foot strike pattern [13], and subject-specific fatigue thresholds [14]. Inter- and intra-subject variability makes it difficult to compare the gait patterns of subjects. Additionally, large inter-individual differences in group-based analyses often result in inconclusive and non-significant findings. A shift from group-based analyses to subject-specific [8,15] or running-style specific [16] analyses would prevent masking of individual responses in the gait pattern. Subject-specific analysis enables monitoring and feedback on deviations from a subject-specific habitual gait pattern, increasing the value of information that can be provided to runners.

Variability between studies

Besides differences in gait patterns between runners, endless possibilities exist for creating running experiments. Variables for running experiments include experience level, injury history, shoe choice, running-induced fatigue, running surface, running speed, continuous versus interval running and running until exhaustion versus reaching a certain distance, heart rate, or perceived exertion. Additionally, choices in data processing, such as the number of strides to include, filtering specifications, and statistical methods, contribute to differences between studies [17]. This abundance of possible running protocols, differences in measurement devices, the number of strides analyzed, and the broad range of methods to analyze gait patterns make comparing findings of studies cumbersome.

The effect of variability between studies became apparent in **Chapter 2** in the form of contradicting findings between studies. We included studies involving fatiguing protocols in meta-analyses to summarize effects of running-induced fatigue on running kinematics. Contradicting findings between studies were likely the result of differences in running protocols. A subject-specific fatigue threshold above which kinematic variables change has been shown previously [14]. Hence, contradicting findings in the literature review might be caused by assuming that all runners were fatigued after completing the running protocol. Additionally, relevant information about the running experience was not always provided, and studies often consisted of small sample sizes. Metabolic measurements of fatigue (e.g., based on respiratory data or blood lactate concentrations) were performed in just 3 out of 28 included studies. Despite the differences between studies investigating running-induced fatigue, in

Chapter 2, we found a general trend to a more compliant but less efficient gait pattern with fatigue, characterized by decreased leg stiffness and increased knee flexion and peak tibial accelerations.

Moving forwards with variability

Investigating running gait patterns is a hot topic. Many papers emerge with contradicting findings, probably caused by intra- and inter-subject differences, differences in running protocols, and small sample sizes. We are convinced that the step forwards is to publish datasets that accompany an article, as demonstrated in **Chapter 3 and Chapter 6**. Publicly available datasets allow researchers to test their hypotheses in different populations without needing large-scale measurements. Additionally, open datasets contribute to scientific transparency, reproducibility, efficiency and are cost-saving. If publishing accompanying datasets is impossible, at a bare minimum, researchers should provide sufficient information about the running protocol and subject population and perform subject-based analyses of running gait patterns instead of group-based analyses. Additional information about subjects and running protocols allows for pinpointing sources of variability and explaining differences between studies. Due to the high variability between studies investigating effects of fatigue, it is of interest to test the reproducibility of these types of studies. Furthermore, subject-specific analysis and reporting of results contribute to a better understanding of individual differences which are often masked in group-based analyses. Finally, large variability between subjects might be something we should not try to solve but embrace in our goal to provide feedback on subject-specific deviations from a habitual gait pattern to reduce injury risk

Moving outside

Laboratory versus outside running biomechanics

Most studies investigating running biomechanics are conducted in a laboratory setting during overground or treadmill running. For overground running in a laboratory, subjects typically need to accelerate and decelerate on a runway of 10 to 32 meters long, while one stride is extracted per trial [18–22]. This process is repeated until the predefined number of successful strides is achieved. Accelerating and decelerating in a constricted volume, together with averaging over a limited number of gait cycles, brings methodological issues concerning repeatability [23], generalizability to continuous (i.e., non-stop) overground running [24], and picking up a natural running pattern that is appropriate for the environment [25]. During continuous running, runners run with flatter and more inverted feet at initial contact, have

reduced braking and propulsion forces variability, and show more variability in ankle joint variables compared to running up and down a runway [24]. Thus, constraints in the experimental setup influence the gait pattern.

Meta-analyses showed that treadmill running is broadly comparable with overground running from a biomechanical perspective [26]. However, even at similar running speeds, multiple essential differences exist with regard to shock and shock attenuation mechanisms. For instance, PTA was higher in overground compared to treadmill running in an unfatigued state but no longer in a fatigued state [12] and peak foot acceleration was higher when running on grass compared to asphalt [27]. Most runners make the bulk of their runs outdoor [28]. Hence, there is a mismatch between the running environment in which most research is performed, and the actual environment where runners run. This limits the generalizability and ecological validity of findings from running studies performed in a laboratory setting.

Measuring running biomechanics outdoors

To gain insight into running biomechanics, runners need to be measured in the environment where most runners run; outdoors. Different wearable devices can be used to monitor running biomechanics like GPS based sports watches to measure speed and location or pressure insoles to measure forces and force distribution of the feet during running. To monitor the gait pattern outdoors, IMUs can be used. IMUs are affordable and small in size, making them attractive for outdoor analyses of the gait pattern. However, the output of IMUs consists of accelerations and angular velocities, while laboratory-based measurement devices typically provide positions and position-derived joint angles. The sensor orientation needs to be estimated based on sensor data to compute similar outputs from IMU data. Sensor orientation can be obtained through different methods, such as sensor fusion or using domain-specific assumptions to correct for orientation drift.

In **Chapters 5 and Chapter 6**, we propose and validate a new method using the quasi-cyclical nature of running to estimate drift-free 3D sensor orientation and displacement. The benefits of this algorithm are that it requires only one IMU and does not need a biomechanical model, Kalman filtering, extensive sensor-to-segment calibration or a magnetometer. Furthermore, the sampling frequency at which satisfactory results are achieved is relatively low (i.e., 60 Hz), making it suitable for data from low-end IMUs. Hence, this algorithm contributes to the growing interest in biomechanics from wearables using a minimal sensor setup.

The algorithms from **Chapter 5 and Chapter 6** provides multiple opportunities with regard to measuring biomechanics. Although no calibration procedure is required to obtain 3D sensor orientation and displacement, one simple short measurement of a subject standing still in a neutral pose would allow computing a vertical axis in a segment fixed coordinate system. Together with the functional flexion-extension rotation axes from the algorithm, this allows for the computation of 3D segment orientation and displacement. Running speed can be calculated based on the forward displacement of the ankle joint with an additional measurement of the distance between the ankle joint center and the sensor on the lower leg. Additionally, joint angles can be computed if time-synchronized data of IMUs on two adjacent body segments are available.

Although the algorithm was tested in treadmill running, it is expected to work for other quasi-2D-cyclical motions such as cycling or rowing. The algorithm can even be applied to quasi-3D-cyclical motions if an alternative for the axis perpendicular to the plane of motion can be defined. Before the algorithm can be used in outdoor running measurements, it should be validated during continuous overground running. Especially the number of strides over which the coordinate system's functional axes are computed can differ between indoor and outdoor measurements. A validation study could be performed in a semi-controlled environment on an extensive indoor track (e.g., [7]) with an optical motion capture system or an uncontrolled environment by comparing estimated lower leg orientation and displacement from a single IMU compared to the estimated orientation output from a full-body IMU sensor setup [29]. The algorithms proposed in **Chapter 5 and Chapter 6** brings us closer to small, affordable, and easy-to-use wearable sensors that provide drift-free 3D orientations, displacements, joint angles, and speed in sport-specific environments without the need for expensive and extensive sensor setups and software programs.

Current use of IMUs in outdoor conditions

Despite the widespread availability of IMUs and their benefits regarding continuous analysis in a sport-specific setting, a recent scoping review showed that IMUs in running biomechanics are typically used indoors for short periods [30]. IMUs were used in a lab in 72% of the studies, while 67% analyzed a single step, stride, or less than 200 meters of running data [30], possibly to exclude effects of fatigue or to validate or combine measurements with force plates. In outdoor settings, runners can freely change their running speed and encounter different surfaces, weather conditions, other runners, traffic, etcetera. The lack of context and the

influence of external factors when measuring in outdoor environments might play a role in the reluctance to measure outdoors. External influences on the gait pattern can burden researchers when trying to answer a research question and burden runners when comparing data of multiple runs.

In **Chapter 2**, PTA was shown to generally increase with fatigue at a constant running speed, indicating higher external forces on the body. However, PTA decreases with a decrease in running speed [31]. Since running speed typically decreases with fatigue, a possible increase in PTA due to fatigue might be masked by a decrease in PTA due to a decrease in running speed. Although a decrease in speed can be a protective mechanism of the body to keep impacts on the body low, an increase in PTA at a certain speed informs us that external forces on the body increase despite a decrease in speed. In **Chapter 3**, we quantified and corrected for the influence of changes in running speed and stride frequency on running mechanics during an outdoor competitive Marathon. After correcting for subject-specific effects of changes in speed and stride frequency, PTA and maximum stance phase knee angles increased during later stages of the marathon. These changes in PTA and knee angles were previously masked by changes in speed and stride frequency. Hence, subject-specific effects of changes in speed and stride frequency on quantities of interest should be investigated and corrected when interpreting, or providing feedback on, running mechanics in an uncontrolled environment.

Moving forwards by going outside

IMUs allow for measuring outside which is important for ecological validity of running research. We believe that the most considerable burden of measuring outdoors is the lack of context and the influence of external factors. The step forwards to using IMUs in outdoor settings is gathering lots of continuous data with sufficient context to quantify the influence of multiple external factors. Although external factors might be confounding when answering research questions, it shows the important disturbances that runners encounter in sport-specific settings and increases our research's ecological validity. The proposed algorithm from **Chapter 5 and Chapter 6** can be adapted to provide a range of exciting quantities of the running gait pattern indoors and outdoors (after validation).

The future of monitoring running biomechanics and injury risk

Running biomechanics and injury risk

A general goal of monitoring running biomechanics is to detect and provide feedback about abnormalities or changes in running biomechanics associated with increased injury risk [32,33]. Often, this is achieved through monitoring changes in running biomechanics due to fatigue [9,20,34]. Prospective studies identified biomechanical risk factors for different running injuries. For instance, female recreational runners who developed patellofemoral pain syndrome had increased stance phase hip adduction compared to healthy controls [35]. Furthermore, increased stance phase iliotibial band strain rate was found in runners who developed iliotibial band syndrome [36], and reduced maximum knee flexion, lower maximal ankle dorsiflexion, and greater maximum rearfoot eversion during the stance phase were found in runners who developed Achilles tendinopathy [37]. Peterson and colleagues [33] summarized nineteen prospective studies about musculoskeletal and biomechanical risk factors and the incidence of running injuries in meta-analyses. They found a significant effect on injury incidence for two out of twenty-five biomechanical quantities; less knee extension strength and lower hip adduction velocity. However, their meta-analyses were limited to six joint angle quantities, and they did not include hip adduction (i.e., linked to patellofemoral pain syndrome), knee angles at initial contact, and midstance (i.e., related to shock attenuation), peak accelerations or shock attenuation in their review. Especially peak accelerations and shock attenuations have been thought to be related to injury risk and can be easily measured in outdoor environments with IMUs. Hence, we recommend further investigating the relationship between peak accelerations, shock attenuation, and knee angles at initial contact and midstance with injury incidence. However, we do agree with Peterson and colleagues [33] that altered running biomechanics on their own do not result in running injuries but that there is an interaction required with training characteristics, for instance, monitored as a cumulative load, when evaluating running injury risk [38–40]. The injury risk concerning running patterns may also be very individual and depend on factors like previous injuries, age, bone geometry, bone density, and sex [41,42]. Hence, differences between runners should be embraced by creating individual longitudinal datasets to investigate deviations in gait patterns on different time scales to identify and understand injury mechanisms and monitor injury risk.

Quantities to monitor

Chapter 4 critically discussed the use of PTA as an indicator for tibial bone loading. PTA was expected to reflect impact forces on the human body and thus loading within the human body and injury risk. However, the contribution of internal forces (i.e., muscle contractions) was overlooked in this thought process. We found a non-clinically relevant relationship between PTA and tibial bone loading for rearfoot striking runners in treadmill running. Perhaps we should take one step back when investigating injury risk in runners.

The things we can observe or easily visualize tend to get our attention. When investigating running biomechanics, we often focus on running kinematics (e.g., joint angles) and external forces (e.g., ground reaction forces). To increase our understanding of running biomechanics, we must investigate the root of the kinematic changes we observe. Hence, we believe that the step forwards would be to take a step back and estimate forces and moments inside the body (i.e., kinetics) instead of their outcomes alone (i.e., kinematics) [43,44]. We suggest using musculoskeletal modeling [45] and estimating 3D ground reaction forces based on IMU data [46] to improve our understanding of biomechanical changes in sport-specific environments. Additionally, individual muscle contributions could be modeled [47] and validated with wearable EMG systems to investigate further if, for instance, an increase in knee flexion at initial contact with fatigue is a consequence of unbalanced muscular fatigue between knee flexors and extensors or a different shock attenuation strategy. Finally, the impulse of tibial acceleration might provide more insight into the forces on the body compared to PTA. Since shock attenuation might cause spreading of the impact force impulse over time, a lower PTA can be found while the impulse of the acceleration during the stance phase might remain constant.

Monitoring methods

The gait pattern differs between runners (**Chapter 3**). A subject-specific model of the habitual gait pattern is therefore required to monitor changes in biomechanical quantities. Since quantities can vary between runs, for instance, due to day-to-day variability or the weather [48], five runs have been suggested to establish a stable subject-specific habitual running pattern when investigating multiple biomechanical quantities [15]. In addition, individual relationships between running speed, stride frequency, and biomechanical quantities of interest can be estimated (**Chapter 3**). These relationships can be used to correct quantities for changes in running speed, making individual longitudinal datasets corrected for effects of speed and stride frequency possible. To obtain more manageable datasets and improve data stability, continuous running data can be split into bins of, for instance, 25 strides [17]. The median [49] value for each bin with 25 strides can then be computed and corrected for running speed and stride frequency for comparison with the habitual gait pattern (**Chapter 3**). We presume that deviations from subject-specific habitual gait patterns provide more value to individual runners than using a rigid threshold above which a quantity is flagged as “high injury risk”. Added value to the runner could be achieved by combining deviations from the habitual gait pattern with training characteristics, such as running speed (as proposed in **Chapter 6**), and physiological parameters, such as heart rate, to create a cumulative load. Feedback about deviations from the habitual gait pattern could help runners to change their gait pattern if desired [50].

Moving forwards with monitoring

To summarize, future (prospective) studies into the etiology of running injuries should focus on combining kinetic and kinematic quantities with training characteristics to provide a cumulative load. The biomechanical quantities to monitor during running depend on the goal for monitoring and will differ between types of running injuries. However, quantities of interest should preferably reflect forces and moments in the body and should be monitored in a sport-specific setting over more extended periods of time, for instance, with IMUs (**Chapter 5 and Chapter 6**). Deviations in quantities should be estimated with regard to a subject-specific habitual gait pattern established over multiple runs.

Strengths and Limitations

Several strengths and limitations of the research presented in this thesis can be stated. One of the strengths of this thesis is that it covers a broad spectrum of running biomechanics, from fundamental research about 3D orientation estimation algorithms to applied research in the form of measuring running mechanics during an actual competitive outdoor marathon. Another strength is that we focused on measuring with IMUs, which allows for findings to be applied in a setting where runners run; outdoors. Finally, based on the findings of this thesis, we created multiple recommendations about how monitoring running biomechanics in an outdoor setting should look in the future.

A significant limitation of this thesis is that despite the clear need for outdoor analysis of running biomechanics, most studies in this thesis were based on indoor treadmill running. This was a necessary step back after the measurement during an outdoor marathon (**Chapter 3**) left us with fundamental questions. In **Chapters 4, 5, and 6**, either force plates or an optical motion capture system were required, which prevented us from performing these measurements outdoors. We strongly recommend evaluating the findings of these chapters outdoors. When performed outdoors, we suspect similar results for **Chapter 4** and somewhat larger orientation and displacement differences in **Chapters 5 and 6** since the gait pattern is expected to behave less cyclical in uncontrolled outdoor settings. Another limitation of this thesis is the small sample sizes in the studies. Especially **Chapter 3** would benefit from a larger sample size due to variability between subjects. However, in **Chapters 3 and 4**, we used subject-specific analyses to reduce the effect of inter-subject variability. In **Chapters 5 and 6**, we introduced and validated a 3D orientation and displacement algorithm. Although this algorithm provided satisfactory results for all four runners in **Chapter 6**, we recommend evaluating this algorithm in more runners.

General conclusions

Studies in this thesis have explored, evaluated, and advanced monitoring of running biomechanics, both in and outside the laboratory. The influence of fatigue and speed on running biomechanics was investigated, the link between PTA and tibial bone load was explored, and a 3D orientation and displacement algorithm was proposed. The answers to the research questions from **Chapter 1** and other main conclusions from the preceding chapters in this thesis are stated below:

- Running-induced fatigue causes runners to move to a more compliant but less efficient gait pattern, characterized by decreased leg stiffness, increased knee flexion together with an increase in PTA (**Chapter 2**)
- The running gait pattern differs between runners, as well as the way runners react to running-induced fatigue and changes in speed and stride frequency (**Chapters 2 and 3**)
- Changes in PTA and knee angles were masked by changes in speed and stride frequency during a fatiguing outdoor run, subject-specific corrections were proposed in **Chapter 3**
- PTA should not be used as an indicator of tibial bone loading since it is unable to reflect internal compressive forces from muscles (**Chapter 4**)
- The quasi-cyclical nature of running can be used to estimate drift-free 3D sensor orientation and displacement with many benefits compared to other methods (**Chapters 5 and 6**)

Moving outside, using the methods proposed in this thesis, is the next step to increase our understanding of running biomechanics. Running biomechanics should be measured and monitored in a sport-specific setting, and the focus should shift from investigating kinematic quantities on a group level to the forces which underly them (i.e., kinetics) on a subject-specific level.

References

1. Dutto, D. J. & Smith, G. A. Changes in spring-mass characteristics during treadmill running to exhaustion. Med. Sci. Sport. Exerc. 34, 1324–31 (2002).
2. Nicol, C., Komi, P. V. & Marconnet, P. Effects of marathon fatigue on running kinematics and economy. Scand. J. Med. Sci. Sports 1, 195–204 (1991).
3. Strohrmann, C., Harms, H., Kappeler-Setz, C. & Tröster, G. Monitoring kinematic changes with fatigue in running using body-worn sensors. IEEE Trans. Inf. Technol. Biomed. 16, 983–990 (2012).
4. Jordan, K., Challis, J. H. & Newell, K. M. Long range correlations in the stride interval of running. Gait Posture 24, 120–125 (2006).
5. Clarke, T. E., Cooper, L. B., Hamill, C. L. & Clark, D. E. The effect of varied stride rate upon shank deceleration in running. J. Sports Sci. 3, 41–49 (1985).
6. Mann, R. et al. Association of previous injury and speed with running style and stride-to-stride fluctuations. Scand. J. Med. Sci. Sport. 25, e638–e645 (2015).
7. Rabita, G., Slawinski, J., Girard, O., Bignet, F. & Hausswirth, C. Spring-mass behavior during exhaustive run at constant velocity in elite triathletes. Med. Sci. Sports Exerc. 43, 685–692 (2011).
8. Siler, W. L. & Martin, P. E. Changes in Running Pattern during a Treadmill Run to Volitional Exhaustion: Fast versus Slower Runners. Int. J. Sport Biomech. 7, 12–28 (1991).
9. Reenalda, J., Maartens, E., Homan, L. & Buurke, J. H. Continuous three dimensional analysis of running mechanics during a marathon by means of inertial magnetic measurement units to objectify changes in running mechanics. J. Biomech. 49, 3362–3367 (2016).
10. Hunter, I. & Smith, G. A. Preferred and optimal stride frequency, stiffness and economy: Changes with fatigue during a 1-h high-intensity run. Eur. J. Appl. Physiol. 100, 653–661 (2007).
11. Bigelow, E. M. R., Elvin, N. G., Elvin, A. A. & Arnoczky, S. P. Peak impact accelerations during track and treadmill running. J. Appl. Biomech. 29, 639–644 (2013).
12. García-Pérez, J. A., Pérez-Soriano, P., Llana Belloch, S., Lucas-Cuevas, Á. G. & Sánchez-Zuriaga, D. Effects of treadmill running and fatigue on impact acceleration in distance running. Sport. Biomech. 13, 259–266 (2014).

13. Ruder, M., Jamison, S. T., Tenforde, A., Mulloy, F. & Davis, I. S. Relationship of Foot Strike Pattern and Landing Impacts during a Marathon. Med. Sci. Sports Exerc. 51, 2073–2079 (2019).

14. Verbitsky, O., Mizrahi, J., Voloshin, A., Treiger, J. & Isakov, E. Shock transmission and fatigue in human running. J. Appl. Biomech. 14, 300–311 (1998).

15. Benson, L. C., Ahamed, N. U., Kobsar, D. & Ferber, R. New considerations for collecting biomechanical data using wearable sensors: Number of level runs to define a stable running pattern with a single IMU. J. Biomech. 85, 187–192 (2019).

16. van Oeveren, B. T., de Ruiter, C. J., Beek, P. J. & van Dieën, J. H. The biomechanics of running and running styles: a synthesis. Sport. Biomech. 00, 1–39 (2021).

17. Oliveira, A. S. & Pirscoveanu, C. I. Implications of sample size and acquired number of steps to investigate running biomechanics. Sci. Rep. 11, 1–15 (2021).

18. Van den Berghe, P., Six, J., Gerlo, J., Leman, M. & De Clercq, D. Validity and reliability of peak tibial accelerations as real-time measure of impact loading during over-ground rearfoot running at different speeds. J. Biomech. 86, 238–242 (2019).

19. Brown, A. M., Zifchock, R. A. & Hillstrom, H. J. The effects of limb dominance and fatigue on running biomechanics. Gait Posture 39, 915–919 (2014).

20. Paquette, M. R. & Melcher, D. A. Impact of a long run on injury-related biomechanics with relation to weekly mileage in trained male runners. J. Appl. Biomech. 33, 216–221 (2017).

21. Bazett-Jones, D. M. et al. Effect of patellofemoral pain on strength and mechanics after an exhaustive run. Med. Sci. Sports Exerc. 45, 1331–1339 (2013).

22. Crowell, H. P. & Davis, I. S. Gait retraining to reduce lower extremity loading in runners. Clin. Biomech. 26, 78–83 (2011).

23. Oriwol, D., Milani, T. L. & Maiwald, C. Methodological issues associated with the mean value of repeated laboratory running measurements. Footwear Sci. 4, 183–190 (2012).

24. Isherwood, J., Hughes, L., Qian, J. Y. & Sterzing, T. Biomechanical effects of continuous loop running in comparison to discontinuous runway running on locomotion and running shoe characterization. Footwear Sci. 12, 39–54 (2020).

25. Meardon, S. A., Hamill, J. & Derrick, T. R. Running injury and stride time variability over a prolonged run. Gait Posture 33, 36–40 (2011).

26. Van Hooren, B. et al. Is Motorized Treadmill Running Biomechanically Comparable to Overground Running? A Systematic Review and Meta-Analysis of Cross-Over Studies. Sport. Med. 50, 785–813 (2020).

27. Kozinc, Ž., Smajla, D. & Šarabon, N. The reliability of wearable commercial sensors for outdoor assessment of running biomechanics: the effect of surface and running speed. Sport. Biomech. 00, 1–14 (2022).
28. Taunton, J. E. et al. A prospective study of running injuries: The Vancouver Sun Run 'In Training' clinics. Br. J. Sports Med. 37, 239–244 (2003).
29. Xsens Technologies B.V. MVN User Manual. MVN Man. 162 (2021).
30. Benson, L. C., Räisänen, A. M., Clermont, C. A. & Ferber, R. Is This the Real Life, or Is This Just Laboratory? A Scoping Review of IMU-Based Running Gait Analysis. Sensors 22, 1–38 (2022).
31. Sheerin, K. R., Besier, T. F. & Reid, D. The influence of running velocity on resultant tibial acceleration in runners. Sport. Biomech. 19, 750–760 (2018).
32. Vannatta, C. N., Heinert, B. L. & Kernozek, T. W. Biomechanical risk factors for running-related injury differ by sample population: A systematic review and meta-analysis. Clin. Biomech. 75, 104991 (2020).
33. Peterson, B. et al. Biomechanical and Musculoskeletal Measurements as Risk Factors for Running-Related Injury in Non-elite Runners: A Systematic Review and Meta-analysis of Prospective Studies. Sport. Med.- Open 8, (2022).
34. Morin, J. B., Samozino, P. & Millet, G. Y. Changes in running kinematics, kinetics, and spring-mass behavior over a 24-h run. Med. Sci. Sports Exerc. 43, 829–836 (2011).
35. Noehren, B., Hamill, J. & Davis, I. Prospective evidence for a hip etiology in patellofemoral pain. Med. Sci. Sports Exerc. 45, 1120–1124 (2013).
36. Hamill, J., Miller, R., Noehren, B. & Davis, I. A prospective study of iliotibial band strain in runners. Clin. Biomech. 23, 1018–1025 (2008).
37. Hein, T., Janssen, P., Wagner-Fritz, U., Haupt, G. & Grau, S. Prospective analysis of intrinsic and extrinsic risk factors on the development of Achilles tendon pain in runners. Scand. J. Med. Sci. Sport. 24, 1–12 (2014).
38. Vanwanseele, B., Beéck, T. Op De, Schütte, K. & Davis, J. Accelerometer Based Data Can Provide a Better Estimate of Cumulative Load During Running Compared to GPS Based Parameters. 2, 1–7 (2020).
39. Kiernan, D. et al. Accelerometer-based prediction of running injury in National Collegiate Athletic Association track athletes. J. Biomech. 73, (2018).
40. Edwards, W. B. Modeling Overuse Injuries in Sport as a Mechanical Fatigue Phenomenon. Exerc. Sport Sci. Rev. 46, 224–231 (2018).
41. Van Der Worp, M. P. et al. Injuries in runners; a systematic review on risk factors and sex differences. PLoS One 10, 1–18 (2015).

42. Romani, W. A., Gieck, J. H., Perrin, D. H., Saliba, E. N. & Kahler, D. M. Mechanisms and management of stress fractures in physically active persons. J. Athl. Train. 37, 306–314 (2002).
43. Scott, S. H. & David, A. W. Internal forces at chronic running injury sites. Med. sci 22, 357–369 (1990).
44. Rooney, B. D. & Derrick, T. R. Joint contact loading in forefoot and rearfoot strike patterns during running. J. Biomech. 46, 2201–2206 (2013).
45. Meardon, S. A. & Derrick, T. R. Effect of step width manipulation on tibial stress during running. J. Biomech. 47, 2738–2744 (2014).
46. Wouda, F. J. et al. Estimation of vertical ground reaction forces and sagittal knee kinematics during running using three inertial sensors. Front. Physiol. (2018) doi:10.3389/fphys.2018.00218.
47. Sasimontonkul, S., Bay, B. K. & Pavol, M. J. Bone contact forces on the distal tibia during the stance phase of running. J. Biomech. 40, 3503–3509 (2007).
48. Ahamed, N. U. et al. Using wearable sensors to classify subject-specific running biomechanical gait patterns based on changes in environmental weather conditions. PLoS One 13, 1–15 (2018).
49. Leys, C., Ley, C., Klein, O., Bernard, P. & Licata, L. Detecting outliers: Do not use standard deviation around the mean, use absolute deviation around the median. J. Exp. Soc. Psychol. 49, 764–766 (2013).
50. Davis, I. S., Tenforde, A. S., Neal, B. S., Roper, J. L. & Willy, R. W. Gait Retraining as an Intervention for Patellofemoral Pain. Curr. Rev. Musculoskelet. Med. 13, 103–114 (2020).

&

Summary
Samenvatting
Dankwoord
About the author
Progress range

Summary

Running is an accessible leisure time activity. In 2020, running was the second most popular sport in The Netherlands, with 12 percent of the Dutch population participating in weekly running sessions. While running has many health benefits, runners are at high risk of developing running-related injuries like medial tibial stress syndrome (i.e., shin splints) or tibial stress fractures. The development of running-related injuries is thought to be caused by training load errors (i.e., running too fast, too far, or too often) and (changes in) the gait pattern of runners. Additionally, running-induced fatigue is believed to affect the gait pattern negatively with regard to injury risk. The link between running biomechanics and injuries sparks our interest in monitoring running biomechanics to eventually decrease the risk of running-related injuries.

Running biomechanics are often studied in a controlled laboratory setting while running on a treadmill. However, most runners run outdoors at various speeds while experiencing different levels of fatigue. Multiple differences in the gait pattern between running in a controlled laboratory setting and outdoor environments have been found, like higher peak tibial accelerations in outdoor running compared to treadmill running. These differences indicate that results from laboratory-based running experiments do not necessarily translate to running outdoors. Since most runners typically run outdoors, monitoring running biomechanics should move from the laboratory to a sport-specific environment.

The running gait pattern can be measured outside of the laboratory with wearable inertial measurement units (IMUs). Quantities like sensor orientation, knee joint angles, and peak accelerations of body segments shortly after the foot hits the ground can be computed from IMU data. However, which quantities should be used to monitor injury risk is unclear. Besides, current algorithms to extract quantities of interest from raw sensor data have many drawbacks. **Hence, this thesis aimed to increase our understanding of running biomechanics as measured in and outside the laboratory and explore the challenges regarding wearable motion analysis during running in a sport-specific setting.**

To accomplish these aims, the following research questions were answered in this thesis:

Chapter 2 How do running kinematics change due to running-induced fatigue?

Chapter 3 How to quantify and correct for the subject-specific effects of changes in running speed and stride frequency on impact-related running mechanics during a fatiguing outdoor run?

Chapter 4 What is the strength of the relationship between peak tibial acceleration and maximal tibial compression force in running?

Chapter 5 Can the cyclical nature of running be used to acquire drift-free 3D orientation of a body segment using a single gyroscope?

Chapter 6 How to estimate 3D orientation and displacement of a single IMU on the lower leg using the quasi-cyclical nature of running?

Chapter 2 investigated the effects of running-induced fatigue on running kinematics. Changes in the running pattern caused by fatigue are thought to reflect a deterioration in running technique and increase the risk of running-related injuries. Many contradicting findings about the effect of fatigue on running kinematics are present in the literature. Hence, we summarised and analyzed current literature about the effect of level running-induced fatigue on the running gait pattern in a systematic literature review with meta-analyses. The effect of running-induced fatigue on nineteen kinematic quantities was investigated based on thirty-three articles. Overall, running-induced fatigue resulted in a more compliant but less efficient gait pattern characterized by increased peak tibial acceleration, knee flexion at initial contact, and maximum swing phase knee flexion while leg stiffness decreased. Experience level influenced the effect of fatigue on running kinematics, as demonstrated by an increase in vertical center of mass displacement with fatigue in novice but not experienced runners. Changes in running kinematics due to fatigue might be explained by a decrease in the tolerance of knee extensors to imposed stretch loads or a decrease in the neuromuscular control resulting in less spreading of the impact force impulse over time.

Chapter 3 focussed on measuring running gait in a sport-specific environment. The running gait pattern is typically analyzed on a group level based on runs in controlled laboratory settings. However, most runners run in uncontrolled outdoor environments. Changes in speed and stride frequency, as often seen in outdoor running, influence the gait pattern and can mask fatigue-related changes in running mechanics. We quantified and corrected for the effects of changes in running speed and stride frequency on running mechanics during a fatiguing outdoor run. The running mechanics of nine runners were analyzed with IMUs during a marathon. Subject-specific multiple linear regression models were created for speed and stride frequency effects on peak tibial acceleration, knee flexion angle at initial contact, and maximum stance phase knee flexion. These individual models were used to correct peak tibial acceleration and knee flexion angles for changes in speed and stride frequency. Regression coefficients for speed and stride frequency varied strongly between subjects, possibly caused by differences in foot strike pattern, tolerance to withstand effects of fatigue, or capacity to sustain a stable gait pattern over a range of speeds. Subject-specific corrections revealed a significant effect of marathon stage on peak tibial acceleration and knee flexion angles, which was previously masked by speed and stride frequency changes. Hence, speed and stride frequency influence the interpretation of changes in mechanical quantities in a subject-specific manner and should be corrected for when interpreting or providing feedback on running mechanics in an uncontrolled environment.

Chapter 4 focussed on investigating the relationship between peak tibial acceleration and tibial compression forces. Peak tibial acceleration is commonly used as a surrogate measure for tibial bone loading and is assumed to be related to tibial stress fracture risk. However, tibial compressive forces are caused by both internal muscle forces and the effect of external ground reaction forces. Peak tibial acceleration is expected to reflect the effect of forces from outside the body on the tibia bone but not the effect of compressive muscle forces. Hence, we investigated the strength of the relationship between peak tibial acceleration and maximum tibial compression forces in rearfoot-striking runners. Twelve runners ran on a treadmill while tibial acceleration was captured with accelerometers. Maximum tibial compression forces were computed with a lower leg model and individually correlated with peak tibial acceleration. The correlation coefficient was, on average, very weak (0.04 ± 0.14) and non-significant, and therefore deemed non-relevant. Peak tibial acceleration does not provide a complete picture of both internal and external compressive forces on the tibial bone. Hence, the assumed link between peak tibial acceleration and peak tibial compression forces and the expected associated risk of tibial stress fractures during treadmill running is not supported by the results of this study.

From **Chapter 3**, it is clear that running biomechanics should be measured in a representative natural environment. With IMUs, we can measure sensor acceleration and angular velocity outside the laboratory. However, we are typically also interested in body segment orientations and joint angles, for which sensor orientation is required. Sensor orientation can be estimated by integrating angular velocity while correcting for integration drift. Many sensor orientation estimation algorithms rely on computationally heavy Kalman filters, magnetometers, multiple IMUs, or extensive calibration procedures, which can burden runners to use IMUs to monitor their gait pattern easily. Alternatively, sensor orientation can be estimated based on domain-specific assumptions to reduce integration drift.

The aim of **Chapter 5** was to investigate if the quasi-cyclical nature of running could be used to define a new set of domain-specific assumptions to acquire drift-free 3D sensor orientation of the lower leg during running based on a single gyroscope. We transformed 3D angular velocities into a new partly functional coordinate system to reduce integration drift during orientation estimation. The rotation axis of the lower leg was aligned with an axis of the partly functional coordinate system, giving one axis a functional meaning. We then estimated the change in sensor orientation for a single runner on a treadmill for 90 seconds. Drift in sensor orientation estimation was drastically reduced after transforming 3D angular velocities to the new partly functional coordinate system compared to the "old" sensor coordinate system. Hence, transforming 3D angular velocities to a partly functional coordinate system before estimating the change in sensor orientation seems promising to reduce drift in 3D orientation based on a single gyroscope in quasi-cyclical and quasi-2D motions like running.

Chapter 6 elaborated on the results of **Chapter 5** and proposed a fully functional coordinate system in which all axes have functional meaning. This method used the quasi-cyclical and quasi-2D nature of many human movements. Additionally, it assumed that the velocity over multiple complete gait cycles was approximately constant, which is often the case for running. Angular velocity was expressed in the functional coordinate system before integration to obtain the change in sensor orientation. The sensor displacement was then computed by assumptions based on a quasi-cyclical movement. 3D sensor orientation and displacement for an IMU on the lower leg were validated with an optical motion capture system in four runners during constant velocity treadmill running. Errors in orientation and displacement were relatively small and comparable to other orientation and displacement algorithms. However, this new method has many advantages over current methods since it does not rely on a constant- or zero-velocity point, a biomechanical model, Kalman filtering, or a magnetometer, and can, therefore, easily be used by runners to measure their gait pattern with a single sensor or minimal sensor setup. Although this method was validated on the lower leg in treadmill running, it is expected to work for other segments and quasi-cyclical movements.

In **Chapter 7**, the main findings of all chapters in this thesis were integrated and discussed. Especially the effect of variability between subjects and studies, differences between running in a laboratory compared to outdoors, and the future of monitoring running biomechanics and injury risk were discussed. Based on the findings of this thesis, we concluded that running-induced fatigue, speed, and stride frequency influence the gait pattern in a subject-specific manner. Additionally, peak tibial acceleration is not an appropriate indicator of tibial bone loading since it does not provide a complete picture of both internal and external compressive forces on the tibial bone. Finally, we concluded that the quasi-cyclical and quasi-2D nature of running could be used to estimate drift-free 3D sensor orientation and displacement with many benefits compared to other methods. We recommend monitoring running biomechanics in a sport-specific setting and shifting the focus from investigating kinematic quantities on a group level to the forces underlying them on a subject-specific level.

Samenvatting

Hardlopen is een toegankelijke vrijetijdsbesteding. In 2020 was hardlopen de op één na populairste sport in Nederland: 12% van de Nederlandse bevolking liep wekelijks hard. Hoewel hardlopen veel voordelen heeft voor de gezondheid, lopen hardlopers een hoog risico op het ontwikkelen van blessures zoals het mediaal tibiaal stresssyndroom (d.w.z. shin splints) of tibiale stressfracturen. Het ontstaan van hardloopblessures wordt vermoedelijk veroorzaakt door fouten in de trainingsbelasting (te snel, te ver of te vaak hardlopen) en (veranderingen in) het hardlooppatroon. Bovendien wordt aangenomen dat vermoeidheid het looppatroon negatief beïnvloed wat het risico op blessures vergroot. Het verband tussen biomechanica en blessures wekt onze belangstelling voor het monitoren van hardloopbiomechanica om uiteindelijk het risico op loopblessures te verminderen.

Hardloopbiomechanica wordt vaak onderzocht tijdens hardlopen op een loopband in een gecontroleerde laboratoriumomgeving. De meeste hardlopers lopen echter buiten op verschillende snelheden en met verschillende mate van vermoeidheid. Er zijn meerdere verschillen gevonden in het looppatroon tussen hardlopen in een gecontroleerde laboratoriumomgeving en buiten, zoals hogere piekversnellingen van het scheenbeen bij het lopen buiten ten opzichte van een loopband. Deze verschillen wijzen erop dat de resultaten van hardloopexperimenten in het laboratorium niet noodzakelijkerwijs te vertalen zijn naar hardlopen in de buitenlucht. Aangezien de meeste hardlopers gewoonlijk buiten lopen, moet het monitoren van hardloopbiomechanica verplaatst worden van het laboratorium naar een sport specifieke omgeving.

Het looppatroon kan buiten het laboratorium worden gemeten met 'Inertial measurement units' (IMU's). Uit IMU data kunnen grootheden als sensororiëntatie, kniegewrichtshoeken en piekversnellingen van lichaamsdelen kort nadat de voet de grond raakt, worden berekend. Het is echter onduidelijk welke grootheden moeten worden gebruikt om het blessurerisico te monitoren. Bovendien hebben de huidige algoritmen om interessante grootheden uit ruwe sensordata te halen veel nadelen. **Daarom was dit proefschrift gericht op het vergroten van ons begrip van de hardloopbiomechanica, zoals gemeten binnen en buiten het laboratorium en het verkennen van de uitdagingen met betrekking tot draagbare bewegingsanalyse tijdens hardlopen in een sport specifieke setting.**

Om deze doelen te bereiken zijn in dit proefschrift de volgende onderzoeksvragen beantwoord:

Hoofdstuk 2	Hoe verandert de hardloopkinematica als gevolg van hardloop-geïnduceerde vermoeidheid?
Hoofdstuk 3	Hoe kan het persoon-specifieke effect van veranderingen in loopsnelheid en stapfrequentie op impact-gerelateerde loopmechanica gekwantificeerd en gecorrigeerd worden tijdens een vermoeiende buitenloop?
Hoofdstuk 4	Hoe sterk is de relatie tussen piek tibiale versnelling en maximale tibiale compressiekracht tijdens hardlopen?
Hoofdstuk 5	Kan het quasi-cyclische karakter van hardlopen gebruikt worden om drift-vrije 3-dimensionale (3D) oriëntatie van een lichaamssegment te schatten op basis van één gyroscoop?
Hoofdstuk 6	Hoe kan de 3D oriëntatie en verplaatsing van één IMU op het onderbeen worden geschat op basis van het quasi-cyclische karakter van hardlopen?

Hoofdstuk 2 onderzocht de effecten van vermoeidheid op de hardloopkinematica. Van veranderingen in het looppatroon als gevolg van vermoeidheid wordt aangenomen dat zij de looptechniek verslechteren en het risico op loopblessures vergroten. De literatuur bevat veel tegenstrijdige bevindingen over het effect van vermoeidheid op de loopkinematica. Daarom hebben wij de huidige literatuur over het effect van hardloop-geïnduceerde vermoeidheid op het looppatroon samengevat en geanalyseerd in een systematisch literatuuroverzicht met meta-analyses. Het effect van vermoeidheid op negentien kinematische grootheden werd onderzocht op basis van drieëndertig artikelen. In het algemeen resulteerde hardloop-geïnduceerde vermoeidheid in een soepeler maar minder efficiënt looppatroon, gekenmerkt door verhoogde piekversnelling van het scheenbeen, een grotere knieflexie bij het eerste grondcontact en meer maximale knieflexie in de zwaaifase, terwijl de beenstijfheid afnam. Het ervaringsniveau beïnvloedde het effect van vermoeidheid op de loopkinematica, zoals bleek uit een toename van de verticale verplaatsing van het massamiddelpunt met vermoeidheid bij beginnende, maar niet bij ervaren lopers. Veranderingen in de loopkinematica als gevolg van vermoeidheid zouden verklaard kunnen worden door een afname in tolerantie van de kniestrekkers voor opgelegde strekbelasting of een afname van de neuromusculaire controle, waardoor de impuls van de botskracht van de voet met de grond minder goed verspreidt wordt over de tijd.

Hoofdstuk 3 richtte zich op het meten van het looppatroon in een sportspecifieke omgeving. Het looppatroon wordt vaak onderzocht op groepsniveau in een gecontroleerde laboratoriumomgeving. De meeste hardlopers lopen echter in een ongecontroleerde buitenomgeving. Veranderingen in snelheid en stapfrequentie, zoals die vaak voorkomen bij buitenlopen, beïnvloeden het looppatroon en kunnen vermoeidheid gerelateerde veranderingen in de looptechniek maskeren. In dit hoofdstuk kwantificeerden en corrigeerden wij voor effecten van veranderingen in loopsnelheid en stapfrequentie op de looptechniek tijdens een vermoeiende buitenloop. De looptechniek van negen lopers werd geanalyseerd met IMU's tijdens een marathon. Persoon-specifieke meervoudige lineaire regressiemodellen werden gemaakt voor effecten van veranderingen in snelheid en stapfrequentie op piek tibiale versnelling, knie flexie hoek bij het eerste grondcontact, en maximale knie flexie hoek tijdens de standfase. Deze individuele modellen werden gebruikt om de piek tibiale versnelling en knieflexiehoeken te corrigeren voor veranderingen in snelheid en stapfrequentie. Regressiecoëfficiënten voor snelheid en stapfrequentie varieerden sterk tussen proefpersonen, deze variatie werd mogelijk veroorzaakt door verschillen in landingspatroon, tolerantie voor effecten van vermoeidheid, of vermogen om een stabiel looppatroon aan te houden over een reeks snelheden. Persoon-specifieke correcties toonden een significant effect van de fase van de marathon op de piekversnelling van het scheenbeen en de knieflexiehoeken, dat eerder werd gemaskeerd door veranderingen in snelheid en stapfrequentie. Snelheid en stapfrequentie beïnvloeden dus de interpretatie van veranderingen in mechanische grootheden op een persoon-specifieke manier. Daar moet voor gecorrigeerd worden bij het interpreteren of geven van feedback op loopmechanica in een ongecontroleerde omgeving.

Hoofdstuk 4 richtte zich op het onderzoeken van de relatie tussen de piekversnelling van het scheenbeen en de compressiekrachten op het scheenbeenbot. De piekversnelling van het scheenbeen wordt gewoonlijk gebruikt als een surrogaatmaat voor de belasting op het scheenbeenbot en er wordt aangenomen dat deze verband houdt met het risico op tibiale stressfracturen. Tibiale compressiekrachten worden echter veroorzaakt door zowel interne spierkrachten als door het effect van externe grondreactiekrachten. De piekversnelling van het scheenbeen weerspiegelt naar verwachting het effect van krachten van buiten het lichaam op het scheenbeenbot, maar niet het effect van compressiekrachten van spieren. Daarom onderzochten wij de sterkte van het verband tussen de maximale tibiale versnelling en de maximale tibiale compressiekrachten bij hardlopers met een haklanding. Twaalf lopers liepen op een loopband terwijl de tibiale versnelling werd gemeten met versnellingsmeters.

De maximale tibiale compressiekrachten werden berekend met een onderbeenmodel en individueel gecorreleerd met de maximale tibiale versnelling. De correlatiecoëfficiënt was gemiddeld zeer zwak (0.04 ± 0.14) en niet-significant en werd vandaar niet relevant geacht. De piekversnelling van het scheenbeen geeft dus geen volledig beeld van zowel de interne als de externe compressiekrachten op het scheenbeenbot. Daarom wordt het veronderstelde verband tussen piekversnelling van het scheenbeen en piekcompressiekrachten op het scheenbeenbot en daarmee waarschijnlijk het risico op tibiale stressfracturen tijdens loopband lopen niet ondersteund door de resultaten van deze studie.

Uit **hoofdstuk 3** bleek duidelijk dat de biomechanica van het hardlopen moet worden gemeten in een representatieve natuurlijke omgeving. Met IMU's kunnen we versnellingen en hoeksnelheden buiten het laboratorium meten. Meestal zijn we echter ook geïnteresseerd in lichaamssegmentoriëntaties en gewrichtshoeken, waarvoor sensor oriëntatie nodig is. Sensor oriëntatie kan worden geschat door de hoeksnelheid te integreren en te corrigeren voor integratiedrift. Veel algoritmen voor het schatten van sensor oriëntatie zijn afhankelijk van computationeel zware Kalman-filters, magnetometers, meerdere IMU's of uitgebreide kalibratieprocedures. Dit kan het voor hardlopers moeilijk maken om hun looppatroon te monitoren met IMU's. Als alternatief kan de sensor oriëntatie worden geschat op basis van domein specifieke aannames om voor integratiedrift te corrigeren.

Het doel van **hoofdstuk 5** was om te onderzoeken of het quasi-cyclische karakter van hardlopen kan worden gebruikt om een nieuwe set domein specifieke aannames te definiëren om driftvrije 3D-sensor oriëntatie van het onderbeen tijdens hardlopen te bepalen op basis van één gyroscoop. Hiervoor transformeerden we 3D hoeksnelheden naar een nieuw gedeeltelijk functioneel coördinatensysteem om de integratiedrift tijdens de oriëntatieschatting te verminderen. De rotatie-as van het onderbeen werd uitgelijnd met een as van het deels functionele coördinatenstelsel, waardoor één as een functionele betekenis kreeg. Vervolgens schatten we de verandering in sensor oriëntatie voor een enkele loper op een loopband gedurende 90 seconden. De afwijking in de schatting van de sensor oriëntatie ten opzichte van een optisch meetsysteem werd drastisch verminderd na transformatie van de 3D-hoeksnelheden naar het nieuwe gedeeltelijk functionele coördinatensysteem in vergelijking met het "oude" sensorcoördinatensysteem. Het transformeren van 3D hoeksnelheden naar een gedeeltelijk functioneel coördinatensysteem voordat de verandering in sensor oriëntatie wordt geschat, lijkt dus veelbelovend om drift in 3D-oriëntatie op basis van één gyroscoop te verminderen bij quasi-cyclische en quasi-2D bewegingen zoals hardlopen.

Hoofdstuk 6 bouwde verder op de resultaten van **hoofdstuk 5** en stelde een volledig functioneel coördinatensysteem voor waarin alle assen een functionele betekenis hebben. Deze methode maakte gebruik van de quasi-cyclische en quasi-2D aard van veel menselijke bewegingen. Bovendien werd aangenomen dat de snelheid over meerdere volledige loopcycli ongeveer constant was, wat vaak het geval is bij hardlopen. De hoeksnelheid werd uitgedrukt in het functionele coördinatensysteem vóór integratie om de verandering in de sensororiëntatie te verkrijgen. De sensorverplaatsing werd vervolgens berekend door aannames gebaseerd op een quasi-cyclische beweging. 3D sensor oriëntatie en -verplaatsing voor een IMU op het onderbeen werden gevalideerd met een optisch meetsysteem bij vier lopers tijdens het lopen op een loopband met constante snelheid. De fouten in oriëntatie en verplaatsing waren relatief klein en vergelijkbaar met andere oriëntatie- en verplaatsingsalgoritmen. Deze nieuwe methode heeft echter veel voordelen ten opzichte van huidige methoden. Dit omdat zij niet afhankelijk is van een punt of lichaamssegment dat stilstaat of een constante snelheid heeft, een biomechanisch model, Kalman filter of een magnetometer, en daarom gemakkelijk door lopers kan worden gebruikt om hun looppatroon te meten met één sensor of een minimale sensorset. Hoewel deze methode werd gevalideerd op het onderbeen bij hardlopen op een loopband, wordt verwacht dat zij ook werkt voor andere lichaamssegmenten en quasi-cyclische bewegingen.

In **hoofdstuk 7** werden de belangrijkste bevindingen van alle hoofdstukken in dit proefschrift geïntegreerd en besproken. Daarbij werd met name het effect van variabiliteit tussen proefpersonen en studies, verschillen tussen binnen en buiten een laboratorium hardlopen en de toekomst van het monitoren van hardloopbiomechanica en het blessurerisico besproken. Op basis van de bevindingen van dit proefschrift concludeerden wij dat vermoeidheid, snelheid en stapfrequentie het looppatroon op een persoon-specifieke manier beïnvloeden. Bovendien is de piekversnelling van het scheenbeen geen geschikte indicator voor de belasting van het scheenbeenbot, omdat zij geen volledig beeld geeft van zowel de interne als de externe compressiekrachten op het scheenbeenbot. Ten slotte concludeerden wij dat de quasi-cyclische en quasi-2D aard van hardlopen kan worden gebruikt om driftvrije 3D sensororiëntatie en verplaatsing te schatten, met vele voordelen ten opzichte van andere methoden. Wij bevelen aan de hardloopbiomechanica in een sport specifieke omgeving te monitoren en de aandacht te verleggen van het onderzoeken van kinematische grootheden op groepsniveau naar de onderliggende krachten op een persoon-specifiek niveau.

&

Dankwoord

Het zit erop! Mijn thesis is goedgekeurd, de promotie plechtigheid en het feest zijn gepland, nu alleen nog het dankwoord en de opmaak van dit boekje afronden. De afgelopen vier jaar zijn voor mij een groot avontuur geweest. Na het afronden van de Research Master bewegingswetenschappen kwam er de mogelijkheid voorbij om een PhD te gaan doen bij Roessingh Research and Development in Twente. Tja, Twente, nooit gedacht dat ik ooit aan die kant van Nederland zou gaan wonen. Het avontuur begon vier jaar terug dan ook met een verhuizing vanuit een studentenflatje op drie hoog in Amsterdam naar een huis met een tuin en kippen aan de rand van Enschede. Na een lange dag achter de computer was het toppunt van ontspanning dan ook lekker met mijn handen bezig zijn in de (moes)tuin of met klussen in huis. Tijdens mijn PhD avontuur heb ik veel mensen leren kennen die ik allemaal wil bedanken.

In het bijzonder wil ik mijn co-promotor en promotoren; Jasper Reenalda, Jaap Buurke en Peter Veltink bedanken. Jasper, dank voor je enthousiasme, inspiratie, motiverende woorden en positieve blik. Als ik het even niet meer zag zitten zorgden onze overleggen er altijd voor dat ik weer met een enthousiastere en positievere blik naar ons onderzoek keek. Ik ben je dankbaar voor je vertrouwen en steun waardoor ik meer zelfvertrouwen als wetenschapper heb ontwikkeld. Jaap, dank voor je nuchtere adviezen en inzichten tijdens mijn hele PhD traject. Jij wist er altijd voor te zorgen dat de grote lijnen in mijn PhD duidelijk bleven en ik niet verstrikt raakte in de details. Peter, dank voor je kritische blik en meer technische kijk op het geheel. Jouw technische inzichten en mechanische visie op het hardlooppatroon lieten mij vaak weer kritisch kijken naar waarom we doen wat we doen. Ik waardeer het ontzettend dat jullie, ondanks jullie drukke agenda's, altijd tijd wisten vrij te maken om stukken tekst van feedback te voorzien. Het gebeurde regelmatig dat ik blij was dat een stuk tekst even "de deur uit" was maar dat hetzelfde stuk binnen 1 á 2 dagen, voorzien van feedback van jullie allemaal, alweer retour in mijn mailbox zat.

I would like to thank the members of the graduation committee for investing their expertise and valuable time in reviewing my thesis and being present at my PhD defence.

Verder was mijn tijd bij RRD lang niet zo gezellig en leerzaam geweest zonder de grote groep junior onderzoekers; Robert, Roos, Silke, Tessa, Eline, Jule, Luca, Bouke, Cindy, Lena, Kira, Marian, Marijke, Anne, Mattiènne en Eline. Bedankt voor de gezelligheid, koffiemomentjes, spelletjes avonden, schaatsuitjes, junioren weekend en uiteraard de gedeelde smart over het leven van een junior onderzoeker. Naast alle andere collega's bij RRD wil ik in het bijzonder graag nog Inger, Jos, Wendy en Leendert bedanken. Inger, bedankt voor alle tips en adviezen over waar (of bij wie) je moet zijn om praktische dingen te regelen, het inplannen van afspraken in onmogelijk volle agenda's maar bovenal de ontzettend fijne gesprekken, lunches en kopjes koffie. Jos, Wendy en Leendert, dank voor jullie hulp op het vlak van ICT, problemen met apparatuur, het meedenken over onderzoeksopstellingen en het ontwerpen van de omslag van dit boekje. Ik zal niet snel vergeten hoe ik jullie kantoor binnen liep met de vraag om een sensor voor het magnetisch veld vlak bij de grond, en met een kompas op een stokje weer naar buiten liep, niet alles in de onderzoekswereld hoeft high-tech te zijn.

Vaste prik op dinsdagochtend was het Immunity (Inertial Measurement Unit Tuesday) overleg. Onder leiding van Jasper discussieerden we over recente artikelen, ideeën voor nieuw onderzoek, interpretaties van resultaten, studentprojecten, et cetera. Graag wil ik dan ook alle (voormalig) leden van het Immunity Team bedanken, maar in het bijzonder Jasper, Luca, Bouke, Robbert en Anne.

Tijdens mijn PhD project ben ik betrokken geweest bij vele studentprojecten. Xanthe, Robbert, Jaline, Jelle, Basile, Bente, Isabella, Emily en Romano, bedankt voor jullie hulp bij metingen, vragen, en inhoudelijke discussies. Het is altijd mooi om het met iemand met een frisse blik over onderzoek te kunnen hebben.

Als junior onderzoeker ben ik aangenomen op het Runner Assist project. Dit project was een samenwerking tussen RRD, Xsens en Trimm. Graag zou ik dan ook Xsens en Trimm, en in het bijzonder Kim, Frank, Martin, Laurens, Janinka, Chris en Marc willen bedanken voor de samenwerking tijdens het Runner Assist project.

Zonder proefpersonen zou dit proefschrift niet mogelijk zijn geweest. Bedankt aan alle lopers die mee hebben gedaan aan één (of meerdere) van de hardloop experimenten. Dank voor jullie tijdsinvestering, inspiratie, motivatie en leuke gesprekken. En dank aan de organisatie van de Enschede Marathon en Singelloop die het mogelijk hebben gemaakt dat wij lopers tijdens hardloopwedstrijden hebben kunnen meten.

Dan de collega's bij OCON. Jullie hebben met name het laatste deel van mijn PhD meegekregen. Een periode waarin ik parallel als bewegingstechnoloog bij OCON werkte en mijn PhD aan het afronden was. Dank allemaal voor de steun en het aanhoren van frustraties. Ik vond het heerlijk (en herkenbaar) om mee te maken hoe Camiel en Quinten net aan de start van hun eigen promotietrajecten staan. Daarnaast was het ook erg fijn om van ervaringsdeskundigen; Judith, Arjan en Alli te horen hoe zij hun eigen promotietrajecten hebben ervaren en om te horen dat ik mij vooral niet zoveel zorgen hoefde te maken en ik ervan moet genieten.

Mijn paranimfen Samantha en Robert. Ik voel mij vereerd dat jullie tijdens mijn verdediging aan mijn zijde zullen staan. Samantha, bedankt voor jouw luisterend oor en adviezen in de afgelopen jaren. Het is ontzettend fijn om mijn hart te kunnen luchten bij jou. Robert, ik vond het spannend om een kantoor te delen met één iemand, want wat nou als het niet klikt? Na mijn eerste dag bij RRD wist ik dat ik mij daar geen zorgen om hoefde te maken. Wat heb ik het getroffen met jou als kamergenoot. Met name jouw nuchterheid en stressbestendigheid hebben mij geholpen om mij te ontwikkelen als kritisch onderzoeker en als mens. Wellicht is onze productiviteit omhoog gegaan toen we noodgedwongen thuis moesten werken maar ik had onze kantoorgesprekken niet willen missen.

Dan mijn (schoon)familie en vrienden, dank voor jullie luisterend oor, ideeën en afleiding. In het bijzonder; Danuše en Puck, dank voor de oprechte interesse, kritische vragen en heerlijke gerechten. Verder wil ik Kirsten en Samantha bedanken voor jullie vriendschap! Onze promotietrajecten liepen parallel aan elkaar waardoor onze afspraakjes een feest der herkenning waren. Wat ontzettend fijn dat wij elkaar negen jaar terug hebben ontmoet! Hoewel iedereen in een andere uithoek van Nederland (of Australië) woont ben ik blij dat wij regelmatig nog een sauna dagje plannen om te kunnen klagen over in de soep gelopen projecten, afgewezen artikelen en de toekomst.

Mama en Fleur, zonder jullie onvoorwaardelijke steun voor dit gekke traject was mijn PhD avontuur een stuk lastiger geweest. Mama, bedankt voor de bemoedigende woorden, het luisterend oor en het oneindige vertrouwen dat ik mijn PhD tot een succesvol einde zou weten te brengen. Fleur, hoewel jij niet per se blij was dat ik aan de andere kant van het land ben gaan wonen waardeer ik het enorm dat je zeer regelmatig met Lucien een weekendje bent komen logeren om zo voor de nodige afleiding te zorgen en om dingen in perspectief te zien. Deze weekenden waren zo gezellig dat ik mij geen zorgen kon maken om mijn PhD. Mama en Fleur, het doet mij goed om te weten dat ik altijd op jullie terug kan vallen. En papa, ik weet zeker dat je trots zou zijn geweest op jouw dochters.

Billie, mijn lieve schat, mijn rots in de branding. Wat zou ik toch zonder jou moeten. De afgelopen 10 jaar weet ik dat wat er ook gebeurd, jij mij zal steunen. Tijdens mijn hele PhD traject was jij fysiek of digitaal vlakbij. Jouw humor, relativeringsvermogen, klushulp en onvoorwaardelijke vertrouwen in mij hebben ervoor gezorgd dat de werk-privé balans niet (te lang) uit evenwicht bleef. Hoe gestrest ik soms ook ben, jij weet mij altijd tot bedaren te brengen. Billie, ik weet dat wij samen alles aankunnen en ik kijk ontzettend uit naar wat de toekomst ons gaat brengen.

About the author

Marit Zandbergen was born in 's-Hertogenbosch, The Netherlands on July 3th 1995. Marit obtained her bachelor's degree Human Movement Sciences with Cum Laude in 2016 at the Vrije Universiteit Amsterdam. She also completed the Honours programme during her bachelor. In 2018, Marit obtained her Research Master's degree in Human Movement Sciences with Cum Laude at the Vrije Universiteit Amsterdam. During her studies, Marit was fascinated by human movement. Why can seemingly simple movements like walking or running be so challenging for some poeple? This interest was reflected in her bachelor and master theses about human movement analysis.

Immediatly after obtaining her master's degree, Marit started as a junior researcher and PhD candidate at Roessingh Research and Development in Enschede. Marit was involved in the runner assist project, where she was responsible for developing and evaluating algorithms to provide real-time feedback on running biomechanics to prevent injuries and improve running performance.

In February 2022, Marit started working as a movement technician at OCON in Hengelo and finished her PhD thesis in parallel.

Awards

- American College of Sports Medicine Biomechanics Interest Group student award 2020
- Society for Movement Analysis Laboratories in the Low Lands award 2018
- Gerrit-Jan van Ingen-Schenau Promising young scientist award 2017
- Student price of the Amsterdam Movement Sciences Innovation Call 2017

Journal publications

- **Zandbergen, M.A.**, ter Wengel, X.J., van Middelaar, R.P., Buurke, J.H., Veltink, P.H., Reenalda, J. Peak tibial acceleration should not be used as indicator of tibial bone loading during running. Sports Biomechanics, accepted for publication. (Included as **Chapter 4**).
- **Zandbergen, M.A.**, Marotta, L., Bulthuis, R., Buurke, J.H., Veltink, P.H., Reenalda, J. (2023). Effects of level-running induced fatigue on running kinematics: A systematic review and meta-analysis. Gait & Posture, 99, 60-75. (Included as **Chapter 2**).

- **Zandbergen, M.A.**, Reenalda, J., van Middelaar, R.P., Ferla, R.I., Buurke, J.H., Veltink, P.H. (2022). Drift-free 3D orientation and displacement estimation for quasi-cyclical movements using one inertial measurement unit: Application to running. Sensors, 22(3), 956. (Included as **Chapter 6**).
- Reenalda, J., **Zandbergen, M.A.**, Harbers, J.D., Paquette, M.R., Milner, C.E. (2021). Detection of foot contact in treadmill running with inertial and optical measurement systems. Journal of Biomechanics, 121, 110419.
- **Zandbergen, M.A.**, Schallig, W., Stebbins, J.A., Harlaar, H., van der Krogt, M.M. (2020). The effect of mono- versus multi-segment musculoskeletal models of the foot on simulated triceps surae lengths in pathological and healthy gait. Gait & Posture, 77, 14-19.
- Brenner, E., Rodriguez, I.A., Munoz, V.E., Schootemeijer, S., Mahieu, Y., Veerkamp, K., **Zandbergen, M.**, Zee, van der T., Smeets, B.J. (2016). How can people be so good at intercepting accelerating objects if they are so poor at visually judging acceleration? i-Perception, 7(1), 1-13.

Submitted for publication

- **Zandbergen, M.A.**, Buurke, J.H., Veltink, P.H., Reenalda, J. Quantifying and correcting for speed and stride frequency effects on running mechanics in fatiguing outdoor running. (Included as **Chapter 3**).

Conference contributions

- **Zandbergen, M.A.**, Ferla, R.I., Buurke, J.H., Reenalda, J., Veltink, P.H. (2020). Estimating 3D orientation of a body segment during running using a single gyroscope. Conference: 3D Analysis of Human Movement symposium 2020. (Included as **Chapter 5**).
- **Zandbergen, M.A.**, Reenalda, J. (2021). Do runners fatigue similarly? Peak accelerations and vertical stiffness during a fatiguing treadmill run. Conference: Americal College of Sports Medicine 2021, Medicine & Science in Sports & Exercise, 53(8S):148-149.
- **Zandbergen, M.A.**, Buurke, J.H., Veltink, P.H., Reenalda, J. (2020). Changes in peak accelerations and shock attenuation over the course of a marathon. Conference: Medicine & Science in Sports & Exercise, 52(7S), 817.
- **Zandbergen, M.A.**, Klaassen, M., Buurke, J.H., Reenalda, J. (2019). Changes in shock absorption and kinematics during a half marathon as measured with inertial sensors. Conference: Medicine & Science in Sports & Exercise, 51(S), 182-183.

Progress range

The following publications have been published in the Progress range by Roessingh Research and Development, Enschede, the Netherlands. Copies can be ordered, when available, via info@rrd.nl.

1. Pot, J.W.G.A, Boer H., van Harten, W.H., Hermens, H.J., Seydel, E.R. Comprehensive Need-Assessment. Ontwikkeling van een meetinstrument voor zorgbehoeften en kwaliteitsbeoordeling door patiënten. September 1994, ISBN 90-25452-01-22
2. van Leerdam, N.G.A, Hermens, H.J. Revalidatietechnologie in Euregio. July 1995, ISBN 90-75452-02-0
3. Duda, L., van Noort, L.O., Röseler, S., Greitemann, B.O.L, van Harten, W.H., Klazinga, N.S. Rehabilitation in Germany and the Netherlands, A comparison of two rehabilitation systems. August 1995, ISBN 90-75452-03-9
4. Hermens, H.J., Nene, A.V., Zilvold, G. Electrophysiological Kinesiology, Proceedings of the 11th congress of the International Society of Electrophysiology and Kinesiology in Enschede, the Netherlands 1996. October 1996, ISBN 90-75452-04- 7
5. van Harten, W.H. Bouwen aan een kwaliteitssysteem in de revalidatiezorg. Een poging tot constructieve technology assessment van een kwaliteitssysteem in een gezondheidszorginstelling. December 1997, ISBN 90-75452-07-1
6. Baardman, G., IJzerman, M.J. Design and evaluation of a hybrid orthosis for people with paraplegia. November 1997, ISBN 90-75452-8-X
7. Hutten, M.M.R. Lumbar Dynamometry: A useful method for assessment of patients with chronic low back pain? November 1999, ISBN 90-75452-13-6
8. van der Salm, A., van Harten W.H., Maathuis, C.G.B. Ketenkwaliteit Cerebrale Parese Zorg. Een beschrijving van de cerebrale parese zorg en mogelijke verbeteringen hierin. April 2001, ISBN 90-75453-19-5
9. Nederhand, M.J. Muscle activation patterns in post traumatic neck pain. March 2003, ISBN 90-75452-27-6
10. Jannink, M.J.A. Usability of custom-made orthopaedic shoes in patients with degenerative disorders of the foot. September 2004, ISBN 90-75452-28-4
11. Blokhorst, M.G.B.G. State-dependent factors and attention in whiplash associated disorder. January 2005, ISBN 90-365-2111-4
12. Buurke, J.H. Walking after stroke. Co-ordination Patterns & Functional Recovery. February 2005, ISBN 90-365-140-8

13. van der Salm, A. Spasticity reduction using electrical stimulation in the lower limb of spinal cord injury patients. October 2005, ISBN 90-365-2253-6
14. Snoek, G.J. Patient preferences for reconstructive interventions of the upper limb in tetraplegia. December 2005, ISBN 90-365-2255-2
15. de Kroon, J.R. Therepeutic electrical stimulation of the upper extremity in stroke. December 2005, ISBN 90-365-2269-2
16. van Dijk, H. Motor skill learning, Age and Augmented feedback. March 2006, ISBN 90-365-202-9
17. Mes, C.A.J. Improving non-optimal results in chronic pain treatment. January 2007, ISBN 90-365-2435-0
18. Voerman, G.E. Musculoskeletal neck-shoulder pain: a new ambulant myofeedback intervention approach. March 2007, ISBN 90-365-2460-1
19. Kallenberg, L.A.C. Multi-channel array EMG in chronic neck-shoulder pain. March 2007, ISBN 90-365-2459-8
20. Huis in 't Veld, M.H.A. Work-releated neck-shoulder pain. The role of cognitivebe-havioural factors and remotely supervised treatment. December 2007, ISBN 978-90-365-2584-8
21. Fleuren, J.F.M. Assessment of spasiticity. From EMG to patients' perception. October 2009, ISBN 978-90-365-2869-6
22. Reenalda, J. Dynamic sitting to prevent pressure ulcers in spinal cord injured. October 2009, ISBN 978-90-365-2884-9
23. Prange, G.B. Rehabilitation robotics. Stimulating restoration of arm function after stroke. October 2009, ISBN 978-90-365-2901-3
24. Vos-van der Hulst, M. Prognostic factors and underlying mechanisms in chronic low back pain. February 2010, ISBN 978-90-365-2881-8
25. Kottink-Hutten, A.I.R. Assessment of a two-channel implantable peroneal nerve stimulator post-stroke. February 2010, ISBN 978-90-365-2959-4
26. van Weering, M.G.H. Towards a new treatment for chronic low back pain patients. Using activity monitoring and personalized feedback. May 2011, ISBN 978-90-365-3305-8
27. Gulmans, J. Crossing boundaries. Improving communication in cerebral palsy care. February 2012, ISBN 978-90-365-3305-8
28. Molier, B.I. Influence of augmented feedback on learning upper extremity tasks after stroke. March 2012, ISBN 978-90-365-3293-9

29. Dubbeldam, R. Towards a better understanding of foot and ankle kinematics in rheumatoid arthritis. The effects of walking speed and structural impairments. October 2012, ISBN 978-90-365-3407-9
30. Evering, R.M.H. Ambulatory feedback at daily physicial activity patterns. A treatment for the chronic fatigue syndrome in the home environment? April 2013, ISBN 978-90-365-3512-0
31. Malhorta, S. Does spasticity interfere with functional recovery after stroke? A novel approach to understand, measure and treat spasticity after acute stroke. November 2013, ISBN 978-90-365-2567-0
32. Tabak, M. Telemedicine for patients with COPD. New treatment approaches to improve daily activity behaviour. Roessingh Research and Development. February 2014, ISBN 978-94-6108-590-0
33. Trompetter, H.R. ACT with pain. Measurement, efficacy and mechanisms of Acceptance and Commitment Therapy. September 2014, ISBN 978-90-365-3708-7
34. op den Akker, H. Smart Tailoring of Real-Time Physical Activity Coaching Systems. October 2014, ISBN 978-90-365-3762-9
35. Jansen-Kosterink, S.M. The added value of telemedicine for physical rehabilitation. December 2014, ISBN 978-90-823196-0-6
36. Velstra, I.M. Advanced insights in upper limb function of individuals with cervical spinal cord injury. December 2015, ISBN 978-90-365-3929-6
37. Kloosterman, M.G.M. Keep on rolling. Functional evaluation of power-assisted wheelchair use. June 2016, ISBN 978-90-365-4299-9
38. Prinsen, E.C. Adapting to change. Influence of a microprocessor-controlled prosthetic knee on gait adaptations. December 2016, ISBN 978-90-365-4206-7
39. Wolvers, M.D.J. A coach in your pocket. On chronic cancer-related fatigue and physical behavior. March 2017, ISBN 978-90-365-4299-9
40. Cabrita, M. Active and Pleasant Ageing supported by Technology. November 2017, ISBN 978-90-365-4407-8
41. Haarman, J.A.M. TIBAR. Therapist Inspired Balance Assisting Robot. November 2017, ISBN 978-90-365-4407-8
42. Nijenhuis, S.M. Roll up your sleeves! Technology-supported arm and hand training at home after stroke. April 2018, ISBN 978-90-365-4510-5
43. Cranen, K. Acceptance of telerehabilitation in chronic pain: the patients' perspective. June 2018, ISBN 978-90-365-4555-6
44. Boerema, S.T. Sensing human activity to improve sedentary lifestyle. September 2018, ISBN 978-90-365-4604-1

45. Radder, B. The wearable hand robot. Supporting impaired hand function in activities of daily living and rehabilitation. November 2018, ISBN 978-90-365-4658-4
46. Krabben T. A reaching hand. Towards an Active Therapeutic device for the upper extremity following stroke. December 2018, ISBN 978-90-365-4660-7
47. Timmerman, J.G. Cancer rehabilitation at home. The potential of telehealthcare to support functional recovery of lung cancer survivors. January 2019, ISBN 978-90-4701-7
48. Nikamp-Simons, C.D.M. The sooner the better?! Providing ankle-foot orthoses in the rehabilitation after stroke. May 2019, ISBN 978-90-365-4747-5
49. Achterkamp, R. Towards a balanced and active lifestyle. June 2019, ISBN 978-94-6323-656-0
50. Engbers, C. Keep Cycling. How Technology can Support Safe and Comfortable Cycling for Older Adults. September 2019, ISBN 978-90-365-4848-9
51. Ommeren, A.L. Offering a helping hand. Getting a grip on needs and preferences of stroke patients regarding soft-robotic technology supporting hand function. October 2019, ISBN 978-90-365-4835-9
52. ter Stal, S. Look Who's Talking. Appearance of Embodied Conversational Agents in eHealth. March 2021, ISBN 978-90-365-5126-7
53. Beinema, T.C. Tailoring coaching conversations with virtual health coaches. December 2021, ISBN 978-90-365-5260-8
54. Hurmuz, M.Z.M. eHealth – In or out of our daily lives? Measuring the (non-)use of eHealth in summative evaluations. June 2022, ISBN 978-90-365-5360-5
55. Broekhuis, M.C. Meet my HUBBI: he's and expert on eHealth usability. September 2022, ISBN 978-90-365-5443-5
56. Schulte, R.V. Up to one's knees in data, data-driven intent recognition using electromyography for the lower limb. December 2022, ISBN: 978-90-365-5486-2
57. Bessler-Etten, J. Safety first in rehabilitation robots! Investigating how safety-related physical human-robot interaction can be assessed. January 2023, ISBN: 978-90-365-5503-6
58. Zandbergen, M.A. Moving forwards by going outside - Inertial measurement unit-based monitoring of running biomechanics. February 2023, ISBN: 978-90-365-5513-5
59. Marotta, L. Development of inertial sensor-based methods to assess physical fatigue in running applications. February 2023, ISBN: 978-90-365-5507-4

ROESSINGH RESEARCH & DEVELOPMENT 58

Progress in rehabilitation science

ISBN 978-90-365-5513-5